

# REGENERATIEF POTENTIEEL VAN BLOEDPLAATJESCONCENTRATEN IN PARODONTALE CHIRURGIE

Ana B. Castro Sardá

**PROMOTOR:**

Prof. Dr. Marc Quirynen

**CO-PROMOTOREN:**

Prof. Dr. Reinhilde Jacobs

Prof. Dr. Joke Duyck

**CHAIR:**

Prof. Dr. Bart Van Meerbeek

**JURY LEDEN:**

Prof. Dr. Constantinus Politis (KU Leuven)

Prof. Dr. Robert Hermans (KU Leuven)

Prof. Dr. Ivo Lambrichts (Hasselt University)

Prof. Dr. Juan Blanco (University of Santiago de Compostela, Spain)

Proefschrift voorgedragen tot het behalen van de graad van  
Doctor in de Biomedische Wetenschappen

Leuven, 2021



KU Leuven  
Biomedical Sciences Group  
Faculty of Medicine  
Department of Oral Health Sciences  
Periodontology and Oral Microbiology



DOCTORAL SCHOOL  
BIOMEDICAL SCIENCES

# REGENERATIVE POTENTIAL OF PLATELET CONCENTRATES IN PERIODONTAL SURGERY

Ana B. Castro Sardá

**PROMOTER:**

Prof. Dr. Marc Quirynen

**CO-PROMOTERS:**

Prof. Dr. Reinhilde Jacobs

Prof. Dr. Joke Duyck

**CHAIR:**

Prof. Dr. Bart Van Meerbeek

**JURY MEMBERS:**

Prof. Dr. Constantinus Politis (KU Leuven)

Prof. Dr. Robert Hermans (KU Leuven)

Prof. Dr. Ivo Lambrichts (Hasselt University)

Prof. Dr. Juan Blanco (University of Santiago de Compostela, Spain)

Dissertation presented in partial fulfilment of the requirements for the degree of  
Doctor in Biomedical Sciences

Leuven, 2021



Thesis submitted in partial fulfilment of the requirements for the degree of *“Doctor in Biomedical Sciences”*

All rights reserved. Except in those cases expressly determined by law, no parts of this publication may be multiplied, saved in an automated data file or made public in any way whatsoever without the express prior written consent of the authors.



# ACKNOWLEDGEMENTS

---

An important chapter of my life is reaching its end today, or it is starting, depending on how you look at it. My interest in research began when I was a kid, always curious to discover new frontiers. During this journey, I have been lucky enough to meet many people who have shown me how exciting science can be. To all of them, big thanks for inspiring me and encouraging me to complete this achievement: a PhD.

My deepest sense of gratitude goes to my promoter **Prof. Dr. Marc Quirynen**, for his contagious enthusiasm in research and constant support. I remember very clearly the day that we met for the first time in Barcelona. I would have never imagined that that moment would change my life completely. Thanks for giving me the opportunity to grow as a clinician, researcher and as a person. You are the best example of tenacity and passion for your work and I feel very proud of being part of this amazing team.

I would also like to thank my two co-promoters **Prof. Dr. Reinhilde Jacobs** and **Prof. Dr. Joke Duyck**, two examples for me of successful women and excellent researchers. Thanks Prof. Reinhilde Jacobs for being always available for me, for opening the doors of your department and for your suggestions. I really admire your solidarity for sharing your knowledge and your tireless desire to learn. To Prof. Joke Duyck, thanks for your humanity, for your excellent advice in research and in life. You have supported me and helped to overcome all difficulties and at the end this made us grow.

As my internal jury members, **Prof. Dr. Constantinus Politis** (KU Leuven) and **Prof. Dr. Robert Hermans** (KU Leuven) have helped me and support me throughout all the yearly evaluation moments. Prof. Constantinus Politis, a big thanks for your suggestions, they inspired me to improve the quality of this thesis. To Prof. Robert Hermans, thanks for your remarks which helped me to enhance the research protocols. Moreover, it was a pleasure to be your “Spanish colleague” at ILT and see the insights of somebody trying to learn my own language.

I am very grateful to the examining committee of this thesis, **Prof. Dr. Ivo Lambrichts** (Hasselt University) and **Prof. Dr. Juan Blanco** (University of Santiago de Compostela, Spain) for their constructive remarks and inspiring suggestions to improve the quality of this PhD thesis. To Prof. Lambrichts, thank you for being always available for advice, for your infinite knowledge in biology. To Prof. Blanco, my sincere thanks for transmitting me your passion for perio and for research and for the amazing congress in Santiago. I am also very grateful to **Prof. Dr. Bart Van Meerbeek** for chairing the public defense of my PhD dissertation.

During this journey, I combined my PhD with the EFP specialization in Periodontology and Implantology. It was not easy, I must say. But at the end, it is very rewarding to see how many things I achieved in the last 7 years. All of this was possible thanks to a strong team behind me, supporting me in all aspects. Since the very beginning, I could count on you, **Prof. Dr. Wim Teughels**, on your knowledge in lab research, brilliant ideas and skills. Also my sincere thanks goes to **Mrs. Christel Dekeyser**. You know how hard some days were for me, how hard I had to fight. Thanks for being always there, for reading my mind sometimes, and for supporting not only me but also, now, my family. A big thanks goes also to **Prof.**

**Dr. Andy Temmerman.** I miss your company and music in the office, the nice chats and laughs. Thanks for adding the fun to the working daily life. I cannot forget the help of **Mrs. Lieve Desmet**, **Mrs. Karine Vranckx** and **Mrs. Andrea Vanobberghen**. Thanks for your kindness and your never-ending smile. Bedankt allemaal!

A big challenge for me was to change the periodontal probe for a pipette. This thesis has a wide section of in vitro studies and I would not have been able to do it without the help of a fantastic team at the 6<sup>th</sup> floor. I would like to thank **Prof. Dr. Wim Teughels** and **Prof. Dr. Kirsten Van Landuyt** for giving me the opportunity to work in the lab. A big thanks goes to **Dr. Martine Pauwels**, **Dr. Vera Slomka**, **Dr. Esteban Rodriguez Herrero**, **Dr. Tim Verspecht**, **Drs. Wannes Van Holm**, **Drs. Naeira Medhat**, **Dr. Ferda Pamuk**, **Dr. Laleh** and **Dr. Ladan Khodoparast**, **Dr. Carolina Morsch**, **Dr. Bernardo Passoni**, **Dr. Marcelo Mesquita**, **Rita Merckx**, **Dr. Stefanie Krausch-Hofmann**, **Drs. Chen Zhong**, **Drs. Amit Rajbhoj** and **Drs. Zuodong Zhao**. To **Martine**, thanks for sharing with me your knowledge in microbiology, for teaching me together with **Esteban** how to work with bacteria. My most sincere gratitude goes to **Vera**, for being my friend, for your delicious dinners and cookies, and for our pleasant conversations. It has never been the same without you.

Daily life of a PhD student can be somehow exhausting and tiresome. However, I was lucky to have the best colleagues and friends who made mine more bearable. These years would not be the same without the best office-mates: **Dr. Isabelle Laleman**, **Drs. Simone Cortellini**, **Drs. Rutger D'Hondt**, **Prof. Dr. Joe Merheb**, **Drs. Mihai Tarce** and **Dr. Jesica Dadamio**. Thank you all for the chats, laughs and untidiness. **Isabelle**, thanks for all your support all these years, for the nice discussions and yoga lessons!. **Simone**, we have shared many unforgettable moments in the last 6 years: EFP training, an animal study (do not underestimate an in vivo study!), many congresses, parties and trips. Together with my other two “boykes”, **Mathieu De Nutte** and **Senne De Winter**, you took care of me during the whole perio training. I feel very lucky to have you guys!

In this line, I cannot forget my other colleagues and friends with whom I shared also so many moments and especially one, the EFP examination: **Valérie Oud**, **Astrid Wylleman** and **Bahoz Sanaan**. Thanks to all the **assistants** of the department of Periodontology with whom I had the opportunity to work with, especially to **Alexander De Greef**, **Drs. Manoetjer Siawasch**, **Tony Vanderstuyft**, **Dominique Van der Veken**, **Bo Molemans**, **Charlotte Favril** and **Charlotte De Hous**. You all inspired me and make me the person and clinician that I am today. To **Manoe**, I wish you all the best with your PhD! Also to the new incorporations to the perio team: **Nina Sidiropoulou**, **Drs. Fabio Rodríguez Sánchez**, **Moaad Alami**, **Pieter-Jan Germonpré**, **Nick Ntovas**, and **Jits Robben**. A word of gratitude goes to the assistants and supervisors of the restorative department for the nice teamwork, especially to **Pieter-Jan Swerts**, **Ellen Van de Maele**, **Tatjana Camps**, **Anna Braeckmans**, **Katrien Blancke**, **Ellen Cloet**, **Laurens De Greef** and **Ellen Wouters**. I would like to thank especially two persons for their patience and kindness with me: **Mrs. Greet De Mars** and **Mr. Marc Meeus**. To **Greet**, you are an example for me. Strong woman who never gave up to achieve her goals, and excellent clinician. Thank you for the amazing teamwork and wonderful Wednesdays. I will miss you. To **Marc**, thanks for transmitting me your passion for surgery, for never stop learning. The same spirit I found in my internship supervisor, **Mr. Dirk Verbist**. Thanks Dirk for introducing me to work in a



private practice, for our pleasant discussions about perio and for your willingness to teach me and show me all you know. I cannot forget my colleagues from **Radix** Antwerpen and Heist-op-den-Berg for their pleasant teamwork.

In a PhD, collaborating with other colleagues is essential. For the systematic reviews of this thesis, I had the great opportunity to collaborate with **Dr. Nastaran Meschi** and **Prof. Em. Paul Lambrechts**. Thanks also to the **CEBAM** (Belgian Centrum for Evidence-Based Medicine) for guiding us in this adventure. I had also the honor to meet and work together with other PhD students from the BIOMAT lab. A big thanks to **Prof. Dr. Bart Van Meerbeek** for opening the doors of the lab, and especially to **Prof. Dr. Simón Pedano**, **Dr. Stevan Čokić**, **Dr. Ivana Nedeljkovic**, **Dr. Xin Li**, **Dr. Pong Pongprueksa**, **Pendithee Chai**, **Dr. Annelies Van Ende**, **Dr. Jan de Munck**, **Dr. Siemon de Nys**, **Dr. Evelyne Putzeys**, **Dr. Mohammed Ahmed Mohammed**, **Drs. Chiulang Tang**, **Dr. Chenmin Yao**, **Prof. Dr. Mariko Matsumoto**, **Dr. Ana Paula Ayres Oliveira**, **Dr. Bernardo Camargo**, **Cassia Katsuki (and Anton)**, **Prof. Dr. Marcio Vivan Cardoso**, and **Ben Mercelis**. **Ivana** and **Xin**, you both became such good friends to me. Thanks for all the moments we have shared together, for the amazing dinners. We will never forget the trip to Serbia!

To **Dr. Stevan Čokić** and **Dr. Jelena Bakušić**, I do not have enough words to express my gratitude to you both. Thanks for our Fridays at Ellis burger, for sharing so many moments together, for becoming a part of our family. I am looking forward to see **Maksim** and Olivia growing together. You both are an example of tenacity and I am sure you will achieve all you propose in the future. Another part of the Leuven family whom I am very grateful too is to **Prof. Dr. María Cadenas**, **Dieter Demeyer** and **Sofía**. Thank you guys for bringing a part of Spain to Leuven, for sharing the same life experiences. **María**, thanks for showing up one day in my office and never leave. Gracias por estar siempre ahí, por tu apoyo incondicional y por compartir esta aventura con nosotros. **Sofía**, **Dieter** y tú ya formáis parte de nuestra familia. A word of gratitude goes also to **Drs. Andrés Torres**, **Ellen Cloet** and **Ana**. Thanks guys for kindness and for your friendship. Also big thanks to **Dr. Giacomo Begnoni** for the nice conversations at lunchtime. And I cannot forget **Dr. Titiaan Dormaar** and **Dr. Deepti Sinha** for their help and support all these years.

In the process of a PhD, one needs to go further and expand her limits. I was very lucky to have the opportunity to work with Prof. Jacobs' team, especially with **Dr. Jeroen Van Dessel**, **Dr. Karla de Faria Vasconcelos**, **Dr. Laura Nicolielo**, **Dr. Anna Ockerman** and **Drs. Catalina Moreno**. Thank you all for your patience, for showing me how amazing imaging can be and let me learn a bit about it. I would also like to acknowledge **Dr. Pieter L'Hoëst** and his team from the Materials Engineering Department at the KU Leuven for their fantastic work analyzing the release of microparticles from the tubes, even in the middle of the pandemic. My gratitude goes also to **Drs. Catherine Andrade** and **Prof. Nelson Pinto** from the University of Los Andes (Chile) for the inspiring meetings and brilliant ideas. **Catherine**, I wish you all the best in your research career!

Everyone who has gone through an animal study will understand how challenging it is. We were privileged to count with the expertise of **Dr. Wouter Merckx**, **Mr. Stijn Massart** and all the staff members of the Centre Zootechnique (**TRANSfarm**) at the KU Leuven in Lovenjoel. You helped us so much during the surgeries and afterwards taking care of the animals during the follow-up period. From that study on, we have intensively worked together with **Dr. Tim Vangansewinkel** and **Mrs. Evelyne Van Kerckhove** from

Hasselt University for the histological analysis. Thanks to both of you for your patience with me and for your willingness to get the best histology out of the samples. Also, I cannot forget the unconditional help of **Dr. Wim Coucke** with the statistics. Thanks Wim for being always available and for our meetings after-hours.

Administration work during a PhD should not be underestimated. I would like to thank **Sandra Winnen** for her infinite help. I also want to have a word of appreciation to the team of the Doctoral School of Biomedical Sciences, in particular to **Mrs. Sophie Collart**, **Mrs. Bieke Tembuyser** and **Mrs. Annemie Janssens** for their continuous support during the whole PhD.

One should never forget where she is coming from, and for me my roots are in my hometown **Albelda (Spain)**. To there, I send my most sincere gratitude to all my friends from **La Figuera**, especially to **Ingrid** and **Sebas**. To **Ingrid**, gràcies nena per estar sempre al meu costat, per les visites, per les xerrades, per ser com ets. To **Sebas**, des de sempre he pogut contar amb tu, gràcies per totes les anades i tornades a l'aeroport i per ser com un germà. **Erika y Vanesa**, qué bonitas son las amistades que aguantan a pesar del tiempo y la distancia. Gracias a las dos por vuestro apoyo incondicional todos estos años. A big thanks goes also to my friends from Barcelona **Sara**, **Alejandra** and **María**. Even though each of us is living in a different country, I feel you very close. Thanks for your absolute support, for encouraging me and believing in me. Cuquis, gracias.

Living abroad is an eye-opener in many aspects and has fulfilled my never-ending desire to explore and discover new frontiers. However, it made me also realise how important my own people are for me. There are no words to express my deepest gratitude and love to my family. **Mama i papa**, gràcies per haver-me donat la llibertat d'escollir, per la confiança infinita i per estar al meu costat, sempre. He sigut sempre una ànima lliure i ho heu sabut entendre i respectar. Heu sabut entendre també la meua necessitat de descobrir coses, d'anar més enllà i gràcies a això he arribat fins aquí. No us puc estar més agraïda per els valors que m'heu ensenyat i pel vostre exemple d'honestetat i treball. **Silvia i Carlos**, gràcies pel suport moral tots aquests anys, per fer que, encara en la distància, segueixi estan present a la vostra vida i a la d'**Arnau i Martí**. Gràcies per totes les abraçades de benvinguda i de despedida. Gracias totales a mi familia madrileña-castellonense-tucumana. **Miguel Ángel y Malena**, gracias por hacerme sentir una más en vuestra familia, a **Miguel, Sergio y Zayda**, gracias por todas las cenas, teatros improvisados, asados y paellas. Y a las primas **Camila, Lucía, Coni, Lola y Malena** por sus abrazos incondicionales.

Last year 2020 will be remembered by all due to the pandemic. It was an unforgettable year for a lot of people, also for me. Several important events happened that year in the middle of the fear and worry, amongst all we had the most amazing experience: becoming parents. **Olivia** brought us light with her permanent smile, giving meaning to our lives. T'estimem petita.

During the whole PhD I had the unconditional support of the best partner, husband, friend, cooker and now the best dad for our lovely daughter. **Simón**, gracias. Vinimos juntos a Leuven en busca de cumplir un sueño que parecía imposible y mira todo lo que hemos conseguido. Gracias por creer siempre en mí, por tu amor infinito. No podría estar más orgullosa de ti. Equipo.

# TABLE OF CONTENTS





# TABLE OF CONTENTS

Acknowledgments .....	7
Table of contents .....	11
Abbreviations .....	14
Hypothesis and Objectives .....	17
General introduction .....	23
<b>Section 1: Systematic Reviews</b> .....	41
Chapter 1: Regenerative potential of leucocyte- and platelet-rich fibrin. Part A. ....	43
Chapter 2: Regenerative potential of leucocyte- and platelet-rich fibrin. Part B. ....	64
<b>Section 2: In vitro studies</b> .....	82
Chapter 3: Characterization of the L-PRF membrane and L-PRF block .....	84
Chapter 4: Impact of g force and timing on the characteristics of PRF matrices .....	98
Chapter 5: Antimicrobial capacity of L-PRF against periodontal pathogens .....	115
Chapter 6: Particle release from silica-coated plastic tubes .....	128
<b>Section 3: In vivo study</b> .....	137
Chapter 7: Peri-implant bone structure at early healing after implant surface functionalization with L-PRF .....	139
<b>Section 4: Clinical study</b> .....	157
Chapter 8: Effect of different PRF matrices in ridge preservation after multiple tooth extractions .....	159
General discussion and Future perspectives .....	177
Summary .....	199
Samenvatting .....	203
Curriculum vitae .....	207
Acknowledgements and conflict of interest .....	213

# ABBREVIATIONS

---

ACD-A	adenosine-citrate-dextrose acid
ARP	alveolar ridge preservation
A. actynomicetemcomitans	Aggregatibacter actynomicetemcomitans
A-PRF	advanced platelet rich fibrin
A-PRF+	advanced platelet rich fibrin +
BIC	bone to implant contact
BMP	bone morphogenetic protein
BV/TV%	percentage of bone volume
C	carbon
CAF	coronally advanced flap
CBCT	cone beam computed tomography
CCT	controlled clinical trial
CAL	clinical attachment level
CTG	connective tissue graft
DBBM	demineralized bovine bone mineral
ELISA	enzyme-linked immuno sorbent assay
EMD	Emdogain®
F. nucleatum	Fusobacterium nucleatum
GBR	guided bone regeneration
GTR	guided tissue regeneration
IBDs	intraony defects
IL	interleukin
i-PRF	injectable platelet rich fibrin
K	potassium
KTW	keratinized tissue width
OFD	open flap debridement
PCs	Platelet concentrates
PD	pocket depth
PPP	platelet-poor plasma
PRF	platelet rich fibrin
PRGF	platelet rich in growth factors
PRP	platelet rich plasma
PDGF	platelet derived growth factor
PDWHF	platelet derived wound healing factors
PTH	parathyroid hormone
L-PRF	leucocyte-and platelet rich fibrin
L-PRP	leucocyte- and platelet rich plasma
O	oxygen
P. gingivalis	Porphyromonas gingivalis
P. intermedia	Prevotella intermedia
P-PRF	pure platelet rich fibrin
P-PRP	pure platelet rich plasma
RCF	relative centrifugal force

RCF <sub>av</sub>	average relative centrifugal force
RCF <sub>clot</sub>	relative centrifugal force at clot
RCF <sub>max</sub>	maximum relative centrifugal force
RCF <sub>min</sub>	minimal relative centrifugal force
RCT	randomized clinical trial
rpm	revolutions per minute
S	sulphur
SEM	scanning electron microscopy
SEM-EDX	scanning electron microscopy with energy dispersive X-Ray spectroscopy
SFE	sinus floor elevation
SiO <sub>2</sub>	silicon dioxide or silica
Tb.N	trabecular number
Tb.Pf	bone trabecular pattern
Tb.Sp	trabecular separation
Tb.Th	trabecular thickness
TGF- $\beta$	transforming growth factor beta
TF	tissue factor
TNF- $\alpha$	tumor necrosis factor alpha
VEGF	vascular endothelial growth factor





# HYPOTHESIS AND OBJECTIVES





# HYPOTHESIS AND OBJECTIVES

The objective of this PhD thesis was to characterize different PRF matrices and to examine their regenerative potential in several oral surgical procedures. The general hypothesis was that PRF products have a positive effect when used alone or as adjuvant in bone grafting. This hypothesis was divided in four subcategories: systematic reviews, *in vitro*, *in vivo*, and clinical studies. Each subcategory presented some specific sub-hypotheses. These are presented below together with their associated research questions (RQ).

## **Section 1: Systematic reviews (SR)**

**SR 1.1:** Regenerative potential of leucocyte- and platelet rich fibrin (L-PRF) in intrabony defects, furcation defects and periodontal plastic surgery.

**RQ 1.1:** Does L-PRF promote regeneration of periodontal tissues in systematically healthy patients (ASA I) during periodontal surgery compared to traditional techniques?

### **This RQ is addressed in:**

Section 1 (chapter 1), page 43-64

Material and Methods: systematic review

*Castro AB, Meschi N, Temmerman A, Pinto N, Lambrechts P, Teughels W & Quirynen M. Regenerative potential of leucocyte- and platelet-rich fibrin. Part A: intra-bony defects, furcation defects and periodontal plastic surgery. A systematic review and meta-analysis. Journal of Clinical Periodontology, 2017; 44(1): 67-82.*

**SR 2.1:** Regenerative potential of leucocyte- and platelet rich fibrin (L-PRF) in alveolar ridge preservation, sinus floor elevation and implant therapy.

**RQ 2.1:** Does L-PRF promote regeneration of periodontal tissues in systematically healthy patients (ASA I) during guided bone regeneration techniques and implant surgery compared to traditional techniques?

### **This RQ is addressed in:**

Section 1 (chapter 2), page 65-81

Material and Methods: systematic review

*Castro AB, Meschi N, Temmerman A, Pinto N, Lambrechts P, Teughels W & Quirynen M. Regenerative potential of leucocyte- and platelet-rich fibrin. Part B: sinus floor elevation, alveolar ridge preservation and implant therapy. A systematic review. Journal of Clinical Periodontology, 2017; 44(2): 225-234.*

## **Section 2: In vitro studies (IV)**

**IV 3.1:** Characterization of Leucocyte- and Platelet Rich Fibrin Block (L-PRF block): release of growth factors, cellular content, and structure.

**RQ 3.1:** Which are the biological properties of an L-PRF Block and its components in terms of growth factors release, cellular content, and structure?

**This RQ is addressed in:**

Section 2 (chapter 3), page 84-97

Material and Methods: in vitro study

*Castro AB, Cortellini S, Temmerman A, Li X, Pinto N, Teughels W & Quirynen M. Characterization of Leucocyte- and Platelet Rich Fibrin Block (L-PRF block): release of growth factors, cellular content, and structure. International Journal of Oral & Maxillofacial Implants. 2019; 34: 855-64.*

**IV 4.1:** The centrifuge type and the time before or after centrifugation do not have any influence on the characteristics of platelet concentrates.

**RQ 4.1:** Are the centrifuge type and time before or after centrifugation a key factor in the preparation of platelet concentrates?

**This RQ is addressed in:**

Section 2 (chapter 4), page 98-114

Material and Methods: in vitro study

*Castro AB, Andrade C, Li X, Pinto N, Teughels W & Quirynen M. Impact of g force and timing on the characteristics of platelet-rich fibrin matrices. Scientific Reports. 2021; 11: 6038.*

**IV 5.1:** L-PRF membrane and L-PRF exudate inhibit bacterial growth of the main periodontal pathogens when applied directly on a cultured agar plate or in planktonic form.

**RQ 5.1:** Does L-PRF membrane and L-PRF exudate have any antimicrobial effect against periodontal pathogens?

**This RQ is addressed in:**

Section 2 (chapter 5), page 115-127

Material and Methods: in vitro study

*Castro AB, Rodriguez EH, Slomka V, Pinto N, Teughels W & Quirynen M. Antimicrobial capacity of Leucocyte- and Platelet Rich Fibrin against periodontal pathogens. Scientific Reports. 2019; 9: 8188.*

**IV 6.1:** Silica microparticles cannot be found in PRF matrices and this is not affected by the centrifugation protocol.

**RQ 6.1.1:** Are silica microparticles present in PRF matrices when prepared with silica-coated plastic tubes?

**RQ 6.1.2:** Does the centrifugation protocol influence the detachment of the silica particles and their presence in PRF matrices?

**These RQ are addressed in:**

Section 2 (chapter 6), page 128-136

Material and Methods: in vitro study

*Castro AB, Andrade C, Teughels W & Quirynen M. Particle release from silica-coated plastic tubes and presence in PRF-matrices. In progress.*

**Section 3: In vivo study (VV)**

**VV 7.1:** Coating dental implants with L-PRF does not influence the peri-implant bone formation at early healing nor bone microstructure in a pig model.

**RQ 7.1.1:** Does the L-PRF coating increase the bone-to-implant contact during early healing (7 to 28 days) in an oversized preparation?

**RQ 7.1.2:** Does L-PRF coating influence the bone microstructure around implants in an oversized preparation?

**These RQ are addressed in:**

Section 3 (chapter 7), page 139-156

Material and Methods: animal study

*Castro AB, Cortellini S, Vasconcelos KF, Pamuk F, Duyck J, Jacobs R & Quirynen M. Peri-implant bone structure after implant surface functionalization with L-PRF at early healing: a micro-CT and histomorphological analysis. In progress.*

**Section 4: Clinical study (CL)**

**CL 8.1:** L-PRF and A-PRF used for alveolar ridge preservation have similar results as an undisturbed healing socket.

**RQ 8.1:** Does L-PRF or A-PRF better preserve the alveolar ridge after multiple tooth extractions compared to natural healing?

**This RQ is addressed in:**

Section 4 (chapter 8), page 159-176

Material and Methods: clinical study

*Castro AB, Van Dessel J, Temmerman A, Jacobs R & Quirynen. Effect of different platelet rich fibrin matrices for ridge preservation in multiple tooth extractions: a split-mouth randomized controlled clinical trial. Journal of Clinical Periodontology. 2021; 48: 984-995.*



GENERAL INTRODUCTION







# GENERAL INTRODUCTION

## 1. Blood composition

Human blood represents about 8% of the total body weight. It is formed in the bone marrow and consists of two basic components: plasma (about 55%), and formed elements (about 45%). Plasma is the liquid portion of blood and about 90% is water. It contains many dissolved substances and three types of formed elements: white blood cells, red blood cells, and platelets (Table 1). The white blood cells account for less than 1% of the total blood volume, the red blood cells for 40-45%, and the platelets, which actually are not cells but rather small fragments of cells called thrombocytes, account for less than 1% of the total blood volume (1, 2).








Formed element	Major subtypes	Description	Number present per microliter and mean range	Summary of functions
Erythrocytes (red blood cells) 		red-colored Ø 7-8 µm	5.2 million (4.4 – 6.0 million)	Transport oxygen and carbon dioxide between tissues and lungs
Leucocytes (white blood cells)			7000 (5000 – 10,000)	All functions in body defences
		<b>Granulocytes</b>		
		Neutrophils 	multilobed nucleus Ø 10-12 µm	4150 (1800 – 7300) Phagocytosis of bacteria and debris Release of cytotoxic chemicals
		Eosinophils 	bilobed nucleus Ø 10-14 µm	165 (0 – 700) Phagocytic cells, release antihistamines
		Basophils 	lobed nucleus Ø 10-14 µm	44 (0 – 150) Promote inflammation
		<b>Agranulocytes</b>		
		Lymphocytes 	spherical/indented nucleus Ø 5-17 µm	2200 (1500 – 4000) Primarily specific immunity: T cells directly attack other cells (cellular immunity); B cells release antibodies (humoral immunity); natural killers
		Monocytes 	U shape/kidney shaped Ø 14-24 µm	455 (200 – 950) Produced in bone marrow (macrophages after leaving circulation) Very effective phagocytic cells of pathogens, also serve as antigen-presenting cells for other components of the immune system
Platelets 			350,000 (150,000 – 500,000)	Haemostasis and release growth factors for repair and tissue healing

Table 1. Characteristics of each blood cell.

## 2. Wound healing

Wound healing is a complex biological process. When an injury occurs, a regulated sequence of biochemical events starts to repair the damage. It consists of four phases: (1) haemostasis, (2) inflammation, (3) proliferation, and (4) remodelling. The haemostasis phase starts immediately after damage with vascular constriction and fibrin clot formation. One of the key cells during this phase are the platelets, a well-known regulator of haemostasis (3). The inflammatory phase begins right after, and during this process a dynamic interaction occurs among endothelial cells, angiogenic cytokines, and the extracellular matrix. Different cell types, including neutrophils, macrophages, lymphocytes, platelets, fibroblasts, and endothelial cells are involved in this process. Platelets release cytokines and growth factors that further attract macrophages and neutrophils to the defect sites to remove debris, necrotic tissue, and bacteria from the wound. The proliferative phase begins around day 3 when the blood clot within the wound is replaced by a provisional matrix. The final phase, the remodelling, begins 2 to 3 weeks after injury and lasts for a year or more. During this stage, all the processes activated after injury dramatically diminish and finally stop. Most of the endothelial cells and macrophages undergo apoptosis or leave the wound (3) (4).

The survival of an organism relies on its ability to repair the damage caused by toxic agents and inflammation. Tissue repair occurs by two types of reactions: (1) regeneration by proliferation of remaining cells and maturation of the tissue, or (2) the deposition of connective tissue to form a scar. The regeneration of injured tissue involving cell proliferation and differentiation is driven by growth factors and is critically dependent on the organization of the extracellular matrix. Several cell types proliferate during tissue repair. These include, firstly, the remaining cell in the injured tissue that attempt to restore normal structure. Secondly, vascular endothelial cells necessary to create new vessels to provide the nutrients required for the repair process. Finally, the fibroblasts that are the source of the fibrous tissue that will fill the defects that cannot be improved by regeneration (5).

Angiogenesis, new blood vessel formation from existing vessels, is also critical in tissue repair. The process of angiogenesis involves several signalling pathways, cell-to-cell communication, interaction between proteins from the extracellular matrix, and tissue enzymes. Vascular endothelial growth factor (VEGF) plays an important role in the initiation of this process (5). It stimulates both migration and proliferation of endothelial cells and thus initiates the process of capillary sprouting. Other growth factors, such as platelet-derived growth factor (PDGF) and transforming growth factor beta (TGF- $\beta$ ), also participate in this process by recruiting smooth muscle cells and enhancing the production of extracellular matrix proteins (6).

Cell proliferation is determined by signals provided by the extracellular matrix and growth factors. Growth factors are normally produced by cells near to the injured area. The most important source of growth factors are macrophages that are activated after tissue injury. Macrophages are cells derived from hematopoietic stem cells that when circulating in blood are known as monocytes. Macrophages are specialised in phagocyte micros and senescent cells, but they serve many other roles in inflammation and repair. In inflammatory reactions, progenitors in the bone marrow produce monocytes that enter the blood and into various tissues and differentiate into macrophages. There are two major pathways for macrophage activation. The classical activation, that may be induce by an external danger (M1), and the alternative activation that is produced by T lymphocytes (M2) (7). These macrophages are not actively microbicide; instead, the function of alternatively activated

macrophages (M2) is tissue repair (8). They secrete growth factors that promote angiogenesis, activate fibroblast, stimulate collagen synthesis and promote osteogenic mineralisation during in vitro studies (9). Although the concept of M1 and M2 macrophages provides a useful framework for understanding macrophage heterogeneity, numerous other subpopulations have also been described. Although the products of activated macrophages eliminate damaging agents and initiate the process of repair, they are also responsible for part of the tissue injury in chronic inflammation. Likewise, epithelial and stromal cells should also be taken into account as they can produce some of these growth factors.

### 3. Coagulation cascade and tissue healing

Blood clotting is a process by which blood changes from a liquid to a insoluble clot. This involves the activation, adhesion, and aggregation of platelets and the deposition and maturation of a fibrin mesh. The coagulation cascade is a sequence of proteolytic events mainly localized on the surface of activated platelets. Once platelets are triggered by being exposed to damaged endothelium, they release mediators such as P-selectin and von Willebrand factor that promote microvesicle formation and platelet adherence. The microvesicles attached to the activated platelet membrane promote the production of tissue factor and its ligand, factor VIIa. Clotting factors bind to adjacent receptors on the membrane, enabling the proteolytic cascade, culminating in thrombin generation (10). Briefly, factor X is cleaved by VIIa to form factor Xa. Prothrombin on the activated platelet surface is converted to thrombin by Xa (Va and calcium ions are cofactors for the reaction). However, little amounts of thrombin are formed by this pathway during the initiation phase of coagulation. The trace amounts of thrombin generated during the initiation phase provide further activation of platelets, factor V, and factor XI. Larger amounts will be generated during the amplification phase (11, 12).

The formation of a complex comprising factors VIIIa, IXa, and calcium ions on the platelet surface, leads to the large-scale generation of factor Xa. Factor Xa, with factor Va and calcium ions, forms the prothrombinase complex that produces the burst of thrombin needed for the conversion of fibrinogen to fibrin. Furthermore, thrombin activates factor XIII, resulting in clot stabilization, and the thrombin-activatable fibrinolysis inhibitor, which modulates fibrinolysis (10). This is known as the common pathway (Figure 1).

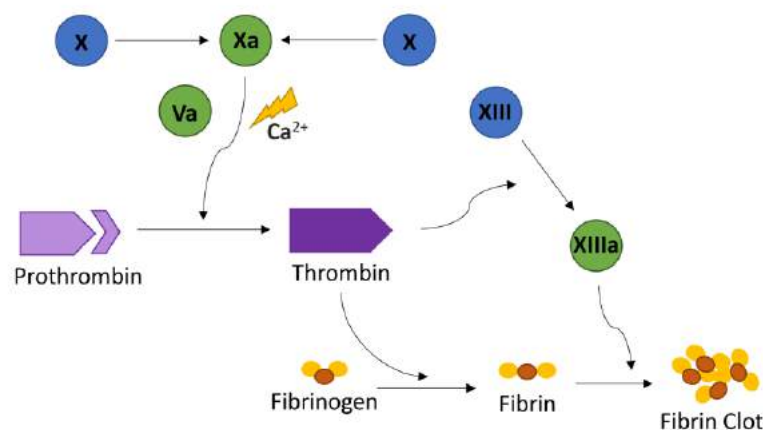


Figure 1. Coagulation cascade: common pathway.

Two major pathways exist for triggering the blood clotting cascade, known as the tissue factor pathway (extrinsic) and the contact activation pathway (intrinsic).

### Extrinsic (tissue factor) pathway

The tissue factor pathway is named for the protein that triggers it: the tissue factor (TF), a cell-surface integral-membrane protein. This pathway is also called the extrinsic pathway because it requires that plasma has contact with something “extrinsic” to trigger it. The TF pathway is the mechanism of triggering blood clotting that functions in normal haemostasis, and probably also in many types of thrombosis. Thus, when cells expressing TF are exposed to blood, this event immediately triggers the clotting cascade (Figure 2). When the circulating factor VII comes into contact with the TF, they form an activated complex TF-VIIa that activates factor X. From here the common pathway starts.

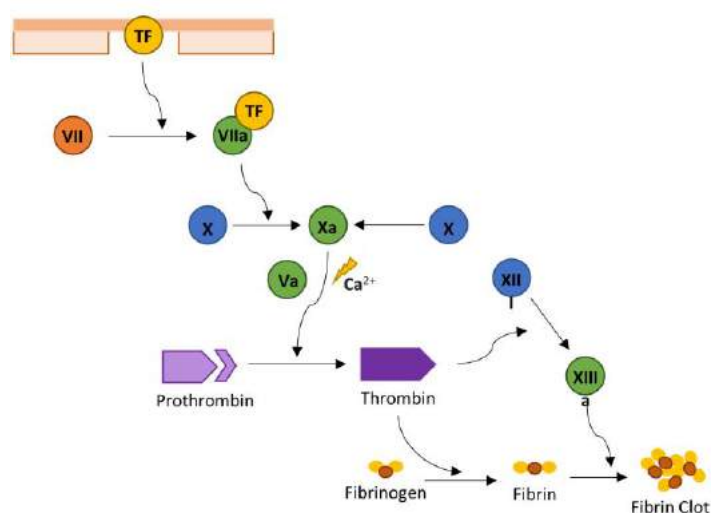


Figure 2. Blood clotting triggering by the extrinsic pathway. (Image from article Smith et al., 2015 (13))

### Intrinsic or contact activation pathway

The contact pathway of triggering blood clotting has also been termed the intrinsic pathway, since it can be triggered without adding a source of TF to the blood or plasma. This pathway is actually triggered when plasma is exposed to certain types of artificial surfaces (Figure 3). For instance, glass tubes or negatively charged artificial surfaces (i.e. silica coated) are especially good activators of the contact pathway. While this pathway does not contribute to normal haemostasis, it is thought to participate in thrombotic diseases (13, 14).

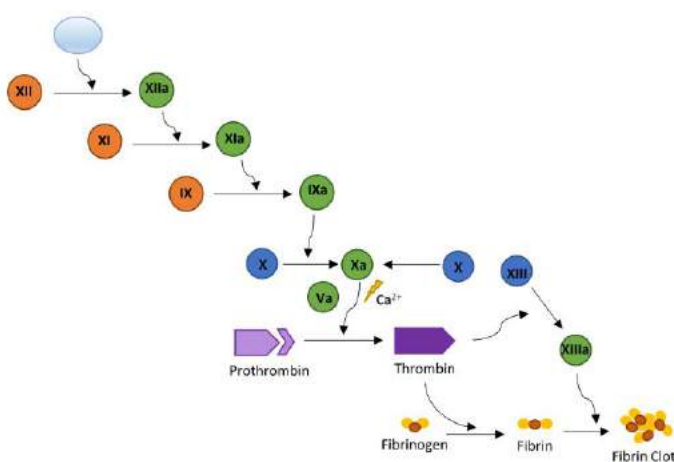


Figure 3. Blood clotting triggering by the intrinsic pathway. (Image from article Smith et al., 2015) (13)

### Fibrin formation

Fibrinogen is a glycoprotein made and secreted into blood primarily by liver hepatocyte cells. After tissue and vascular injury, it is enzymatically converted by thrombin into fibrin. This fibrin is an essential component of a blood clot, which primary function is to occlude blood vessels to stop bleeding. Mature fibrinogen is a long flexible protein array of three nodules: two end nodules (termed D regions or domains) and a slightly smaller nodule (termed the E region or domain) in the centre. The length of a dried fibrinogen molecule is  $475 \pm 25$  Å.

Stimulus of the coagulation cascade ultimately produces the transformation of fibrinogen into fibrin monomers by the cleavage of 2 small fragments (fibrinopeptides A and B, small blue cycles in Figure 4) from the molecule by thrombin. During this process, the negative charge of the E domain of fibrinogen (orange circle) is converted to a positive charge, permitting spontaneous polymerization of the fibrin monomers into a polymer stabilized by hydrogen bonds. Thrombin and factor XIII stabilize the initial fibrin polymer by catalysing the formation of cross-linked covalent bonds between adjacent D domains.

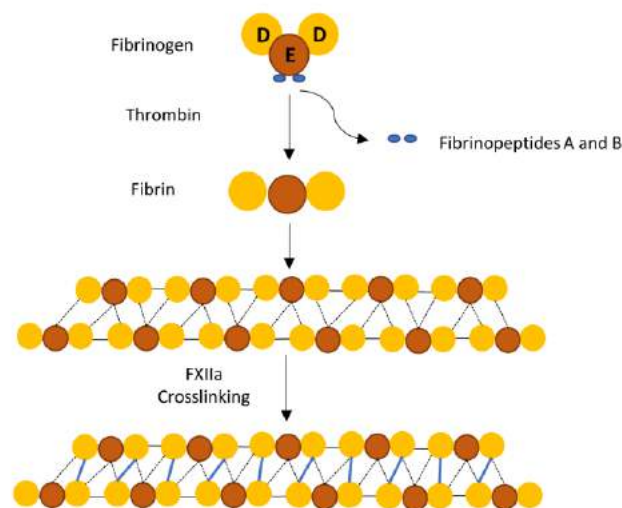


Figure 4. Process of fibrin formation. Fibrinogen is converted into fibrin by thrombin. After the spontaneous formation of a polymer stabilized by hydrogen bonds (dotted line), cross-covalent bonds appear between adjacent D domains (blue bold line) for the crosslinking of the fibrin. (Image from article Smith et al., 2015) (13)

## 4. From fibrin glue to the 1<sup>st</sup> generation of platelet concentrates

The use of autologous blood products to enhance tissue healing started with the reports of Matras and co-workers in 1970 (16). They introduced the concept of platelet concentrates (PCs) by using fibrin glue (fibrin sealers) to improve skin wound healing. Platelet concentrates are blood extracts obtained after various processing of a whole blood sample, through centrifugation. Fibrin sealers were the derivatives of human plasma that mimicked the last steps in the process of blood coagulation by the formation of a fibrin clot. The main action of these fibrin sealers was to stimulate local angiogenesis, to minimize oedema or hematoma formation, and to reduce post-operative pain. The fibrin matrix was the main component of fibrin sealers. The properties of this matrix were determined by interactions between the circulating fibrinogen, platelet aggregation and molecules produced by the platelets. Further research led to an upgraded version of the sealers, called "Platelet Derived Wound Healing

Factors" (PDWHF). This group of sealers contained a significant concentration of platelets, to strengthen the fibrin gel and simultaneously promote the healing capacities.

However, it was not until Marx's studies (15, 16) that the use of PCs also gained interest in the oral and maxillofacial field. Since then, different techniques have been developed and with them, a variety of preparations. The first PCs generation include platelet-rich plasma (PRP) and plasma rich in growth factors (PRGF). Their preparation requires anticoagulants at the moment of blood collection to avoid coagulation during centrifugation and the addition of a coagulate activator at a later stage for fibrin polymerization (Table 2). Consequently, the fibrin polymerization occurs rapidly, resulting in a weak fibrin network (17). The preparation is quite complex. Briefly, 27 mL of blood is collected in a 30-mL syringe containing 3 mL of adenosine-citrate-dextrose acid (ACD-A) anticoagulant. The content of the syringe is transferred into the 30-mL separation tube and centrifuged for 15 minutes (1900xg) at room temperature. After removing the plasma, the buffy coat is re-suspended in the leftover plasma by shaking the tube for 30 seconds. A second syringe containing 1 mL of ACD-A is used to collect an additional 11 mL of blood, which is transferred into a Clotallyst disposable tube (Biomet Inc) containing 4 mL thrombin. After gentle mixing, the tube is placed into a Clotallyst disposable tube heater for 25 minutes. Subsequently, the mix is centrifuged for 5 minutes at 1900 x g. Coagulation is performed using a double syringe (spray applicator), allowing uniform mixing of the two components that results in the formation of a clot. The time between centrifugation and clinical use is  $\pm 45$  min.

The benefits of using PRP in medicine have been extensively studied. Most reviews are found within the field of orthopaedics and sports medicine (18, 19). According to a recent meta-analysis (20), the intra-articular injection of PRP in patients with osteoarthritis of the knee is beneficial. However, results are not conclusive (21). Within oral and maxillofacial surgery, PRP is particularly used after extraction of 3<sup>rd</sup> molars (22), in the treatment of periodontal intra-bony defects (23), in sinus elevation techniques (24) and for hard and soft tissue augmentation (25). The purpose of using PRP in these types of surgeries was to accelerate the vascularization of the graft, to improve soft tissue healing and bone regeneration and to reduce post-operative morbidity. However, results remained inconclusive.

	Process				Cellular content		Fibrin matrix	
	Centrifugation	Additives	Duration	Simplicity	Platelets	Leucocytes	Density	Polymerization
<i>1<sup>st</sup> generation</i>								
<b>PRP</b>	2x + pipetting	Yes	30-45 min	-	Medium	Yes/No	Weak	Fast
<b>PRGF</b>	1x + pipetting	Yes	20-25 min	-	Low	No	Weak	Fast
<i>2<sup>nd</sup> generation</i>								
<b>PRF</b>	1x	No	10-12 min	+	High	Yes/No	Strong	Slow

Table 2. Description of platelet concentrates (PCs) characteristics. PRP: platelet rich plasma; PRGF: platelet rich in growth factors; PRF: platelet rich fibrin.

To improve its efficacy, the preparation protocol for this platelet concentrate has been changed and adapted several times over the years. A well-known example is "Platelet Rich Growth Factors" (PRGF), which was first described by Anitua and co-workers (26). PRGF differs from other platelet concentrates in its versatility. Depending on the degree of coagulation and activation of the blood, different types of preparations with a different therapeutic potential were obtained (as a liquid substance and a dense or elastic fibrin). Research showed that PRGF may be used as a treatment modality for osteoarthritis (27), treatment of ulcers (28), tissue engineering and oral surgery (29, 30). However, the results should be interpreted with some precaution.

Overall, we can say that there is a shortage of critical scientific data on the positive effects of PRP in clinical procedures. There is a great variability in study designs (small groups of patients, no control groups), but also in preparation protocols without clear classification, which makes a comparison difficult. Furthermore, it is important to note that the use of PRP has a number of significant disadvantages: the preparation protocol is expensive, complicated, operator sensitive, and the need for animal thrombin as a coagulant rises legal issues in some countries (31).

## 5. 2<sup>nd</sup> generation of platelet concentrates: Platelet rich fibrin (PRF)

Due to the difficulties in the preparation and the inconsistent outcome of PRP and PRGF formulations, a second PCs generation was introduced in 2001 (17, 32) (Table 2). The use of platelet-rich fibrin (PRF) is simple and requires neither anticoagulant, bovine thrombin nor calcium chloride. In this case, the whole blood is centrifuged without anticoagulants at high spin using glass tubes or silica-coated tubes so that three layers are obtained: red blood corpuscles (RBCs) at the bottom of the tube, platelet-poor plasma (PPP) on the top and an intermediate layer called "buffy coat" where most leucocytes and platelets are concentrated. According to the literature, PRF accelerates neoangiogenesis (33), stimulates the local environment for differentiation and proliferation of surrounding cells (34), and continuously releases growth factors over a period of 7-14 days (35).

In 2014, a new classification was published dividing the platelet concentrates into four categories depending on the leucocyte inclusion and their architecture (36):

- No leucocyte inclusion + low density fibrin matrix: Pure platelet rich plasma (P-PRP).
- No leucocyte inclusion + high density fibrin matrix: Pure platelet rich fibrin (P-PRF).
- Leucocyte inclusion + low density fibrin matrix: Leucocyte and platelet rich plasma (L-PRP).
- Leucocyte inclusion + high density fibrin matrix: Leucocyte and platelet rich fibrin (L-PRF).

Due to the poor standardization of the manual process of PRP formulations as well as the use of exogenous agents (anticoagulants, bovine thrombin and calcium chloride), the use of L-PRF increased exponentially.

### 5.1. Leucocyte and platelet rich fibrin (L-PRF): preparation protocol

Leucocyte and platelet rich fibrin is an autologous fibrin matrix containing platelets and leucocytes obtained after blood centrifugation. Blood samples are collected in 9-10 ml sterile glass or silica-coated plastic tubes. The tubes are immediately placed in pairs in the centrifuge and centrifuged at 408 g ( $R_{CF_{clot}}$ ) for 12 minutes (Figure 5). There is no chemical manipulation of the blood.

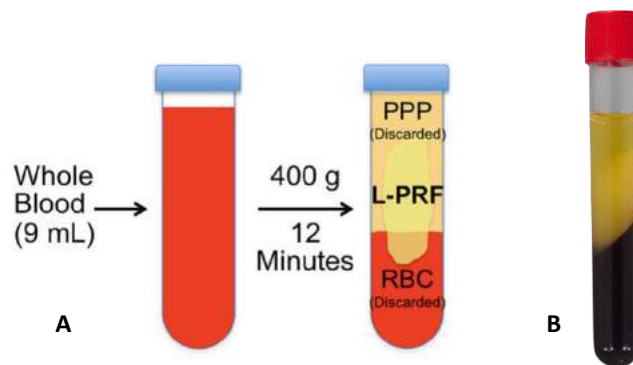


Figure 5. L-PRF preparation. A. L-PRF tube after centrifugation, with its 3 compartments (drawing from Schär et al. 2015). B. Real view of a tube after the preparation of L-PRF.

The loading of the centrifuge should be performed two by two to ensure the balance during centrifugation. In case that there would be only one tube, a tube filled with the same amount of glycerine or saline should be used (Figure 6). Blood collection is performed always in pairs (2 tubes). When the first and the second tube are filled, they are immediately placed in the centrifuge and centrifuged. At this moment, the third tube starts to get filled. As soon as the fourth tube is half-filled, the centrifuge should be stopped and while the centrifugation is stopping, this last tube is finally fully filled. Then, tubes 3 and 4 are placed in balance inside the device and all four tubes are centrifuged. The same sequence is repeated for tubes 5 and 6.

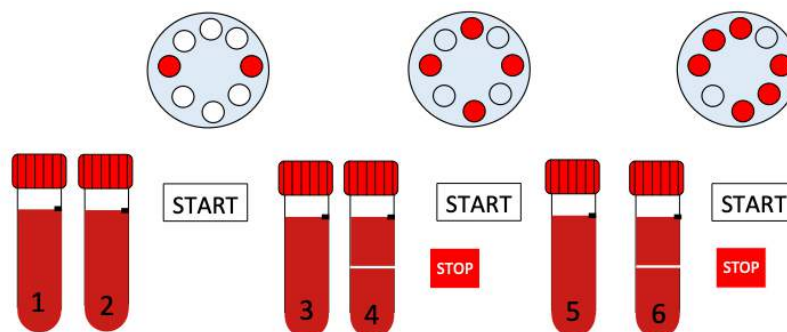


Figure 6. Blood collection sequence for six tubes and loading of the centrifuge.

After centrifugation the L-PRF clot can be collected from the tube with surgical tweezers. With an instrument, similar to a spatula, the red blood cell fraction can be gently separated from the fibrin clot (Figure 7). The clot by itself contains a great amount of exudate (the L-PRF exudate). By gentle compression using a specific box designed for this purpose, the L-PRF clot can be transformed into a 1-mm thick membrane.





Figure 7. Protocol to prepare L-PRF clots and membranes. A: three layers can be found in the tubes after centrifugation: platelet-poor plasma (top), L-PRF clot (middle) and red blood cells (bottom); B: careful removal of clot from the tube; C: L-PRF clot; D: L-PRF membrane after compression; E: L-PRF membrane.

This special engineered box (Figure 8) contains a weighted press plate designed to express exudate from the L-PRF clot in a controlled manner. It forms standard 1 mm thick L-PRF membranes (Figure 1). One can also compress the clots into different shapes, such as a cylinder form (L-PRF plugs). The L-PRF constructs (membranes/plugs) remain stable at room temperature for several hours, if one can prevent them to dry out.

Figure 8. Especially designed kit to compress L-PRF clots into L-PRF membranes with a consistent thickness of 1 mm. A piston (left top) and cylinder assembly (in white) can be used for the creation of L-PRF plugs.



## 5.2. Principles of blood centrifugation

A centrifuge is a device that creates a centrifugal force for separating substances of different densities in a liquid by rotating at a certain speed (measured as revolutions per minute, RPM). The force applied during centrifugation is called relative centrifugal force (RCF) (37). It causes denser substances and particles to move outward in the radial direction. Denser particles thus settle at the bottom of the tube, while low-density substances move to the top (38).

The final composition of the L-PRF constructs depends on several factors including: the time of spinning, the speed (rotation/revolutions per minute, RPM) and the  $g$  force (RCF), as illustrated by the following formula:

$$RCF = 11.18 \times r \times (N/1000)^2.$$

For this equation,  $r$  is the radius in centimetres of the centrifuge and  $N$  is the rotor speed in RPM. During centrifugation of blood with a fixed-angle centrifugation device, cells are pushed towards the back of the tube and then downwards based on their density. The separation occurs at a certain angle, which corresponds to the fixed angle at which the tubes rotate. There exist three locations to calculate the RCF with a rotor with fixed angle: the minimal RCF ( $RCF_{\min}$ ) at the top of the tube (shortest distance to the rotor axis), the average RCF ( $RCF_{\text{av}}$  or  $RCF_{\text{clot}}$ ) in the middle, and the maximum RCF ( $RCF_{\max}$ ) at the largest distance to the rotor axis (39, 40).

The original L-PRF protocol foresees an  $RCF_{\text{clot}}$  of 408 g for 12 minutes. These settings can be completely different for other centrifuges due to, for example, differences in rotor diameter and/or rotor angulation (39, 40). Moreover, in vitro studies reported significant differences between centrifuges due rotor radial vibration (41). A stable positioning of the centrifuge on an immobile table is thus crucial.

### 5.3. General characteristics of L-PRF matrices

#### Platelets in L-PRF

After centrifugation,  $\geq 80\%$  of the platelets present in the blood sample will be collected in the fibrin clot (42). The platelets are mainly present in the lower portion of the clot, at the border between the red blood cells and the clot itself. As a result, the lower portion of the clot (with a red colour due to some remaining red blood cells), also called “the face”, is considered to be the most biologically active.

The platelet-cytoplasm contains several granules (43). The content is released at the time of activation. These granules contain many cytokines and substances like serotonin, von Willebrand factor, factor V, osteonectin and anti-microbial proteins. When platelets come in contact with the collagen of a damaged blood vessel or the inner wall of blood tubes (glass or silica-coated), they become activated. This activation is necessary for platelet aggregation and as such starts and maintains the haemostasis. Activation of the platelets involves degranulation and sequentially the release of various cytokines. They will stimulate cell migration and proliferation into the fibrin matrix.

The principal role of the platelets is the maintenance of homeostasis. However, they are also capable of binding, aggregating and internalizing microorganisms, which enhances the clearance of pathogens from the bloodstream. Platelets participate in antibody-dependent cell cytotoxicity functions to kill protozoal pathogens as well as to release an array of potent antimicrobial peptides (43, 44).

#### Leucocytes in L-PRF

Leucocytes are the other main cell type present in L-PRF. Dohan and co-workers (42) analysed the cellular content of L-PRF membranes and concluded that more than 50% of the leucocytes are concentrated in the fibrin matrix. The presence of leucocytes in platelet concentrates is of great importance. Leucocytes have potential antibacterial characteristics but can also regulate cell proliferation and cell differentiation. In addition, they are the basic cells responsible for the wound healing process and the first cells to start the neoangiogenesis. In fact, they contain vascular endothelial growth factor (VEGF) that acts as a potent vascular growth factor. Leucocytes also play a role as immune regulator via the secretion of key immune cytokines such as interleukin-1 $\beta$ , IL-6, IL-4, and tumor necrosis factor alpha (TNF- $\alpha$ ).

Neutrophils are recruited to the site of injury within minutes following trauma, and are the hallmark of acute inflammation. They migrate towards the damaged site and become embedded in the fibrin network, in order to form a dense barrier against pathogens and prevent infection. Their main function is the production of inflammatory cytokines and growth factors (26).

Monocytes are the largest type of leucocytes and can differentiate into macrophages; playing a central role in the healing. They have immunological functions as antigen presenting cells and phagocytes.

Macrophages have been implicated in the inflammation processes. However, they also play an essential role in bone repair. The role of the monocytes and macrophages in bone repair has become an area of increased interest in the recent years. Macrophages apparently direct osteogenic cells signals and promote mineralization during in vitro studies (9). During bone injury, monocytes and macrophages modulate the acute inflammatory response, produce growth factors such as BMP-2 and PDGF-BB, and induce osteogenesis in mesenchymal stem cells (8, 45).

Macrophages secrete collagenase, which promotes the cleaning of the wound. Additionally, they are a source of growth factors such as Transforming Growth Factor (TGF), which stimulates the keratinocytes and Platelet-Derived Growth Factor (PDGF) that plays an important role in the angiogenesis. Granulocytes and macrophages promote the production of inflammatory mediators such as leukotriene B4 and platelet activating factor that stimulates the expansion and increased permeability of blood vessels as well as the production of inflammatory cytokines and proteolytic enzymes. These factors also act on the endothelial cells of the blood vessels, stimulating the adhesion of neutrophils and lymphocytes and their migration out of blood vessel (Anitua et al. 1999).

Despite the release of activated oxygen species (free radicals) from leucocytes during phagocytosis activity and the ischemia reperfusion process, it seems that the inclusion of leucocytes in the blood derivatives like L-PRF may play beneficial role (46).

#### Fibrin in L-PRF

Fibrin is an insoluble clotting protein, which plays a major role in platelet aggregation during haemostasis and wound healing. Fibrinogen, the precursor of fibrin, is converted by thrombin into fibrin, which forms long non-soluble strands that bind to platelets. Present in physiological concentrations, thrombin allows the formation of a fibrin matrix in a slow and physiological manner. The fibrin wires tend to polymerize and form a biochemical structure with tri-molecular or equilateral junctions providing a fine and flexible fibrin-network, favouring the entrapment of cytokines and cell migration. This three-dimensional network has an important function as a matrix, promoting the invasion of various types of inflammatory, endothelial and other cells. This matrix is also able to capture glycosaminoglycans (originating from the blood platelets). These glycosaminoglycans have a high affinity for circulating peptides (such as cytokines) and a large capacity to support cell migration and the healing processes (Dohan et al. 2006a). The three-dimensional fibrin matrix present in the L-PRF serves as a scaffold for the cells entrapped in it but also for the growth factors produced by these cells, resulting in a slow and gradual releasing rate.

## 6. New protocols

Recently, new PRF protocols [advanced platelet rich fibrin (A-PRF) and advanced platelet rich fibrin+ (A-PRF+)] have been proposed reducing the relative centrifugal force and duration of the centrifugation (Table 3) (47, 48). By reducing the relative centrifugal force (the low-speed centrifugation concept), an increase in the release of growth factors and in the concentration of leucocytes and platelets was envisaged. Theoretically, less centrifugation time would reduce pull-down forces during centrifugation, which would increase the total number of cells contained within the L-PRF clot. Ghanaati and co-workers (48) reported a higher concentration of cells at the red part of the L-PRF clot (face, part in contact with the red blood cells) compared to A-PRF where the cells were distributed throughout the clot. The same group of researchers formulated another PRF preparation

called A-PRF+, reducing even more the g-force and the duration of centrifugation (207 g, 8 min). They claimed a significantly higher release of growth factors after 10 days as well as greater migration of human gingival fibroblasts to the A-PRF and A-PRF+ compared to L-PRF. In 2019, Miron and co-workers introduced a new protocol with horizontal centrifugation (49). They also reported an even higher concentration of cells compared to L-PRF and A-PRF. However, the clinical relevance of these difference centrifugation protocols still needs to be demonstrated in clinical studies.

	DEVICE	TUBE	SETTING			INTRODUCED BY
			rpm	time	RCF <sub>clot</sub>	
solid PRF matrices						
L-PRF	Intra-Lock, USA	Plastic-coated	2700	12 min	408 g	Choukroun et al. 2001 (32)
A-PRF	Process for PRF, France	Glass	1500	14 min	276 g	Ghanaati et al. 2014 (48)
A-PRF+	Process for PRF, France	Glass	1300	8 min	208 g	Fujjoka-Kobayashi et al. 2017 (50)
H-PRF	Eppendorf	Glass	-	8 min	700 g	Miron et al. 2019 (49)
liquid PRF matrices						
Liquid Fibrinogen	Intra-Lock, USA	Plastic-coated	2700	3 min	408 g	Cortellini et al. 2018 (51)
i-PRF	Process for PRF, France	Glass	700	3 min	60 g	Choukroun et al. 2018 (52)

Table 3. Platelet rich fibrin constructs prepared with the centrifuge Process for PRF, Nice, France, (DUO)] and the Intra-Spin centrifuge [Intra-Lock, Boca Raton, Florida, USA, (IL)].

The development of the liquid PRF formulation allowed the easy combination with bone substitutes to create stronger constructs. The liquid fibrinogen, prepared with the same *g* force as for L-PRF but reducing the time (3 min), was used to prepare the L-PRF block (51). This block has been used for horizontal bone regeneration or in sinus floor elevations. It combines the properties of bone blocks and particulated grafts, reducing the disadvantages of both.

On the other hand, injectable-PRF (i-PRF) was also introduced for the same purpose. i-PRF demonstrated the ability to release higher concentrations of various growth factors and induced higher fibroblast migration and expression of PDGF, TGF- $\beta$ , and collagen than PRP (53).

## References

1. Betts GYKAW, J. A.; Johnson, E.; Poe, B.; Kruse, D. H.; Korol, O.; Johnson, J. E.; Womble, M.; DeSaix, P. *Anatomy and Physiology*. 4th ed 2017.
2. Mader S. *Laboratory Manual for Human Biology*. 14 ed 2015.
3. Gurtner GC, Werner S, Barrandon Y, Longaker MT. Wound repair and regeneration. *Nature*. 2008;453(7193):314-21.
4. Guo S, Dipietro LA. Factors affecting wound healing. *J Dent Res*. 2010;89(3):219-29.
5. Kumar V, Abbas A. K., Aster, J. *Robbins Basic Pathology*, 10th Edition. 10th ed 2018 2018. 952 p.
6. Morgan C, Nigam Y. Naturally derived factors and their role in the promotion of angiogenesis for the healing of chronic wounds. *Angiogenesis*. 2013;16(3):493-502.
7. Winkler IG, Sims NA, Pettit AR, Barbier V, Nowlan B, Helwani F, et al. Bone marrow macrophages maintain hematopoietic stem cell (HSC) niches and their depletion mobilizes HSCs. *Blood*. 2010;116(23):4815-28.
8. Champagne CM, Takebe J, Offenbacher S, Cooper LF. Macrophage cell lines produce osteoinductive signals that include bone morphogenetic protein-2. *Bone*. 2002;30(1):26-31.
9. Chang MK, Raggatt LJ, Alexander KA, Kuliwaba JS, Fazzalari NL, Schroder K, et al. Osteal tissue macrophages are intercalated throughout human and mouse bone lining tissues and regulate osteoblast function in vitro and in vivo. *J Immunol*. 2008;181(2):1232-44.
10. Green D. Coagulation cascade. *Hemodial Int*. 2006;10 Suppl 2:S2-4.
11. Monkovic DD, Tracy PB. Functional characterization of human platelet-released factor V and its activation by factor Xa and thrombin. *J Biol Chem*. 1990;265(28):17132-40.
12. Hoffman M, Monroe DM, 3rd. A cell-based model of hemostasis. *Thromb Haemost*. 2001;85(6):958-65.
13. Smith SA, Travers RJ, Morrissey JH. How it all starts: Initiation of the clotting cascade. *Crit Rev Biochem Mol Biol*. 2015;50(4):326-36.
14. Nossel HL. Differential consumption of coagulation factors resulting from activation of the extrinsic (tissue thromboplastin) or the intrinsic (foreign surface contact) pathways. *Blood*. 1967;29(3):331-40.
15. Marx RE, Carlson ER, Eichstaedt RM, Schimmele SR, Strauss JE, Georgeff KR. Platelet-rich plasma: Growth factor enhancement for bone grafts. *Oral Surg Oral Med Oral Pathol Oral Radiol Endod*. 1998;85(6):638-46.
16. Marx RE. Platelet-rich plasma (PRP): what is PRP and what is not PRP? *Implant Dent*. 2001;10(4):225-8.
17. Dohan DM, Choukroun J, Diss A, Dohan SL, Dohan AJ, Mouhyi J, et al. Platelet-rich fibrin (PRF): a second-generation platelet concentrate. Part I: technological concepts and evolution. *Oral Surg Oral Med Oral Pathol Oral Radiol Endod*. 2006;101(3):e37-44.
18. Houck DA, Kraeutler MJ, Thornton LB, McCarty EC, Bravman JT. Treatment of Lateral Epicondylitis With Autologous Blood, Platelet-Rich Plasma, or Corticosteroid Injections: A Systematic Review of Overlapping Meta-analyses. *Orthop J Sports Med*. 2019;7(3):2325967119831052.
19. Shen L, Yuan T, Chen S, Xie X, Zhang C. The temporal effect of platelet-rich plasma on pain and physical function in the treatment of knee osteoarthritis: systematic review and meta-analysis of randomized controlled trials. *J Orthop Surg Res*. 2017;12(1):16.

20. Campbell KA, Saltzman BM, Mascarenhas R, Khair MM, Verma NN, Bach BR, Jr., et al. Does Intra-articular Platelet-Rich Plasma Injection Provide Clinically Superior Outcomes Compared With Other Therapies in the Treatment of Knee Osteoarthritis? A Systematic Review of Overlapping Meta-analyses. *Arthroscopy*. 2015;31(11):2213-21.
21. Lai LP, Stitik TP, Foye PM, Georgy JS, Patibanda V, Chen B. Use of Platelet-Rich Plasma in Intra-Articular Knee Injections for Osteoarthritis: A Systematic Review. *PM R*. 2015;7(6):637-48.
22. Barona-Dorado C, Gonzalez-Regueiro I, Martin-Ares M, Arias-Irimia O, Martinez-Gonzalez JM. Efficacy of platelet-rich plasma applied to post-extraction retained lower third molar alveoli. A systematic review. *Med Oral Patol Oral Cir Bucal*. 2014;19(2):e142-8.
23. Dori F, Arweiler N, Huszar T, Gera I, Miron RJ, Sculean A. Five-year results evaluating the effects of platelet-rich plasma on the healing of intrabony defects treated with enamel matrix derivative and natural bone mineral. *J Periodontol*. 2013;84(11):1546-55.
24. Khairy NM, Shendy EE, Askar NA, El-Rouby DH. Effect of platelet rich plasma on bone regeneration in maxillary sinus augmentation (randomized clinical trial). *Int J Oral Maxillofac Surg*. 2013;42(2):249-55.
25. Pocaterra A, Caruso S, Bernardi S, Scagnoli L, Continenza MA, Gatto R. Effectiveness of platelet-rich plasma as an adjunctive material to bone graft: a systematic review and meta-analysis of randomized controlled clinical trials. *Int J Oral Maxillofac Surg*. 2016;45(8):1027-34.
26. Anitua E. Plasma rich in growth factors: preliminary results of use in the preparation of future sites for implants. *Int J Oral Maxillofac Implants*. 1999;14(4):529-35.
27. Haigler MC, Abdulrehman E, Siddappa S, Kishore R, Padilla M, Enciso R. Use of platelet-rich plasma, platelet-rich growth factor with arthrocentesis or arthroscopy to treat temporomandibular joint osteoarthritis: Systematic review with meta-analyses. *J Am Dent Assoc*. 2018;149(11):940-52.e2.
28. Anitua E, Sanchez M, Orive G, Andia I. The potential impact of the preparation rich in growth factors (PRGF) in different medical fields. *Biomaterials*. 2007;28(31):4551-60.
29. Anitua E, Prado R, Orive G. Bilateral sinus elevation evaluating plasma rich in growth factors technology: a report of five cases. *Clin Implant Dent Relat Res*. 2012;14(1):51-60.
30. Batas L, Tsalikis L, Stavropoulos A. PRGF as adjunct to DBB in maxillary sinus floor augmentation: histological results of a pilot split-mouth study. *Int J Implant Dent*. 2019;5(1):14.
31. Kawase T. Platelet-rich plasma and its derivatives as promising bioactive materials for regenerative medicine: basic principles and concepts underlying recent advances. *Odontology*. 2015;103(2):126-35.
32. Choukroun J. Une opportunité en paro-implantologie: le PRF. . *Implantodontie*. 2001;42:55-62.
33. Ratajczak J, Vanganswinkel T, Gervois P, Merckx G, Hilken P, Quirynen M, et al. Angiogenic Properties of 'Leukocyte- and Platelet-Rich Fibrin'. *Sci Rep*. 2018;8(1):14632.
34. Dohan Ehrenfest DM, Doglioli P, de Peppo GM, Del Corso M, Charrier JB. Choukroun's platelet-rich fibrin (PRF) stimulates in vitro proliferation and differentiation of human oral bone mesenchymal stem cell in a dose-dependent way. *Arch Oral Biol*. 2010;55(3):185-94.
35. Schär MO, Diaz-Romero J, Kohl S, Zumstein MA, Nesic D. Platelet-rich concentrates differentially release growth factors and induce cell migration in vitro. *Clin Orthop Relat Res*. 2015;473(5):1635-43.
36. Dohan Ehrenfest DM, Andia I, Zumstein MA, Zhang CQ, Pinto NR, Bielecki T. Classification of platelet concentrates (Platelet-Rich Plasma-PRP, Platelet-Rich Fibrin-PRF) for topical and infiltrative

use in orthopedic and sports medicine: current consensus, clinical implications and perspectives. *Muscles Ligaments Tendons J.* 2014;4(1):3-9.

37. Larson D. *Clinical Chemistry: Fundamentals and Laboratory Techniques.* 1st ed 2016.
38. Rahmanian N, Bozorgmehr M, Torabi M, Akbari A, Zarnani AH. Cell separation: Potentials and pitfalls. *Prep Biochem Biotechnol.* 2017;47(1):38-51.
39. Pinto N, Quirynen M. Letter to the editor: RE: Optimized platelet-rich fibrin with the low-speed concept: Growth factor release, biocompatibility, and cellular response. *J Periodontol.* 2019;90(2):119-21.
40. Miron RJ, Pinto NR, Quirynen M, Ghanaati S. Standardization of relative centrifugal forces in studies related to platelet-rich fibrin. *J Periodontol.* 2019;90(8):817-20.
41. Dohan Ehrenfest DM, Pinto NR, Pereda A, Jimenez P, Corso MD, Kang BS, et al. The impact of the centrifuge characteristics and centrifugation protocols on the cells, growth factors, and fibrin architecture of a leukocyte- and platelet-rich fibrin (L-PRF) clot and membrane. *Platelets.* 2018;29(2):171-84.
42. Dohan Ehrenfest DM, Del Corso M, Diss A, Mouhyi J, Charrier JB. Three-dimensional architecture and cell composition of a Choukroun's platelet-rich fibrin clot and membrane. *J Periodontol.* 2010;81(4):546-55.
43. Blair P, Flaumenhaft R. Platelet alpha-granules: basic biology and clinical correlates. *Blood Rev.* 2009;23(4):177-89.
44. Tang YQ, Yeaman MR, Selsted ME. Antimicrobial peptides from human platelets. *Infect Immun.* 2002;70(12):6524-33.
45. Wu AC, Raggatt LJ, Alexander KA, Pettit AR. Unraveling macrophage contributions to bone repair. *Bonekey Rep.* 2013;2:373.
46. Fantone JC, Ward PA. Role of oxygen-derived free radicals and metabolites in leukocyte-dependent inflammatory reactions. *Am J Pathol.* 1982;107(3):395-418.
47. El Bagdadi K, Kubesch A, Yu X, Al-Maawi S, Orłowska A, Dias A, et al. Reduction of relative centrifugal forces increases growth factor release within solid platelet-rich-fibrin (PRF)-based matrices: a proof of concept of LSCC (low speed centrifugation concept). *Eur J Trauma Emerg Surg.* 2017.
48. Ghanaati S, Booms P, Orłowska A, Kubesch A, Lorenz J, Rutkowski J, et al. Advanced platelet-rich fibrin: a new concept for cell-based tissue engineering by means of inflammatory cells. *J Oral Implantol.* 2014;40(6):679-89.
49. Miron RJ, Chai J, Zheng S, Feng M, Sculean A, Zhang Y. A novel method for evaluating and quantifying cell types in platelet rich fibrin and an introduction to horizontal centrifugation. *J Biomed Mater Res A.* 2019;107(10):2257-71.
50. Fujioka-Kobayashi M, Miron RJ, Hernandez M, Kandam U, Zhang Y, Choukroun J. Optimized Platelet-Rich Fibrin With the Low-Speed Concept: Growth Factor Release, Biocompatibility, and Cellular Response. *J Periodontol.* 2017;88(1):112-21.
51. Cortellini S, Castro AB, Temmerman A, Van Dessel J, Pinto N, Jacobs R, et al. Leucocyte- and platelet-rich fibrin block for bone augmentation procedure: A proof-of-concept study. *J Clin Periodontol.* 2018;45(5):624-34.
52. Choukroun J, Ghanaati S. Reduction of relative centrifugation force within injectable platelet-rich-fibrin (PRF) concentrates advances patients' own inflammatory cells, platelets and growth factors: the first introduction to the low speed centrifugation concept. *Eur J Trauma Emerg Surg.* 2018;44(1):87-95.

53. Wang X, Zhang Y, Choukroun J, Ghanaati S, Miron RJ. Effects of an injectable platelet-rich fibrin on osteoblast behavior and bone tissue formation in comparison to platelet-rich plasma. *Platelets*. 2018;29(1):48-55.



# SECTION 1



Systematic reviews



# CHAPTER 1

## Regenerative potential of leucocyte- and platelet-rich fibrin. Part A: intra-bony defects, furcation defects and periodontal plastic surgery. A systematic review and meta-analysis

Castro Ana B, Meschi Nastaran, Temmerman Andy, Pinto Nelson, Lambrechts Paul,  
Teughels Wim & Quirynen Marc. (2017) *Journal of Clinical Periodontology* 44; 225-234.

### **Abstract**

**Aim:** To analyse the regenerative potential of leucocyte- and platelet-rich fibrin (L-PRF) during periodontal surgery.

**Material & Methods:** An electronic and hand search were conducted in three databases. Only randomized clinical trials were selected and no follow-up limitation was applied. Pocket depth (PD), clinical attachment level (CAL), bone fill, keratinized tissue width (KTW), recession reduction and root coverage (%) were considered as outcome. When possible, meta-analysis was performed.

**Results:** Twenty-four articles fulfilled the inclusion and exclusion criteria. Three subgroups were created: intra-bony defects (IBDs), furcation defects and periodontal plastic surgery. Meta-analysis was performed in all the subgroups. Significant PD reduction ( $1.1 \pm 0.5$  mm,  $p < 0.001$ ), CAL gain ( $1.2 \pm 0.6$  mm,  $p < 0.001$ ) and bone fill ( $1.7 \pm 0.7$  mm,  $p < 0.001$ ) were found when comparing L-PRF to open flap debridement (OFD) in IBDs. For furcation defects, significant PD reduction ( $1.9 \pm 1.5$  mm,  $p = 0.01$ ), CAL gain ( $1.3 \pm 0.4$  mm,  $p < 0.001$ ) and bone fill ( $1.5 \pm 0.3$  mm,  $p < 0.001$ ) were reported when comparing L-PRF to OFD. When L-PRF was compared to a connective tissue graft, similar outcomes were recorded for PD reduction ( $0.2 \pm 0.3$  mm,  $p > 0.05$ ), CAL gain ( $0.2 \pm 0.5$  mm,  $p > 0.05$ ), KTW ( $0.3 \pm 0.4$  mm,  $p > 0.05$ ) and recession reduction ( $0.2 \pm 0.3$  mm,  $p > 0.05$ ).

**Conclusions:** L-PRF enhances periodontal wound healing.

### **Introduction**

In the last 20 years, platelet concentrates (PCs) have emerged as a potential regenerative material, used alone or as scaffold for other graft materials. PCs are blood extracts, obtained after processing a whole blood sample, mostly through centrifugation (1). In 1970, Matras (1970) (2) published the first article on PCs using fibrin glue to improve skin wound healing. But it was not until Marx's studies (3, 4) that the use of PCs also gained interest in oral and maxillofacial surgery. Since then, different techniques have been developed and with them, a variety of preparations. The first PCs generation (Figure 1) include platelet-rich plasma (PRP) and plasma rich in growth factors (PRGF). Their preparation requires anticoagulants at the moment of blood collection to avoid coagulation. Consequently, the fibrin polymerization occurs rapidly, resulting in a weak fibrin network (5). They are used as liquid solution or in gel form after adding bovine thrombin and calcium chloride.

Due to the difficulties in the preparation and the inconsistent outcome of PRP and PRGF formulations, a second PCs generation was introduced in 2001 by Choukroun and co-workers (5-7). The use of platelet-rich fibrin (PRF) is simple and requires neither anticoagulant, bovine thrombin nor calcium chloride. It is nothing more than centrifuged blood without any additives (Table 1). Whole blood

is centrifuged without anticoagulants at high spin so that three layers are obtained: red blood corpuscles (RBCs) at the bottom of the tube, platelet-poor plasma (PPP) on the top and an intermediate layer called “buffy coat” where most leucocytes and platelets are concentrated.

This buffy coat or L-PRF is a bioactive construct that stimulates the local environment for differentiation and proliferation of stem and progenitor cells (8). It acts as an immune regulation node with inflammation control abilities, including a slow continuous release of growth factors over a period of 7–14 days (9). Rich in fibrin, platelets ( $\pm 95$  % of initial blood), leucocytes ( $\pm 50$  % of initial blood), monocytes and stem cells, L-PRF can be further transformed into a membrane, circa 1 mm in thickness, by careful compression (10) (Figure 2). Its strong fibrin architecture and its superior mechanical properties distinguish it from other kinds of PCs (11). PRP, for example, has a thin and non-condensed fibrin network with a low tensile strength so that it is less useful as a space maintainer (12). The strong fibrin network in L-PRF is explained by the physiological concentrations of thrombin during its preparation. Rowe et al. (2007) (13) concluded that a high thrombin concentration resulted in a high-interconnected fibre mesh with a fine fibre structure. However, as thrombin concentration decreased, fibre size increased as well as the mechanical properties. Apart from the biological and mechanical properties, antimicrobial effects have also been described (14).

The main aim of this systematic review was to study the beneficial effect of L-PRF used as sole filling material and as adjunct to conventional techniques in periodontal surgery.

## **Materials & Methods**

The protocol of this systematic review was based on the guidelines of the Belgian Centre for Evidence-Based Medicine (CEBAM), Belgian Branch of the Dutch Cochrane Centre. It was conducted in accordance with the Transparent Reporting of Systematic Reviews and Meta-analyses (PRISMA statement, Moher et al. 2009).

### **Focused PICO question**

The following statements were used to conduct the systematic search (PICO question):

- Population (P) = systemically healthy humans (ASA I) with loss of periodontal tissues.
- Intervention (I) = use of L-PRF (protocol 2700 r.p.m./12 min. or 3000 r.p.m./10 min.) as sole biomaterial or in combination to other biomaterials in periodontal surgery.
- Comparison (C) = traditional techniques: open flap debridement with or without grafting, periodontal plastic surgery via coronally advanced flap, with or without connective tissue graft.
- Outcome (O) = alveolar bone and/or periodontal wound healing.

A PICO question was created to define the search strategy: *Does L-PRF promote periodontal wound healing in systemically healthy patients (ASA I) during periodontal surgery compared to traditional techniques?*

### **Search strategy**

An electronic search was performed in three Internet databases: the National Library of Medicine, Washington, DC (MEDLINE-PubMed), EMBASE (Excerpta Medical Database by Elsevier), and Cochrane Central Register of Controlled Trials (CENTRAL). The search strategy is shown Table S2. The last electronic search was performed on the 31st of July 2015. This search was enriched by hand searches, citation screening and expert recommendations.

### Screening and selection

The titles and abstracts obtained from the first search were screened independently by two reviewers (A.C., N.M.). When publications did not meet the inclusion criteria, they were excluded upon reviewer's agreement. Any disagreement between the two reviewers was resolved by discussion. All full texts of the eligible articles were obtained and examined by both reviewers. The articles that fulfilled all selection criteria were processed for data extraction. Given some variability in the preparation of L-PRF, two different protocols (2700 r.p.m./12 min. or 3000 r.p.m./10 min.) were included. The inclusion and exclusion criteria are summarized in Table S3.

### Assessment of heterogeneity

The heterogeneity of the included studies was judged based on following factors: (1) study design and evaluation period, (2) subject characteristics and smoking habits, and (3) surgical protocol used: (a) centrifugation protocol (2700 r.p.m./12 min. or 3000 r.p.m./10 min.), (b) mL blood used to prepare L-PRF and (c) number of clots/membranes (if used).

### Quality assessment

The quality assessment, performed by both reviewers (A.C., N.M.), was based on the Cochrane Collaboration's tool for assessing risk of bias. Six quality criteria were verified: (1) sequence generation or randomization component, (2) allocation concealment, (3) blinding of participants, personnel and outcome assessors, (4) incomplete/missing outcome data, (5) selective outcome reporting and (6) other sources of bias. In case of any doubt, the authors were contacted for clarification or to provide missing information. Low risk of bias was indicated if all quality criteria were “present”, moderate risk of bias if one or more key domains were “unclear” and high risk of bias if one or more key domains were “absent”.

### Data analysis

The analysed variables were as follows: pocket depth (PD) reduction, clinical attachment level (CAL) gain, bone fill (mm and %), keratinized tissue width (KTW) gain, tissue thickness gain, recession reduction and root coverage (%) at 6 months. For all variables in each group, mean values and standard deviation (SD) were extracted. All data were arranged in groups for the inter-group comparison (L-PRF *versus* control group). When possible, a meta-analysis was performed. The mean difference was calculated and a 95% confidence interval (CI) was computed.

## **Results**

### Search and selection

As a result of the electronic and hand search, 205 articles were obtained, of which 23 were duplicate and consequently removed (Figure 3). A total of 182 articles was included for title and abstract screening. From those, 25 articles were included for full text review. One article was excluded after full text screening, which was conducted independently by two reviewers (A.C., N.M.). Twenty-four randomized control trials (RCTs) fulfilled the inclusion criteria and were included for analysis. The included articles were classified into three subgroups, depending on the indication for the use of L-PRF (Tables 1, 2, 3):

- Intra-bony defect fill:  $n = 13$

L-PRF *versus* open flap debridement (OFD):  $n = 5$ , Sharma & Pradeep (2011b) (15), Thorat et al. (2011) (16), Rosamma et al. (2012) (17), Ajwani et al. (2015) (18), and Pradeep et al. (2015) (19).

L-PRF *versus* PRP *versus* OFD:  $n = 1$ , Pradeep et al. (2012) (20).

L-PRF *versus* bovine porous bone mineral (BPBM):  $n = 1$ , Lekovic et al. (2012) (21).

L-PRF *versus* demineralized freeze-dried bone allograft (DFDBA):  $n = 3$ , Bansal & Bharti (2013) (22), Shah et al. (2015) (23), and Agarwal et al. (2016) (24).

L-PRF *versus* Emdogain®:  $n = 1$ , Gupta et al. (2014) (25).

L-PRF *versus* nano-bone®:  $n = 1$ , Elgendy & Abo Shady (2015) (26).

L-PRF *versus* autologous bone graft (ABG):  $n = 1$ , Mathur et al. (2015) (27).

- Furcation defects:  $n = 2$ , Sharma & Pradeep (2011a) (28), and Bajaj et al. (2013) (29).

- Periodontal plastic surgery:  $n = 9$

Coronally advanced flap (CAF) *versus* CAF + L-PRF:  $n = 4$ , Aroca et al. (2009) (30), Padma et al. (2013) (31), Gupta et al. (2015) (32), and Thamaraiselvan et al. (2015) (33).

CAF + L-PRF *versus* CAF + connective tissue graft (CTG):  $n = 4$ , Jankovic et al. (2012) (34), Eren & Atilla (2014) (35), Keceli et al. (2015) (36), and Tunali et al. (2015) (37).

CAF + L-PRF *versus* CAF + Emdogain® (EMD):  $n = 1$ , Jankovic et al. (2010) (38).

### Assessment of heterogeneity

#### Study design and evaluation period

All studies were RCTs and frequently presented a split-mouth design. The articles with these characteristics are the following: intra-bony defects (IBDs) 7/13 (Lekovic et al. 2012, Rosamma et al. 2012, Bansal & Bharti 2013, Ajwani et al. 2015, Elgendy & Abo Shady 2015, Shah et al. 2015, Agarwal et al. 2016), furcation defects 1/2 (Sharma & Pradeep 2011a), plastic surgery 7/9 (Aroca et al. 2009, Jankovic et al. 2010, 2012, Padma et al. 2013, Eren & Atilla 2014, Keceli et al. 2015, Tunali et al. 2015). The follow-up ranged slightly (IBDs 6–12 months, furcation defects 9 months and plastic surgery 6–12 months).

#### Subject characteristics, smoking habits and surgical protocol

Healthy subjects with no active periodontal disease were included in all the studies. The studies that did not include smokers are the following: IBDs 9/13 (Sharma & Pradeep 2011a,b, Lekovic et al. 2012, Rosamma et al. 2012, Pradeep et al. 2012, 2015, Gupta et al. 2014, Ajwani et al. 2015, Shah et al. 2015, Agarwal et al. 2016), furcation defects 1/2 (Sharma & Pradeep 2011a), plastic surgery 8/9 (Jankovic et al. 2010, 2012, Padma et al. 2013, Eren & Atilla 2014, Gupta et al. 2015, Keceli et al. 2015, Thamaraiselvan et al. 2015, Tunali et al. 2015).

A wide variety of surgical protocols was used. This heterogeneity can be derived from Tables 1, 2, 3.

#### Quality assessment

Figures 4, 5, 6 show the quality assessment for the included studies. All articles on furcation defects and periodontal plastic surgery showed a moderate risk of bias. Similarly, 12 articles using L-PRF in IBD had a moderate risk, and one had a low risk of bias.

#### Quantitative assessment

The extracted data were continuous. The articles with split-mouth design and parallel design were not analysed separately. The control group and test group from the articles with split-mouth design were considered as independent. As shown in the Figs 3 and 4, the studies with split-mouth design do

not differ from those with parallel design. Random effects were used due to the heterogeneity of the data.

#### *Intra-bony defects*

In the articles on IBDs, benefits in terms of PD reduction, CAL gain and bone fill were shown when L-PRF was used alone or in combination with other biomaterials (Table 2). Six out of 13 articles (Sharma & Pradeep 2011b, Thorat et al. 2011, Pradeep et al. 2012, 2015, Rosamma et al. 2012, Ajwani et al. 2015) could be used for a meta-analysis since they reported on similar outcome measures comparing OFD to OFD + L-PRF (Figures 7-9). The meta-analysis of IBDs showed a statistical significant difference for PD reduction (mean difference: 1.1 mm,  $p < 0.001$ , CI: 0.6–1.6), CAL gain (mean difference: 1.2 mm,  $p < 0.001$ , CI: 0.5–1.9), amount of bone fill in mm (mean difference: 1.7 mm,  $p < 0.001$ , CI: 1.0–2.3) and bone fill when scored as % (mean difference: 46.0%,  $p < 0.001$ , CI: 33.2–58.7), all in favour of L-PRF.

#### *Furcation defects*

Two articles were included for furcation defects (Sharma & Pradeep 2011a, Bajaj et al. 2013). A meta-analysis could be performed for both articles, comparing OFD to OFD + L-PRF (Figures 10-11). Statistical significant differences could be found for PD reduction (mean difference: 1.9 mm,  $p = 0.01$ , CI: 0.4–3.5), CAL gain (mean difference: 1.3 mm,  $p < 0.001$ , CI: 0.8–1.7), amount of bone fill in mm (mean difference: 1.5 mm,  $p < 0.001$ , CI: 1.2–1.9), bone fill when scored as % (37.6%,  $p < 0.001$ , CI: 30.6–44.5), again in favour of L-PRF (Table 3).

#### *Periodontal plastic surgery*

In case of a CAF, some studies reported some benefits when L-PRF membranes were added, but others failed to show this advantage (Table 4). When the use of a CTG in a CAF procedure was compared to the use of L-PRF membranes, similar results were obtained. Two meta-analyses could be performed, one comparing a CAF alone *versus* a CAF with L-PRF, and another comparing a CAF with L-PRF *versus* a CAF with a CTG. The following variables were considered: PD reduction, CAL gain, KTW gain, tissue thickness gain, recession reduction and root coverage at 6 months.

For the first comparison (CAF + L-PRF *versus* CAF, Figures 12-13), three articles could be included for a meta-analysis (Aroca et al. 2009, Gupta et al. 2015, Thamaraiselvan et al. 2015). The analysis showed no statistical significant difference in PD reduction (mean difference: 0.2 mm,  $p = 0.2$ , CI: -0.08 to 0.4), CAL gain (mean difference: 0.4 mm,  $p = 0.09$ , CI: -0.06 to 0.8), KTW gain (mean difference: 0.3 mm,  $p = 0.1$ , CI: -0.06 to 0.6), tissue thickness (mean difference: 0.2 mm,  $p = 0.09$ , CI: -0.03 to 0.4) and root coverage at 6 months (mean difference: 9.6%,  $p = 0.6$ , CI: -23.2 to 42.4), although the results showed a trend that L-PRF was superior for all of these variables. However, statistically significant difference could be found for recession depth reduction (mean difference: 0.6 mm,  $p < 0.01$ , CI: 0.2–1.1), in favour of the for the L-PRF treatment.

For the second comparison (CAF + L-PRF *versus* CAF + CTG, Figure 14) also three articles could be used for a meta-analysis (Jankovic et al. 2012, Eren & Atilla 2014, Tunali et al. 2015). No statistical significant differences could be found for all of the variables: PD reduction (mean difference: 0.2 mm,  $p = 0.4$ , CI: -0.5 to 0.2), CAL gain (mean difference: 0.2 mm,  $p = 0.3$ , CI: -0.3 to 0.7), KTW gain (mean difference: 0.3 mm,  $p = 0.2$ , CI: -0.7 to 0.2) and recession reduction (mean difference: 0.2 mm,  $p = 0.2$ , CI: -0.4 to 0.1). Root coverage could not be included in this meta-analysis since only

one article (Jankovic et al. 2012) fully analysed this variable; Eren & Atilla (2014), and Tunali et al. (2015) did not include the standard deviations.

The adverse events were only registered in some articles within the group of periodontal plastic surgery (Aroca et al. 2009, Jankovic et al. 2010, 2012, Eren & Atilla 2014, Gupta et al. 2015). Each article analysed the adverse events with a different scale, so no meta-analysis could be performed. Five out of the nine articles on periodontal plastic surgery reported on pain, swelling and hypersensitivity. All of them observed less side effects in L-PRF sites.

## **Discussion**

L-PRF has often shown a positive effect when applied during periodontal surgery. Although it has been classified as a platelet concentrates(1) (Dohan et al. 2014a), it can also be considered as a living tissue graft due to its cellular content and its constant release of growth factors for more than 7 days (8).

This review demonstrates that L-PRF has many applications but there is no clear standard protocol per surgical procedure. For example, the number of clots used varies enormously, as well as the amount of blood drawn to prepare L-PRF. The type of centrifuge and setting also differed from one study to another. More standardized protocols are necessary in order to better compare and standardize outcomes.

The effectiveness of L-PRF in the treatment of intra-bony defects has been studied by different research groups (39, 40). In these studies, L-PRF was placed in the defect and L-PRF membranes were used to cover the defect similar to a guided tissue regeneration (GTR) membrane. Clinical and radiographic evaluations showed statistically significant greater PD reduction, CAL gain and radiographic intra-bony defect fill in the L-PRF group (Table 3). Different graft materials were also compared to L-PRF during GTR. The outcomes showed a favourable effect of L-PRF in all clinical parameters measured, or an improvement of the outcomes in studies where L-PRF was combined with other biomaterials (Table 3). Although very limited data exist, the use of L-PRF in furcation defects has also shown favourable results.

For periodontal plastic surgery, the comparison of CAF + L-PRF *versus* CAF led to controversial results. Although most articles did not show statistically significant differences, L-PRF was superior for all of the parameters recorded. Comparing CAF + L-PRF *versus* CAF + CTG, L-PRF might be an alternative to a connective tissue graft. The latter is supported by some case reports (41-43). In this systematic review, a mean root coverage of 86.5% at 6 months has been recorded for CAF + L-PRF treatment. For CAF + EMD and CAF + CTG, a mean root coverage of 91.2% and 90.3% was, respectively, reported in a recent systematic review at 6 months (44).

Some limitations have to be taken into consideration while processing this systematic review. Most of the included articles showed a moderate risk of bias. In those articles, the power analysis was often performed after the recruitment of the participants, where for a RCT it should be done prior to the recruitment in order to determine the sample size. Working in the opposite way, a selective outcome reporting bias can be introduced. Additionally, the allocation concealment and blinding methods were frequently not applied which increased the risk of bias.

Meta-analysis could be performed in the three indications. However, also here the results of certain studies have to be considered very cautiously. For instance, for the IBDs subgroup, Ajwani et al. (2015) (18) obtained the worst results compared to the rest of the selected articles. The reason could be that two- and three-wall IBDs were included but not analysed separately. Moreover, only one L-PRF



clot without membrane was used, so the stability of one L-PRF clot in a two-wall defect without the use of a membrane might not have been ideal. Given the importance of stability in GTR, the use of L-PRF clots in two- or one-wall defects should be accompanied by a L-PRF membrane. In periodontal plastic surgery, Aroca et al. (2009) (30) published the only article that reported better outcome for the control group (CAF). However, smokers (<20 cig/day) were also included, though smoking negatively influences the healing process and affects complete root coverage (45, 46). Tobacco smoke might directly affect the peripheral blood cells within the L-PRF (47), yielding to uncertain outcomes.

Regardless the limitations of the included studies, it is worth pointing out some strengths of this systematic review. A total number of 722 participants was enrolled in the selected studies (479 in intra-bony defects, 55 in furcation defects, 188 in periodontal plastic surgery). Taking into consideration the rather short history of L-PRF, this review comprehends a quite large sample of patients. Moreover, the follow-up varied slightly in the articles included for meta-analysis. The duration in the follow-up ranged from 9 to 12 months in the studies selected for quantitative assessment for the IBDs group. Considering furcation defects and periodontal plastic surgery, all of them had a follow-up of 9 and 6 months, respectively. Moreover, only the two most accepted protocols of centrifugation (3000 r.p.m./10 min. or 2,700 r.p.m./12 min.) were included. All other protocols that were not explained in detail or with a non-standardized procedure were excluded. A correct handling of L-PRF is of the outmost importance. It should be clearly distinguished what L-PRF is and what not. For example, L-PRF and PRP contain different cell concentrations, release different amount of growth factors, and have different mechanical properties although both come from a blood sample (5).

## **Conclusion**

Favourable effects on hard and soft tissue healing and postoperative discomfort reduction were often reported when L-PRF was used. Nevertheless, standardization of the protocol is needed to obtain an optimal effect of L-PRF in regenerative procedures. Correct handling of L-PRF as well as the use of enough clots/membranes per surgical site might be crucial to obtain benefits from this technique. This biomaterial can be taken into consideration due to its reported good biological effects, low costs and ease of preparation.

## Figures

Figure 1. Differences among PCs preparation. (a) platelet-rich plasma (PRP): after the first centrifugation, the platelet-poor plasma, the “yellow” part called buffy coat and a few red blood cells are carefully collected (pipetting) and centrifuged again in order to obtain the PRP (b) PRGF: after centrifugation, the blood is divided in five layers; by pipetting, the undesired parts are discarded; the most concentrated part with growth factors (PRGF) is collected (48); (c) PRF: after centrifugation, a fibrin clot is obtained in the middle of the tube, which is ready to be used (5).

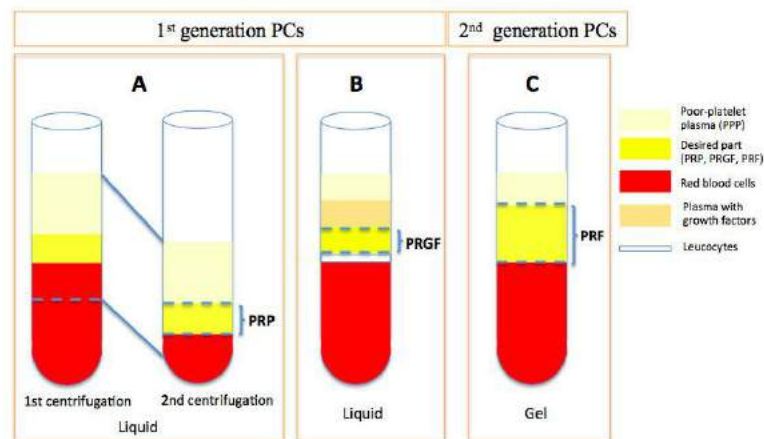


Figure 2. L-PRF preparation. A. Blood is withdrawn from the patient. B. Tubes are centrifuged within 60 s after blood collection without any additives. C. After 12 min. of centrifugation, a clear separation between the platelet-poor plasma, the buffy coat and the red blood cells is obtained. D. L-PRF is presented in the middle of the tube. E. Different L-PRF forms can be produced: liquid, clots or membranes.

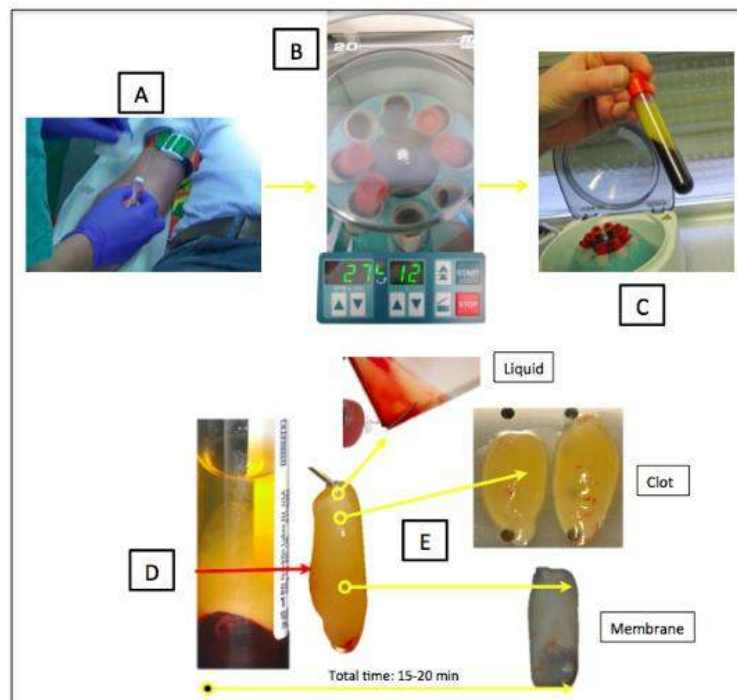


Figure 3. PRISMA flow diagram.

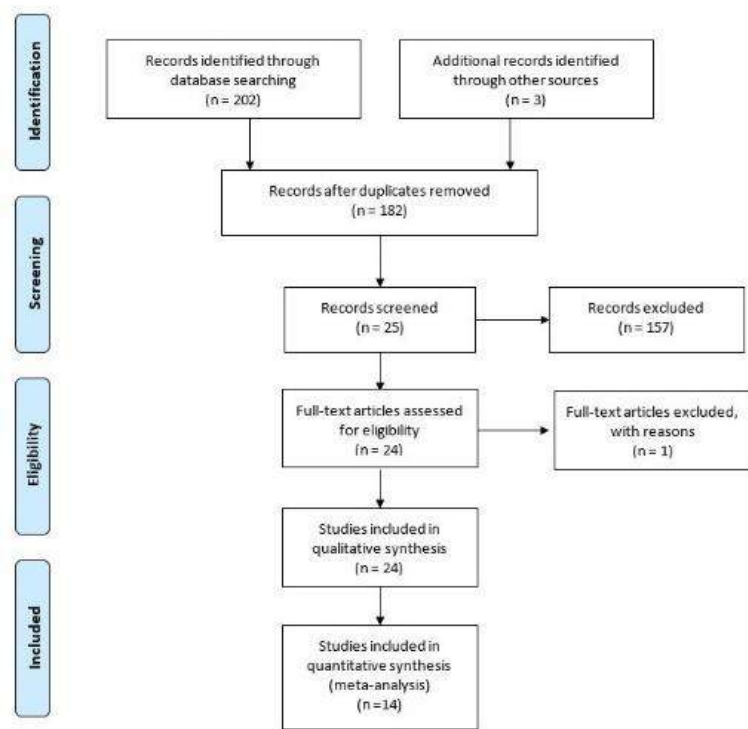


Figure 4. Quality assessment for IBS.

Sharma & Pradeep (2011a)	●	●	●	●	●	●
Bajaj et al. (2013)	●	●	●	●	●	●
Random sequence generation (selection bias)	●	●	●	●	●	●
Allocation concealment (selection bias)	●	●	●	●	●	●
Blinding of participants and personnel (performance bias)	●	●	●	●	●	●
Blinding of outcome assessment (detection bias)	●	●	●	●	●	●
Incomplete outcome data (attrition bias)	●	●	●	●	●	●
Selective reporting (reporting bias)	●	●	●	●	●	●
Other bias	●	●	●	●	●	●

Figure 5. Quality assessment for furcation defects.

Sharma & Pradeep (2011b)	●	●	●	●	●	●
Thor et al. (2011)	●	●	●	●	●	●
Rosier et al. (2012)	●	●	●	●	●	●
Pradeep et al. (2015)	●	●	●	●	●	●
Pradeep et al. (2012)	●	●	●	●	●	●
Mathur et al. (2015)	●	●	●	●	●	●
Lehok et al. (2012)	●	●	●	●	●	●
Cupira et al. (2014)	●	●	●	●	●	●
Björndal & Alvo Study (2015)	●	●	●	●	●	●
Bajaj & Bhatt (2013)	●	●	●	●	●	●
Agarwal et al. (2016)	●	●	●	●	●	●
Alwan et al. (2015)	●	●	●	●	●	●
Random sequence generation (selection bias)	●	●	●	●	●	●
Allocation concealment (selection bias)	●	●	●	●	●	●
Blinding of participants and personnel (performance bias)	●	●	●	●	●	●
Blinding of outcome assessment (detection bias)	●	●	●	●	●	●
Incomplete outcome data (attrition bias)	●	●	●	●	●	●
Selective reporting (reporting bias)	●	●	●	●	●	●
Other bias	●	●	●	●	●	●

Figure 6. Quality assessment for periodontal plastic surgery.

Tunali et al. (2015)	●	●	●	●	●	●
Thammaselvan et al. (2015)	●	●	●	●	●	●
Padma et al. (2013)	●	●	●	●	●	●
Kerell et al. (2015)	●	●	●	●	●	●
Jankovic et al. (2010)	●	●	●	●	●	●
Jankovic et al. (2012)	●	●	●	●	●	●
Cupira et al. (2015)	●	●	●	●	●	●
Eren & Adigil (2014)	●	●	●	●	●	●
Arora et al. (2009)	●	●	●	●	●	●
Random sequence generation (selection bias)	●	●	●	●	●	●
Allocation concealment (selection bias)	●	●	●	●	●	●
Blinding of participants and personnel (performance bias)	●	●	●	●	●	●
Blinding of outcome assessment (detection bias)	●	●	●	●	●	●
Incomplete outcome data (attrition bias)	●	●	●	●	●	●
Selective reporting (reporting bias)	●	●	●	●	●	●
Other bias	●	●	●	●	●	●

Figure 7. Forest plot comparing OFD vs. OFD + L-PRF in the treatment of IBDs, PD reduction (mm).

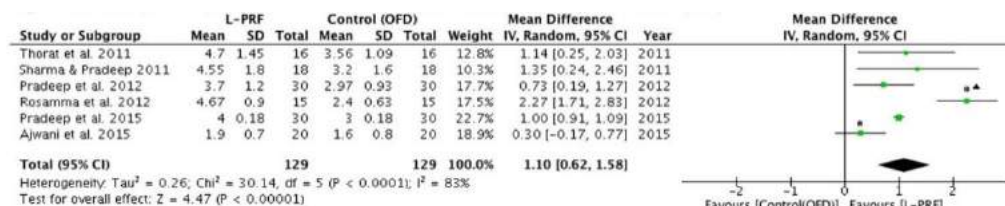


Figure 8. Forest plot comparing OFD vs. OFD + L-PRF in the treatment of IBDs, CAL gain (mm).

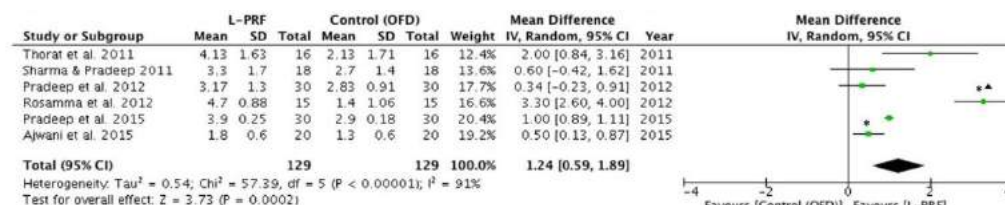


Figure 9. Forest plot comparing OFD vs. OFD + L-PRF in the treatment of IBDs, bone fill (mm).

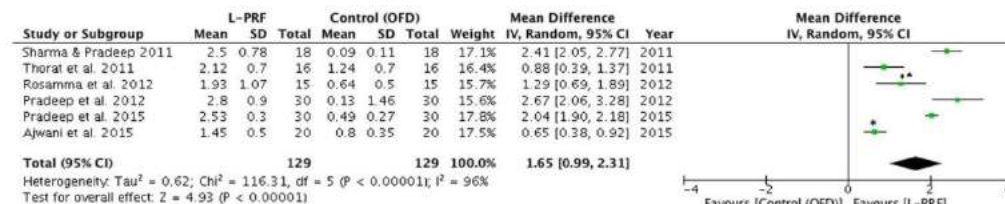


Figure 10. Forest plot comparing OFD vs. OFD + L-PRF in the treatment of furcation defects, CAL gain (mm).

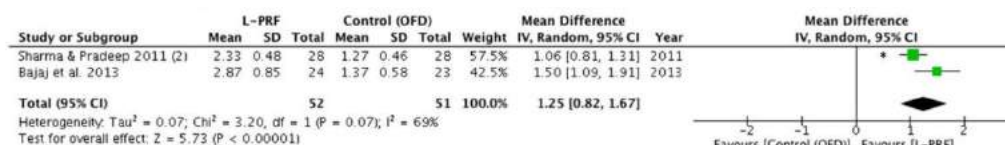


Figure 11. Forest plot comparing OFD vs. OFD + L-PRF in the treatment of furcation defects, bone fill (mm).

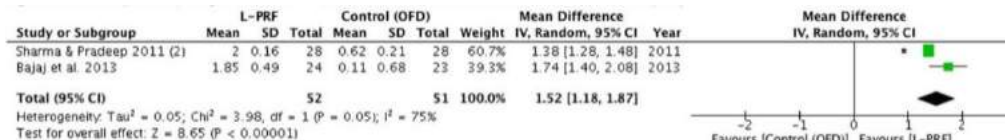


Figure 12. Forest plot comparing CAF vs. CAF + L-PRF in periodontal plastic surgery, recession reduction (mm).

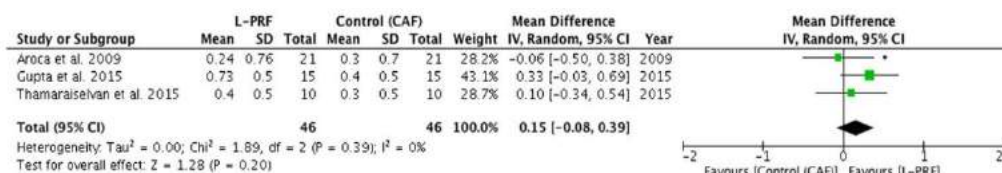


Figure 13. Forest plot comparing CAF vs. CAF + L-PRF in periodontal plastic surgery, root coverage (%).

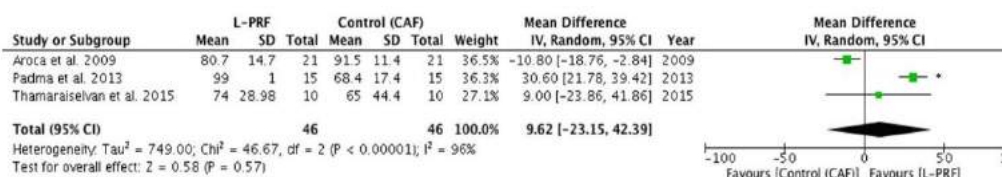
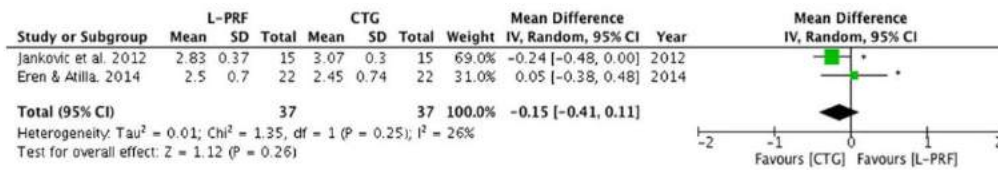


Figure 14. Forest plot comparing CAF + CTG vs. CAF + L-PRF in periodontal plastic surgery, recession reduction (mm).



## Tables

Table 1. Description of platelet concentrates (PCs) characteristics. Although PRP and PRF can be prepared with or without leucocytes (Dohan et al. 2009, 2014a), this table presents the most common formulations.

	1 <sup>st</sup> generation		2 <sup>nd</sup> generation
	PRP	PRGF	PRF
<b>Process</b>			
<b>Centrifugation</b>	2x + pipetting	1x + pipetting	1x
<b>Additives</b>	Yes	Yes	No
<b>Duration</b>	30-45 min	20-25 min	10-12 min
<b>Simplicity</b>	-	-	+
<b>Cellular content</b>			
<b>Volume</b>	-	+/-	+
<b>Platelets</b>	Medium	Low	High
<b>Leucocytes</b>	No	No	Yes
<b>Fibrin</b>			
<b>Density</b>	Weak	Weak	Strong
<b>Polymerization</b>	Fast	Fast	Slow

Table 2. L-PRF for intrabony defects. Papers have been arranged by subapplications (L-PRF + OFD vs. OFD, L-PRF vs. PRP, L-PRF vs. L-PRF + BPBM, L-PRF + DFDBA vs. DFDBA, L-PRF vs. Emdogain®, L-PRF vs. nano-bone®, L-PRF vs. ABG, L-PRF in furcation lesions: L-PRF + OFD vs. OFD).

Authors (year)	Study design, Duration	No. of participants baseline (end), gender, age Smoking	Groups C: control T: test	L-PRF preparation	Surgical protocol	Results
<i>L-PRF + OFD vs. OFD</i>						
Thorat <i>et al.</i> (2011)	RCT	40 – (32)	2 and 3 walls IBDs  C: n= 16, OFD  T: n= 16, OFD + L-PRF	Hardware: <sup>1</sup>  Setting: 400 g / 12 min	1 L-PRF clot 1 L-PRF membrane  10 mL blood/clot	<b>L-PRF + OFD vs. OFD</b> SS more PD reduction (4.5 vs. 3.5 mm), CAL gain (3.7 vs. 2.1 mm) and bone fill (47% vs. 29%) in favour of L-PRF group (p<0.05).
	Parallel Single-blind  9 months	18 ♀, 22 ♂  Mean age: 31 ± 2 Range: ?  Smoking: ?				
Sharma & Pradeep (2011b)	RCT	42 – (35)	3 walls IBDs  C: n= 17 (28 sites), OFD  T: n= 18 (28 sites), L-PRF	Hardware: ?  Setting: 3000 rpm / 10 min	1 L-PRF clot 2 L-PRF membrane  10 mL blood/clot	<b>L-PRF + OFD vs. OFD</b> SS more PD reduction (4.5 vs. 3.2mm) and bone fill (48.2% vs. 1.8%) in L-PRF group (p<0.001). NSS CAL gain between groups (3.1 vs. 2.7 mm) (p>0.05).
	Parallel Double-blind  9 months	18 ♀, 24 ♂  Mean age: 35 ± 6 Range: 30-50  Smoking: No				
Rosamma <i>et al.</i> (2012)	RCT	15 – (15)	3 walls IBDs  C: n=15, OFD  T: n= 15, OFD + L-PRF	Hardware: <sup>2</sup>  Setting: 3000 rpm / 10 min	1 L-PRF clot 0 L-PRF membrane  10 mL blood/clot	<b>L-PRF + OFD vs. OFD</b> SS PD reduction (4.6 vs. 2.4 mm), CAL gain (4.7 vs. 1.4 mm) and radiographic intrabony defect depth (1.9 vs. 0.6 mm) in favour of L-PRF sites (p<0.00).
	Split-mouth Not blind  12 months	9 ♀, 6 ♂  Mean age: 29 ± 7 Range: 17-44  Smoking: No				
Ajwani <i>et al.</i> (2015)	RCT	20 – (20)	2 and 3 walls IBDs  C: n= 20, OFD  T: n= 20, OFD + L-PRF	Hardware: <sup>3</sup>  Setting: 3000 rpm / 10 min	1 L-PRF clot 0 L-PRF membrane  10 mL blood/clot	<b>L-PRF + OFD vs. OFD</b> NSS improvement in PD (1.9 vs. 1.6 mm) and CAL (1.8 vs. 1.3 mm) (p>0.05).  SS more bone fill (2.6 vs. 1.3 mm) in favour of L-PRF group (p<0.05).
	Split-mouth Single-blind  9 months	10 ♀, 10 ♂  Mean age: 30.5 Range: ?  Smoking: No				



<i>Pradeep et al. (2015)</i>	RCT	126 – (120)	3 walls IBDs			
	Parallel Triple-blind	60 ♀, 60 ♂ Mean age: 41 ± 6 Range: 30-50 Smoking: No	C: n=30, OFD T <sub>1</sub> : n= 30, OFD + L-PRF T <sub>2</sub> : n= 30, OFD + 1% MF T <sub>3</sub> : n= 30, OFD + L-PRF + 1% MF	Hardware: ? Setting: 3000 rpm / 10 min	2 L-PRF clot 0 L-PRF membrane 10 mL blood/clot	<b>L-PRF + OFD vs. OFD</b> SS PD reduction (4.0 vs. 3.0 mm), CAL gain (4.0 vs. 2.9 mm) in favour of T <sub>1</sub> compared to C (p<0.05).
<i>L-PRF vs. PRP</i>						
<i>Pradeep et al. (2012)</i>	RCT	54 – (50)	3 wall IBDs			
	Parallel Double-blind	27 ♀, 27 ♂ Mean age: 36.8 Range: ? Smoking: No	C: n=17 (30 sites), OFD T <sub>1</sub> : n= 16 (30 sites), L-PRF T <sub>2</sub> : n= 17 (30 sites), PRP	Hardware: ? Setting: 3000 rpm / 10 min	1 L-PRF clot 2 L-PRF membrane 10 mL blood/clot	<b>L-PRF vs. PRP</b> SS PD reduction (T <sub>1</sub> : 3.7 vs. T <sub>2</sub> : 3.7 vs. C: 2.7mm) and bone fill (T <sub>1</sub> 55% vs. C: 2.9 mm ) and bone fill (T <sub>1</sub> 55% vs. T <sub>2</sub> : 56% vs. C: 1.5%) in favour of L-PRF and PRP groups (p<0.05).  NSS CAL gain (T <sub>1</sub> : 3.17 vs. T <sub>2</sub> : 2.9 vs. C: 2.9 mm) (p>0.05).
<i>L-PRF vs. L-PRF + BPBM</i>						
<i>Lekovic et al. (2012)</i>	RCT	17 – (17)	2 and 3 walls IBDs			
	Split-mouth Double-blind	11 ♀, 6 ♂ Mean age: 44 ± 9 Range: ? Smoking: 12 non smokers/5 smokers	C: n= 17, L-PRF T: n= 17, L-PRF+ BPBM	Hardware: <sup>4</sup> Setting: 1000 g / 10 min	1 L-PRF clot 1 L-PRF membrane 10 mL blood/clot	<b>L-PRF vs. L-PRF + BPBM</b> SS PD reduction (4.4 vs. 3.3 mm), CAL gain (2.4 vs. 3.8 mm), and bone fill (2.1 vs. 4.6 mm) in favour of L-PRF-BPBM group (p<0.001).

*L-PRF + DFDBA vs. DFDBA*

<i>Bansal &amp; Bharti (2013)</i>	RCT Split-mouth Not blind 6 months	10 – (10) Gender: ? Mean age: ? Range: ? Smoking: ?	walls IBDs not mentioned C: n= 10, DFDBA T: n= 10, L-PRF + DFDBA	Hardware: ? Setting: 3000 rpm / 10 min	1 L-PRF clot 0 L-PRF membrane 10 mL blood/clot	<b>L-PRF + DFDBA vs. DFDBA</b> SS PD reduction (4.0 vs. 3.1 mm) and CAL gain (3.4 vs. 2.3 mm) in favour of L-PRF group (p<0.05). NNSD for bone fill (2.3 vs. 1.9 mm) and alveolar crest resorption (0.02 vs. 0.04 mm) (p>0.01) .
	RCT Split-mouth Not blind 6 months	20 – (20) Gender: ? Mean age: ? Range: 20-55 Smoking: No	2 and 3 walls IBDs C: n= 20, OFD + DFDBA T: n= 20, OFD + L-PRF	Hardware: ? Setting: 3000 rpm / 10 min	? L-PRF clot 0 L-PRF membrane 10 mL blood/clot	<b>L-PRF + DFDBA vs. DFDBA</b> NSS PD reduction (3.6 vs. 3.7 mm), CAL (2.9 vs. 2.9 mm) and GML (-0.4 vs. -0.3 mm).
	RCT Split-mouth Double-blind 12 months	32 – (30) 14 ♀, 18 ♂ Mean age: 52 ± 7 Range: ? Smoking: No	2 and 3 walls IBDs C: n= 32, DFDBA + saline T: n= 32, DFDBA + L-PRF	Hardware: ? Setting: 400 g / 12min	1? L-PRF clot >1 L-PRF membrane 10 mL blood/clot	<b>L-PRF + DFDBA vs. DFDBA</b> SS PD reduction (4.2 vs. 3.6 mm), CAL gain (3.7 vs. 2.6 mm), REC (0.5 vs. 1.0 mm), bone fill (3.5 vs. 2.5 mm) and defect resolution (3.7 vs. 2.7 mm) in favour of DFDBA + L-PRF group (p<0.05).
<i>L-PRF vs. Emdogain®</i>						
<i>Gupta et al. (2014)</i>	RCT 6 months	30 – (30) 15 ♀, 15 ♂ Mean age: ? Range: 30-65 Smoking: No	3 walls IBDs C: n= 22, OFD + Emdogain® T: n= 22, OFD + L-PRF	Hardware: <sup>3</sup> Setting: 3000 rpm / 12 min	? L-PRF clot 0 L-PRF membrane 10 mL blood/clot	<b>L-PRF vs. Emdogain®</b> NSS PD reduction (1.8 vs. 1.8 mm) and CAL gain (2.0 vs. 1.8 mm) (p>0.05). SS more defect resolution in Emdogain® group (43% vs. 32%) (p<0.05).



<i>L-PRF vs. nano-bone®</i>						
<i>Elgendy &amp; Abo Shady (2015)</i>	RCT Split-mouth Not blind 6 months	20 – (20) Gender: ? Mean age: C: 40 ± 6, T: 44 ± 8 Range: ? Smoking: No or light smokers (<10cig/day)	walls IBDs not mentioned C: n= 20, OFD + nano-bone® T: n= 20, L-PRF + nano-bone®	Hardware: ? Setting: 3000 rpm / 10 min	? L-PRF clot 0 L-PRF membrane 10 mL blood/clot	<b>L-PRF vs. nano-bone®</b> SS PD reduction (7.1 vs. 6.7 mm) and CAL gain (7.4 vs. 7.1 mm) in favour of L-PRF group (p<0.01).
<i>L-PRF vs. ABG</i>						
<i>Mathur et al. (2015)</i>	RCT Parallel Not blind 6 months	25 – (25) 11 ♀, 14 ♂ Mean age: 40 ± 5 Range: ? Smoking: ?	3 walls IBDs C: n= 19, OFD + ABG T: n= 19, OFD + L-PRF	Hardware: <sup>3</sup> Setting: 3000 rpm / 10 min	? L-PRF clot 0 L-PRF membrane 10 mL blood/clot	<b>L-PRF vs. ABG</b> NSS PD reduction (2.6 vs. 2.4 mm), and CAL gain (2.5 vs. 2.6 mm) (p>0.05).

<sup>1</sup>: Process protocol, Nice, France, <sup>2</sup>: KW-70, Almicro™ Instruments, Ambala Cantt., Haryana, India, <sup>3</sup>: R-4C, REMI, Mumbai, India. <sup>4</sup>: Labofuge 300, Kendro Laboratory Products GmbH, Osterode, Germany. C: control group, T: test group, OFD: open flap debridement, SS: statistically significant, NSS: no statistically significant, PD: pocket depth, CAL: clinical attachment level, REC: gingival recession, PRP: platelet rich plasma, BPBM: Bovine porous bone mineral, DFDBA: demineralized freeze-dried bone allograft, ABG: autologous bone graft.

Table 3. L-PRF for furcation defects. Papers have been arranged by subapplications (L-PRF + OFD vs. OFD).

Authors (year)	Study design, Duration	No. of participants baseline (end), gender, age, Smoking	Groups C: control T: test	L-PRF preparation	Surgical protocol	Results
<i>L-PRF + OFD vs. OFD</i>						
Sharma & Pradeep (2011a)	RCT	18 – (18)	Furcation degree II	Hardware: ?	1 L-PRF clot	<b>L-PRF + OFD vs. OFD</b> SS PD reduction (4.1 vs. 2.9 mm), CAL gain (2.3 vs. 1.2 mm) and bone fill (50% vs. 16.7%) in favour of L-PRF group (p<0.001).
	Split-mouth Double-blind 9 months	8 ♀, 10 ♂ Mean age: 34.2 Range: ? Smoking: No	C: n= 18, OFD T: n= 18, L-PRF	Setting: 3000 rpm / 10 min	2 L-PRF membrane 10 mL blood/clot	
Bajaj et al. (2013)	RCT	42 – (37)	Furcation degree II	Hardware: <sup>1</sup>	1 L-PRF clot	<b>L-PRF + OFD vs. OFD</b> SS PD reduction (T <sub>1</sub> : 4.2 vs. T <sub>2</sub> : 3.9 vs. C: 1.5 mm), CAL gain (T <sub>1</sub> : 2.8 vs. T <sub>2</sub> : 2.7 vs. C: 1.3 mm) and bone fill (T <sub>1</sub> : 44% vs. T <sub>2</sub> : 42% vs. C: 2.8%) (p<0.001).
	Parallel Double-blind 9 months	20 ♀, 22 ♂ Mean age: 39.4 Range: ? Smoking: ?	C: n= 12 (23), OFD T <sub>1</sub> : n= 12 (24), L-PRF T <sub>2</sub> : n= 13 (25), PRP	Setting: 400g / 10 min	2 L-PRF membrane 10 mL blood/clot	

<sup>1</sup>: R-4C, REMI, Mumbai, India. C: control group, T: test group, OFD: open flap debridement, PD: pocket depth, CAL: clinical attachment level, SS: statistically significant.

Table 4. L-PRF for periodontal plastic surgery. Papers have been arranged by subapplications (CAF + L-PRF vs. CAF, CAF + L-PRF vs. CAF + CTG, L-PRF vs. EMD).

Authors (year)	Study design, Duration	No. of participants baseline (end), gender, age, Smoking	Groups C: control T: test	L-PRF preparation	Surgical protocol	Results
<i>CAF + L-PRF vs. CAF</i>						
<i>Aroca et al. (2009)</i>	RCT	20 – (20)				<b>CAF + L-PRF vs. CAF</b> SS more root coverage at 3 months (91.5% vs. 80%) and 6 months (88% vs. 81%) in favour of control group (p<0.01).  NSSD for PD reduction in both groups. more CAL gain (2.6 vs. 2.5 mm) and GTH (0.0 vs. 0.3 mm) in favour of control group (p>0.05).
	Split-mouth Not blind  6 months	15 ♀, 5 ♂  Mean age: 31.7 Range: 22-47  Smoking: No or ≤ 20 cig/day	C: n= 21, CAF  T: n= 21, CAF + L-PRF	Hardware: <sup>1</sup>  Setting: 3000 rpm / 10min	4? L-PRF membrane Modified CAF  10 mL blood/clot	
<i>Padma et al. (2013)</i>	RCT	15 – (15)				<b>CAF + L-PRF vs. CAF</b> SS more root coverage (100% vs. 68%) in favour of L- PRF group (p<0.05).  SS more WKG (2.4 vs. 2.2 mm) in favour of L-PRF group (p<0.05).
	Split-mouth Not blind  6 months	Gender: ?  Mean age: ? Range: 18-35  Smoking: No	C: n= 15, CAF  T: n= 15, CAF + L-PRF	Hardware: ?  Setting: 3000 rpm / 10 min	1 L-PRF membrane CAF  10 mL blood/clot	
<i>Gupta et al. (2015)</i>	RCT	26 – (26)				<b>CAF + L-PRF vs. CAF</b> NSSD for outcomes in both groups for any parameter (p>0.05).
	Parallel Not blind  6 months	10 ♀, 16 ♂  Mean age: 37 ± 9 Range: ?  Smoking: No	C: n= 15, CAF  T: n= 15, CAF + L-PRF	Hardware: <sup>2</sup>  Setting: 2700 rpm / 12 min	1 L-PRF membrane Modified CAF  10 mL blood/clot	
<i>Thamaraiselv an et al. (2015)</i>	RCT	20 – (20)				<b>CAF + L-PRF vs. CAF</b> NSSD for outcomes in both groups for any parameter (p>0.05).
	Parallel Single-blind  6 months	2 ♀, 18 ♂  Mean age: ? Range: 21-47  Smoking: No	C: n= 10, CAF  T: n= 10, CAF + L-PRF	Hardware: ?  Setting: 3000 rpm / 10 min	1 L-PRF membrane + surgical site rinsed with L- PRF exudate CAF  10 mL blood/clot	

CAF + L-PRF vs. CAF + CTG						
<i>Jankovic et al. (2012)</i>	RCT Split-mouth Single-blind 6 months	15 – (15) 10 ♀, 5 ♂ Mean age: ? Range: 19-47 Smoking: No	C: n= 15, CAF + CTG T: n= 15, CAF + L-PRF	Hardware: ? Setting: 3000 rpm / 10 min	1 L-PRF membrane CAF 10 mL blood/clot	<b>CAF + L-PRF vs. CAF + CTG</b> NSSD for PD, CAL and root coverage for L-PRF and CTG group (p>0.05). SS more gain of keratinized tissue width (0.8 vs. 1.4 mm) for CTG group (p<0.05).
<i>Eren &amp; Atilla (2014)</i>	RCT Split-mouth Single-blind 6 months	27 – (22) 13 ♀, 9 ♂ Mean age: 34 ± 13 Range 18.5 Smoking: No	C: n= 22, CAF+ SCTG T: n= 22, CAF+ L-PRF	Hardware: <sup>3</sup> Setting: 400 g / 12min	1 L-PRF membrane CAF 10 mL blood/clot	<b>CAF + L-PRF vs. CAF + CTG</b> NSSD for root coverage in L-PRF group (92.7%) and control group (94.2%) (p>0.05). NSSD for complete root coverage in L-PRF group (72.7%) and control group (77.3%) (p>0.05).
<i>Keceli et al. (2015)</i>	RCT Split-mouth Single-blind 6 months	40 – (40) 27 ♀, 13 ♂ Mean age: 40 ± 7 Range: ? Smoking: No	C: n= 20, CAF + CTG T: n= 20, CAF + CG + L-PRF	Hardware: ? Setting: 3000 rpm / 10 min	1 L-PRF membrane CAF 10 mL blood/clot	<b>CAF + L-PRF vs. CAF + CTG</b> NSSD for outcomes in both groups for any parameter (p>0.05).
<i>Tunali et al. (2015)</i>	RCT Split-mouth Single-blind 12 months	10 – (10) 6 ♀, 4 ♂ Mean age: 34.2 Range: 25-52 Smoking: No	C: n= 10, CAF + CTG T: n= 10, CAF + L-PRF	Hardware: <sup>1</sup> Setting: 2700 rpm / 12 min	1 L-PRF membrane CAF 10 mL blood/clot	<b>CAF + L-PRF vs. CAF + CTG</b> similar outcomes in both groups for any parameter.
L-PRF vs. EMD						
<i>Jankovic et al. (2010)</i>	RCT Split-mouth Not blind 12 months	20 – (20) 12 ♀, 8 ♂ Mean age: ? Range: 21-48 Smoking: No	C: n= 20, CAF + EMD T: n= 20, CAF + L-PRF	Hardware: ? Setting: 3000 rpm / 10 min	1 L-PRF membrane Modified CAF 10 mL blood/clot	<b>L-PRF vs. EMD</b> more complete root coverage (65% vs. 60%) in L-PRF group. similar WKG between groups.

<sup>1</sup>: EBA 20, Hettich GmbH & Co KG, Tuttlingen, Germany. <sup>2</sup>: RC-4, REMI, Mumbai, India. <sup>3</sup>: Nüve Laboratory Equipments, NF200, Ankara, Turkey. C: control group, T: test group, CAF: coronally advanced flap, PD: pocket depth, CAL: clinical attachment level, GTH: gingival thickness, WKG: width of keratinized gingiva, EMD: Emdogain®, CTG: connective tissue graft, SCTG: subepithelial connective tissue graft.

## References

1. Dohan Ehrenfest DM, Andia I, Zumstein MA, Zhang CQ, Pinto NR, Bielecki T. Classification of platelet concentrates (Platelet-Rich Plasma-PRP, Platelet-Rich Fibrin-PRF) for topical and infiltrative use in orthopedic and sports medicine: current consensus, clinical implications and perspectives. *Muscles Ligaments Tendons J.* 2014;4(1):3-9.
2. Matras H. [Effect of various fibrin preparations on reimplantations in the rat skin]. *Osterr Z Stomatol.* 1970;67(9):338-59.
3. Marx RE. Platelet-rich plasma (PRP): what is PRP and what is not PRP? *Implant Dent.* 2001;10(4):225-8.
4. Marx RE, Carlson ER, Eichstaedt RM, Schimmele SR, Strauss JE, Georgeff KR. Platelet-rich plasma: Growth factor enhancement for bone grafts. *Oral Surg Oral Med Oral Pathol Oral Radiol Endod.* 1998;85(6):638-46.
5. Dohan DM, Choukroun J, Diss A, Dohan SL, Dohan AJ, Mouhyi J, et al. Platelet-rich fibrin (PRF): a second-generation platelet concentrate. Part I: technological concepts and evolution. *Oral Surg Oral Med Oral Pathol Oral Radiol Endod.* 2006;101(3):e37-44.
6. Dohan Ehrenfest DM, Rasmusson L, Albrektsson T. Classification of platelet concentrates: from pure platelet-rich plasma (P-PRP) to leucocyte- and platelet-rich fibrin (L-PRF). *Trends Biotechnol.* 2009;27(3):158-67.
7. Choukroun J. Une opportunité en paro-implantologie: le PRF. *Implantodontie.* 2001;42:55-62.
8. Dohan DM, Choukroun J, Diss A, Dohan SL, Dohan AJ, Mouhyi J, et al. Platelet-rich fibrin (PRF): a second-generation platelet concentrate. Part II: platelet-related biologic features. *Oral Surg Oral Med Oral Pathol Oral Radiol Endod.* 2006;101(3):e45-50.
9. Dohan DM, Choukroun J, Diss A, Dohan SL, Dohan AJ, Mouhyi J, et al. Platelet-rich fibrin (PRF): a second-generation platelet concentrate. Part III: leucocyte activation: a new feature for platelet concentrates? *Oral Surg Oral Med Oral Pathol Oral Radiol Endod.* 2006;101(3):e51-5.
10. Dohan Ehrenfest DM, Del Corso M, Diss A, Mouhyi J, Charrier JB. Three-dimensional architecture and cell composition of a Choukroun's platelet-rich fibrin clot and membrane. *J Periodontol.* 2010;81(4):546-55.
11. Khorshidi H, Raoofi S, Bagheri R, Banihashemi H. Comparison of the Mechanical Properties of Early Leukocyte- and Platelet-Rich Fibrin versus PRGF/Endoret Membranes. *Int J Dent.* 2016;2016:1849207.
12. Burnouf T, Goubran HA, Chen TM, Ou KL, El-Ekiaby M, Radoscovic M. Blood-derived biomaterials and platelet growth factors in regenerative medicine. *Blood Rev.* 2013;27(2):77-89.
13. Rowe SL, Lee S, Stegmann JP. Influence of thrombin concentration on the mechanical and morphological properties of cell-seeded fibrin hydrogels. *Acta Biomater.* 2007;3(1):59-67.
14. Yang LC, Hu SW, Yan M, Yang JJ, Tsou SH, Lin YY. Antimicrobial activity of platelet-rich plasma and other plasma preparations against periodontal pathogens. *J Periodontol.* 2015;86(2):310-8.
15. Sharma A, Pradeep AR. Treatment of 3-wall intrabony defects in patients with chronic periodontitis with autologous platelet-rich fibrin: a randomized controlled clinical trial. *J Periodontol.* 2011;82(12):1705-12.
16. Thorat M, Pradeep AR, Pallavi B. Clinical effect of autologous platelet-rich fibrin in the treatment of intra-bony defects: a controlled clinical trial. *J Clin Periodontol.* 2011;38(10):925-32.
17. Rosamma Joseph V, Raghunath A, Sharma N. Clinical effectiveness of autologous platelet rich fibrin in the management of infrabony periodontal defects. *Singapore Dent J.* 2012;33(1):5-12.

18. Ajwani H, Shetty S, Gopalakrishnan D, Kathariya R, Kulloli A, Dolas RS, et al. Comparative evaluation of platelet-rich fibrin biomaterial and open flap debridement in the treatment of two and three wall intrabony defects. *J Int Oral Health*. 2015;7(4):32-7.
19. Pradeep AR, Nagpal K, Karvekar S, Patnaik K, Naik SB, Guruprasad CN. Platelet-rich fibrin with 1% metformin for the treatment of intrabony defects in chronic periodontitis: a randomized controlled clinical trial. *J Periodontol*. 2015;86(6):729-37.
20. Pradeep AR, Rao NS, Agarwal E, Bajaj P, Kumari M, Naik SB. Comparative evaluation of autologous platelet-rich fibrin and platelet-rich plasma in the treatment of 3-wall intrabony defects in chronic periodontitis: a randomized controlled clinical trial. *J Periodontol*. 2012;83(12):1499-507.
21. Lekovic V, Milinkovic I, Aleksic Z, Jankovic S, Stankovic P, Kenney EB, et al. Platelet-rich fibrin and bovine porous bone mineral vs. platelet-rich fibrin in the treatment of intrabony periodontal defects. *J Periodontal Res*. 2012;47(4):409-17.
22. Bansal C, Bharti V. Evaluation of efficacy of autologous platelet-rich fibrin with demineralized-freeze dried bone allograft in the treatment of periodontal intrabony defects. *J Indian Soc Periodontol*. 2013;17(3):361-6.
23. Shah M, Patel J, Dave D, Shah S. Comparative evaluation of platelet-rich fibrin with demineralized freeze-dried bone allograft in periodontal infrabony defects: A randomized controlled clinical study. *J Indian Soc Periodontol*. 2015;19(1):56-60.
24. Agarwal A, Gupta ND, Jain A. Platelet rich fibrin combined with decalcified freeze-dried bone allograft for the treatment of human intrabony periodontal defects: a randomized split mouth clinical trail. *Acta Odontol Scand*. 2016;74(1):36-43.
25. Gupta SJ, Jhingran R, Gupta V, Bains VK, Madan R, Rizvi I. Efficacy of platelet-rich fibrin vs. enamel matrix derivative in the treatment of periodontal intrabony defects: a clinical and cone beam computed tomography study. *J Int Acad Periodontol*. 2014;16(3):86-96.
26. Elgendy EA, Abo Shady TE. Clinical and radiographic evaluation of nanocrystalline hydroxyapatite with or without platelet-rich fibrin membrane in the treatment of periodontal intrabony defects. *J Indian Soc Periodontol*. 2015;19(1):61-5.
27. Mathur A, Bains VK, Gupta V, Jhingran R, Singh GP. Evaluation of intrabony defects treated with platelet-rich fibrin or autogenous bone graft: A comparative analysis. *Eur J Dent*. 2015;9(1):100-8.
28. Sharma A, Pradeep AR. Autologous platelet-rich fibrin in the treatment of mandibular degree II furcation defects: a randomized clinical trial. *J Periodontol*. 2011;82(10):1396-403.
29. Bajaj P, Pradeep AR, Agarwal E, Rao NS, Naik SB, Priyanka N, et al. Comparative evaluation of autologous platelet-rich fibrin and platelet-rich plasma in the treatment of mandibular degree II furcation defects: a randomized controlled clinical trial. *J Periodontal Res*. 2013;48(5):573-81.
30. Aroca S, Keglevich T, Barbieri B, Gera I, Etienne D. Clinical evaluation of a modified coronally advanced flap alone or in combination with a platelet-rich fibrin membrane for the treatment of adjacent multiple gingival recessions: a 6-month study. *J Periodontol*. 2009;80(2):244-52.
31. Padma R, Shilpa A, Kumar PA, Nagasri M, Kumar C, Sreedhar A. A split mouth randomized controlled study to evaluate the adjunctive effect of platelet-rich fibrin to coronally advanced flap in Miller's class-I and II recession defects. *J Indian Soc Periodontol*. 2013;17(5):631-6.
32. Gupta S, Banthia R, Singh P, Banthia P, Raje S, Aggarwal N. Clinical evaluation and comparison of the efficacy of coronally advanced flap alone and in combination with platelet rich fibrin membrane in the treatment of Miller Class I and II gingival recessions. *Contemp Clin Dent*. 2015;6(2):153-60.

33. Thamaraiselvan M, Elavarasu S, Thangakumaran S, Gadagi JS, Arthie T. Comparative clinical evaluation of coronally advanced flap with or without platelet rich fibrin membrane in the treatment of isolated gingival recession. *J Indian Soc Periodontol*. 2015;19(1):66-71.
34. Jankovic S, Aleksic Z, Klokkevold P, Lekovic V, Dimitrijevic B, Kenney EB, et al. Use of platelet-rich fibrin membrane following treatment of gingival recession: a randomized clinical trial. *Int J Periodontics Restorative Dent*. 2012;32(2):e41-50.
35. Eren G, Atilla G. Platelet-rich fibrin in the treatment of localized gingival recessions: a split-mouth randomized clinical trial. *Clin Oral Investig*. 2014;18(8):1941-8.
36. Keceli HG, Kamak G, Erdemir EO, Evginer MS, Dolgun A. The Adjunctive Effect of Platelet-Rich Fibrin to Connective Tissue Graft in the Treatment of Buccal Recession Defects: Results of a Randomized, Parallel-Group Controlled Trial. *J Periodontol*. 2015;86(11):1221-30.
37. Tunalı M, Özdemir H, Arabacı T, Gürbüz B, Pıkdöken L, Firatlı E. Clinical evaluation of autologous platelet-rich fibrin in the treatment of multiple adjacent gingival recession defects: a 12-month study. *Int J Periodontics Restorative Dent*. 2015;35(1):105-14.
38. Jankovic S, Aleksic Z, Milinkovic I, Dimitrijevic B. The coronally advanced flap in combination with platelet-rich fibrin (PRF) and enamel matrix derivative in the treatment of gingival recession: a comparative study. *Eur J Esthet Dent*. 2010;5(3):260-73.
39. Rock L. Potential of platelet rich fibrin in regenerative periodontal therapy: literature review. *The Canadian Journal of Dental Hygiene*. 2013;47:33-7.
40. Shah M, Deshpande N, Bharwani A, Nadig P, Doshi V, Dave D. Effectiveness of autologous platelet-rich fibrin in the treatment of intra-bony defects: A systematic review and meta-analysis. *J Indian Soc Periodontol*. 2014;18(6):698-704.
41. Anilkumar K, Geetha A, Umasudhakar, Ramakrishnan T, Vijayalakshmi R, Pameela E. Platelet-rich-fibrin: A novel root coverage approach. *J Indian Soc Periodontol*. 2009;13(1):50-4.
42. Agarwal K, Chandra C, Agarwal K, Kumar N. Lateral sliding bridge flap technique along with platelet rich fibrin and guided tissue regeneration for root coverage. *J Indian Soc Periodontol*. 2013;17(6):801-5.
43. Singh J, Bharti V. Laterally positioned flap-revised technique along with platelet rich fibrin in the management of Miller class II gingival recession. *Dent Res J (Isfahan)*. 2013;10(2):268-73.
44. Cairo F, Pagliaro U, Nieri M. Treatment of gingival recession with coronally advanced flap procedures: a systematic review. *J Clin Periodontol*. 2008;35(8 Suppl):136-62.
45. Chambrone L, Chambrone D, Pustiglioni FE, Chambrone LA, Lima LA. The influence of tobacco smoking on the outcomes achieved by root-coverage procedures: a systematic review. *J Am Dent Assoc*. 2009;140(3):294-306.
46. de Sanctis M, Clementini M. Flap approaches in plastic periodontal and implant surgery: critical elements in design and execution. *J Clin Periodontol*. 2014;41 Suppl 15:S108-22.
47. Arimilli S, Damratoski BE, Bombick B, Borgerding MF, Prasad GL. Evaluation of cytotoxicity of different tobacco product preparations. *Regul Toxicol Pharmacol*. 2012;64(3):350-60.
48. Anitua E. The use of plasma-rich growth factors (PRGF) in oral surgery. *Pract Proced Aesthet Dent*. 2001;13(6):487-93; quiz -93.

## CHAPTER 2

### Regenerative potential of leucocyte- and platelet-rich fibrin. Part B: sinus floor elevation, alveolar ridge preservation and implant therapy.

#### A systematic review

Castro Ana B, Meschi Nastaran, Temmerman Andy, Pinto Nelson, Lambrechts Paul, Teughels Wim & Quirynen Marc. (2017) *Journal of Clinical Periodontology* 44; 67-82.

#### **Abstract**

**Aim:** To analyse the effect of leucocyte- and platelet-rich fibrin (L-PRF) on bone regeneration procedures and osseointegration.

**Material & Methods:** An electronic and hand search was conducted in three databases (MEDLINE, EMBASE and Cochrane). Only randomized clinical trials, written in English where L-PRF was applied in bone regeneration and implant procedures, were selected. No follow-up restrictions were applied.

**Results:** A total of 14 articles were included and processed. Three subgroups were created depending on the application: sinus floor elevation (SFE), alveolar ridge preservation and implant therapy. In SFE, for a lateral window as well as for the trans-alveolar technique, histologically faster bone healing was reported when L-PRF was added to most common xenografts. L-PRF alone improved the preservation of the alveolar width, resulting in less buccal bone resorption compared to natural healing. In implant therapy, better implant stability over time and less marginal bone loss were observed when L-PRF was applied. Meta-analyses could not be performed due to the heterogeneity of the data.

**Conclusions:** Despite the lack of strong evidence found in this systematic review, L-PRF might have a positive effect on bone regeneration and osseointegration.

#### **Introduction**

After tooth extraction, a marked resorption of the alveolar ridge occurs due to the tooth-bundle bone-dependent relationship (1), both horizontally and vertically. A more recent study (2) with analysis of the alveolar ridge after tooth extraction via CBCT, reported even 3.5 times more severe bone resorption than the findings described in the existing literature. These changes in the alveolar ridge after tooth extraction have to be taken into account when implants are planned. Farmer & Darby (2014) (3) concluded that the majority of the implants placed in aesthetic zones required simultaneous bone augmentation due to the resorption in the mid-buccal aspect.

Several bone substitutes and/or procedures have been described in the literature but no specific technique neither for sinus augmentation nor for guided bone regeneration (GBR) procedures have been strongly recommended (4, 5). The use of growth factors has also been proposed as adjuvant of bone grafting. Jung et al. (2008) (6) concluded that bone morphogenetic proteins (BMP-2, BMP-7), growth-differentiation factor-5 (GDF-5), platelet-derived growth factor (PDGF) and parathyroid hormone (PTH) might stimulate local bone augmentation during ridge preservation procedures. For sinus augmentation, also BMP-2 has been proposed as adjuvant of conventional techniques (7).

Platelet concentrates were suggested for bone augmentation procedures because of their constant release of growth factors. Platelet concentrates were initially used as fibrin glue to improve



wound healing (8). Later, the first generation of platelet concentrates, which included platelet-rich plasma (PRP) (Marx 2001) and plasma rich in growth factors (PRGF) (9), were developed. However, they had some disadvantages: expensive, operator dependent and extended production time. The second generation of platelet concentrates appeared to improve and ease the use of this technique (10, 11). Leucocyte- and platelet-rich fibrin (L-PRF) belongs to the second generation of platelet concentrates (12). For its preparation, 9–10 ml blood is withdrawn from the patient in plastic/glass-coated tubes through venepuncture. No anticoagulants or additives are used. The blood is immediately centrifuged at 400 g during 10–12 min. After centrifugation, three layers are obtained: at the bottom, red blood corpuscles (RBC); at the top, platelet-poor plasma (PPP); and in the middle, a fibrin clot (L-PRF). L-PRF contains a dense fibrin fibre network where platelets and leucocytes are enmeshed and it can serve as scaffold for other type of cells due to its favourable mechanical properties (13, 14). Its content in leucocytes and platelets results in a constant release of growth factors such as PDGF, transforming growth factor (TGF), vascular endothelial growth factor (VEGF) and insulin-like growth factor (IGF) for 7–14 days (15, 16). Its biological characteristics could also improve/facilitate the osseointegration process (17).

The main aim of this systematic review was to analyse the capacity of L-PRF to promote bone regeneration in systemically healthy patients (ASA I). Its influence on potential adverse events after surgery was considered as a secondary aim.

## **Materials & Methods**

This systematic review follows the guidelines of the Belgian Centre for Evidence-Based Medicine (CEBAM), Belgian Branch of the Dutch Cochrane Centre. It was conducted in accordance with the Transparent Reporting of Systematic Reviews and Meta-analyses (18).

### **Focused PICO question**

The following statements were used to conduct the systematic search:

- Population (P) = systemically healthy humans (ASA I) with lack of alveolar bone and/or with need of implant therapy.
- Intervention (I) = use of L-PRF (protocol 2700 r.p.m./12 min. or 3000 r.p.m./10 min.) as biomaterial (alone or in combination with a graft material) in guided bone regeneration techniques and implant surgery.
- Comparison (C) = traditional techniques using bone substitute (xenograft, allograft, etc.) with/without collagen membrane or connective tissue graft.
- Outcome (O) = alveolar bone regeneration (reported as newly formed bone (%), soft tissue and bone healing (reported as healing index scores, bone resorption in mm and/or in technetium-99 m methylene diphosphonate uptake) and implant osseointegration (reported as ISQ values and/or marginal bone loss in mm).

A PICO question was created to define the search strategy: *Does L-PRF promote regeneration in systemically healthy patients (ASA I) during guided bone regeneration techniques and implant surgery compared to traditional techniques?*

### **Search strategy**

An electronic search was performed in three Internet databases: the National Library of Medicine, Washington, DC (MEDLINE-PubMed), EMBASE (Excerpta Medical Database by Elsevier), and Cochrane Central Register of Controlled Trials (CENTRAL). The search strategy is shown in Table 1. No

language or time restrictions were applied in the first search. However, only studies written in English were included for selection. The search was limited to human studies. The last electronic search was performed on the 31st of July 2015. This search was enriched by hand searches, citation screening and expert recommendations.

### Screening and selection

Two reviewers (A.C., N.M.) screened independently the titles and abstract obtained from the first search. When publications did not meet the inclusion criteria, they were excluded upon reviewer's agreement. Any disagreement between the two reviewers was resolved by discussion. All full texts of the eligible articles were examined by both reviewers. The articles that fulfilled all selection criteria were processed for data extraction. The two most accepted protocols for the preparation of L-PRF (2700 r.p.m./12 min. or 3000 r.p.m./10 min.) were included. The inclusion and exclusion criteria are summarized in Table 2.

### Assessment of heterogeneity

The heterogeneity of the included studies was evaluated based on following factors: (1) study design and follow-up duration, (2) subject characteristics and smoking habits, and (3) surgical protocol: (a) centrifugation protocol (2700 r.p.m./12 min. or 3000 r.p.m./10 min.), (b) ml blood used to prepare L-PRF and (c) number of clots/membranes (if used).

### Data extraction and quality assessment

Data extraction was performed for the included studies. All variables analysed in each study were processed. Where possible, a meta-analysis was performed.

Both reviewers (A.C., N.M.) independently performed the quality assessment using the Cochrane Collaboration's tool for assessing risk of bias. Six quality criteria were verified: (1) sequence generation or randomization component, (2) allocation concealment, (3) blinding of participants, personnel and outcome assessors, (4) incomplete/missing outcome data, (5) selective outcome reporting and (6) other sources of bias. In case of any doubt, the authors were contacted for clarification or to provide missing information. Each study was classified into the following groups: low risk of bias if all quality criteria were judged as "present", moderate risk of bias if one or more key domains were "unclear", and high risk of bias if one or more key domains were "absent".

## Results

### Search and selection

As a result of the electronic and hand search, 603 articles were obtained, of which 154 were duplicate and consequently removed (Figure 1).

A total of 449 articles were included for title and abstract screening. From those, 26 articles were included for full text review. Twelve articles were excluded after full text screening, which was conducted independently by two reviewers (A.C., N.M.) (Table 3).

Fourteen randomized control trials (RCTs) fulfilled the inclusion criteria and were included for analysis. The included articles were classified into three subgroups, depending on the indication for the use of L-PRF (Tables 1, 2, 3).

1. Sinus floor elevation procedures (SFE):  $n = 3$ , Tatullo et al. (2012) (19), Zhang et al. (2012) (20) and Gassling et al. (2013) (21).

2. Alveolar ridge preservation:  $n = 8$ , Gürbüz et al. (2010) (22), Singh et al. (2012) (23), Hauser et al. (2013) (24), Suttapreyasri & Leepong (2013) (25), Baslarli et al. (2015) (26), Marenzi et al. (2015) (27), Kumar et al. (2015) (28) and Yelamali & Saikrishna (2015) (29).
3. Implant therapy:  $n = 3$ , Boora et al. (2015) (30), Hamzacebi et al. (2015) (31) and Öncü & Alaadinöglu (2015) (32).

### Assessment of heterogeneity

#### *Study design and evaluation period*

All studies were RCTs and often a split-mouth design was applied. The following articles fulfilled both study designs: SFE 1/3 (Gassling et al. 2013), ridge preservation 4/8 (Gürbüz et al. 2010, Singh et al. 2012, Marenzi et al. 2015, Yelamali & Saikrishna 2015), and implant therapy 0/3. The follow-up ranged considerably (SFE 5–6 months, ridge preservation 7 days to 4 months, implant therapy 1–6 months).

#### *Subject characteristics, smoking habits and surgical protocol*

Healthy subjects with no active periodontal disease were included in all the studies. The articles that exclude the smokers are the following: SFE 1/3 (Tatullo et al. 2012), ridge preservation 4/8 (Gürbüz et al. 2010, Singh et al. 2012, Baslarli et al. 2015, Marenzi et al. 2015), and implant therapy 0/3. However, in alveolar ridge preservation and implant therapy, most of the studies did not mention the smoking status (ridge preservation 4/8 (Hauser et al. 2013, Suttapreyasri & Leepong 2013, Kumar et al. 2015, and Yelamali & Saikrishna 2015), and implant therapy 2/3 (Boora et al. 2015, Hamzacebi et al. 2015). This heterogeneity in the surgical protocols is shown in Tables 1, 2, 3.

#### *Data extraction*

The variables processed as primary outcome were mean newly formed bone (%) for the SFE subgroup; soft tissue and bone healing (reported as healing index scores, bone resorption in mm and/or in technetium-99 m methylene diphosphonate uptake) for alveolar ridge preservation; and peri-implant bone stability (ISQ values and/or marginal bone loss in mm) for implant therapy. Post-operative pain was considered as secondary outcome. All the data presented a high heterogeneity, so a meta-analysis was impossible. The follow-up also differed substantially, therefore a comparison between studies was difficult.

### Sinus floor elevation

All included studies used L-PRF in combination with a xenograft material and compared it to the xenograft alone (Table 4). One study compared, in a split-mouth set-up, an L-PRF membrane with a collagen membrane to cover a lateral window and reported a similar outcome in terms of percentage of mean vital bone formation and residual xenograft (Gassling et al. 2013). Zhang et al. (2012) evaluated the addition of L-PRF to the xenograft during a lateral window sinus augmentation. They observed 1.4 times more percentage of newly formed bone in the L-PRF group. Also, when L-PRF was used in a trans-alveolar approach, histologically, a faster bone healing was observed (Tatullo et al. 2012). Due to the heterogeneity of the data, meta-analysis could not be conducted.

### Alveolar ridge preservation

In general, L-PRF improved the preservation of the alveolar ridge and resulted in less buccal bone resorption compared to the natural healing (Singh et al. 2012, Hauser et al. 2013, Suttapreyasri &

Leepong 2013, Kumar et al. 2015). A better soft tissue healing and less post-extraction pain was frequently reported (Singh et al. 2012, Hauser et al. 2013, Kumar et al. 2015, Marenzi et al. 2015). However, scintigraphic analyses (after 4 and 8 weeks) did not show enhanced bone healing in L-PRF sites (Table 5). The wide variability of the data did not allow a meta-analysis. Most studies used only one L-PRF clot/membrane per extraction site, which might be insufficient.

The adverse events were only registered in four out of the eight articles within this group. Each article analysed the adverse events with a different scale, so no meta-analysis could be performed. In all of them, less pain for L-PRF sites compared to control sites was reported (Singh et al. 2012, Hauser et al. 2013, Kumar et al. 2015, Marenzi et al. 2015).

### Implant therapy

The RCTs (Hamzacebi et al. 2015, Öncü & Alaadinöglu 2015) evaluated the benefits of the application of L-PRF on the osseointegration process (Table 6). Öncü & Alaadinöglu (2015) evaluated the impact of implant coating with L-PRF. Implant stability was measured through resonance frequency analysis with implant stability quotients (ISQ values). The use of L-PRF at implant insertion resulted in statistically significant higher ISQ values which increased continuously over time. Boora et al. (2015) recorded the early bone remodelling around implants coated or not with L-PRF at insertion. The L-PRF-coated implants showed 50% less initial bone loss. Both after 1 and 3 months, respectively, (at 3 months: L-PRF sites:  $0.3 \pm 0.6$  mm mesially and  $0.3 \pm 0.7$  mm distally, non-L-PRF site:  $0.6 \pm 0.2$  mm mesially and  $0.7 \pm 0.3$  mm distally). Hamzacebi et al. (2015) assessed the effectiveness of the application of L-PRF and conventional flap surgery for the treatment of peri-implantitis bone loss. They reported more PD reduction (at 3 and 6 months: L-PRF sites:  $2.4 \pm 1.1$  mm and  $2.8 \pm 1.0$  mm, non-L-PRF sites:  $1.65 \pm 1.0$  mm and  $2.0 \pm 0.7$  mm), and CAL gain (L-PRF sites:  $2.9 \pm 1.0$  mm, non-L-PRF sites:  $1.4 \pm 1.0$  mm).

### Quality assessment

All articles on SFE and implant therapy showed a moderate risk of bias. Six articles using L-PRF for alveolar ridge preservation had a moderate risk and two had a high risk of bias. Figure 2 shows the quality assessment for the included studies.

For the groups of SFE and alveolar ridge preservation, a good inter-rater agreement or weighted kappa was found (0.67, 95% CI, 0.4–0.9, and 0.63, 95% CI, 0.5–0.8 respectively). A fair inter-rater agreement (0.55, 95% CI, 0.2–0.9) was observed for the group of implant therapy. In the latest, the most disagreement was on the “incomplete outcome data” and “selective outcome reporting”.

### Discussion

In recent years, L-PRF has been used in sinus floor elevation (SFE) either as a sole filling material or in combination with other graft materials. As mentioned in the results section, when L-PRF was used in combination with a graft material, better results were often obtained. However, no RCT or controlled clinical trial (CCT) could be retrieved in which L-PRF was used as the sole filling material or in combination with autologous bone grafts. The use of L-PRF as sole filling material has been analysed in several case series and case reports. In these studies, L-PRF was always used in combination with implant placement so that the implants could maintain the sinus membrane in an elevated position. Using the lateral window technique, Mazar et al. (2009) (33), Simonpieri et al. (2011) (34) and Tajima et al. (2013) (35) evaluated the effectiveness of L-PRF as a sole graft material in SFE with simultaneous implant placement. In the first two articles, a bone gain of 7.5 mm (SD not mentioned) and  $10.1 \text{ mm} \pm 0.9 \text{ mm}$ , respectively, at 6 months was reported. Tajima et al. (2013) (35) found a bone gain of  $10.4 \text{ mm} \pm 1.2$  at 1-year follow-

up. They all concluded that L-PRF as a sole filling material could promote natural bone regeneration producing dense bone-like tissue, at least when implants are placed simultaneously. L-PRF has also been used as the sole filling material in a transalveolar approach. Using this approach, the case series of Diss et al. (2008) (36) reported that a healing period of 2–3 months was sufficient to resist a torque of 25 Ncm applied during abutment tightening. At 1-year follow-up, formation of a new recognizable bone structure delimiting the sinus floor was identified radiographically. Toffler et al. (2010) (37) reported on 110 cases of osteotome-mediated SFE, with L-PRF as sole filling material during implant placement. The mean increase in the height at implant sites was 3–4 mm (range 2.5–5 mm), similar to the traditional osteotomes procedures. In a recent study (38), the mean bone gain around two different types of implant surfaces [hydroxyapatite (HA) and sandblasted acid-etched (SA)] was analysed using L-PRF as sole filling material in a transalveolar approach. Similar bone gain around both implant surfaces was reported ( $4.0 \pm 1.6$  mm and  $4.4 \pm 1.7$  mm respectively) after 1-year follow-up. The main challenge in SFE procedures is to avoid the perforation of the Schneiderian membrane (39). It has been reported that L-PRF can be used to cover the perforation since it has a good intrinsic adherence to the Schneiderian membrane. Consequently, it can also be used preventively to reduce the risk of perforation during SFE procedures (34).

L-PRF has been applied after tooth extraction to prevent bone resorption and alveolar ridge collapse. Most studies confirmed that L-PRF decreased the healing time as well as reduced the resorption of the buccal plate. However, five out of the eight studies evaluated the use of L-PRF in third molar extraction sites, which might have a distinct healing process when compared to extraction sites in the aesthetic region. Moreover, most of the studies used only one L-PRF clot or membrane to fill the extraction socket. One could question whether one clot or membrane is sufficient to completely fill the alveolus in order to create an adequate environment to stimulate the migration of osteoblasts and endothelial cells. The use of an L-PRF membrane on top, to close the alveolar socket, might have a significant influence on the outcome. Also, the amount of cells brought to the surgical site, as well as the quantity of fibrin might be crucial for success.

Although the application of L-PRF during implant placement or for the treatment of peri-implant defects is quite new, several studies already showed clinical benefits (higher ISQ values, less marginal bone resorption). Lee et al. (2012) (40) revealed in an animal study more bone-to-implant contact ( $39.4\% \pm 7.4$  versus  $17.1\% \pm 8.1$ ) after the treatment of peri-implantitis defects with L-PRF.

Some limitations are needed to be taken into account regarding this systematic review. Most of the included articles showed a moderate risk of bias and some even a high risk. In this last case, the allocation concealment was not correctly applied what increased the risk of bias. In addition, no meta-analysis could be performed in any of the groups due to the heterogeneity of the data. Therefore, this systematic review can only analyse the included articles qualitatively. Consequently, the varied nature of the data resulted in a lack of strong evidence for this systematic review.

However, it is also worth to highlight the strengths. A total number of 296 participants were enrolled in the selected studies (161 in alveolar ridge preservation, 76 in sinus floor elevation and 59 in implant therapy). The surgical protocol of all these studies was examined, giving a detailed information about the use of L-PRF in each application. Consequently, we could observe that to use the correct protocol is extremely important to obtain an optimal effect.

L-PRF should be certainly distinguished from other types of platelet concentrates. The architecture of the fibrin matrix and its cellular content differ from the other products, as well as the biological activity.

**Conclusion**

Despite the lack of strong evidence found in the included articles, beneficial effects on bone regeneration and in implant surgery are suggested when L-PRF is applied. Given its ease of preparation, low cost and biological properties, L-PRF could be considered as a reliable option of treatment. However, standardization of the protocol is required to obtain reproducible results. The use of enough L-PRF clots or membranes seems to be crucial to obtain an optimal effect.

Due to the lack in the standardization of the study design and variables analysed, further RCTs with long-term follow-up are needed to assess the beneficial effect of L-PRF on bone augmentation procedures and osseointegration.

Figure 1. PRISMA flow diagram.

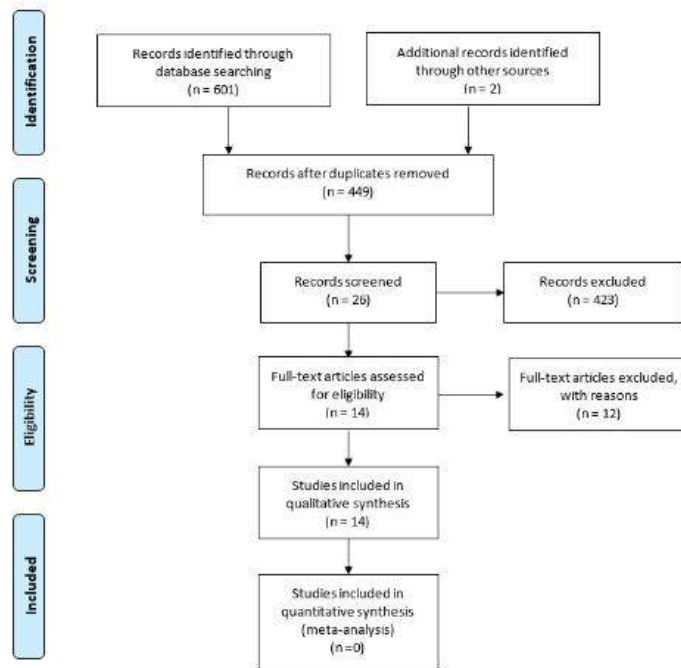


Figure 2. Quality assessment for the included studies. Cochrane tools for assessment of risk of bias for RCTs.

Study	Random sequence generation (selection bias)	Allocation concealment (selection bias)	Blinding of participants and personnel (performance bias)	Blinding of outcome assessment (detection bias)	Incomplete outcome data (attrition bias)	Selective reporting (reporting bias)	Other bias
Basler et al. 2015	●	●	●	●	●	●	●
Boora et al. 2015	●	●	●	●	●	●	●
Cassling et al. 2013	●	●	●	●	●	●	●
Gditzlzer et al. 2010	●	●	●	●	●	●	●
Hannacheb et al. 2015	●	●	●	●	●	●	●
Hausser et al. 2013	●	●	●	●	●	●	●
Kumar et al. 2015	●	●	●	●	●	●	●
Marenzi et al. 2015	●	●	●	●	●	●	●
Oncu & Alaadinoglu 2015	●	●	●	●	●	●	●
Smith et al. 2012	●	●	●	●	●	●	●
Sutarpavasi et al. 2013	●	●	●	●	●	●	●
Tautilo et al. 2012	●	●	●	●	●	●	●
Tiorat et al. 2011	●	●	●	●	●	●	●
Yelamali et al. 2015	●	●	●	●	●	●	●
Zhang et al. 2012	●	●	●	●	●	●	●



## Tables

Table 1. Search terms used for PUBMED, EMBASE and CENTRAL.

<b>PUBMED</b>	<b>Population (P)</b>	Mesh Terms	“guided bone regeneration”, “bone regeneration”, “alveolar ridge augmentation”, “alveolar bone atrophy”, “alveolar process atrophy”, “maxillary sinus”, “alveolar bone loss”
		Key Words	“tooth extraction”, “socket preservation”, “alveolar ridge preservation”, “alveolar ridge augmentation”, “guided bone regeneration”, “bone resorption”, “sinus floor augmentation”, “sinus lift”, “maxillary sinus”, “sinus floor elevation”, “graft material”
	<b>Intervention (I)</b>	Mesh Terms	“platelet rich plasma”, “blood buffy coat”
		Key Words	“leucocyte platelet rich fibrin”, “platelet rich fibrin”
<b>EMBASE</b>	<b>Population (P)</b>	Emtree terms	“Platelet rich Plasma”
		Key Words	“tooth extraction”, “socket preservation”, “alveolar ridge preservation”, “alveolar ridge augmentation”, “guided bone regeneration”, “bone resorption”, “sinus floor augmentation”, “sinus lift”, “maxillary sinus”, “sinus floor elevation”, “graft material”
	<b>Intervention (I)</b>	Emtree terms	“platelet rich plasma”
		Key Words	“leucocyte platelet rich fibrin”, “platelet rich fibrin”
<b>COCHRANE</b>	<b>Population (P)</b>	Mesh Terms	“bone regeneration”, “alveolar resorption”, “bone atrophy, alveolar”, “maxillary sinus”, “Bone loss, alveolar”, “Bone loss, periodontal”
		Key Words	“tooth extraction”, “socket preservation”, “alveolar ridge preservation”, “alveolar ridge augmentation”, “guided bone regeneration”, “bone resorption”, “sinus floor augmentation”, “sinus lift”, “maxillary sinus”, “sinus floor elevation”, “graft material”
	<b>Intervention (I)</b>	Mesh Terms	“platelet rich plasma”, “blood buffy coat”
		Key Words	“leucocyte platelet rich fibrin”, “platelet rich fibrin”

Table 2. Inclusion and exclusion criteria.

Inclusion criteria	Exclusion criteria
randomised controlled clinical trials (RCTs) or controlled clinical trials (CCTs)	case reports, case series, retrospective studies, ...
studies regarding bone augmentation procedures, ridge preservation or implant surgery.	studies regarding periodontal surgery: intrabony defects, furcation defects and periodontal plastic surgery.
L-PRF prepared following the protocol 2.700 rpm/12 min or 3.000 rpm/10 min	other types of platelet concentrates (fibrin glues, PRP, PRGF, A-PRF, I-PRF...)
studies conducted in humans	animal studies, in vitro studies
no limitation in publication date nor in follow-up duration	other applications of L-PRF in Medicine (Traumatology, Ophthalmology, Dermatology, etc.) or in Dentistry (Endodontics,...)
articles written in English	



Table 3. Excluded articles and reason for exclusion.

Author	Year	Reason for exclusion
Angelo et al.	2015	Use of A-PRF
Anilkumar et al.	2009	Case report
Barone et al.	2015	Single cohort study
Bolukbasi et al.	2015	Retrospective study
Chang et al.	2011	Retrospective study
Choukroun et al.	2006	Report of clinical cases
Diss et al.	2008	Case series, no control group
Inchingolo et al.	2010	Case series, no control group
Mazor et al.	2009	Case series, no control group
Simonpieri et al.	2011	Case series, no control group
Tajima et al.	2013	Case series, no control group
Toffler et al.	2010	Case series, no control group

Table 4. L-PRF for sinus floor elevation. LW: Lateral window, imm. impl.: immediate implant, TT: Transalveolar technique, NSSD: No statistically significant difference, ISQ: implant stability quotient, SL: sinus lift. Papers have been arranged by subapplications (L-PRF as coverage of lateral window and L-PRF bone quality).

Authors (year)	Study design, Duration	No. of participants baseline (end), gender, age, smoking	Groups C: control T: test	L-PRF preparation	Surgical protocol	Results
<i>L-PRF as coverage of lateral window</i>						
<i>Gassling et al. (2013)</i>	RCT Split-mouth Single-blind 5 months	6 – (6) Gender: ? Mean age: 61 Range: 54-69 Smoking: ?	C: n= 6, Bio-Oss® + Bio-Guide® membrane T: n= 6, Bio-Oss® + L-PRF membrane	Hardware: ? Setting: 400g / 12 min	1 L-PRF membrane + Bio-Oss® LW no imm. impl. 10 mL blood/clot	mean vital bone formation 17.0% and 17.2% for L-PRF and collagen sites, respectively. NSSD in mean residual bone-substitute (15.9% and 17.3% respectively).
<i>L-PRF bone quality</i>						
<i>Tatullo et al. (2012)</i>	RCT Parallel Single- blind 5 months	60 – (60) 48 ♀, 12 ♂ Mean age: ? Range: 43-62 Smoking: No	* “Early”: n= 20 - n= 6: SL + Bio-Oss® - n= 10: SL + Bio-Oss® + LPRF - n= 4: bilateral atrophy: - Bio-Oss® - Bio-Oss® + L-PRF * “Intermediate”: n= 20, idem * “Late”: n= 20, idem	Hardware: ? Setting: 3000 rpm / 10 min	2 L-PRF membranes + Bio-Oss® TT + piezosurgery no imm. impl. 10 mL blood/clot	NSSDs for ISQ mean values. L-PRF showed histologically faster bone healing (106 days compared to 120-150 days).
<i>Zhang et al. (2012)</i>	RCT Parallel Not blind 6 months	10 – (10) 2 ♀, 8 ♂ Mean age: C: 46, T: 43 Range: C: 37-53, T: 30-49 Smoking: ?	C: n= 5, SL + Bio-Oss® T: n= 6, SL + Bio-Oss® + L-PRF	Hardware: <sup>1</sup> Setting: 300 g / 10 min	1 L-PRF membrane + Bio-Oss® LW no imm. impl. 10 mL blood/clot	similar bone morphological characteristics in both groups. L-PRF group had 1.4 times higher percentage of new-formed bone than control group.

<sup>1</sup>: Labofuge 300, Kendro Laboratory Products GmbH, Osterrode, Germany.

Table 5. PRF for alveolar ridge preservation. NSSD: no statistically significant difference, NSS: no statistically significant, SS: statistically.

Authors (year)	Study design, duration	No. of participants baseline (end), gender, age, smoking	Groups C: control T: test	L-PRF preparation	Surgical protocol	Results
<i>L-PRF vs. “natural healing”: bone quality</i>						
<i>Singh et al. (2012)</i>	CCT Split-mouth Not blind 3 months	20 – (20) 10 ♀, 10 ♂ Mean age: 32 Range 18-50 Smoking: No	20 bilateral impacted 3 <sup>rd</sup> molar:  C: n= 20, no filling  T: n= 20, L-PRF filling	Hardware: ?  Setting: 3000 rpm / 10 min	1 L-PRF clot 0 L-PRF membrane  5-10? mL blood/clot	Healing Index scores statistically better in L-PRF group.  NSSD in trabecular bone formation. SS higher bone density at 12 weeks for L-PRF group.
<i>Hauser et al. (2013)</i>	RCT Parallel Double-blind 8 weeks	23 – (22) 14 ♀, 9 ♂ Mean age: 47 Range: 22-75 Smoking: ?	Premolar extractions:  C: n= 7  T <sub>1</sub> : n= 9, L-PRF filling  T <sub>2</sub> : n= 6, L-PRF filling + flap	Hardware: ?  Setting: 2700 rpm / 12 min	1 L-PRF clot ? L-PRF membrane  8 mL blood/clot	L-PRF: SS better bone healing. L-PRF: SS better intrinsic bone tissue quality and preservation of alveolar width. Flap: invasive surgical procedure seemed to neutralize advantages of L-PRF.
<i>Suttapreyasri et al. (2013)</i>	RCT Parallel Split-mouth 8 weeks	8 – (8) 5 ♀, 3 ♂ Mean age: 22 ± 2 Range 20.3-27.6 Smoking: ?	10 bilateral premolar extractions:  C: n= 10, no filling  T: n= 10, L-PRF filling	Hardware: <sup>2</sup>  Setting: 3000 rpm / 10 min	1 L-PRF clot 0 L-PRF membrane  10 mL blood/clot	L-PRF: NSSD faster soft-tissue healing. L-PRF: less buccal/lingual resorption (SS buccally) NSSD in rx evaluation.
<i>Kumar et al. (2015)</i>	RCT Parallel Single-blind 3 months	31 – (31) Gender: ? Mean age: 26.1 Range: ? Smoking: ?	3 <sup>rd</sup> molar extractions:  C: n= 15, no filling  T: n= 16, L-PRF filling	Hardware: ?  Setting: 3000 rpm / 10 min	1 L-PRF clot 0 L-PRF membrane  5 mL blood/clot	SS more PD reduction (distal 2 <sup>nd</sup> molar) in L-PRF group. NSS greater bone density with L-PRF after 3 months less adverse events recorded in L-PRF group.

<i>L-PRF vs. PRP</i>						
<i>Yelamali et al. (2015)</i>	RCT Split-mouth Not blind 4 months	20 – (20) 8 ♀, 12 ♂ Mean age: ? Range: 21-27 Smoking:?	20 bilateral impacted 3 <sup>rd</sup> molar: C: PRP: n= 20, PRP filling T: L-PRF: n= 20, L-PRF filling	Hardware: ? Setting: 3000 rpm / 10 min	1 L-PRF clot 0 L-PRF membrane 6 mL blood/clot	SS better soft tissue healing in L-PRF group. SS higher bone density in L-PRF group.
<i>L-PRF pain</i>						
<i>Marenzi et al. (2015)</i>	RCT Split-mouth Single-blind 7 days	26 – (26) 17 ♀, 9 ♂ Mean age: 53 ± 4 Range: ? Smoking: No or light smokers (<5/day)	26 bilateral canine/premolar/molar: C: n= 26, no filling T: n= 26, L-PRF filling	Hardware: <sup>3</sup> Setting: 2700 rpm / 12 min	2-6 L-PRF clot 0 L-PRF membrane 9 mL blood/clot	SS better and faster healing in L-PRF group at 3 and 7 days. less post-extraction pain is L-PRF group.
<i>L-PRF uptake technetium-99m methylene diphosphonat</i>						
<i>Gürbüz et al. (2010)</i>	RCT Split-mouth Not blind 4 weeks	20 – (14) 7 ♀, 7 ♂ Mean age: 24 ± 4 Range: ? Smoking: No	14 bilateral impacted 3 <sup>rd</sup> molar: C: n= 14, no filling T: n= 14, L-PRF filling	Hardware : <sup>4</sup> Setting: 400g / 10 min	1 L-PRF clot 0 L-PRF membrane 10 mL blood/clot	NSSD between groups in the average increase in technetium-99m methylene diphosphonat uptake (as indicator of enhanced bone healing).
<i>Baslarli et al. (2015)</i>	RCT Parallel Single-blind 2 months	20 – (20) 13 ♀, 7 ♂ Mean age: 23 Range: 10-34 Smoking: No	20 bilateral impacted 3 <sup>rd</sup> molar: C: n= 20, no filling T: n= 20, L- PRF filling	Hardware : ? Setting: 3000 rpm / 10 min	0 L-PRF clot 1 L-PRF membrane 9 mL blood/clot	NSSD between groups in the average increase in technetium-99m methylene diphosphonat uptake (as indicator of enhanced bone healing). NSSD in PD reduction.

<sup>2</sup>: EBA 20, Hettich GmbH&Co, KG, Tuttlingen, Germany, <sup>3</sup>: Intra-Spin L-PRF kit, Intra-Lock, Boca-Raton, FL, USA, <sup>4</sup>: Universal 320 Hettich, Tuttlingen, Germany.

Table 6. L-PRF for implant therapy. NSSD: no statistically significant difference, SS: statistically significant, PD: pocket depth, CAL: clinical attachment level, BoP: bleeding on probing, imm. function: immediate function, ISQ: implant stability quotient. Papers have been arranged by subapplications (L-PRF at implant placement, L-PRF in peri-implant defects).

Authors (year)	Study design, Duration	No. of participants baseline (end), gender, age, Smoking	Groups C: control T: test	L-PRF preparation	Surgical protocol	Results
<i>L-PRF at implant placement</i>						
<i>Boora et al. (2015)</i>	RCT  Parallel Not blind  3 months	20 – (20)  5 ♀, 15 ♂  Mean age: 24.6 Range: 18-33  Smoking: ?	C: n= 10, no L-PRF  T: n= 10, L-PRF	Hardware: ?  Setting: 3000 rpm / 10-12 min	1 L-PRF membrane  Adin Dental Implant System (Israel)  10-14d non-functional prov. crown  10 mL blood/clot	SS less initial marginal bone loss in L-PRF group. NSSD in PD and BoP between groups.
<i>Öncü &amp; Alaadinöglu (2015)</i>	RCT  Parallel Not blind  1 month	20 – (20)  6 ♀, 14 ♂  Mean age: 44 ± 12 Range: ?  Smoking: < 10cig/day	C: n= 33, no L-PRF  T: n= 31, L-PRF	Hardware: <sup>9</sup>  Setting: 2700 rpm / 12 min	1 L-PRF membrane + exudate  Ankylos Implant System (Dentsply)  no imm. function  10 mL blood/clot	SS higher ISQ values in L-PRF group by the end of the 1 <sup>st</sup> week (69 vs. 64) and 4 <sup>th</sup> week (77 vs. 70.5).  Mean ISQ values in L-PRF group increased continuously.
<i>L-PRF in peri-implant defects</i>						
<i>Hamzacebi et al. (2015)</i>	RCT  Parallel Not blind  6 months	19 – (19)  8 ♀, 11 ♂  Mean age: 61 ± 12 Range: ?  Smoking: ?	C: n= 19, OFD  T: n= 19, OFD + L-PRF	Hardware: ?  Setting: 3000 rpm / 10 min	1 L-PRF clot >1 L-PRF membrane  Type implant not mentioned  imm. function  10 mL blood/clot	SS more PD reduction (2.8 vs. 2.05mm) and CAL gain (3.3 vs. 1.84mm).

## References

1. Cardaropoli G, Araujo M, Lindhe J. Dynamics of bone tissue formation in tooth extraction sites. An experimental study in dogs. *Journal of clinical periodontology*. 2003;30(9):809-18.
2. Chappuis V, Engel O, Reyes M, Shahim K, Nolte LP, Buser D. Ridge alterations post-extraction in the esthetic zone: a 3D analysis with CBCT. *J Dent Res*. 2013;92(12 Suppl):195s-201s.
3. Farmer M, Darby I. Ridge dimensional changes following single-tooth extraction in the aesthetic zone. *Clinical oral implants research*. 2014;25(2):272-7.
4. McAllister BS, Haghighat K. Bone augmentation techniques. *Journal of periodontology*. 2007;78(3):377-96.
5. Vignoletti F, Sanz M. Immediate implants at fresh extraction sockets: from myth to reality. *Periodontology 2000*. 2014;66(1):132-52.
6. Jung RE, Thoma DS, Hammerle CH. Assessment of the potential of growth factors for localized alveolar ridge augmentation: a systematic review. *Journal of clinical periodontology*. 2008;35(8 Suppl):255-81.
7. Lin GH, Lim G, Chan HL, Giannobile WV, Wang HL. Recombinant human bone morphogenetic protein 2 outcomes for maxillary sinus floor augmentation: a systematic review and meta-analysis. *Clinical oral implants research*. 2016;27(11):1349-59.
8. Matras H. [Effect of various fibrin preparations on reimplantations in the rat skin]. *Osterreichische Zeitschrift fur Stomatologie*. 1970;67(9):338-59.
9. Anitua E. Plasma rich in growth factors: preliminary results of use in the preparation of future sites for implants. *The International journal of oral & maxillofacial implants*. 1999;14(4):529-35.
10. Choukroun J. Une opportunité en paro-implantologie: le PRF. *Implantodontie*. 2001;42:55-62.
11. Dohan DM, Choukroun J, Diss A, Dohan SL, Dohan AJ, Mouhyi J, et al. Platelet-rich fibrin (PRF): a second-generation platelet concentrate. Part I: technological concepts and evolution. *Oral surgery, oral medicine, oral pathology, oral radiology, and endodontics*. 2006;101(3):e37-44.
12. Dohan Ehrenfest DM, Andia I, Zumstein MA, Zhang CQ, Pinto NR, Bielecki T. Classification of platelet concentrates (Platelet-Rich Plasma-PRP, Platelet-Rich Fibrin-PRF) for topical and infiltrative use in orthopedic and sports medicine: current consensus, clinical implications and perspectives. *Muscles, ligaments and tendons journal*. 2014;4(1):3-9.
13. Rowe SL, Lee S, Stegemann JP. Influence of thrombin concentration on the mechanical and morphological properties of cell-seeded fibrin hydrogels. *Acta biomaterialia*. 2007;3(1):59-67.
14. Khorshidi H, Raoofi S, Bagheri R, Banihashemi H. Comparison of the Mechanical Properties of Early Leukocyte- and Platelet-Rich Fibrin versus PRGF/Endoret Membranes. *International journal of dentistry*. 2016;2016:1849207.
15. Dohan DM, Choukroun J, Diss A, Dohan SL, Dohan AJ, Mouhyi J, et al. Platelet-rich fibrin (PRF): a second-generation platelet concentrate. Part II: platelet-related biologic features. *Oral surgery, oral medicine, oral pathology, oral radiology, and endodontics*. 2006;101(3):e45-50.
16. Schär MO, Diaz-Romero J, Kohl S, Zumstein MA, Nesic D. Platelet-rich concentrates differentially release growth factors and induce cell migration in vitro. *Clinical orthopaedics and related research*. 2015;473(5):1635-43.
17. Öncü E, Bayram B, Kantarci A, Gülsever S, Alaaddinoğlu EE. Positive effect of platelet rich fibrin on osseointegration. *Medicina oral, patologia oral y cirugía bucal*. 2016;21(5):e601-7.

18. Moher D, Hopewell S, Schulz KF, Montori V, Gotzsche PC, Devereaux PJ, et al. CONSORT 2010 explanation and elaboration: updated guidelines for reporting parallel group randomised trials. *International journal of surgery (London, England)*. 2012;10(1):28-55.
19. Tatullo M, Marrelli M, Cassetta M, Pacifici A, Stefanelli LV, Scacco S, et al. Platelet Rich Fibrin (P.R.F.) in reconstructive surgery of atrophied maxillary bones: clinical and histological evaluations. *International journal of medical sciences*. 2012;9(10):872-80.
20. Zhang Y, Tangl S, Huber CD, Lin Y, Qiu L, Rausch-Fan X. Effects of Choukroun's platelet-rich fibrin on bone regeneration in combination with deproteinized bovine bone mineral in maxillary sinus augmentation: a histological and histomorphometric study. *Journal of cranio-maxillo-facial surgery : official publication of the European Association for Cranio-Maxillo-Facial Surgery*. 2012;40(4):321-8.
21. Gassling V, Purcz N, Braesen JH, Will M, Gierloff M, Behrens E, et al. Comparison of two different absorbable membranes for the coverage of lateral osteotomy sites in maxillary sinus augmentation: a preliminary study. *Journal of cranio-maxillo-facial surgery : official publication of the European Association for Cranio-Maxillo-Facial Surgery*. 2013;41(1):76-82.
22. Gürbüz B, Pıkdöken L, Tunalı M, Urhan M, Küçükodacı Z, Ercan F. Scintigraphic evaluation of osteoblastic activity in extraction sockets treated with platelet-rich fibrin. *Journal of oral and maxillofacial surgery : official journal of the American Association of Oral and Maxillofacial Surgeons*. 2010;68(5):980-9.
23. Singh A, Kohli M, Gupta N. Platelet rich fibrin: a novel approach for osseous regeneration. *Journal of maxillofacial and oral surgery*. 2012;11(4):430-4.
24. Hauser F, Gaydarov N, Badoud I, Vazquez L, Bernard JP, Ammann P. Clinical and histological evaluation of postextraction platelet-rich fibrin socket filling: a prospective randomized controlled study. *Implant dentistry*. 2013;22(3):295-303.
25. Suttapreyasri S, Leepong N. Influence of platelet-rich fibrin on alveolar ridge preservation. *The Journal of craniofacial surgery*. 2013;24(4):1088-94.
26. Baslarlı O, Tümer C, Ugur O, Vatankulu B. Evaluation of osteoblastic activity in extraction sockets treated with platelet-rich fibrin. *Medicina oral, patologia oral y cirugía bucal*. 2015;20(1):e111-6.
27. Marenzi G, Riccitiello F, Tia M, di Lauro A, Sammartino G. Influence of Leukocyte- and Platelet-Rich Fibrin (L-PRF) in the Healing of Simple Postextraction Sockets: A Split-Mouth Study. *BioMed research international*. 2015;2015:369273.
28. Kumar N, Prasad K, Ramanujam L, K R, Dexith J, Chauhan A. Evaluation of treatment outcome after impacted mandibular third molar surgery with the use of autologous platelet-rich fibrin: a randomized controlled clinical study. *Journal of oral and maxillofacial surgery : official journal of the American Association of Oral and Maxillofacial Surgeons*. 2015;73(6):1042-9.
29. Yelamali T, Saikrishna D. Role of platelet rich fibrin and platelet rich plasma in wound healing of extracted third molar sockets: a comparative study. *Journal of maxillofacial and oral surgery*. 2015;14(2):410-6.
30. Boora P, Rathee M, Bhorla M. Effect of Platelet Rich Fibrin (PRF) on Peri-implant Soft Tissue and Crestal Bone in One-Stage Implant Placement: A Randomized Controlled Trial. *Journal of clinical and diagnostic research : JCDR*. 2015;9(4):Zc18-21.
31. Hamzacebi B, Oduncuoglu B, Alaaddinoglu EE. Treatment of Peri-implant Bone Defects with Platelet-Rich Fibrin. *The International journal of periodontics & restorative dentistry*. 2015;35(3):415-22.
32. Öncü E, Alaaddinoğlu EE. The effect of platelet-rich fibrin on implant stability. *The International journal of oral & maxillofacial implants*. 2015;30(3):578-82.

33. Mazor Z, Horowitz RA, Del Corso M, Prasad HS, Rohrer MD, Dohan Ehrenfest DM. Sinus floor augmentation with simultaneous implant placement using Choukroun's platelet-rich fibrin as the sole grafting material: a radiologic and histologic study at 6 months. *Journal of periodontology*. 2009;80(12):2056-64.
34. Simonpieri A, Choukroun J, Del Corso M, Sammartino G, Dohan Ehrenfest DM. Simultaneous sinus-lift and implantation using microthreaded implants and leukocyte- and platelet-rich fibrin as sole grafting material: a six-year experience. *Implant dentistry*. 2011;20(1):2-12.
35. Tajima N, Ohba S, Sawase T, Asahina I. Evaluation of sinus floor augmentation with simultaneous implant placement using platelet-rich fibrin as sole grafting material. *The International journal of oral & maxillofacial implants*. 2013;28(1):77-83.
36. Diss A, Dohan DM, Mouhyi J, Mahler P. Osteotome sinus floor elevation using Choukroun's platelet-rich fibrin as grafting material: a 1-year prospective pilot study with microthreaded implants. *Oral surgery, oral medicine, oral pathology, oral radiology, and endodontics*. 2008;105(5):572-9.
37. Toffler M, Toscano N, Holtzclaw D. Osteotome-mediated sinus floor elevation using only platelet-rich fibrin: an early report on 110 patients. *Implant dentistry*. 2010;19(5):447-56.
38. Kanayama T, Horii K, Senga Y, Shibuya Y. Crestal Approach to Sinus Floor Elevation for Atrophic Maxilla Using Platelet-Rich Fibrin as the Only Grafting Material: A 1-Year Prospective Study. *Implant dentistry*. 2016;25(1):32-8.
39. Pjetursson BE, Lang NP. Sinus floor elevation utilizing the transalveolar approach. *Periodontology 2000*. 2014;66(1):59-71.
40. Lee JW, Kim SG, Kim JY, Lee YC, Choi JY, Dragos R, et al. Restoration of a peri-implant defect by platelet-rich fibrin. *Oral surgery, oral medicine, oral pathology and oral radiology*. 2012;113(4):459-63.





## SECTION 2



*In vitro* studies



## CHAPTER 3

### Characterization of the Leucocyte-and Platelet Rich Fibrin Membrane and Block: release of growth factors, cellular content and structure

Castro Ana B, Cortellini Simone, Temmerman Andy, Li Xin, Pinto Nelson,  
Teughels Wim & Quirynen Marc. (2019)  
*International Journal of Oral & Maxillofacial Implants* 34; 855-64.

#### **Abstract**

**Aim:** The Leucocyte and Platelet Rich Fibrin Block (L-PRF Block) is a composite graft that combine a xenograft that is acting as a scaffold with L-PRF membranes that serve as a bioactive nodule with osteoinductive capacity. This study evaluated the properties of the L-PRF Block and its components in terms of release of growth factors, cellular content and structure.

**Material & Methods:** The concentration of transforming growth factor- $\beta$ 1 (TGF- $\beta$ 1), vascular endothelial growth factor (VEGF), platelet-derived growth factor-AB (PDGF-AB) and bone morphogenetic protein-1 (BMP-1) released by a L-PRF membrane (mb) and a L-PRF Block were examined with ELISA for 5 time intervals (0-4h, 4h-1day, 1-3d, 3-7d, 7-14d). Those levels in L-PRF exudate and Liquid Fibrinogen were also evaluated. The cellular content of the Liquid Fibrinogen, L-PRF membrane and exudate was calculated. The L-PRF Block was also analysed by means of a microCT scan and scanning electron microscopy (SEM).

**Results:** TGF- $\beta$ 1 was the most released growth factor after 14 days, followed by PDGF-AB, VEGF, and BMP-1. All L-PRF blocks constantly release the four growth factors up to 14 days. L-PRF membrane and Liquid Fibrinogen presented high concentration of leucocytes and platelets. The microCT and SEM images revealed the bone substitute particles surrounded by platelets and leucocytes, embedded in a dens fibrin network.

**Conclusions:** The L-PRF Block consists of deproteinized bovine bone mineral particles surrounded by platelets, leucocytes and embedded in a fibrin network that releases growth factors up to 14 days.

#### **Introduction**

Various surgical procedures have been proposed to horizontally and/or vertically augment the residual bone after tooth extraction. However, no specific surgical techniques have been described as the gold standard, being the autologous bone the ideal grafting material for bone augmentation procedures (1, 2). Thus, the treatment of an atrophic maxilla or a resorbed mandibular ridge remains a major challenge. In a systematic review with meta-analysis, Sanz-Sánchez et al. (2015) concluded that the combination of a xenograft and a bioresorbable membrane was the most frequently used technique for lateral bone augmentation in combination with implant placement. On the other hand, autogenous bone blocks were the most suitable for a staged approach. More recently, a composite bone graft combining a xenograft with particulated autogenous bone has been suggested to increase the osteogenic properties of the graft and to reduce morbidity, especially when compared to autogenous blocks (3, 4).

Despite the lack of osteoinductive capacity, deproteinized bovine bone mineral (DBBM) is considered as the gold standard xenograft for guided bone regeneration (GBR) (1). In the last decade,

tissue engineering approaches have been introduced to combine biologically inactive matrices (scaffolds) with bioactive agents, since cell-enriched bone grafts have been demonstrated to be more effective in regenerating the alveolar bone (5). Fibrin-based scaffolds are one of the classical biomaterials and have been widely utilized for a variety of applications (6, 7). The fibrin network provides a physical support for different cells such as neutrophils, macrophages and fibroblasts, which will produce collagen, fibronectin and other extracellular matrix components (8).

Composite fibrin gels have been often created to give the desired mechanical properties to the material. Fibrin gels copolymerized with polyurethane (9), heparin (10) or collagen(11) have been already described in the literature. The Leucocyte and Platelet Rich Fibrin Block (L-PRF Block) has arisen from this concept: a combination of a xenograft that is acting as a scaffold with osteoconductive ability and L-PRF membranes that serve as a bioactive nodule with osteoinductive capacity (12-15). The combination of activated platelets in the L-PRF membranes and the Liquid Fibrinogen results in a mass production of fibrin, integrating the bone substitute into a strong construct. Leucocyte- and Platelet Rich Fibrin (L-PRF), a 2<sup>nd</sup> generation platelet concentrate, has been shown to stimulate the cellularity in the surgical site due to the continuous release of growth factors and cytokines (16). L-PRF is 100% autogenous and is formed via a simple process of centrifugation without the incorporation of additives.

The aim of this study was to characterize the L-PRF Block and its components (L-PRF membrane, L-PRF exudate and Liquid Fibrinogen) in terms of release of growth factors, cellular content, and their distribution inside the L-PRF Block.

## **Materials & Methods**

### **Participants in the study**

Eight systemically healthy volunteers were enrolled in this study. The exclusion criteria included: anticoagulant medication or antibiotics 3 months before the study, pregnancy or lactation, history of periodontal disease or any active systemic infection. Seven 9-ml tubes of blood were collected per participant. Four tubes were used for the analysis of growth factors: three tubes to make an L-PRF Block and one tube for an L-PRF membrane. The last three tubes were used for cellular counting: one tube for the L-PRF membrane, one tube for the Liquid Fibrinogen, and one tube for the initial cellular counting. In four out of the eight volunteers, seven extra tubes were withdrawn for the microCT (three tubes for the L-PRF Block), and SEM imaging (three tubes for the L-PRF Block and one tube for the L-PRF membrane).

The use of human blood was approved by the ethical committee of the KU Leuven and registered with identifier B322201628215. All procedures were performed according to the Helsinki Declaration and the regulations of the University Hospital. An informed consent was obtained from all subjects after having explained the purpose of the study.

### **Preparation of the L-PRF Block**

As described by Cortellini et al. (2018) (17), two 9-ml glass-coated plastic tubes (red cap, BVBCTP-2, Intra-Spin, Intra-Lock, Florida, USA) and one 9-ml plastic tube without coating (white cap, WCT, Intra-Spin, Intra-Lock, Florida, USA) were collected per participant (n=8) in this order and immediately centrifuged at 408 g force (IntraSpin, Intra-Lock, Florida, USA). The centrifugation was interrupted after 3 minutes and the white cap tube was removed from the centrifuge. The remaining red cap tubes were further centrifuged for 9 minutes, completing the cycle of 12 minutes of centrifugation. Immediately after removing the white cap tube from the centrifuge, the yellow liquid obtained above the red blood cells

was collected with a sterile (5 ml) syringe. This liquid is called Liquid Fibrinogen. When the full centrifugation (12 min) was finalized, the red cap tubes were removed and two L-PRF membranes were prepared following the protocol described by Temmerman et al. (2016)(18). Briefly, each L-PRF clot was collected from the tube and transformed into a membrane by gentle compression (Xpression kit, Intra-Lock, Florida, USA).

Both L-PRF membranes were chopped into small pieces using scissors and mixed with 0,5 g of particulated deproteinized bovine bone mineral (DBBM, Bio-Oss®, Geistlich Biomaterials, Wolhusen, Switzerland) in a sterile titanium dish providing a volume ratio of 50:50. After obtaining a homogeneous mix,  $\pm$  2 ml of Liquid Fibrinogen were added while carefully modelling the block during 5-10 seconds (Figure 1). After 3 min, the L-PRF Block was ready for use.

#### Cellular counting of L-PRF Block components

One 9-ml glass-coated plastic tube (red cap, BVBCTP-2, Intra-Spin, Intra-Lock, Florida, USA) and one 9-ml plastic tube without coating (white cap, WCT, Intra-Spin, Intra-Lock, Florida, USA) were collected per participant (n=8). The white tube was centrifuged, as described before, to obtain the Liquid Fibrinogen, whereas the red cap tube followed the protocol for L-PRF membranes. During the compression of the L-PRF clot from the red cap tube, the exudate released from the L-PRF clot was collected for analysis. A 9-ml tube of blood with EDTA was withdrawn to examine the initial blood composition.

Cellular counting was performed for all components of the L-PRF Block: the L-PRF membrane, the L-PRF exudate and the Liquid Fibrinogen by means of a haematology analyser (CELL-DYN® 3700, Abbott GmbH & Co, Wiesbaden, Germany). Given the difficulty to dissolve the L-PRF membrane without damaging the cells, cellular counting for the latter was carried out indirectly as follows: after removal of the L-PRF clot, the remaining tube was refilled with sterile saline until the initial volume (9 ml) was obtained. The exudate obtained from the compression of the L-PRF clot was also diluted into sterile saline until a volume of 9 ml. For the calculation of the cellular content of the L-PRF membrane, the cellular content of the exudate and the remaining tube were added and subtracted from the initial blood composition. All samples were immediately frozen at -80°C to avoid coagulation. In order to avoid the formation of crystals inside the cells, 10% Dimethylsulfoxide (DMSO) was added to all samples.

#### Growth factors release from the L-PRF Block and its components

Each L-PRF Block and L-PRF membrane was placed in a 15 ml-tube with 5 ml of Dulbecco's Modified Eagle medium (Sigma-Aldrich BVBA, Overijse, Belgium) without antibiotics and changed to a new tube with a sterile tweezer after 4 hours and on day 1, 3, and 7. After collecting the L-PRF membrane/L-PRF Block at each time interval, the remaining medium was centrifuged at 1.000 rpm for 10 minutes (VWR® Mega Star 6000R, VWR International BVBA, Leuven, Belgium) to remove any residue and thereafter frozen at -80°C.

The L-PRF exudate and the Liquid Fibrinogen were analysed at the time of collection (one time point). These concentrations were presented in pg/ml.

The levels of vascular endothelial growth factor (VEGF), transforming growth factor beta1 (TGF- $\beta$ 1), and platelet derived growth factor-AB (PDGF-AB) were measured in duplicate aliquots using commercially available enzyme-linked immunosorbent assay kits (ELISA, R&D Systems Europe, Abingdon, UK) following the manufacturer's instructions. For the concentrations of bone morphogenetic protein-1 (BMP-1) another ELISA system was used (Abbexa, Cambridge Science Park, UK). Measurements were conducted with a microplate reader (Multiskan Ascent®, Rev 1.2, Thermo Electron

Corporation, Vantaa, Finland) set to 450 nm and subtracted at 550 nm from the 450nm measurements. The concentrations were calculated per block and per membrane.

To guarantee the quality of the ELISA for growth factors release analysis, careful validation and standardisation of the tests were performed. The sensitivity of the test was determined by calculating the minimum detectable dose (MDD) and adapting the samples concentrations to the MDD for each growth factor. Similarly, all ELISA kits were assayed for cross-reactivity by the manufacturer and no significant cross-reactivity or interference was observed (19).

#### MicroCT scanning, object reconstruction and volumetric percentage of particles

A microCT scan (Skyscan 1172, Bruker microCT, Kontich, Belgium) was performed for four additional L-PRF Blocks. Each specimen was positioned in a plastic tube and stabilized from the base with silicone. The specimens were scanned at 100kV, 360° rotation with a step of 0,7°, a pixel size of 15,6 µm, and aluminium filter (0,5 mm of thickness). The average scanning time was 20 minutes per sample. The images were reconstructed using the software NRecon (version 1.6.10.4; Bruker, Kontich, Belgium) and analysed with CTAn (version 1.11.5.1; Bruker, Kontich, Belgium). In each L-PRF Block, the region of interest (ROI) which coincided with the visible outer surface of the block, was manually outlined along the block. Volumes of interest (VOI) were determined from the manually drawn ROI. A three-dimensional model per block was automatically created considering the DBBM particles as hard tissue (radiopaque) and the L-PRF membranes/Liquid Fibrinogen as soft tissue (radiolucent). The percentage of the particles in the total volume was calculated.

#### Scanning Electron Microscopy (SEM)

One extra L-PRF Block and L-PRF membrane were fixed immediately after preparation in 2,5% glutaraldehyde in 0,1 M sodium cacodylate buffer for 24h, rinsed with 0,2 M sodium cacodylate buffer and distilled water, and dehydrated in ascending dilutions of ethanol (25, 50, 75, 95, and 100%). After dehydration, each sample was immersed in hexamethyldisilazane 98% (Acros Organics, Geel, Belgium) for 10 min and then air-dried at room temperature. The specimens were coated with gold by an auto fine coater (JFC-1300, JEOL, Tokyo, Japan). The surface and a cross-sectional part of the L-PRF Block were taken for SEM analysis (JSM-6610LV, JEOL). For the L-PRF membrane, the red part (face, the area previously in contact with the red blood cells) and the middle part (tail) were also examined using SEM.

#### Data analysis

For every growth factor, a linear mixed model was fit with the sample (L-PRF membrane/L-PRF Block/L-PRF exudate/Liquid Fibrinogen) and time as fixed factors and volunteer as random factor. All samples were compared for each time interval and comparisons were corrected for simultaneous hypothesis testing according to Sidak. Normality and homoscedasticity of the residuals were assessed by means of a normal quantile plot and a residual dot plot. Data were once analyzed as concentration per time interval and once as cumulative concentrations over time. Mean values and standard deviations were calculated from the data of the cellular counting. The percentage of each cell type present in the L-PRF membrane/L-PRF exudate/Liquid Fibrinogen in relation to the initial blood sample was also computed.

## Results

### Demographic data

Eight systemically healthy subjects (4 women, 4 men) participated in this study. The mean age was 42,8 ± 14,2 years (range 29-60 years). No complications during blood collection were reported.

### Cellular counting of L-PRF Block components

More than 80% of platelets and 72% of leucocytes in the initial blood sample were still present in the L-PRF membranes. The same applied to the Liquid Fibrinogen, with 88% and 70%, respectively. The L-PRF exudate showed a low cellular content with 2,5% of platelets and 0,9% of leucocytes (Table 1).

### Growth factors release from the L-PRF Block and its components

#### *L-PRF exudate and Liquid Fibrinogen (Figure 2)*

All four growth factors could be detected in both L-PRF exudate and Liquid Fibrinogen, with TGF-β1 as the most released (20.079,1 pg/ml, 95% CI: 10.824,0-29.334,2). For the levels of TGF-β1 and PDGF-AB, no statistically significant difference could be observed ( $p>0,05$ ) between both fluids. The levels of VEGF ( $p<0,05$ ) and BMP-1 ( $p<0,01$ ) were statistically significantly higher in the L-PRF exudate in comparison to Liquid Fibrinogen.

#### *L-PRF Block and L-PRF membrane: time interval (Figure 2)*

All four growth factors were continuously released until day 14. TGF-β1 was the most released by both the L-PRF Block and the L-PRF membrane ( $p<0,01$ ). During the interval 7-14d, statistically significant higher levels of TGF-β1 were detected for the L-PRF Block (24.052,7 pg/block, 95% CI: 19.377,3-28.728,3; 9.614,6 pg/mb, 95% CI: 3.533,2-15.695,9,  $p<0,05$ ) compared with the L-PRF membrane. For the L-PRF membrane, the highest concentration (41.000,1 pg/mb, 95% CI: 23.129,7-58.870,5,  $p>0,005$ ) was observed for the interval 1-3d. Afterwards, release of TGF-β1 progressively decreased.

The L-PRF membrane produced significantly higher levels of PDGF-AB, at the intervals 4-1d and 1-3d ( $p<0,01$ ) compared to the PDGF-AB levels for the L-PRF Block. After these time intervals, the difference was no longer statistically significant.

The initial concentrations of VEGF were similar for L-PRF membrane and the L-PRF Block. However, the later released significantly larger concentrations at later interval 7-14d ( $p<0,01$ ).

For BMP-1, statistically significant higher levels were detected in the L-PRF Block at 1-3d and 7-14d compared to that of the L-PRF membrane (324,8pg/block, 95% CI: 174,8-474,8; 89,4pg/mb, 95% CI: 27-8-151,0,  $p<0,05$ ).

#### *L-PRF Block and L-PRF membrane: cumulative concentration (Figure 2)*

For the L-PRF Block, TGF-β1 was the most released after 14 days (96.232,5 pg/block, 95% CI: 85.453,8-107.011,3,  $p<0,01$ ). It was followed by PDGF-AB (23.051,3 pg/block, 95% CI: 8.963,9-37.138,7), VEGF (9.491,4 pg/block, 95% CI: 5.462,5-13.520,3), and BMP-1 (1.916,9 pg/block, 95% CI: 1.279,0-2.554,9). The same trend was observed for the L-PRF membrane.

Figure 2. Release of growth factors (TGF-β1, PDGF-AB, VEGF, BMP-1) from the L-PRF membrane and the L-PRF Block per time interval as well as its cumulative concentration up to 14 days. The respective concentrations in the L-PRF exudate and Liquid Fibrinogen are also indicated. \*:  $p<0,05$ , Δ:  $p<0,01$ .

For TGF-β1 and BMP-1, no statistically significant difference could be observed when comparing the L-PRF membrane and the L-PRF Block after 14 days ( $p>0,05$ ). However, the L-PRF membrane released



significantly more PDGF-AB ( $p < 0,01$ ), and the L-PRF Block showed larger levels of VEGF than that of the membrane ( $p < 0,05$ ).

#### Volumetric percentage of particles ( $\mu$ CT analysis)

The micro-CT analysis revealed a mean volume of  $37.7 \pm 1.7\%$  for the DBBM particles in the L-PRF Block (Figure 3). The particles were homogeneously distributed within the L-PRF Block, without being in close contact with each other.

#### SEM analysis

##### *L-PRF membrane*

The red part of the membrane also called the face presented a large number of cells, mostly platelets and leucocytes (Figure 4A). In the middle part (tail), fewer cells were detected than in the red part (Figure 4B). However, the same pattern of fibrin fibres was noticed in both parts.

##### *L-PRF Block*

The SEM images from the surface of the L-PRF Block showed a dense fibrin mesh covering the whole surface of the block. However, the fibrin network was less dense than in the membrane (Figure 4C). Numerous cells were embedded in this mesh, which seemed to keep the components of the block assembled (Figure 4). In the cross-sectional images (Figure 4E), bundles of fibres could be seen connecting different DBBM particles. These bundles contained clusters of platelets, leucocytes and some red blood cells (Figure 4F).

#### Discussion

This study presented an innovative method to assemble bone graft particles in a bioactive structure, combining a xenograft with autologous tissue. The study shows a continuous release of growth factors up to 14 days by both L-PRF Block and L-PRF membrane. In addition, the L-PRF exudate and the Liquid Fibrinogen can be considered as bioactive agents due to their active participation in the release of growth factors and their cellular content. To our best knowledge, this is the first investigation on the biological properties of the L-PRF Block.

Considering that the L-PRF Block comprises two L-PRF membranes and  $\pm 2$  ml of Liquid Fibrinogen, although not all gets into the block, it could be expected that the L-PRF Block would produce a greater amount of growth factors. This was the case for VEGF and BMP-1, which showed both higher cumulative levels and per time interval for the L-PRF Block. However, the L-PRF membrane produced higher concentration of TGF- $\beta$ 1 and three times more PDGF-AB than the L-PRF Block.

Growth factors delivery can rely on different mechanisms: physical entrapment of proteins within the scaffold, direct binding of the proteins to the scaffold, or the use of micro- or nanoparticles as protein reservoir (20). In the first situation, the growth factors become immobilized within the scaffold and the release occurs passively as the fibrin is being degraded, which is mediated by the serine protease plasmin. Plasmin acts on either fibrinogen or cross-linked fibrin and yield to a number of fibrin degradation products (21). This method generally reduces the rapid release of growth factors and allow a prolonged release of the growth factor that are entrapped into the carrier.

This might be a possible theory for the release of growth factors from the L-PRF Block. TGF- $\beta$ 1 and PDGF-AB both have a higher molecular weight (43 and 49 kDa, respectively), compared to those of VEGF (18 kDa) and BMP-1 (20 kDa). It might be more difficult for the large-sized proteins to escape from

the structure created by the Liquid Fibrinogen in the L-PRF Block, whereas the smallest ones may be released more easily. Due to this retention, the release of TGF- $\beta$ 1 and PDGF-AB gradually increased over time for the L-PRF Block as the fibrin network was becoming looser.

However, several biomaterials have been developed to control the release of growth factors from scaffolds (22). Fibrin-based matrices are well-known for the delivering of growth factors. Fibrin contains numerous binding sites for cells, proteins and growth factors that contribute to its role in modulation a number of complexes cellular responses (8, 21). Some growth factors such as TGF- $\beta$ 1, VEGF, and PDGF are covalently cross-linked to fibrin during the formation of fibrin (23-26). Thus, its release might be also influenced by this binding.

Many of other techniques involve encapsulation of the growth factors within degradable polymer so that they can be slowly released from the degrading scaffold into the wound site. This process has the capacity to obtain a constant therapeutic dose for longer than the rapidly releasing scaffolds (20). Microspheres and hydrogels are the most frequently used matrices for encapsulation (21). The precise quantification of growth factors encapsulated in delivery devices is equally critical and complex as achieving efficient delivery of active growth factors (27). The release of growth factors is frequently measured by ELISA assays. This method has the advantage of being simple and that the detection of protein level is immediate. However, beyond the release kinetics assays, in vitro cellular models allow for more detail study of growth factors release profile. They enable us to determine bioactivity of the released growth factor and to gain insight into the appropriate therapeutic dosage (21). However, the bioactivity of PDGF-AB, TGF- $\beta$ 1, VEGF, and BMP-1 was not examined in this study. Further research should consider the analysis of the bioactivity is these growth factors released by the L-PRF Block.

This is the first time that the release of BMP-1 from the L-PRF membrane and derivatives has been reported. Bone morphogenetic proteins form a unique group of proteins within the Transforming Growth Factor beta (TGF-  $\beta$ ) superfamily. BMPs play a role in differentiation and proliferation of a wide variety of cells, depending on the cellular micro-environment and the interactions with other regulatory factors (28). BMP-1 is a metalloproteinase that functions in collagen maturation and is not part of the TGF-  $\beta$  family (28, 29). Recent findings indicate that BMP-1 is identical to pro-collagen C-proteinase, which is a proteinase involved in extracellular matrix formation (30, 31).

The L-PRF exudate presented a low cellular content, with 6% of platelets and 0.9% of leucocytes. Schär et al. (2015)(15) examined the exudate released from the L-PRF clot (without compression) after a short time period. They reported smaller levels of PDGF-BB and TGF- $\beta$ 1 than those observed in the present study. The high presence of PDGF-AB and TGF- $\beta$ 1 in the L-PRF exudate in our study might suggest that as the clot was squeezed, most of the liquid inside and its molecular content was also released, leading to a higher concentration of those growth factors.

Both the L-PRF membrane and Liquid Fibrinogen presented a high concentration in leucocytes. In Figure 4, the leucocytes marked in the SEM images could have corresponded with lymphocytes given its shape and size. Taking into account the cellular concentrations shown in Table 1, lymphocytes were the most abundant leucocyte type in the Liquid Fibrinogen and the second in the L-PRF membrane. However, a specific staining under fluorescence microscopy would be necessary to distinguish every cell type.

The role of the Liquid Fibrinogen in the L-PRF Block seems to be crucial and twofold: it mechanically glues all the components of the L-PRF Block together and at the same time, it has bioactive properties. The protocol used to produce the Liquid Fibrinogen is derived from a protocol to prepare platelet rich plasma (PRP) without using anticoagulants and with a single centrifugation technique

(Arthex Autologous Conditioned Plasma ACP®, Naples, FL, USA). In the original protocol, the blood was centrifuged at 350 *g* for 5 minutes, resulting in a 2,1x platelet concentration (32, 33). In order to facilitate the preparation of Liquid Fibrinogen, the blood was centrifuged at 408 *g* for 3 minutes, using the same *g* force as for producing L-PRF.

The microCT analysis revealed a ratio of 40:60 between DBBM particles and autologous tissue (L-PRF membrane and Liquid Fibrinogen). Initially, the block was prepared with an estimated ratio of 50:50. However, after having added Liquid Fibrinogen the proportion changed in favour of the autologous tissue. Cortellini et al. (2018)(17) reported an average resorption of the L-PRF Block around 15% after 5-8 months healing. Given the well-known slow resorption rate of the DBBM (34), they assumed that the remaining 45% of the healed graft was generated from the L-PRF, which seemed to be new bone tissue on CBCT images. However, these statements should be confirmed with histological analysis.

The ultrastructural similarity of the DBBM particles with natural bone has been demonstrated in various transmission electron microscopy (TEM) studies (35, 36). Rosen et al. (2002)(35) reported that the diameter of the mineral fibres of the DBBM particles (65-80µm) was similar to the diameter of the type I collagen that comprises bone. This biomaterial, with a porosity of 75%-80% and a crystal size of 10 µm, has shown osteoconductive properties and a slow resorption rate (37, 38). A recent study suggested that the porous structure might serve as a scaffold for in-growth of blood vessels (39). For instance, Degidi et al. (2006)(40) observed that the bone augmented with DBBM after 6 months had statistically higher microvessel density values and more vessels positive to VEGF than the pre-existing bone. Moreover, several *in vitro* studies concluded that DBBM can support osteoblast attachment and proliferation, and can be further enhanced when PDGF is on the surface (41, 42). This would support the hypothesis that growth factors on/or near to the xenograft can influence osteogenesis *in vivo*. Likewise, Schwartz et al. (2000)(43) suggested that DBBM might have tissue-specific osteoinductive properties and might contain growth factors such as TGF-β1 and BMP-2. Given the active production of growth factors by the L-PRF membrane and derivatives, it might further stimulate the biological properties of the DBBM particles becoming a bioactive scaffold.

## **Conclusions**

Within the limitations of this study, it can be concluded that the L-PRF Block is composed by bovine bone particles surrounded by platelets, leucocytes and embedded in a fibrin network that releases growth factors up to 14 days. It might be considered as a biomaterial for tissue engineering.

## Figures

Figure 1. Preparation of an L-PRF Block. A: chop two L-PRF membranes in small pieces; B and C: mix chopped L-PRF membranes with bone substitute (DBBM particles); D: add  $\pm 2$  ml of Liquid Fibrinogen; this liquid can only be stored for  $\leq 30$  min; E: mix carefully during 5-10 seconds and stir gently; and F: wait 3 minutes until the block is formed. Keep the block covered in the dish to prevent it from drying out.

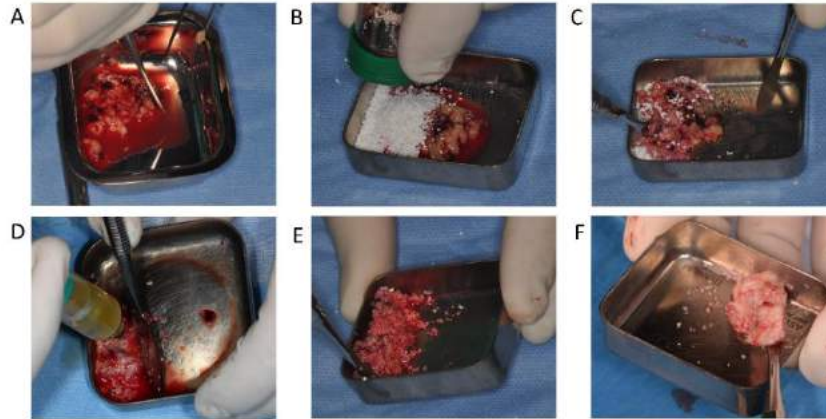


Figure 2. Release of growth factors (TGF- $\beta$ 1, PDGF-AB, VEGF, BMP-1) from the L-PRF membrane and the L-PRF Block per time interval as well as its cumulative concentration up to 14 days. The respective concentrations in the L-PRF exudate and Liquid Fibrinogen are also indicated. \*:  $p < 0.05$ ,  $\Delta$ :  $p < 0.01$ .

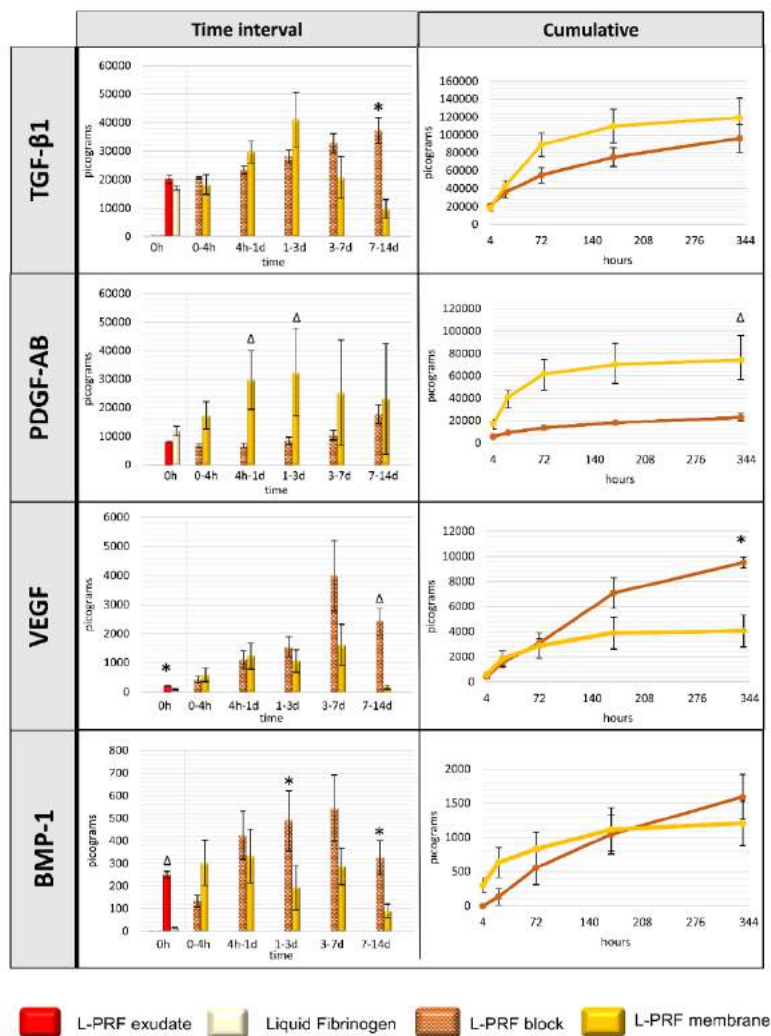


Figure 3. Reconstruction images of the microCT. Sections selected at 7.3 and 14.0 mm from a total length of 21.0 mm. Deproteinized bovine bone mineral were detected as radiopaque particles.

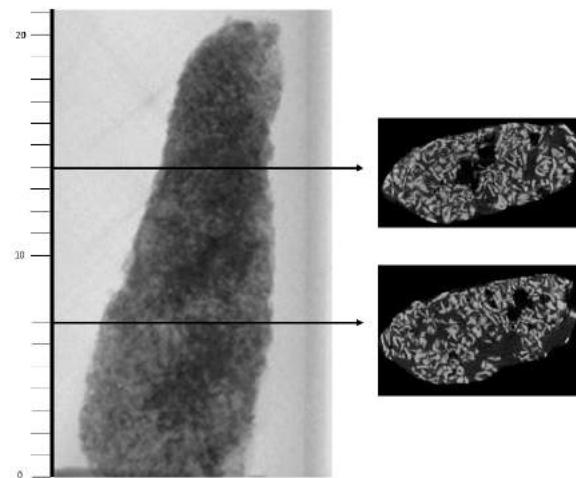
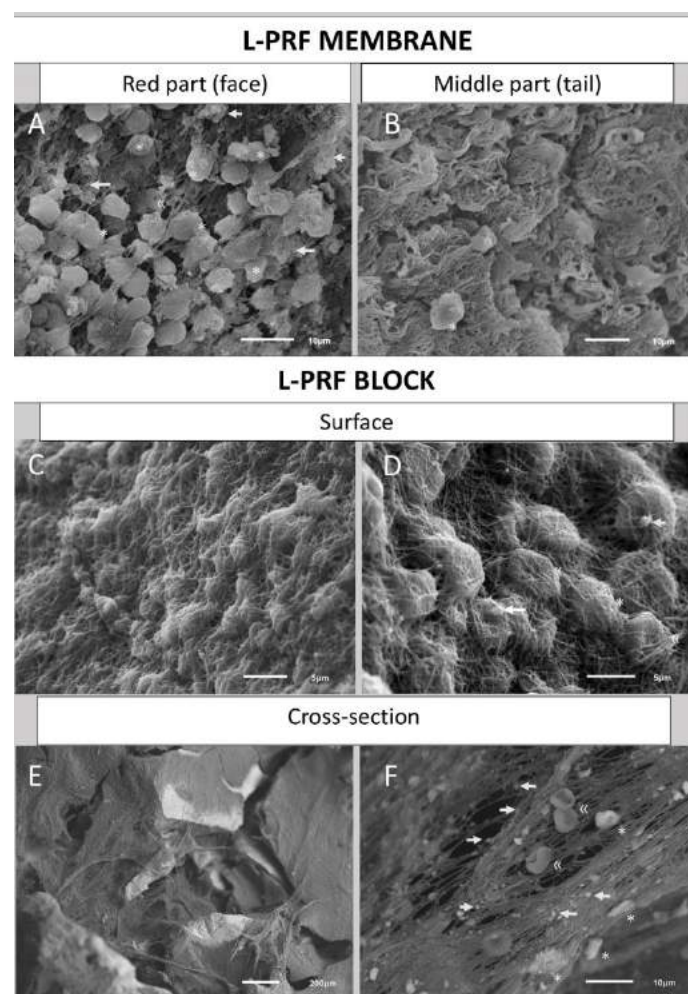


Figure 4. SEM images of the L-PRF Block (surface and cross-section) and L-PRF membrane (face and tail). A: High concentration of cells present in the red part (face) of the L-PRF membrane. B: Fibrin fibres of the middle part of the L-PRF membrane with the presence of some cells. C: Dense fibrin network with embedded cells covering the block. D: Cells embedded in the fibrin network. E: Fibres of the Liquid Fibrinogen connecting the DBBM particles inside the block. F: Cells present in the Liquid Fibrinogen at higher magnification. ( → : platelets, \*: leucocytes, and «: red blood cells).



**Tables**

Table 1. Cellular counting for L-PRF membrane (per mb), L-PRF exudate (per ml) and Liquid Fibrinogen (per ml), and their relative percentage. †: relative percentage in relation to the initial blood sample.

	L-PRF membrane (per mb)				L-PRF exudate (per ml)				Liquid Fibrinogen (per ml)			
	mean	<i>sd</i>	% <sup>†</sup>	<i>sd</i>	mean	<i>sd</i>	% <sup>†</sup>	<i>sd</i>	mean	<i>sd</i>	% <sup>†</sup>	<i>sd</i>
<b>Platelets</b>	$1.9 \times 10^9$	$4.5 \times 10^8$	81.3	17.1	$6.1 \times 10^7$	$6.1 \times 10^7$	2.5	2.3	$2.1 \times 10^9$	$2.3 \times 10^8$	88.9	5.6
<b>Leucocytes</b>	$3.6 \times 10^7$	$1.9 \times 10^7$	72.6	13.9	$5.0 \times 10^5$	$7.5 \times 10^5$	0.9	1.2	$3.3 \times 10^7$	$1.5 \times 10^7$	70.3	16.0
<b>Neutrophils</b>	$2.0 \times 10^7$	$1.3 \times 10^7$	69.3	29.1	$1.4 \times 10^5$	$2.7 \times 10^5$	0.5	0.8	$1.5 \times 10^7$	$1.4 \times 10^7$	52.3	41.6
<b>Lymphocytes</b>	$1.2 \times 10^7$	$4.7 \times 10^6$	60.9	14.0	$2.9 \times 10^5$	$3.7 \times 10^5$	1.4	1.6	$1.7 \times 10^7$	$4.7 \times 10^6$	84.7	16.8
<b>Monocytes</b>	$3.5 \times 10^6$	$1.7 \times 10^6$	76.9	21.1	$3.8 \times 10^4$	$8.4 \times 10^4$	1.4	3.4	$3.0 \times 10^6$	$1.4 \times 10^6$	78.7	25.9
<b>Eosinophils</b>	$3.1 \times 10^6$	$2.9 \times 10^6$	28.0	20.8	$1.5 \times 10^4$	$1.4 \times 10^4$	2.0	2.3	$9.9 \times 10^5$	$1.2 \times 10^6$	71.8	36.0
<b>Basophils</b>	$4.4 \times 10^5$	$3.3 \times 10^5$	59.7	36.9	$1.1 \times 10^4$	$2.8 \times 10^4$	1.3	3.3	$3.5 \times 10^5$	$3.0 \times 10^5$	44.3	40.3



## References

1. Benic GI, Hämmerle CH. Horizontal bone augmentation by means of guided bone regeneration. *Periodontol* 2000. 2014;66(1):13-40.
2. Esposito M, Grusovin MG, Felice P, Karatzopoulos G, Worthington HV, Coulthard P. The efficacy of horizontal and vertical bone augmentation procedures for dental implants - a Cochrane systematic review. *Eur J Oral Implantol*. 2009;2(3):167-84.
3. Urban IA, Nagursky H, Lozada JL. Horizontal ridge augmentation with a resorbable membrane and particulated autogenous bone with or without anorganic bovine bone-derived mineral: a prospective case series in 22 patients. *Int J Oral Maxillofac Implants*. 2011;26(2):404-14.
4. Altıparmak N, Soydan SS, Uckan S. The effect of conventional surgery and piezoelectric surgery bone harvesting techniques on the donor site morbidity of the mandibular ramus and symphysis. *Int J Oral Maxillofac Surg*. 2015;44(9):1131-7.
5. Avila-Ortiz G, Bartold PM, Giannobile W, Katagiri W, Nares S, Rios H, et al. Biologics and Cell Therapy Tissue Engineering Approaches for the Management of the Edentulous Maxilla: A Systematic Review. *Int J Oral Maxillofac Implants*. 2016;31 Suppl:s121-64.
6. Janmey PA, Winer JP, Weisel JW. Fibrin gels and their clinical and bioengineering applications. *Journal of The Royal Society Interface*. 2009;6(30):1-10.
7. Nürnberger S, Wolbank S, Peterbauer-Scherb A, Morton TJ, Feichtinger GA, Gugerell A, et al. Properties and Potential Alternative Applications of Fibrin Glue. In: von Byern J, Grunwald I, editors. *Biological Adhesive Systems: From Nature to Technical and Medical Application*. Vienna: Springer Vienna; 2010. p. 237-59.
8. Brown AC, Barker TH. Fibrin-based biomaterials: modulation of macroscopic properties through rational design at the molecular level. *Acta Biomater*. 2014;10(4):1502-14.
9. Lee CR, Grad S, Gorna K, Gogolewski S, Goessl A, Alini M. Fibrin–Polyurethane Composites for Articular Cartilage Tissue Engineering: A Preliminary Analysis. *Tissue Engineering*. 2005;11(9-10):1562-73.
10. Collen A, Smorenburg SM, Peters E, Lupu F, Koolwijk P, Van Noorden C, et al. Unfractionated and low molecular weight heparin affect fibrin structure and angiogenesis in vitro. *Cancer Res*. 2000;60(21):6196-200.
11. Rao RR, Peterson AW, Ceccarelli J, Putnam AJ, Stegemann JP. Matrix composition regulates three-dimensional network formation by endothelial cells and mesenchymal stem cells in collagen/fibrin materials. *Angiogenesis*. 2012;15(2):253-64.
12. Testori T, Wallace SS, Trisi P, Capelli M, Zuffetti F, Del Fabbro M. Effect of xenograft (ABBM) particle size on vital bone formation following maxillary sinus augmentation: a multicenter, randomized, controlled, clinical histomorphometric trial. *Int J Periodontics Restorative Dent*. 2013;33(4):467-75.
13. Miron RJ, Zhang Q, Sculean A, Buser D, Pippenger BE, Dard M, et al. Osteoinductive potential of 4 commonly employed bone grafts. *Clin Oral Investig*. 2016;20(8):2259-65.
14. Dohan Ehrenfest DM, Doglioli P, de Peppo GM, Del Corso M, Charrier JB. Choukroun's platelet-rich fibrin (PRF) stimulates in vitro proliferation and differentiation of human oral bone mesenchymal stem cell in a dose-dependent way. *Arch Oral Biol*. 2010;55(3):185-94.
15. Schär MO, Diaz-Romero J, Kohl S, Zumstein MA, Nesic D. Platelet-rich concentrates differentially release growth factors and induce cell migration in vitro. *Clin Orthop Relat Res*. 2015;473(5):1635-43.

16. Dohan DM, Choukroun J, Diss A, Dohan SL, Dohan AJJ, Mouhyi J, et al. Platelet-rich fibrin (PRF): A second-generation platelet concentrate. Part II: Platelet-related biologic features. *Oral Surgery, Oral Medicine, Oral Pathology, Oral Radiology, and Endodontics*. 2006;101(3):E45-E50.
17. Cortellini S, Castro AB, Temmerman A, Van Dessel J, Pinto N, Jacobs R, et al. Leucocyte- and platelet-rich fibrin block for bone augmentation procedure: A proof-of-concept study. *J Clin Periodontol*. 2018;45(5):624-34.
18. Temmerman A, Vandessel J, Castro A, Jacobs R, Teughels W, Pinto N, et al. The use of leucocyte and platelet-rich fibrin in socket management and ridge preservation: a split-mouth, randomized, controlled clinical trial. *J Clin Periodontol*. 2016;43(11):990-9.
19. Schrijver RS, Kramps JA. Critical factors affecting the diagnostic reliability of enzyme-linked immunosorbent assay formats. *Rev Sci Tech*. 1998;17(2):550-61.
20. De Witte TM, Fratila-Apachitei LE, Zadpoor AA, Peppas NA. Bone tissue engineering via growth factor delivery: from scaffolds to complex matrices. *Regen Biomater*. 2018;5(4):197-211.
21. Blackwood KA, Bock N, Dargaville TR, Ann Woodruff M. Scaffolds for Growth Factor Delivery as Applied to Bone Tissue Engineering. *International Journal of Polymer Science*. 2012;2012:25.
22. Polo-Corrales L, Latorre-Esteves M, Ramirez-Vick JE. Scaffold design for bone regeneration. *J Nanosci Nanotechnol*. 2014;14(1):15-56.
23. Catelas I, Dwyer JF, Helgersson S. Controlled release of bioactive transforming growth factor beta-1 from fibrin gels in vitro. *Tissue Eng Part C Methods*. 2008;14(2):119-28.
24. Sahni A, Francis CW. Vascular endothelial growth factor binds to fibrinogen and fibrin and stimulates endothelial cell proliferation. *Blood*. 2000;96(12):3772-8.
25. Zisch AH, Schenk U, Schense JC, Sakiyama-Elbert SE, Hubbell JA. Covalently conjugated VEGF--fibrin matrices for endothelialization. *J Control Release*. 2001;72(1-3):101-13.
26. Mittermayr R, Branski L, Moritz M, Jeschke MG, Herndon DN, Traber D, et al. Fibrin biomatrix-conjugated platelet-derived growth factor AB accelerates wound healing in severe thermal injury. *J Tissue Eng Regen Med*. 2016;10(5):E275-85.
27. Bock N, Dargaville TR, Kirby GT, Hutmacher DW, Woodruff MA. Growth Factor-Loaded Microparticles for Tissue Engineering: The Discrepancies of In Vitro Characterization Assays. *Tissue Eng Part C Methods*. 2015.
28. Sykaras N, Opperman LA. Bone morphogenetic proteins (BMPs): how do they function and what can they offer the clinician? *J Oral Sci*. 2003;45(2):57-73.
29. Wang RN, Green J, Wang Z, Deng Y, Qiao M, Peabody M, et al. Bone Morphogenetic Protein (BMP) signaling in development and human diseases. *Genes Dis*. 2014;1(1):87-105.
30. Kessler E, Takahara K, Biniaminov L, Brusel M, Greenspan DS. Bone morphogenetic protein-1: the type I procollagen C-proteinase. *Science*. 1996;271(5247):360-2.
31. Sarras MP, Jr. BMP-1 and the astacin family of metalloproteinases: a potential link between the extracellular matrix, growth factors and pattern formation. *Bioessays*. 1996;18(6):439-42.
32. Franklin SP, Cook JL. Prospective trial of autologous conditioned plasma versus hyaluronan plus corticosteroid for elbow osteoarthritis in dogs. *Can Vet J*. 2013;54(9):881-4.
33. Lebiezinski R, Borowski A, Synder M, Grzegorzewski A, Marciniak M, Sibinski M. Comparison Analysis of Autologous Conditioned Plasma. *Ortop Traumatol Rehabil*. 2016;18(6):563-8.
34. Galindo-Moreno P, Hernandez-Cortes P, Aneiros-Fernandez J, Camara M, Mesa F, Wallace S, et al. Morphological evidences of Bio-Oss(R) colonization by CD44-positive cells. *Clin Oral Implants Res*. 2014;25(3):366-71.



35. Rosen VB, Hobbs LW, Spector M. The ultrastructure of anorganic bovine bone and selected synthetic hydroxyapatites used as bone graft substitute materials. *Biomaterials*. 2002;23(3):921-8.
36. Landis WJ, Hodgins KJ, Arena J, Song MJ, McEwen BF. Structural relations between collagen and mineral in bone as determined by high voltage electron microscopic tomography. *Microsc Res Tech*. 1996;33(2):192-202.
37. Piattelli M, Favero GA, Scarano A, Orsini G, Piattelli A. Bone reactions to anorganic bovine bone (Bio-Oss) used in sinus augmentation procedures: a histologic long-term report of 20 cases in humans. *Int J Oral Maxillofac Implants*. 1999;14(6):835-40.
38. Sartori S, Silvestri M, Forni F, Icaro Cornaglia A, Tesei P, Cattaneo V. Ten-year follow-up in a maxillary sinus augmentation using anorganic bovine bone (Bio-Oss). A case report with histomorphometric evaluation. *Clin Oral Implants Res*. 2003;14(3):369-72.
39. Weibrich G, Trettn R, Gnoth SH, Gotz H, Duschner H, Wagner W. [Determining the size of the specific surface of bone substitutes with gas adsorption]. *Mund Kiefer Gesichtschir*. 2000;4(3):148-52.
40. Degidi M, Artese L, Rubini C, Perrotti V, Iezzi G, Piattelli A. Microvessel density and vascular endothelial growth factor expression in sinus augmentation using Bio-Oss. *Oral Dis*. 2006;12(5):469-75.
41. Jiang D, Dziak R, Lynch SE, Stephan EB. Modification of an osteoconductive anorganic bovine bone mineral matrix with growth factors. *J Periodontol*. 1999;70(8):834-9.
42. Stephan EB, Jiang D, Lynch S, Bush P, Dziak R. Anorganic bovine bone supports osteoblastic cell attachment and proliferation. *J Periodontol*. 1999;70(4):364-9.
43. Schwartz Z, Weesner T, van Dijk S, Cochran DL, Mellonig JT, Lohmann CH, et al. Ability of deproteinized cancellous bovine bone to induce new bone formation. *J Periodontol*. 2000;71(8):1258-69.

## CHAPTER 4

### Impact of *g* force and timing on the characteristics of PRF matrices

Castro Ana B\*, Andrade Catherine\*, Li Xin, Pinto Nelson, Teughels Wim & Quirynen Marc. (2021) Scientific Reports 11; 6038

\* shared first-authorship

#### **Abstract**

**Aim:** This in vitro study aimed to compare the biological and physical characteristics of 3 types of PRF membranes using 2 different centrifuges (Intra-Spin and Duo) with adapted relative centrifugal forces (RCF): leucocyte- and platelet-rich fibrin (L-PRF: 408 g, 12min); advanced platelet-rich fibrin (A-PRF: 276 g, 14min); advanced platelet-rich fibrin<sup>+</sup> (A-PRF<sup>+</sup>: 208 g, 8min).

**Material & methods:** The release of growth factors, the macroscopic dimensions, cellular content and the mechanical properties (Young's modulus) of the respective membranes, prepared from blood of the same individual, were explored. Also the impact of timing (blood draw - centrifugation and centrifugation - membrane preparation) was assessed morphologically including scanning electron microscopy.

**Results:** No statistically significant differences between the 3 PRF modifications could be observed, neither in their release of growth factors or the cellular content, nor in clot/membrane dimensions. The difference between both centrifuges were neglectable when using the same *g* force. A lower *g* force, however, reduced the membrane tensile strength. Timing in the preparation had a significant impact. Ideally the time between blood draw and centrifugation should be  $\leq 1$  min, and between centrifugation and membrane preparation  $\leq 30$  min.

**Conclusions:** The suggested changes in RCF had minimal impact on the final characteristics of the PRF membranes.

#### **Introduction**

A centrifuge creates a centrifugal force for separating substances of different densities in a liquid by rotating at a certain speed measured as revolutions per minute, RPM. The force applied during centrifugation is called relative centrifugal force (RCF). (1) It causes denser substances and particles to move outward in the radial direction. Denser particles thus settle at the bottom of the tube, while low-density substances move to the top. (2) This technique is often used to separate red blood cells from serum or plasma. Based on this procedure, the concept of platelet concentrates (PCs) arose in the '70s, (3) and in the late '90s and beginning of the 00's their use gained more interest in the oral and maxillofacial field. (4, 5) In 2009, PCs were newly classified into four categories depending on leucocyte inclusion and architecture: (6) pure platelet-rich plasma (P-PRP), leucocyte and platelet-rich plasma (L-PRP), pure platelet-rich fibrin (P-PRF), and leucocyte- and platelet-rich fibrin (L-PRF). L-PRF is obtained after centrifugation of blood in glass or silica-coated plastic tubes without the use of anticoagulants, such as EDTA. Three layers are obtained: red blood cells at the bottom, a buffy coat (clot) consisting of leucocytes and platelets in the middle, and a-cellular plasma at the top. The original protocol for L-PRF provided centrifugation at RCF<sub>clot</sub>: 408 g (RCF<sub>max</sub>: 653 g, RCF<sub>min</sub>: 326 g, RCF<sub>average</sub>: 489 g, distance

to rotor for RCFclot: 50 mm) for 12 minutes in order to reach high concentrations of platelets and leucocytes in the buffy coat (7). In the past decade, the use of L-PRF has increased exponentially. (8, 9)

Separating substances of different densities by centrifugation depends on several aspects, including speed (rotation/revolutions per minute), and duration of spinning. The g- force is influenced by the angulation and radius of the rotor in the centrifuge and these differ widely depending on the type of centrifuge. (10) Rotor stability also has a significant impact, with reduced separation in case of radial vibration. In any evaluation or comparison of medical devices and protocols in this area, factual accuracy is of the utmost importance. Even centrifugation at identical RPM will exert different centrifugal forces if centrifuge rotors have different radius sizes, bucket types or bucket sizes. In 2014, Ghanaati and co-workers (11) proposed a new protocol increasing the time of centrifugation and decreasing speed (A-PRF, RCFclot 193 g, RCFmax: 276 g for 14 min), using glass tubes for blood collection. Recently, the same group introduced another modification (12) by reducing centrifugation speed and duration even further (A-PRF +, RCFclot 145 g, RCFmax: 208 g for 8 min). Reducing RCF resulted in an increase in the release of growth factors and in the concentration of leucocytes and platelets.

Studies comparing A-PRF or A-PRF+ with L-PRF have led to controversial data (12-14). For instance, Ehrenfest and co-workers (15) (2018) compared L-PRF vs. A-PRF prepared with various centrifugation devices and concluded that the L-PRF protocol allowed producing larger clots/membranes and a more intense release of growth factors. In contrast, in a similar study El Bagdadi and co-workers (13) (2019) compared L-PRF vs. A-PRF vs. A-PRF+ and observed an increased in growth factors release when RCF was reduced. Comparing findings is complicated by the heterogeneity in methods used, such as type of tube (plastic or glass) and adaptation of RCF to the rcf-max or rcf-clot. Moreover, neither of these studies evaluated the real effect of the centrifuge when the same PRF matrices were prepared with the g force adapted for each device nor the impact of using a glass or plastic tube.

Therefore, the primary aim of this study was to investigate whether the adaptation of the g force for the above-mentioned PRF modifications (L-PRF, A-PRF, and A-PRF+) in 2 centrifuges have any influence on their characteristics in terms of release of growth factors, morphology, cellular content, and mechanical properties. Although speed and duration of centrifugation are crucial, timing of the entire process also appears to be an important factor. Therefore, the secondary aim was to assess the influence of time before and after centrifugation on L-PRF membrane morphology.

## **Material & Methods**

Eight healthy volunteers were included in this study. The exclusion criteria comprised the following conditions: anticoagulant medication 3 months before the study, pregnancy or lactation, history of periodontal disease or any active systemic infection. A total of six 9-ml silica-coated plastic tubes (BVBCTP-2, Intra-Spin, Intra-Lock, Florida, USA), and six 10-ml glass tubes (A-PRF tubes, Process for PRF, Nice, France) were collected per participant. Three out of eight volunteers donated an extra 12 tubes of blood for the timing experiments: six for the blood draw - centrifugation time (time before centrifugation), and six for the centrifugation - membrane preparation time (time after centrifugation). The tube distribution for each experiment is shown in Figure 1.

The use of human blood was approved by the KU Leuven ethical committee and registered with identifier B322201628215. The procedures were executed according to the Helsinki Declaration and the regulations of the University Hospital, which are approved by the ethical committee. An informed consent was obtained from all subjects.

### A. Comparison PRF modifications

#### *Preparation of the PRF clots/membranes*

Three types of platelet concentrates were prepared with two different centrifuges and the g-force was adapted for each protocol: leucocyte- and platelet-rich fibrin (L-PRF) (RCFclot 408 g, RCFmax: 653 g, for 12 min) (16); advanced platelet-rich fibrin (A-PRF) (RCFclot 193 g, RCFmax: 276 g for 14 min) (11); and advanced platelet-rich fibrin+ (A-PRF+) (RCFclot 145 g, RCFmax: 208 g for 8 min) (12).

These clots were gently compressed into membranes using the specific design box for each protocol (L-PRF: Xpression kit, Biohorizons, Birmingham, Alabama, USA ; A-PRF and A-PRF+: PRF Box, Process for PRF, Nice, France). Two centrifuges were used, in which the g-force could be adapted: the DUO centrifuge [Process for PRF, Nice, France, (DUO)] and the Intra-Spin centrifuge [Biohorizons, Birmingham, Alabama, USA, (IL)].

Six different membranes were prepared: L-PRF-DUO, A-PRF-DUO, A-PRF+-DUO; and L-PRF-IL, A-PRF-IL, A-PRF +-IL (Table 1). Following the manufacturer's instructions, 10-ml glass tubes were used for all the preparations in the DUO centrifuge, and 9-ml silica-coated plastic tubes for the Intra-Spin centrifuge.

#### *Release of growth factors*

Each membrane (L-PRF-DUO, L-PRF-IL, A-PRF-DUO, A-PRF-IL, A-PRF+-DUO, A-PRF+-IL) was placed in a 15 ml-tube with 5 ml of Dulbecco's Modified Eagle medium (Sigma-Aldrich BVBA, Overijse, Belgium) without antibiotics and changed to a new tube with sterile tweezers after 4 hours and then on day 1, 3, 7, and 14. After membrane collection at each time interval, the remaining medium was centrifuged at 1000 rpm for 10 minutes (VWR® Mega Star 6000R, VWR International BVBA, Haasrode, Belgium) to remove any residue and thereafter frozen at -80° Celsius.

The concentrations of vascular endothelial growth factor (VEGF), transforming growth factor beta-1 (TGF-β1), and platelet-derived growth factor-AB (PDGF-AB) were measured in duplicate with commercially available enzyme-linked immunosorbent assay kits (ELISA, R&D Systems Europe, Abingdon, UK) following the manufacturer's instructions. The levels of bone morphogenetic protein-1 (BMP-1) were also recorded by another ELISA test (Abbexa, Cambridge Science Park, UK). Measurements were conducted with a microplate reader (Multiskan Ascent®, Rev 1.2, Thermo Electron Corporation, Vantaa, Finland) set to 450 nm (using 550 nm as a background reference). The exudate released during compression of the clot into a membrane was kept to analyse the cellular content.

#### *Cellular counting*

Cellular counting was performed for all the membranes with a haematology analyser (CELL-DYN 3700, Abbott GmbH & Co, Wiesbaden, Germany). Given the difficulty to dissolve the membranes without damaging the cells, cellular counting was carried out indirectly following the protocol described by Castro et al., (2019) (17) (Figure 2). All samples were frozen at -80° Celsius after addition of 10% dimethylsulfoxide (DMSO) to avoid the formation of crystals inside the cells.

#### *Macroscopic analysis*

After centrifugation, the clots were removed from the tubes and weighed immediately. Standardized pictures were taken of all the clots on a graph paper. Afterwards, the clots were transformed into a membrane by gentle compression; membranes were weighed and standardized pictures taken. The

length and the width of each clot and membrane were measured with software ImageJ® (Image Processing and Analysis in Java, 1.8.0\_77). A horizontal (length) and a vertical (width) line were drawn from the middle point of the clot or membrane with an angle of 90°.

#### *Physical characteristics*

Tensile tests were carried out on a TA.XT plus Texture Analyser (Stable Microsystems, Surrey, UK). The membranes had previously been cut with a specially designed metal mould with a “dog-bone” shape. The dimensions were 5 mm width in the narrowest middle part, 10 mm width at both ends, and 1 mm in thickness. The shaped membranes were held with the tensile grips of the Texture Analyser (A/MTG Mini), leaving the specimen free of tension. Next, the test was programmed on Exponent software (Stable Microsystems, Surrey, UK) applying the tensile load at a constant speed of 0.5 mm/sec. Stress-strain curve data were recorded and the elastic modulus was calculated by using the slope of the stress/strain curve.

For the compression test, the same equipment was used but the membranes were cut with a 10-mm diameter metal punch, and the tensile grips were changed by a cylinder probe P/0.5 (Stable Microsystems, UK). The specimens were compressed to about 50% (50% deformation) at a constant speed of 0.5 mm/sec. Stress-strain curve data were recorded and the elastic modulus was calculated by using the slope of the stress/strain curve.

### B. Influence of Time in the Preparation of Platelet Concentrates

#### *Timing: blood draw - centrifugation*

Six extra 9-ml plastic silica-coated tubes were collected from three participants. One tube was centrifuged immediately (< 1 minute) at 408 g for 12 min, whereas the remaining five were gently shaken for 1, 3, 5, 7, and 10 min before centrifugation. Standardized pictures were taken of the corresponding membranes. Morphology (length and width) was measured with ImageJ as described for the macroscopic analysis.

One L-PRF membrane from each time point (if a membrane could be obtained) was processed for SEM analysis following the protocol described by Castro and co-workers(17) (2019). Briefly, each membrane was fixed immediately after preparation in 2.5% glutaraldehyde in 0.1 M sodium cacodylate buffer for 24 h, rinsed with 0.2 M sodium cacodylate buffer and distilled water, and dehydrated in ascending dilutions of ethanol (25, 50, 75, 95, and 100%). After dehydration, each sample was immersed in hexamethyldisilazane 98% (Acros Organics, Geel, Belgium) for 10 min and air-dried at room temperature. The specimens were coated with gold by an auto fine coater (JFC-1300, JEOL, Tokyo, Japan). The images from the red part (face, the area previously in contact with the red blood cells) and the middle part (tail) were taken using SEM (JSM-6610LV, JEOL).

#### *Timing: centrifugation - membrane preparation*

Another six 9-ml plastic silica-coated tubes from 3 patients were immediately centrifuged at 408 g for 12 min. L-PRF membrane were prepared immediately after centrifugation and after 30 min, 1h, 2h, and 3h, respectively.

## Data Analysis

In order to analyse growth factor release, the fixed effects coefficients and their variance-covariance matrix were subjected to a multiple comparisons procedure with the best <sup>49</sup>. The concentrations of growth factors for each membrane were calculated, per time interval and cumulative concentration.

A linear mixed model was set up for each haematological cell type separately, with each protocol as fixed factor and the subject as random factor. Normality of the residuals was assessed by means of a normal quantile plot and data were log-transformed if the normal quantile plot indicated a distribution that approached a log-normal distribution.

The data for the mechanical testing were analysed using descriptive statistics by reporting the mean and standard deviation. An unpaired student t-test was used to compare all groups.

For the data of the time before/after centrifugation, a linear mixed model was applied with donor as random factor. A normal quantile plot was used to assess the normality of the residuals. Comparisons between timings were corrected for simultaneous hypothesis testing according to Tukey.

## Results

Eight healthy subjects (4 women, 4 men) participated in this study. The mean age was  $42.8 \pm 14.2$  years (range 29-60 years). No complications during blood collection were reported. In one subject, the L-PRF-DUO membrane was completely dissolved at the 7-14 day time interval. The same occurred with the A-PRF+IL of another subject at the same time interval.

### A. Comparison PRF modifications

#### *Release of growth factors per time interval (Figure 3)*

The highest amount of VEGF was released by A-PRF-DUO at 1-3 days (2241.4 pg/mb, 95%CI 917.8-3565.0). No statistically significant differences could be observed among any of the membranes (different device/different setting) ( $p > 0.05$ ). For PDGF-AB, the maximum concentration of protein released occurred during the 1-3 day time interval for all membranes. However, no statistically significant difference amongst all membranes was observed ( $p > 0.05$ ). All membranes produced the highest amount of TGF- $\beta$ 1 at the 1-3 day time interval. Statistically significant difference could only be observed between A-PRF-DUO and A-PRF-IL in favour of the latter ( $p < 0.05$ ). Similarly, all membranes produced the highest amount of BMP-1 at a 4h-1-day time interval. No significant differences could be found between the membranes ( $p > 0.05$ ).

#### *Cumulative measurement on release of growth factors (Figure 3)*

The highest amount of VEGF over 14 days was released by L-PRF-DUO (6306.8 pg/mb, 95%CI 1351.3-9075.6). However, no statistically significance difference was found in comparison with other membranes ( $p > 0.05$ ). For PDGF-AB, the highest amount was released by A-PRF-IL (83692.3 pg/mb, 95%CI 63976.9-103407.7), but no statistically significant difference could be found between all membranes ( $p > 0.05$ ). A-PRF+-DUO released the highest amount of TGF- $\beta$ 1 after 14 days (177974.1 pg/mb, 95%CI 136761.3-2191896.9). This did not reach statistical significance compared with the other membranes ( $p > 0.05$ ). Likewise, A-PRF-IL produced the highest amount of BMP-1 after 14 days (1723.4 pg/mb, 95%CI 731.5-4033.5) but no differences could be observed among any of the membranes ( $p > 0.05$ ).

Women released slightly more growth factors compared with men except for VEGF (L-PRF-IL), PDGF (L-PRF-IL and L-PRF-DUO), and TGF- $\beta$ 1 (L-PRF-IL and A-PRF<sup>+</sup>-IL), albeit not statistically significant ( $p < 0.05$ ).

#### *Cellular counting*

All membranes contained more than 60% of leucocytes available in the initial blood sample. No statistically significant differences were observed for any leucocyte cell type amongst protocols ( $p > 0.05$ ). Similarly, all membranes presented more than 80% of platelets, except L-PRF-DUO (74.0%) and A-PRF<sup>+</sup>-DUO (76.9%). These differences did not reach statistical significance (Figure 4).

The exudate showed a low cellular content with less than 3% of platelets and 1% of leucocytes for all settings. No statistically significant differences were observed for the platelet count ( $p > 0.05$ ). Statistically significant differences amongst white blood cells are shown in Figure 4E.

#### *Macroscopic analysis (Table 2)*

In terms of length or width no statistically significant differences could be observed among the different clots. In terms of weight statistically significant differences ( $1.6 \pm 0.4$  g vs.  $2.1 \pm 0.6$  g,  $p < 0.05$ ) were only observed between L-PRF-IL clots vs. L-PRF-DUO clots. No differences in length, width, or weight were observed in the membranes ( $p > 0.05$ ) (Figure 5).

After gentle compression of the clot in membranes, a minimal change in length of 0.08 cm, 0.09 cm, 0.10 cm, 0.08 cm, 0.06, and 0.10 cm was measured for L-PRF-IL, L-PRF-DUO, A-PRF-IL, A-PRF-DUO, A-PRF<sup>+</sup>-IL, and A-PRF<sup>+</sup>-DUO, respectively. At the same time, a mean loss of 85.5% in weight was recorded (L-PRF-IL: 81.7%, L-PRF-DUO: 87.1%, A-PRF-IL: 84.2%, A-PRF-DUO: 87.2%, A-PRF<sup>+</sup>-IL: 86.1%, and A-PRF<sup>+</sup>-DUO: 86.6%).

#### *Mechanical testing.*

Figure 6 shows Young's modulus obtained for the different membranes (mean and standard deviation). In the tensile test, statistically significant differences were observed between L-PRF-IL vs. A-PRF-IL ( $p < 0.01$ ), L-PRF-DUO vs. A-PRF<sup>+</sup>-DUO ( $p < 0.001$ ), and A-PRF-DUO vs. A-PRF<sup>+</sup>-DUO ( $p < 0.05$ ). No statistically significant difference was found within the same protocol when the g force was adapted in each device, i.e. L-PRF-IL vs. L-PRF-DUO.

For the compression test, statistically significant differences were observed between the different centrifugation protocols and within the same protocol using different devices (Figure 6).

### B. Influence of time in the preparation

#### *Timing: blood draw - centrifugation.*

The time interval between blood draw and centrifugation played a significant role. If the delay was  $> 5$  min (in one patient even  $> 3$  min) an amorphous blood clot was obtained and compression into a membrane became impossible (Figure 7). Even shorter delays had an impact. For example, delays caused a reduction in membrane length: for time intervals of  $<1$ , 1, 3, and 5 min lengths were  $3.0 \pm 0.2$  cm,  $2.4 \pm 0.5$  cm,  $1.7 \pm 0.1$  cm, and  $0.9 \pm 0.0$  cm, respectively). The difference between  $<1$  or 1 min on the one hand and 3 min or 5 min on the other hand reached statistical significance ( $p < 0.05$ ). No statistical significant difference could be observed for width measurements ( $p > 0.05$ ).



SEM images from the above-mentioned membranes are shown in Figure 8. Membranes prepared within 1 min after blood draw showed clusters of platelets, leucocytes and red blood cells embedded in a well-organized fibrin matrix. As the time interval increased, looser cells and a denser and disorganized matrix were observed.

*Timing: centrifugation - membrane preparation (Figure 7).*

The time interval between the end of centrifugation and the compression of the clot into a membrane also had an impact. The longer this time interval, the smaller the membranes. Both in length and width, statistically significant differences were found between membranes prepared immediately after centrifugation and those prepared after 2 or 3 hours ( $p < 0.05$ ).

## **Discussion**

The present study showed both the importance of adapting RCF of the centrifuge to obtain similar PRF matrices and the differences among different PRF modifications. No statistically significant differences could be observed among all six protocols in terms of growth factors release, cellular content, and dimensions. The release of growth factors by L-PRF, A-PRF and A-PRF + had already been reported in literature, but to date PRF clots had been examined and not the membranes. (13, 19) Ours is the first study to test PRF membranes. Choosing membranes rather than clots is important because membranes are most frequently used in oral surgery and treatment of chronic wounds. (20-22)

The role of growth factors in bone formation is widely recognised, particularly for bone morphogenetic proteins (BMPs), PDGF, TGF- $\beta$  and VEGF. (23, 24) BMPs and PDGF induce migration and proliferation of osteoprogenitor cells, whereas TGF- $\beta$  stimulates cell growth and the synthesis of extracellular matrix. (25) VEGF is known as a potent inducer of angiogenesis and osteoblast proliferation. (26) Recently, Ratajczak and co-workers (27) described the angiogenic potential of L-PRF in an in-vitro study. They concluded that L-PRF induced key steps of the angiogenic process such as endothelial proliferation, migration, and tube formation. They also demonstrated that L-PRF was able to induce blood vessel formation in vivo with a chorioallantoic membrane assay. Platelet concentrates may release other bioactive factors that also play a role in the regeneration process. Some studies have revealed that PRF constructs produced key immune cytokines, such as interleukin (IL) 1 $\beta$ , IL-6, IL-4, and tumor necrosis factor. (28, 29)

Several papers (13, 15, 30) reported contradictory data on the impact of g-force on the above-mentioned release in growth factors, but unfortunately with some methodological shortcomings (7, 31). It is indeed important to use the same RCF of the centrifuge when comparing different protocols. When adapting RCF for different centrifuges, the previously reported differences between different protocols were no longer observed. Indeed, in the current study, no statistically significant differences could be found among all membranes, prepared with different protocols, in terms of growth factors release, cellular content, and dimensions.

In literature, the common way to express rotor speed is in terms of revolutions per minute (rpm). (32, 33) However, rpm does not take into account the radius of the centrifuge. Since the radius is not standardized for all centrifuges, RCF should be used because it also considers the distance of the tubes to the axis of rotation. (34) Therefore, the rpm of two centrifuges can be the same, but the forces applied to the particles in the tubes will differ significantly. Both the Intra-Spin and the PRF DUO centrifuge have a fixed-angle rotor but they present a different rotation angle and radius (Table 2). Consequently, RCF should be adjusted in both centrifuges if one would like to apply similar forces on the



blood cells. If not, PRF constructs will be completely different. One limitation of this study is that the angulation of the tubes inside the centrifuge is a variable that cannot be adapted. Thus, we assumed that the angulation would have some effect on the distribution of the cells in the clot/membrane. However, even without adapting this variable, no differences could be observed among all membranes.

The L-PRF clot lost 85% of its weight when compressed into a membrane. However, the clots were compressed using a box where the force applied could not be registered, which may be a limitation of this study. Nevertheless, this finding needs to be taken into consideration when using L-PRF clots in a clinical application, for instance, for alveolar ridge preservation. If clots are used, it will be more difficult to place 4-6 clots in one socket since their volume is larger than that of the membranes. (16, 35) After some time, the clots will lose the exudate, leaving an almost empty socket. The latter might explain the unfavourable clinical results when clots were used for ridge preservation instead of membranes. (36)

Although there was no statistically significant difference, PRF clots produced with glass tubes showed higher weight (mean  $1.9 \pm 0.4$  g) compared with those from silica-coated plastic tubes (mean  $1.6 \pm 0.3$  g). Recently, the importance of centrifugation tubes on the final production of PRF matrices has been highlighted(37). Bonazza and co-workers (38) already showed the influence of the material and shape of the blood collection tube on the platelet concentrate, with differences in morphology, fibrin network architecture, and cell distribution. They reported a higher weight of Concentrated Growth Factors (CFG), a PRF-like product, obtained with a glass round-bottom tube. In glass tubes, blood begins to coagulate immediately after blood collection, with larger fibrin recruitment. The use of these tubes allowed to obtain CFGs that were larger, thicker and weighed more compared with those obtained with plastic silica-coated tubes. (38, 39) However, their weight after compression, in membrane form, did not differ between protocols in our study. Yamaguchi and co-workers(40) reported different platelet distribution in the concentrated growth factors matrix when prepared with silica-coated plastic tubes or glass tubes. Platelets were distributed mainly in the distal side of the glass-prepared CGF matrix, but homogeneously in the plastic-prepared CGF matrix.

In this present study, statistically significant differences were found amongst different protocols for both mechanical tests. Moreover, the results for the tensile testing were similar and showed no statistically significant differences for the same protocol when the g-force was adapted in both centrifuges, suggesting that the adaptation of the g-force may result in similar PRF matrices independently of the device used. The results obtained from the mechanical testing for the six protocols ranged between 0.3-0.6 MPa and between 0.1-0.3 MPa for the tensile strength and compression strength, respectively. These data are similar to the results found in literature. (41), (42) For instance, when compared with the elastic modulus in tension of a porcine dermal collagen membrane ( $0.3 \pm 0.1$  MPa), (43) all PRF constructs showed higher values except A-PRF+-IL and A-PRF+-DUO.

In this study, and for the first time, the relevance of timing before and after centrifugation in obtaining an optimal PRF construct is highlighted. The blood coagulation cascade has been studied intensively. (44-46) Butenas and co-workers (47) reported that this first stage of the coagulation finished after two minutes. The in-vivo clot formation has also been studied with real-time confocal microscopy. (48) After 20 seconds, fibrin appeared on the upstream edge of the thrombus. Between 34 and 60 seconds, fibrin extended throughout the platelet thrombus. Accordingly, our findings showed the importance of centrifuging blood within the first 60 seconds to avoid early formation (before centrifugation and separation of the cells) of a coagulum inside the tube. These findings are in accordance with those observed by Miron and co-workers (2019) (49). They also reported a 60- to 90 seconds interval between blood draw and the start of centrifugation.

## **Conclusions**

Within the limitations of this study, one can conclude that the adaptation of RCF for each centrifuge did not result in differences in terms of release of growth factors, cellular content, dimensions, and mechanical properties. However, the time between blood collection and centrifugation strongly influenced the dimension and structure of the L-PRF membranes obtained.

## Figures

Figure 1. Scheme of the tube distribution for each experiment.

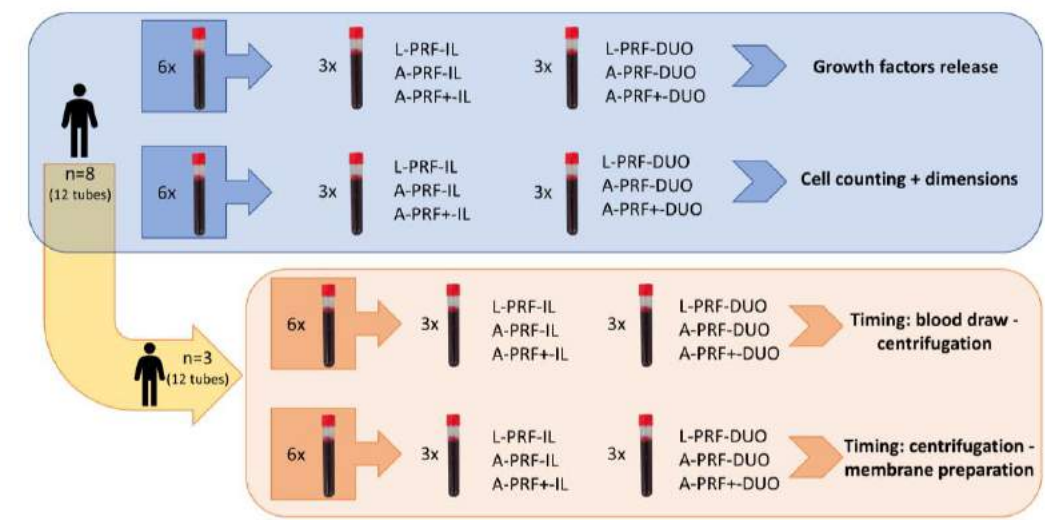


Figure 2. Representation of steps for cellular counting. (A) initial blood; (B) tube after centrifugation with three layers: platelet-poor plasma (PPP), fibrin clot (L-PRF clot), and red blood cells (RBC); (C) tube after removal of the fibrin clot (PPP + RBC). (D) same tube of step C with physiological water (PW) until a volume of 9 ml (initial volume); (E) L-PRF membrane prepared after compression of the clot; (F) tube with L-PRF exudate release during the compression of the L-PRF clot + physiological water (PW) until a volume of 9 ml; (G) tube with initial blood composition.

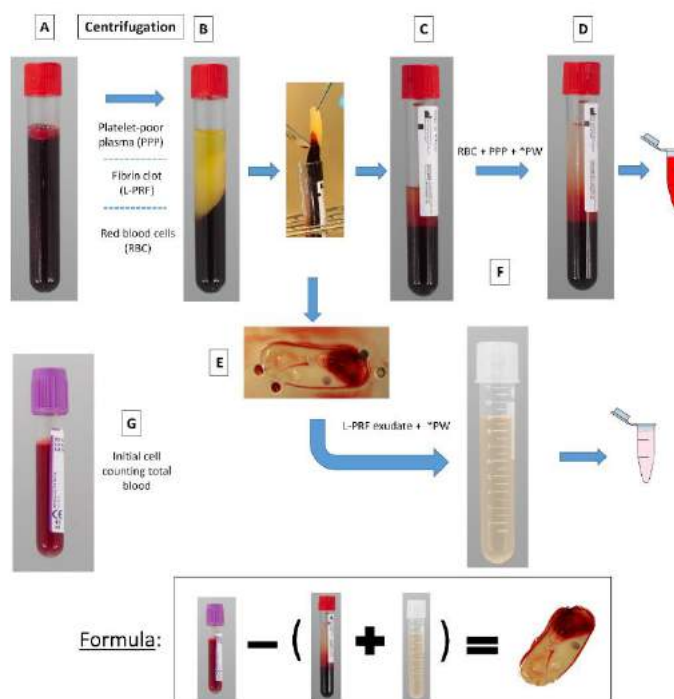


Figure 3. Release of growth factors (VEGF, BMP-1, PDGF-AB, and TGF- $\beta$ 1). A: release per time interval; B: cumulative release up to 14 days. Data from eight participants. \*:  $p < 0.05$ .

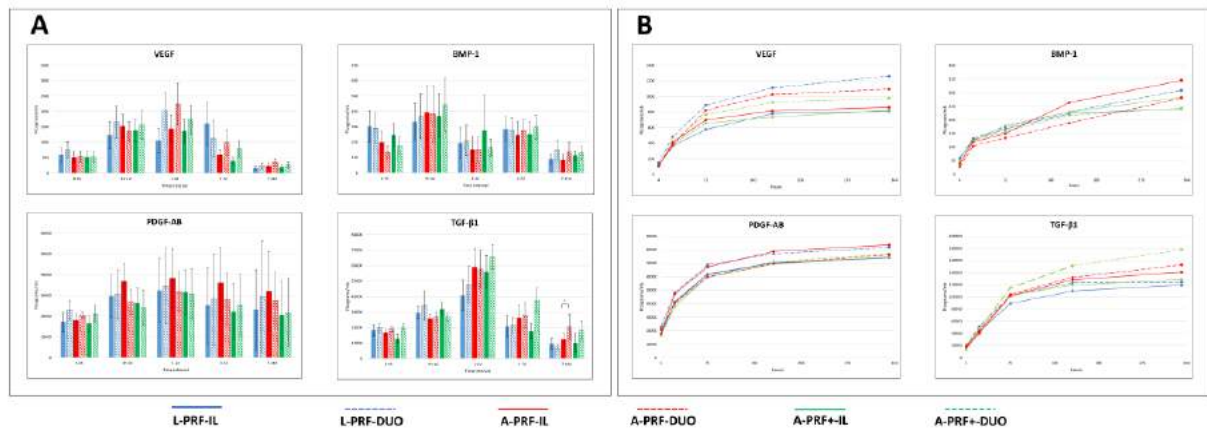
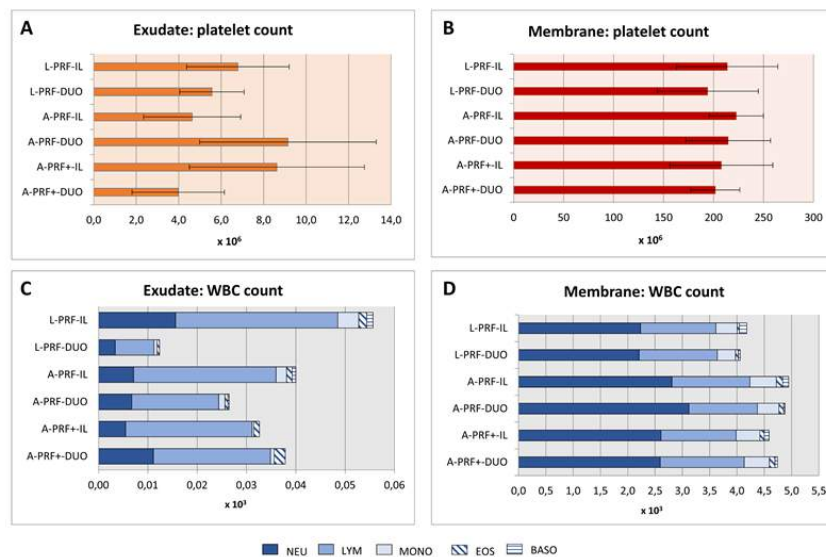


Figure 4. Cellular counting of the exudate and the membranes for each protocol. (A) platelet count for exudate; (B): platelet count for membrane; (C) white blood cell count for each exudate; (D) white blood cell count for each membrane; (E) mean and standard deviation (*sd*) of the white blood cells count for the exudate. For each cell type, different letters (a-c) indicate statistical significant difference ( $p>0.05$ ) between protocols.



E	L-PRF IL		L-PRF DUO		A-PRF IL		A-PRF DUO		A-PRF+IL		A-PRF+DUO	
$\times 10^3$	mean	<i>sd</i>	mean	<i>sd</i>	mean	<i>sd</i>	mean	<i>sd</i>	mean	<i>sd</i>	mean	<i>sd</i>
Total WBC	0.06 <sup>a</sup>	0.04	0.01 <sup>b</sup>	0.01	0.03 <sup>a,b</sup>	0.03	0.04 <sup>a,b</sup>	0.02	0.04 <sup>a,b</sup>	0.03	0.03 <sup>a,b</sup>	0.01
Neutrophils	0.02 <sup>a</sup>	0.02	0.00 <sup>b</sup>	0.00	0.01 <sup>a</sup>	0.01	0.01 <sup>a</sup>	0.01	0.01 <sup>a</sup>	0.00	0.01 <sup>a</sup>	0.00
Lymphocytes	0.03 <sup>a,c</sup>	0.03	0.01 <sup>b</sup>	0.01	0.02 <sup>a,b,c</sup>	0.02	0.02 <sup>a,b,c</sup>	0.02	0.03 <sup>a,c</sup>	0.03	0.02 <sup>a,b,c</sup>	0.01
Monocytes	0.01 <sup>a</sup>	0.00	0.00 <sup>b</sup>	0.00	0.00 <sup>b</sup>	0.00	0.00 <sup>a</sup>	0.00	0.00 <sup>b</sup>	0.00	0.00 <sup>a</sup>	0.00
Eosinophils	0.00 <sup>a</sup>	0.00	0.00 <sup>b</sup>	0.00	0.00 <sup>b</sup>	0.00	0.00 <sup>b</sup>	0.00	0.00 <sup>a</sup>	0.00	0.00 <sup>a</sup>	0.00
Basophils	0.00 <sup>a</sup>	0.00	0.00 <sup>b</sup>	0.00	0.00 <sup>b</sup>	0.00	0.00 <sup>b</sup>	0.00	0.00 <sup>a</sup>	0.00	0.00 <sup>a</sup>	0.00

Figure 5. Standardized pictures and measurements of the clots and membranes. The length and the width of each clot and membrane were measured with a horizontal (length) and a vertical (width) line drawn from the middle point of the clot or membrane with an angle of 90°.

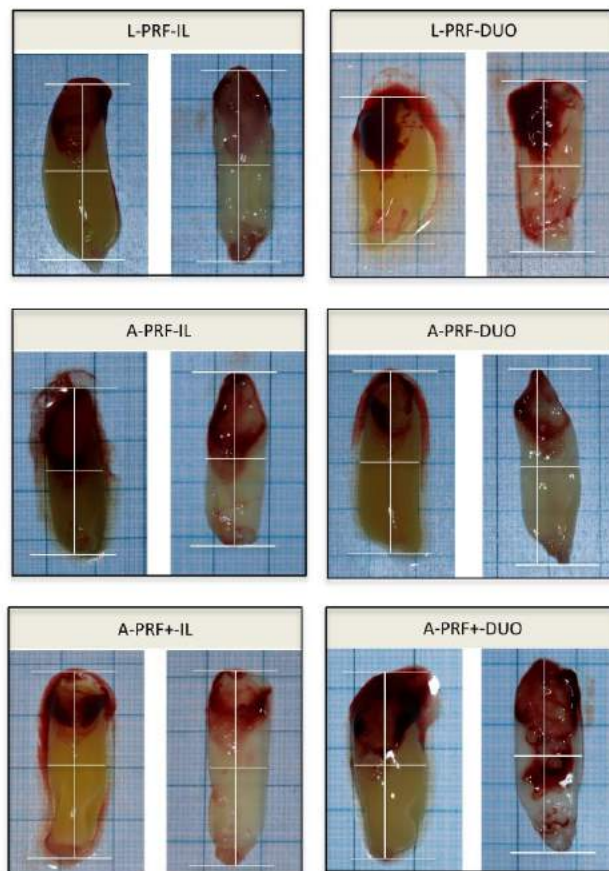


Figure 6. Graphical representation of the compression tests and tensile tests. Data from eight participants. \*  $p < 0.05$ , \*\*  $p < 0.01$ , \*\*\*  $p < 0.001$ .

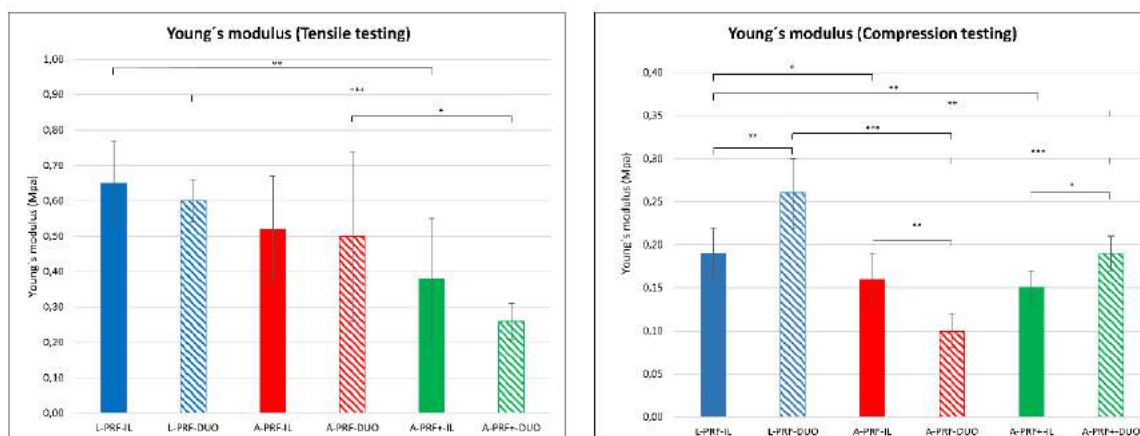




Figure 7. Morphology of the L-PRF membranes depending on the time before and after centrifugation (n=3). A: Timing between blood collection and centrifugation; B: Timing between centrifugation and L-PRF membrane preparation.

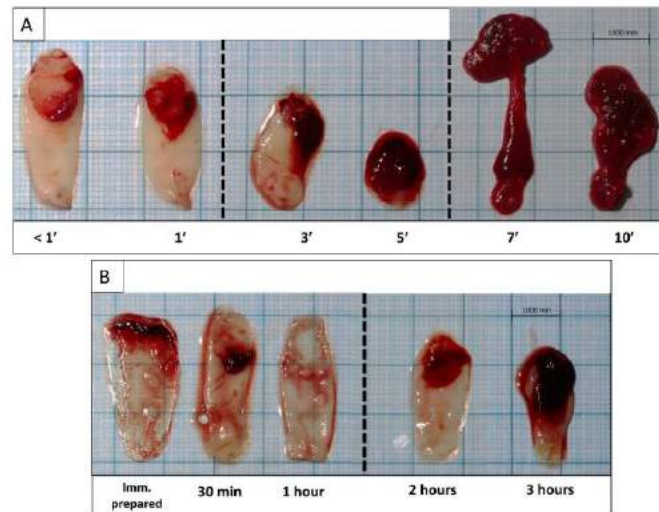
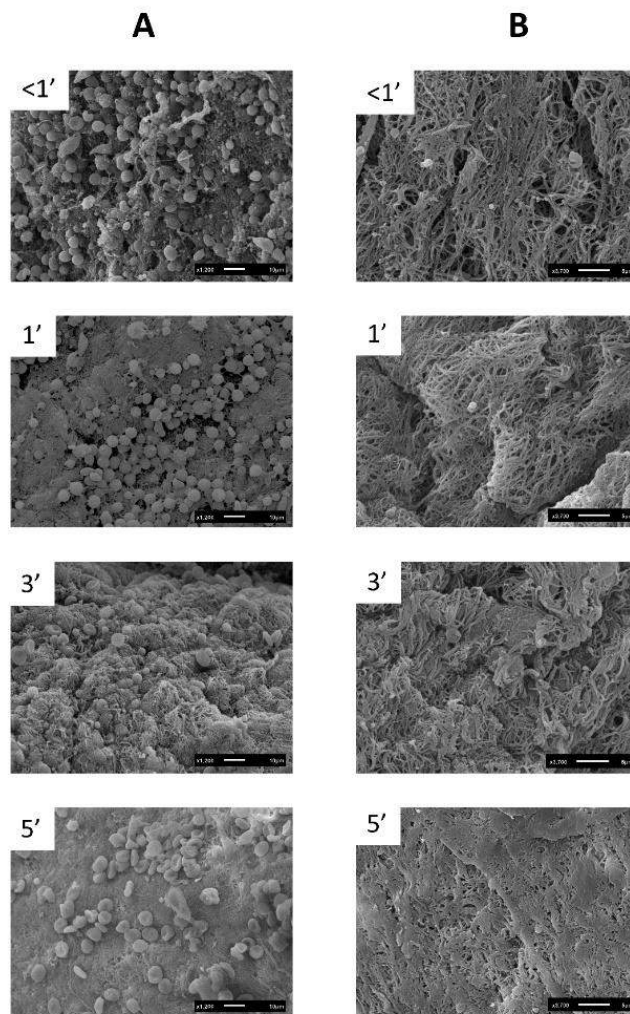


Figure 8. Scanning electron microscopy images of the L-PRF membranes with different time points (<1 min, 1 min, 3 min, and 5 min) before centrifugation. (A) Represents the red part (face) of the membrane; (B) represents the yellow part (tail).



## Tables

Table 1. Platelet rich fibrin matrices (L-PRF, A-PRF, and A-PRF<sup>+</sup>) prepared with the centrifuge Process for PRF, Nice, France, (DUO)] and the Intra-Spin centrifuge [Biohorizons, Birmingham, Alabama, USA, (IL)].<sup>7</sup>

	DEVICE	TUBE	SETTING				
			RCF <sub>clot</sub>	RCF <sub>max</sub>	rotor angulation	rpm	time
L-PRF-IL	Intra-Lock, USA	Plastic-coated	408 g	653 g	33°	27000	12 min
L-PRF-DUO	Process for PRF, France	Glass	408 g	653 g	40°	1825	12 min
A-PRF-IL	Intra-Lock, USA	Plastic-coated	193 g	276 g	33°	2200	14 min
A-PRF-DUO	Process for PRF, France	Glass	193 g	276 g	40°	1500	14 min
A-PRF <sup>+</sup> -IL	Intra-Lock, USA	Plastic-coated	145 g	208 g	33°	1900	8 min
A-PRF <sup>+</sup> -DUO	Process for PRF, France	Glass	145 g	208 g	40°	1300	8 min

Table 2. Clots and membrane dimensions (mean and standard deviation) in all protocols (n=8). Difference ( $\Delta$ ) between clots and membranes in terms of length, width, and weight. *sd*: standard deviation.

	Length (cm)		Width (cm)		Weight (g)	
Clot						
	mean	<i>sd</i>	mean	<i>sd</i>	mean	<i>sd</i>
L-PRF-IL	3.0	0.3	1.2	0.08	1.6	0.5
L-PRF-DUO	3.3	0.7	1.2	0.1	2.1	0.6
A-PRF-IL	2.9	0.3	1.2	0.1	1.6	0.3
A-PRF-DUO	3.0	0.3	1.1	0.1	2.0	0.3
A-PRF + -IL	2.9	0.3	1.1	0.1	1.5	0.3
A-PRF + -DUO	3.0	0.2	1.1	0.1	1.7	0.2
Membrane						
	mean	<i>sd</i>	mean	<i>sd</i>	mean	<i>sd</i>
L-PRF-IL	2.9	0.7	1.0	0.1	0.26	0.09
L-PRF-DUO	3.2	0.5	1.0	0.1	0.27	0.08
A-PRF-IL	2.8	0.4	1.0	0.06	0.22	0.08
A-PRF-DUO	3.0	0.4	1.0	0.07	0.27	0.06
A-PRF + -IL	3.0	0.2	0.9	0.1	0.23	0.08
A-PRF + -DUO	2.9	0.5	0.9	0.1	0.22	0.06
Difference membrane-clot						
	mean	<i>sd</i>	mean	<i>sd</i>	mean	<i>sd</i>
L-PRF-IL	-0.08	0.6	-0.2	0.1	-1.3	0.4
L-PRF-DUO	-0.09	0.2	-0.2	0.3	-1.8	0.6
A-PRF-IL	-0.1	0.2	-0.2	0.2	-1.4	0.2
A-PRF-DUO	-0.08	0.6	-0.1	0.6	-1.7	0.2
A-PRF + -IL	0.06	0.2	-0.2	0.2	-1.3	0.2
A-PRF + -DUO	-0.1	0.3	-0.2	0.2	-1.5	0.3

## References

1. Larson D. Clinical Chemistry: Fundamentals and Laboratory Techniques. 1st ed 2016.
2. Rahmanian N, Bozorgmehr M, Torabi M, Akbari A, Zarnani AH. Cell separation: Potentials and pitfalls. *Prep Biochem Biotechnol*. 2017;47(1):38-51.
3. Matras H. [Effect of various fibrin preparations on reimplantations in the rat skin]. *Osterr Z Stomatol*. 1970;67(9):338-59.
4. Marx RE, Carlson ER, Eichstaedt RM, Schimmele SR, Strauss JE, Georgeff KR. Platelet-rich plasma: Growth factor enhancement for bone grafts. *Oral Surg Oral Med Oral Pathol Oral Radiol Endod*. 1998;85(6):638-46.
5. Choukroun J. Une opportunité en parodontologie: le PRF. *Implantodontie*. 2001;42:55-62.
6. Dohan Ehrenfest DM, Rasmusson L, Albrektsson T. Classification of platelet concentrates: from pure platelet-rich plasma (P-PRP) to leucocyte- and platelet-rich fibrin (L-PRF). *Trends Biotechnol*. 2009;27(3):158-67.
7. Miron RJ, Pinto NR, Quirynen M, Ghanaati S. Standardization of relative centrifugal forces in studies related to platelet-rich fibrin. *J Periodontol*. 2019;90(8):817-20.
8. Castro AB, Meschi N, Temmerman A, Pinto N, Lambrechts P, Teughels W, et al. Regenerative potential of leucocyte- and platelet-rich fibrin. Part A: intra-bony defects, furcation defects and periodontal plastic surgery. A systematic review and meta-analysis. *J Clin Periodontol*. 2017;44(1):67-82.
9. Castro AB, Meschi N, Temmerman A, Pinto N, Lambrechts P, Teughels W, et al. Regenerative potential of leucocyte- and platelet-rich fibrin. Part B: sinus floor elevation, alveolar ridge preservation and implant therapy. A systematic review. *J Clin Periodontol*. 2017;44(2):225-34.
10. Pinto N, Quirynen M. Letter to the Editor regarding Fujioka-Kobayashi et al. 2017 (JOP-16-0443.R1). *J Periodontol*. 2018.
11. Ghanaati S, Booms P, Orlowska A, Kubesch A, Lorenz J, Rutkowski J, et al. Advanced platelet-rich fibrin: a new concept for cell-based tissue engineering by means of inflammatory cells. *J Oral Implantol*. 2014;40(6):679-89.
12. Choukroun J, Ghanaati S. Reduction of relative centrifugation force within injectable platelet-rich-fibrin (PRF) concentrates advances patients' own inflammatory cells, platelets and growth factors: the first introduction to the low speed centrifugation concept. *Eur J Trauma Emerg Surg*. 2018;44(1):87-95.
13. El Bagdadi K, Kubesch A, Yu X, Al-Maawi S, Orlowska A, Dias A, et al. Reduction of relative centrifugal forces increases growth factor release within solid platelet-rich-fibrin (PRF)-based matrices: a proof of concept of LSCC (low speed centrifugation concept). *Eur J Trauma Emerg Surg*. 2017.
14. Kobayashi E, Flückiger L, Fujioka-Kobayashi M, Sawada K, Sculean A, Schaller B, et al. Comparative release of growth factors from PRP, PRF, and advanced-PRF. *Clin Oral Investig*. 2016;20(9):2353-60.
15. Dohan Ehrenfest DM, Pinto NR, Pereda A, Jimenez P, Corso MD, Kang BS, et al. The impact of the centrifuge characteristics and centrifugation protocols on the cells, growth factors, and fibrin architecture of a leukocyte- and platelet-rich fibrin (L-PRF) clot and membrane. *Platelets*. 2018;29(2):171-84.
16. Temmerman A, Vandessel J, Castro A, Jacobs R, Teughels W, Pinto N, et al. The use of leucocyte and platelet-rich fibrin in socket management and ridge preservation: a split-mouth, randomized, controlled clinical trial. *J Clin Periodontol*. 2016;43(11):990-9.



17. Castro AB, Cortellini S, Temmerman A, Li X, Pinto N, Teughels W, et al. Characterization of the Leukocyte- and Platelet-Rich Fibrin Block: Release of Growth Factors, Cellular Content, and Structure. *Int J Oral Maxillofac Implants*. 2019;34(4):855-64.
18. Hsu CJ. Multiple comparisons-theory and methods. 1st ed1996.
19. Ghanaati S, Booms P, Orlowska A, Kubesch A, Lorenz J, Rutkowski J, et al. Advanced Platelet-Rich Fibrin (A-PRF) - A new concept for cell-based tissue engineering by means of inflammatory cells. *J Oral Implantol*. 2014.
20. Miron RJ, Zucchelli G, Pikos MA, Salama M, Lee S, Guillemette V, et al. Use of platelet-rich fibrin in regenerative dentistry: a systematic review. *Clin Oral Investig*. 2017;21(6):1913-27.
21. Strauss FJ, Stähli A, Gruber R. The use of platelet-rich fibrin to enhance the outcomes of implant therapy: A systematic review. *Clin Oral Implants Res*. 2018;29 Suppl 18(Suppl Suppl 18):6-19.
22. de Carvalho CKL, Fernandes BL, de Souza MA. Autologous Matrix of Platelet-Rich Fibrin in Wound Care Settings: A Systematic Review of Randomized Clinical Trials. *J Funct Biomater*. 2020;11(2).
23. Gothard D, Smith EL, Kanczler JM, Rashidi H, Qutachi O, Henstock J, et al. Tissue engineered bone using select growth factors: A comprehensive review of animal studies and clinical translation studies in man. *Eur Cell Mater*. 2014;28:166-207; discussion -8.
24. Devescovi V, Leonardi E, Ciapetti G, Cenni E. Growth factors in bone repair. *Chir Organi Mov*. 2008;92(3):161-8.
25. Chen G, Deng C, Li YP. TGF-beta and BMP signaling in osteoblast differentiation and bone formation. *Int J Biol Sci*. 2012;8(2):272-88.
26. Hu K, Olsen BR. The roles of vascular endothelial growth factor in bone repair and regeneration. *Bone*. 2016;91:30-8.
27. Ratajczak J, Vangansewinkel T, Gervois P, Merckx G, Hilkens P, Quirynen M, et al. Angiogenic Properties of 'Leukocyte- and Platelet-Rich Fibrin'. *Sci Rep*. 2018;8(1):14632.
28. Dohan DM, Choukroun J, Diss A, Dohan SL, Dohan AJ, Mouhyi J, et al. Platelet-rich fibrin (PRF): a second-generation platelet concentrate. Part II: platelet-related biologic features. *Oral Surg Oral Med Oral Pathol Oral Radiol Endod*. 2006;101(3):e45-50.
29. Gassling VL, Acil Y, Springer IN, Hubert N, Wiltfang J. Platelet-rich plasma and platelet-rich fibrin in human cell culture. *Oral Surg Oral Med Oral Pathol Oral Radiol Endod*. 2009;108(1):48-55.
30. Fujioka-Kobayashi M, Miron RJ, Hernandez M, Kandalam U, Zhang Y, Choukroun J. Optimized Platelet-Rich Fibrin With the Low-Speed Concept: Growth Factor Release, Biocompatibility, and Cellular Response. *J Periodontol*. 2017;88(1):112-21.
31. Pinto N, Quirynen M. Letter to the editor: RE: Optimized platelet-rich fibrin with the low-speed concept: Growth factor release, biocompatibility, and cellular response. *J Periodontol*. 2019;90(2):119-21.
32. Son D, Choi T, Yeo H, Kim J, Han K. The effect of centrifugation condition on mature adipocytes and adipose stem cell viability. *Ann Plast Surg*. 2014;72(5):589-93.
33. Kim IH, Yang JD, Lee DG, Chung HY, Cho BC. Evaluation of centrifugation technique and effect of epinephrine on fat cell viability in autologous fat injection. *Aesthet Surg J*. 2009;29(1):35-9.
34. Wilson KW, J. Principles and Techniques of Practical Biochemistry. 5th ed2000.
35. Canellas J, da Costa RC, Breves RC, de Oliveira GP, Figueredo C, Fischer RG, et al. Tomographic and histomorphometric evaluation of socket healing after tooth extraction using leukocyte- and platelet-rich fibrin: A randomized, single-blind, controlled clinical trial. *J Craniomaxillofac Surg*. 2020;48(1):24-32.

36. Suttapreyasri S, Leepong N. Influence of platelet-rich fibrin on alveolar ridge preservation. *J Craniofac Surg*. 2013;24(4):1088-94.
37. Miron RJ, Xu H, Chai J, Wang J, Zheng S, Feng M, et al. Comparison of platelet-rich fibrin (PRF) produced using 3 commercially available centrifuges at both high (~ 700 g) and low (~ 200 g) relative centrifugation forces. *Clin Oral Investig*. 2020;24(3):1171-82.
38. Bonazza V, Borsani E, Buffoli B, Castrezzati S, Rezzani R, Rodella LF. How the different material and shape of the blood collection tube influences the Concentrated Growth Factors production. *Microsc Res Tech*. 2016;79(12):1173-8.
39. Margolis J. Initiation of blood coagulation by glass and related surfaces. *J Physiol*. 1957;137(1):95-109.
40. Yamaguchi S, Aizawa H, Sato A, Tsujino T, Isobe K, Kitamura Y, et al. Concentrated Growth Factor Matrices Prepared Using Silica-Coated Plastic Tubes Are Distinguishable From Those Prepared Using Glass Tubes in Platelet Distribution: Application of a Novel Near-Infrared Imaging-Based, Quantitative Technique. *Front Bioeng Biotechnol*. 2020;8:600.
41. Madurantakam P, Yoganarasimha S, Hasan FK. Characterization of Leukocyte-platelet Rich Fibrin, A Novel Biomaterial. *J Vis Exp*. 2015(103).
42. Khorshidi H, Raoofi S, Bagheri R, Banihashemi H. Comparison of the Mechanical Properties of Early Leukocyte- and Platelet-Rich Fibrin versus PRGF/Endoret Membranes. *Int J Dent*. 2016;2016:1849207.
43. Lu HK, Lee SY, Lin FP. Elastic modulus, permeation time and swelling ratio of a new porcine dermal collagen membrane. *J Periodontal Res*. 1998;33(5):243-8.
44. Travers RJ, Smith SA, Morrissey JH. Polyphosphate, platelets, and coagulation. *Int J Lab Hematol*. 2015;37 Suppl 1:31-5.
45. Weiss HJ, Turitto VT, Baumgartner HR, Nemerson Y, Hoffmann T. Evidence for the presence of tissue factor activity on subendothelium. *Blood*. 1989;73(4):968-75.
46. Davie EW, Ratnoff OD. WATERFALL SEQUENCE FOR INTRINSIC BLOOD CLOTTING. *Science*. 1964;145(3638):1310-2.
47. Butenas S, van 't Veer C, Mann KG. Evaluation of the initiation phase of blood coagulation using ultrasensitive assays for serine proteases. *J Biol Chem*. 1997;272(34):21527-33.
48. Falati S, Gross P, Merrill-Skoloff G, Furie BC, Furie B. Real-time in vivo imaging of platelets, tissue factor and fibrin during arterial thrombus formation in the mouse. *Nat Med*. 2002;8(10):1175-81.
49. Miron RJ, Dham A, Dham U, Zhang Y, Pikos MA, Sculean A. The effect of age, gender, and time between blood draw and start of centrifugation on the size outcomes of platelet-rich fibrin (PRF) membranes. *Clin Oral Investig*. 2019;23(5):2179-85.

## CHAPTER 5

## Antimicrobial capacity of Leucocyte- and Platelet Rich Fibrin against periodontal pathogens

Castro Ana B, Rodriguez Esteban H, Slomka Vera, Pinto Nelson, Teughels Wim & Quirynen Marc. (2019) *Scientific Reports* 9; 8188.

### Abstract

**Aim:** To evaluate the antibacterial properties against the main periopathogens cultured on agar plates and in planktonic solution.

**Materials & Methods:** L-PRF membranes and 25µl L-PRF exudate were applied on different agar plates seeded with *Porphyromonas gingivalis*, *Prevotella intermedia*, *Fusobacterium nucleatum*, and *Aggregatibacter actinomycetemcomitans*. The plates were incubated for 72h. After incubation, the areas of inhibition were measured. When L-PRF exudate showed inhibition against the plated bacteria, vitality-qPCR was performed for the planktonic culture. Three different dilutions of L-PRF exudate were used for vitality-qPCR and colony counting.

**Results:** The mean area of inhibition for *P. gingivalis*, *P. intermedia*, *F. nucleatum*, and *A. actinomycetemcomitans* was  $11.8 \pm 5.0 \text{ mm}^2$  ( $p < 0.05$ ),  $4.6 \pm 5.2 \text{ mm}^2$  ( $p < 0.05$ ),  $2.6 \pm 3.0 \text{ mm}^2$  ( $p > 0.05$ ), and  $2.0 \pm 1.8 \text{ mm}^2$  ( $p > 0.05$ ), respectively. L-PRF exudate showed an area of inhibition against *P.gingivalis* of  $18.0 \pm 2.6 \text{ mm}^2$  ( $p < 0.05$ ). No inhibition could be seen for the rest of the bacterial strains. The vitality-qPCR performed for *P.gingivalis* and the 3 dilutions of L-PRF exudate showed a decrease of bacterial growth of 86%, 38%, and 24%, when compared to the control.

**Conclusions:** An L-PRF membrane has antimicrobial effect against the main periopathogens, especially against *P.gingivalis*. The L-PRF exudate showed a strong inhibition against *P.gingivalis* on agar plates and it decreases the number of viable *P.gingivalis* in a dose-dependent way.

### Introduction

The classic experimental gingivitis studies in the 60s (1, 2) demonstrated the direct relation between the accumulation of dental plaque and gingival inflammation. Dental plaque or dental biofilms are defined as a matrix-embedded microbial population, adherent to each other and/or to surfaces or interfaces (3). Studies on biofilm development in deep periodontal pockets showed that the deepest sites are colonized predominantly by motile species (e.g. spirochetes) and gram-negative bacteria, located adjacent to the epithelial lining of the pocket. Some of these bacteria are part of the red complex (*Porphyromonas gingivalis*, *Treponema denticola*, *Tannerella forsythia*) and the orange complex (e.g. *Fusobacterium nucleatum*) (4). On the other hand, gram-positive rods and cocci are more dominant in shallow sites, forming a firmly adherent band of microorganisms on the enamel or root surface (4)(5)(6). One of the most solid associations between a periodontal pathogen and destructive periodontal disease is provided by *Aggregatibacter actinomycetemcomitans* JP2, a potential etiologic agent of localized aggressive periodontitis (7)(8)(9).

Traditionally, the goal of non-surgical periodontal therapy is to eliminate the microbial and/or inflammatory etiology and to reduce the initial pockets to  $\leq 5 \text{ mm}$ . Antimicrobial agents are often used

as adjuncts to initial therapy (10). If the desired pocket depths are not achieved, surgical treatment is required (11, 12).

Recently, new tissue-engineering techniques have been proposed for regenerative procedures after non-surgical periodontal therapy (13) or for bone augmentation (14, 15). Leucocyte- and platelet-rich fibrin (L-PRF), a second-generation platelet concentrate, was introduced as an autologous biomaterial that serves as a scaffold for regenerating cells. L-PRF is prepared from the patient's own blood, without adding any additives, and concentrates >90% of the platelets and >75% of the leucocytes from the initial blood composition (16). It offers a continuous release of growth factors and other bioactive substances that stimulate and protect the surgical site (17, 18). Different forms of L-PRF can be prepared, the membrane most commonly used.

Two recent systematic reviews (19, 20) have shown the various applications of L-PRF, concluding that favourable effects on hard and soft tissue healing and a decrease of postoperative discomfort could be obtained when L-PRF was used. Several studies have described other biological properties of L-PRF such as the antimicrobial effect against wound bacteria (21)–(22). Given the cellular composition of L-PRF (16) and its bioactive nature (17), the aim of this study was to evaluate the antimicrobial capacity of an L-PRF membrane and L-PRF exudate against key periodontal pathogens (*Porphyromonas gingivalis*, *Prevotella intermedia*, *Fusobacterium nucleatum*, and *Aggregatibacter actinomycetemcomitans*). The null-hypothesis was postulated as (1) an L-PRF membrane and its exudate do not inhibit the four tested bacterial strains when applied directly on a cultured Brain Heart Infusion (BHI) agar plate, and (2), L-PRF exudate does not inhibit bacterial growth of the tested bacterial strains in planktonic form.

## **Materials & Methods**

### **Bacterial strains**

All bacterial species (*P. gingivalis* ATCC 33277, *P. intermedia* ATCC 25611, *F. nucleatum* ATCC 20482, *A. actinomycetemcomitans* ATCC 43718) were maintained on blood agar (Oxoid, Basingstoke, UK) supplemented with 5mg/ml hemin (Sigma, St. Louis, USA), 1mg/ml menadione (Calbiochem-Novabiochem, La Jolla, CA, USA), and 5% sterile horse blood (E&O Laboratories, Bonnybridge, Scotland). Overnight liquid cultures were prepared in BHI broth (Difco, Detroit, MI, USA). The bacteria were cultured under anaerobic conditions (80% N<sub>2</sub>, 10% H<sub>2</sub> and 10% CO<sub>2</sub>) for *P. gingivalis*, *P. intermedia*, and *F. nucleatum* or aerobic conditions (5% CO<sub>2</sub>) for *A. actinomycetemcomitans*.

### **Leucocyte- and Platelet-Rich Fibrin (L-PRF) preparation**

The participants in this study (n=9) were systemically healthy, non-smokers, without a history of periodontal disease and who had not taken any antibiotics for at least 6 months before the study. Four blood samples were collected from each volunteer (n=9) in a 9mL glass-coated plastic tube and immediately centrifuged at 408 g for 12 minutes (Intraspin™, Intra-Lock, Boca Raton, FL, USA). The L-PRF clot was compressed and transformed into a standardized membrane of 1 mm in thickness (Xpression® box, Intra-Lock, Boca Raton, FL, USA). During this process, the released exudate was also kept for further use at -80°C. Due to the low cellular content of L-PRF exudate (<2.5% of platelets and <0.9% of leucocytes for the initial blood composition) (23), we could freeze it without damaging the possible active molecules.

### Agar plate test

#### *L-PRF membrane*

BHI agar plates (Difco, Sparks, MD, USA) were seeded with an overnight culture 2 h before the application of an L-PRF membrane and incubated in anaerobic (80% N<sub>2</sub>, 10% H<sub>2</sub> and 10% CO<sub>2</sub>) or aerobic (5% CO<sub>2</sub>) conditions, depending on the bacteria. The L-PRF membranes on the surface of a BHI agar plate were in direct contact with *P. gingivalis*, *P. intermedia*, *F. nucleatum* or *A. actinomycetemcomitans*. The incubation time was 72 h.

Standardized pictures (constant distance between agar plate and camera) were taken at baseline and after 72 h. In order to verify the shrinkage, the difference in surface area of the membrane between pictures at baseline and those after 72h was computed with PictZar® Pro 7.1 (Digital Planimetry Software). Each image was calibrated based on the ruler that was attached to the agar plate. First, the area of the L-PRF membrane at baseline was coloured (red) and its area was calculated. The same was done for the L-PRF membrane after 72 h of incubation. The area free of bacterial growth around each membrane was coloured (green) and calculated. To evaluate the shrinkage, the area of the L-PRF membrane at baseline was subtracted from the area after 72 h (Figure 1).

The length and width of each membrane were measured at baseline and after 72 h with the software ImageJ® (Image Processing and Analysis in Java, 1.8.0\_77). All images were individually calibrated based on the ruler that was fixed to each agar plate. A horizontal (length) and a vertical (width) line were drawn from the middle point of the membrane with an angle of 90°.

#### *L-PRF exudate*

Twenty-five microliters of L-PRF exudate, 25 µl of pure chlorhexidine (CHX) 0.12% (positive control) and 25 µl of BHI broth (negative control) were applied directly to the surface of each BHI agar plate, prepared and inoculated in the same way as in the previous experiment. The incubation time was 72 h. Standardized pictures were taken at baseline and after 72 h. The area free of bacterial growth around each drop of L-PRF exudate was measured with the software PictZar® Pro 7.1.

### L-PRF exudate dilution test

If inhibition with L-PRF exudate was detected, bacteria were cultured in BHI broth and optical densities were adjusted using spectrophotometry (OD<sub>600</sub>, GeneQuant Spectrophotometer, Buckinghamshire, UK) to an OD of 0.5-0.7 (OD<sub>600</sub> = 0.5  $\approx$  1x10<sup>8</sup> colony forming unit/ml (CFU/ml). Three dilutions of L-PRF exudate were prepared in a 96-well plate, for a total volume of 300 µl/well: ratio 1:1 (150 µl of bacteria + 150 µl of L-PRF exudate), ratio 1:2 (150 µl of bacteria + 75 µl of L-PRF exudate + 75 µl of saline), and ratio 1:4 (150 µl of bacteria + 37.5 µl of L-PRF exudate + 112.5 µl of saline). The positive control consisted of 150 µl of bacteria + 150 µl of saline. The incubation time was 24 h. One bacterial strain that was not inhibited during the agar plate test was also cultured.

After 24 h, 90 µl of the mixtures mentioned above was taken for vitality quantitative PCR (qPCR). Another 50 µl was used for microbial culturing and colony counting (CFU/ml). This experiment was performed in triplicate.

#### *Vitality qPCR*

The vitality-DNA extraction was performed with a QIAamp DNA Mini kit (Qiagen, Hilden, Germany) (24). Briefly, 90 µl aliquots of the samples were immediately incubated with 10 µl of propidium monoazide (PMA) (Biotium, Hayward, CA, USA) at a final concentration of 100 µg/ml (24). Samples were incubated in the dark for 5 min, following photo-induced cross-linking of PMA by 10-min light exposure using a 400

W (500 lm) light source, placed 20 cm above the sample, while samples were kept on ice. The PMA treated bacteria were pelleted by centrifugation at  $20,000 \times g$  for 10 min and DNA extraction was performed using the QIAamp DNA Mini kit following the manufacturer's instruction, extending the incubation step of the bacteria in the lytic enzyme solution at 37°C to 2 h.

A qPCR assay was performed with a CFX96 Real-Time System (Biorad, Hercules, CA, USA) using the Taqman 5' nuclease assay PCR method for detection and quantification of bacterial DNA. Primers and probes were targeted against the 16S rRNA gene for the test group and for the negative control. Taqman reactions contained 12.5 µl Mastermix (Eurogentec, Seraing, Belgium), 4.5 µl sterile H<sub>2</sub>O, 1 ml of each primer and probe, and 5 ml template DNA. Assay conditions for all primer/probe sets consisted of an initial 2 min at 50°C, followed by a denaturation step at 95°C for 10 min, followed by 45 cycles of 95°C for 15 s and 60°C for 60 seconds. Quantification was based on a plasmid standard curve (Table 1).

#### *Colony counting (CFU/ml)*

All samples were also diluted from  $10^{-1}$  to  $10^{-9}$  in PBS and plated by means of a spiral plater on blood agar plates supplemented with 5mg/ml hemin (Sigma, St. Louis, USA), 1mg/ml menadione, and 5% sterile horse blood. After 7 days of anaerobic (80% N<sub>2</sub>, 10% H<sub>2</sub> and 10% CO<sub>2</sub>) or aerobic (5% CO<sub>2</sub>) incubation (depending on the bacteria), the total number of CFU/ml was counted by means of Fiji software (Image Processing and Analysis in Java, 1.8.0\_77). Briefly, all images were transformed into a 16-bit-image and a region of interest (ROI) with all colonies was selected. The image was then converted into a binary image. The latter was modified (watershed) to improve the separation of each colony when the colonies were too close. Finally, the count was performed based on the size and the circularity<sup>43</sup> (Figure S1). If the number of colonies on an agar plate was above 300, this plate was considered not countable. CFU/ml were calculated according to the dilution point.

#### *Gram negative staining*

Given the differences in values between the qPCR and the CFU reported in Table 3, a gram negative staining was performed for *A. actinomycetemcomitans* (control and ratio 1:1). The samples were analysed with the Axio Imager 2 Microscope (Carl Zeiss MicroImaging GmbH, Germany) with a 40x magnification.

#### Ethical Statement

The use of human blood was approved by the ethical committee of the KU Leuven and registered with identifier B322201628215. The procedures were executed according to the Helsinki Declaration and the regulations of the University Hospital, approved by the ethical committee. Informed consent was obtained from all subjects after the purpose of the study had been explained. The subjects were aware that the results would be used in a scientific study.

#### Statistical analysis

For all variables, mean values and standard deviations were calculated. The normality of the data was tested with the Kolmogorov-Smirnov test. The normally distributed data were then analysed with Student's T-test (parametric test) and the 95% confidence interval was computed. For non-parametric data, the Wilcoxon test was used. A p value < 0.05 was considered statistically significant.



## Results

### Demographic data

Nine systemically healthy adult volunteers (6 women, 3 men) participated in this study. Their mean age was  $37.7 \pm 15.3$  years (range 25-60 years). No complications were reported during blood collection.

### Agar plate test

#### L-PRF membrane

The mean area of inhibition was  $11.8 \pm 5.0$  mm<sup>2</sup>,  $2.7 \pm 5.2$  mm<sup>2</sup>,  $2.6 \pm 3.0$  mm<sup>2</sup>, and  $0.6 \pm 1.7$  mm<sup>2</sup> for *P. gingivalis*, *P. intermedia*, *F. nucleatum*, and *A. actinomycetemcomitans*, respectively (Table 2). More inhibition was found for *P. gingivalis* when compared to *P. intermedia* ( $p < 0.05$ ), *F. nucleatum* ( $p < 0.05$ ), and *A. actinomycetemcomitans* ( $p < 0.05$ ).

Over the 72-hour time incubation period, shrinkage of the membranes was observed. The mean shrinkage of the L-PRF membrane was  $5.7 \pm 3.7$  % after 72h of incubation at 37°C in both aerobic and anaerobic conditions. The mean reduction in length and width was  $1.0 \pm 0.5$  mm and  $0.5 \pm 0.1$  mm, respectively. None of these changes (Table 2) were statistically significant ( $p > 0.05$ ).

However, since membrane shrinkage could have influenced the mean area of inhibition, it was subtracted from the area of inhibition. After subtracting membrane shrinkage, *P. gingivalis* showed an area of inhibition of  $9.1 \pm 3.2$  mm<sup>2</sup> ( $p < 0.05$ ). For *P. intermedia*, *F. nucleatum* and *A. actinomycetemcomitans* no statistically significant inhibition could be measured ( $p > 0.05$ ).

#### L-PRF exudate

For the L-PRF exudate, only inhibition against *P. gingivalis* could be observed, with a mean area of inhibition of  $17 \pm 2.6$  mm<sup>2</sup> (Table 3). For the positive control (CHX 0.12%), the mean area of inhibition was statistically significantly larger ( $48.8 \pm 4.2$  mm<sup>2</sup>,  $p < 0.005$ ).

### Planktonic bacteria

#### Vitality qPCR

*P. gingivalis* and *A. actinomycetemcomitans* were considered for this analysis since they showed the highest and the lowest amount of inhibition induced by the membranes, respectively. The vitality qPCR analysis showed a mean reduction of 0.9 log (86%,  $p < 0.001$ ), 0.2 log (38%,  $p < 0.05$ ), and 0.1 log (24%,  $p > 0.05$ ) in the growth of *P. gingivalis* when exposed to the L-PRF exudate with the ratios 1:1, 1:2, and 1:4, respectively. For the *A. actinomycetemcomitans*, a mean increase of 0.9 log ( $p < 0.05$ ), 0.7 log ( $p < 0.05$ ), and 0.5 log ( $p < 0.05$ ) was observed for the respective ratios (Figure 2).

#### Colonies counting (CFU/ml)

For *P. gingivalis*, the standard culture test showed a mean of  $2.4 \times 10^{12}$  CFU/ml in the control condition and of  $9.4 \times 10^9$ ,  $3.8 \times 10^{10}$ , and  $2.0 \times 10^{11}$  for the ratios 1:1, 1:2, and 1:4, respectively. For *A. actinomycetemcomitans*, the mean CFU/ml for the control was  $3.1 \times 10^7$ , whereas the counting was  $3.0 \times 10^{11}$ ,  $1.8 \times 10^{11}$ , and  $5.5 \times 10^{10}$  for the respective ratios 1:1, 1:2, and 1:4 (Table 4).

#### Gram negative staining

In order to find an explanation for the differences observed between the vitality qPCR data and the culture data for *A. actinomycetemcomitans*, gram staining was performed. As shown in Figure 2, in the control group (Figure 2A) *A. actinomycetemcomitans* formed aggregated clusters known as auto-

aggregation. In the ratio 1:1, the bacteria appeared looser than those in the control group and no auto-aggregation was observed (Figure 2B). Since clusters of bacteria were counted as one colony in the culturing method, and, all bacteria were counted as independent bacteria in the qPCR analysis, the discrepancy between culturing and vitality qPCR could be explained via inhibition of auto-aggregation.

## **Discussion**

The results in this study demonstrated antimicrobial activity of the L-PRF membrane against *P. gingivalis*. No statistically significant inhibition could be observed for *P. intermedia*, *F. nucleatum*, and *A. actinomycetemcomitans*. The L-PRF exudate also showed a clear inhibition against *P. gingivalis* on agar plates. In planktonic form, a dose-dependent inhibition against *P. gingivalis* was observed for the L-PRF exudate, whereas for *A. actinomycetemcomitans* an increase in bacterial growth was detected.

Several studies showed an antimicrobial effect of platelet concentrates against wound bacteria. Burnouf and co-workers (21) described bacterial inhibition by platelet-rich plasma (PRP) against *Pseudomonas aeruginosa*, *Staphylococcus aureus*, and *Escherichia coli* in planktonic form, after 3h of aerobic incubation. Similar results were reported by Edelblute and co-workers (22) on using a clotted form of platelet-rich plasma (PRP), after having added bovine thrombin. They concluded that the human platelet gel supernatant inactivated opportunistic pathogens on the skin, such as *S. aureus* and *Acinetobacter baumannii*, but not *P. aeruginosa*. However, controversial results were shown by Chen and co-workers (26) stating that PRP had an antibacterial effect against *S. aureus* but not against *E. coli* or against *P. aeruginosa* in patients with diabetes.

Only few articles examined oral microorganisms. For instance, *Enterococcus faecalis* and *Candida albicans* isolated from the oral cavity were inhibited by pure-platelet-rich plasma (P-PRP), a type of PRP without leucocytes (27, 28). Yang and co-workers (29) showed inhibition on *P. gingivalis* and *A. actinomycetemcomitans* by PRP whereas no inhibition could be observed for *F. nucleatum*. In this study, the effect of PRP and PRF was compared, concluding that PRP showed superior activity. It should be noted that PRF was prepared by adding calcium chloride to PRP in order to activate the platelets and convert fibrinogen into fibrin, which is not in line with the protocol to prepare PRF. Moreover, the authors affirmed that in their study PRF had neither platelets nor leucocytes. However, by definition, platelet concentrates are blood-derived products with an increased concentration in platelets, with or without the presence of leucocytes (28, 30). Therefore, these results must be interpreted with caution. More recently, Kour and co-workers (2018)(31) compared the antibacterial capacity of PRP, PRF, and injectable-PRF (I-PRF) on *P. gingivalis* and *A. actinomycetemcomitans*. They concluded that all three platelet concentrates showed some antibacterial activity against both bacteria. However, PRP and I-PRF presented significantly greater inhibition against *P. gingivalis* compared to PRF. In the present study, limited inhibition could be observed on *A. actinomycetemcomitans*, which differs from their results. The bacterial strain used and the fact that they incubated *A. actinomycetemcomitans* anaerobically might have influenced the effect of PRF.

*P. gingivalis* was the most inhibited bacteria strain in this study. However, there is no evidence in the literature showing a direct effect of blood components on *P. gingivalis*. Proteinase inhibitors constitute 10% of the protein content of human plasma and they can affect the gingipain activity, known as the primary virulence factor of those bacteria. These proteinases also play an important role in the survival of the bacterium within host cells, due to their implication in the cellular invasion and in overcoming the protective defense mechanisms of epithelial cells(32, 33). An example of proteinase inhibitors is the human alpha-2-macroglobulin, a large plasma protein found in blood, that inhibited



RgpA and RgpB, but not Kgp in an in-vitro study(34). The alpha-granules from the platelets are also an important intracellular storage of biologically active proteins(35, 36). Seven antimicrobial peptides have been identified from human platelets, suggesting a direct antimicrobial role(37). However, the direct relation between those peptides and the antimicrobial capacity of the L-PRF has not been proved yet. For the L-PRF membrane, two theories could be advocated: (1) the living cells inside the fibrin matrix constantly released antimicrobial peptides against the targeted bacteria, or (2) the antimicrobial peptides were entrapped in the fibrin matrix and they were gently released as the fibrin matrix was being disintegrated. Concerning the L-PRF exudate, no specific pathways are known between blood-derived products and *P. gingivalis*. Therefore, further research should investigate this association.

Two effects on *A. actinomycetemcomitans* could be observed in this present study. First, there was an effect on the auto-aggregation of these bacteria. One possible explanation is that the L-PRF exudate might impair the aggregation of those bacteria(38). Given that most bacteria exist in environments with fluctuating conditions (e.g. shear forces, nutrient availability or physiological conditions), the bacteria within co-aggregated communities will survive and proliferate under conditions that reduce the prevalence of single non-aggregated cells. For these reasons, co-aggregation processes are likely to have an important ecological role in the development and maintenance of multiple-species biofilm(39, 40). Regarding the second effect, bacterial growth stimulation of *A. actinomycetemcomitans* was detected when it was in contact with the L-PRF exudate. Fresh human serum is known for enhancing leukotoxic activity of these bacteria(41, 42). Johansson and co-workers (43) indicated that the increased leukotoxicity of *A. actinomycetemcomitans* observed in the presence of human serum is caused by the serum protease inhibitors, which counteract the proteolytic degradation of the leukotoxin.

To the best of our knowledge, this was the first time that the shrinkage of the L-PRF membrane was considered, in surface as well as in length and width. A mean surface shrinkage of 5% *in vitro* after 3 days was reported. These results cannot be straightforwardly extrapolated to the clinical situation. However, they provide insight into the dimensional changes that might occur when used in the oral cavity. It must be noted that the shrinkage of the L-PRF membrane probably occurred progressively. The area of shrinkage was thus gradually exposed, but not colonised by the surrounding bacteria. The explanation for the absence of microbial growth in the area that became exposed after membrane shrinkage is more complex, including factors such as antimicrobial activity at distance, antimicrobial activity due to direct contact or growth inhibition due to mechanical coverage.

Within the limitations of this study, it can be concluded that an L-PRF membrane has antimicrobial properties against *P. gingivalis*, whereas the inhibition against *P. intermedia*, *F. nucleatum*, and *A. actinomycetemcomitans* was not statistically significant on agar plates. The L-PRF exudate showed a strong inhibition against *P. gingivalis* on agar plates, but no inhibition could be observed for the rest of the bacterial strains. Therefore, we cannot reject the first null-hypothesis. For the L-PRF exudate, the second hypothesis cannot be rejected because *A. actinomycetemcomitans* even showed increased growth. However, the L-PRF exudate has an antimicrobial effect against *P. gingivalis* in a dose-dependent way.

## Figures

Figure 1. A: L-PRF membrane on BHI agar plate previously inoculated with an overnight culture of *P. gingivalis*. B: Calculation of initial membrane surface area using PictZar® software (red area). C: After 72 hours of anaerobic incubation, bacterial growth became visible (white colonies). D: Calculation of the membrane's new surface area (red area), in order to detect membrane shrinkage. E: Calculation of area without bacterial growth (green area).

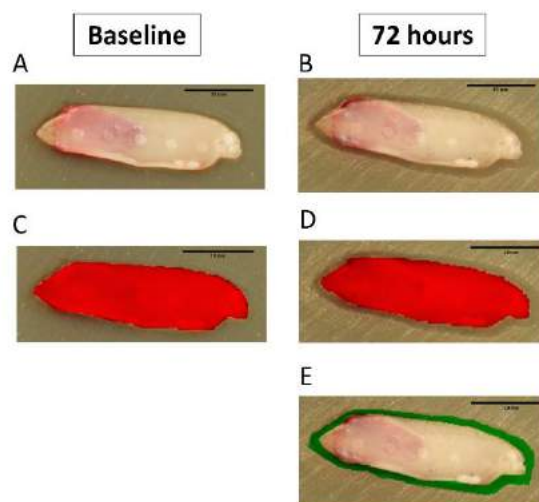


Figure 2. Effect of L-PRF exudate (1:1, 1:2, and 1:4 ratios) on *P. gingivalis* and *A. actinomycetemcomitans* in planktonic form. Results of the vitality qPCR shown after log transformation related to the control (*P.g* and *A.a*, respectively). Positive values represent bacterial growth. Negative values indicate bacterial inhibition. \*\*:  $p < 0.001$ ; \*:  $p < 0.05$

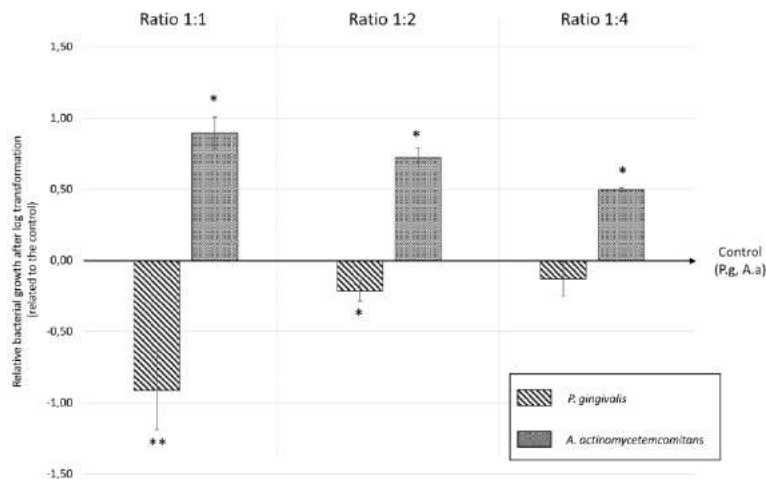
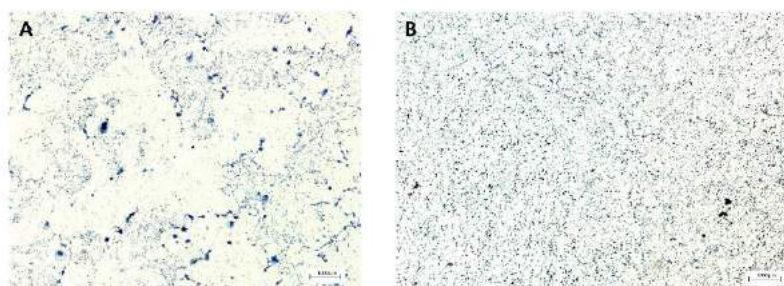


Figure 3. Gram negative staining of *A. actinomycetemcomitans*. A: Control, bacteria in aggregated clusters; B: ratio 1:1, bacteria in separate colonies.



## Tables

Table 1. Primers and probes used for the detection and qualification by vitality qPCR.

STRAIN		Primer/Probe (5'-3')	Fragment length
<i>P. gingivalis</i>	Forward Reverse Probe	GCG CTC AAC GTT CAG CC CAC GAA TTC CGC CTG C CAC TGA ACT CAA GCC CGG CAG TTT CAA	68 bp
<i>P. intermedia</i>	Forward Reverse Probe	CGG TCT GTT AAG CGT GTT GTG CAC CAT GAA TTC CGC ATA CG TGG CGG ACT TGA GTG CAC GC	99 bp
<i>F. nucleatum</i>	Forward Reverse Probe	GGA TTT ATT GGG CGT AAA GC GGC ATT CCT ACA AAT ATC TAC GAA CTC TAC ACT TGT AGT TCC G	162 bp
<i>A. actinomycetemcomitans</i>	Forward Reverse Probe	GAA CCT TAC CTA CTC TTG ACA TCC GAA TGC AGC ACC TGT CTC AAA GC AGA ACT CAG AGA TGG GTT TGT GCC TTA GGG	80 bp

Table 2. Dimensions of L-PRF membranes at baseline and after 72h of incubation as well as the difference between both observations (▲), and bacteria-free area (mm<sup>2</sup>) for nine participants (mean and standard deviation). \* p < 0.05

		<i>P. gingivalis</i>		<i>P. intermedia</i>		<i>F. nucleatum</i>		<i>A. actinomycetemcomitans</i>	
L-PRF membrane		mean	sd	mean	sd	mean	sd	mean	sd
Length and Width (mm)									
Baseline	length	39.4	3.3	35.9	3.5	35.8	4.7	35.1	7.0
	width	10.5	1.2	11.3	1.0	11.1	2.3	10.4	1.3
72 h	length	39.0	3.3	34.2	3.2	35.1	4.6	34.3	6.4
	width	8.8	4.1	9.7	3.8	9.5	3.9	8.9	3.8
▲	length mm	0.4	0.6	1.6	0.2	0.7	0.7	0.8	0.8
	width mm	0.6	0.5	0.4	0.5	0.3	0.2	0.4	0.3
	length %	1.1	1.6	4.4	1.5	2.1	2.0	2.1	1.7
	width %	6.7	4.9	3.7	2.9	5.5	7.6	4.1	3.5
Surface (mm <sup>2</sup> )									
Baseline	membrane surface	37.0	4.6	33.3	6.0	35.4	5.1	32.2	7.9
72 h	membrane surface	34.4	4.4	31.1	11.1	33.6	5.0	30.5	7.0
▲	shrinkage mm <sup>2</sup>	2.7	1.1	2.1	1.1	1.9	0.9	1.7	2.0
	shrinkage %	7.2	2.9	5.5	3.9	5.3	2.5	4.8	5.1
Area of bacterial growth inhibition (mm <sup>2</sup> )									
72 h	full area	11.8*	5.0	2.7	5.2	2.6	3.0	0.6	1.8
	area without shrinkage	9.1*	3.2	0.5	1.3	0.5	0.9	0.2	0.7

Table 3. Mean bacteria-free area (mm<sup>2</sup>) and standard deviation for the L-PRF exudate and chlorhexidine 0.12% (positive control). Data for nine participants. \* p < 0.05.

		<b>P. gingivalis</b>		<b>P. intermedia</b>		<b>F. nucleatum</b>		<b>A. actinomycetemcomitans</b>	
<b>L-PRF exudate (mm<sup>2</sup>)</b>		<b>mean</b>	<b>sd</b>	<b>mean</b>	<b>sd</b>	<b>mean</b>	<b>sd</b>	<b>mean</b>	<b>sd</b>
72 h	L-PRF exudate	17.5*	2.0	0.0	0.0	0.0	0.0	0.0	0.0
	chlorhexidine 0.12%	48.0*	4.2	79.4*	7.0	28.8*	4.0	27.4*	3.0

Table 4. Mean ( $\pm$  standard deviation, SD) qPCR and CFU counting (log values) for *P. gingivalis* and *A. actinomycetemcomitans*. Control: 150  $\mu$ l bacteria + 150  $\mu$ l physiological water. Ratio 1:1 : 150  $\mu$ l bacteria + 150  $\mu$ l L-PRF exudate, ratio 1:2 : 150  $\mu$ l bacteria + 75  $\mu$ l L-PRF exudate + 75  $\mu$ l physiological water, and ratio 1:4 : 150  $\mu$ l bacteria + 37,5  $\mu$ l L-PRF exudate + 112,5  $\mu$ l physiological water. Data for 9 volunteers.

		<b>Vitality qPCR (Log<sub>10</sub> Geq/ml)</b>		<b>Culturing (Log<sub>10</sub> CFU/ml)</b>	
Groups		<b>mean</b>	<b>sd</b>	<b>Mean</b>	<b>sd</b>
<b>P. g</b>	Control	9.6	0.08	12.4	0.6
	1:1	8.6	0.4	9.7	0.4
	1:2	9.4	0.2	10.4	0.4
	1:4	9.5	0.2	11.0	0.5
<b>A. a</b>	Control	10.4	0.2	7.5	0.2
	1:1	11.3	0.3	11.2	0.6
	1:2	11.1	0.3	11.2	0.3
	1:4	10.9	0.2	10.7	0.3

## References

1. Loe H, Theilade E, Jensen SB. Experimental Gingivitis in Man. *J Periodontol*. 1965;36:177-87.
2. Loe H, Theilade E, Jensen SB, Schiott CR. Experimental gingivitis in man. 3. Influence of antibiotics on gingival plaque development. *J Periodontol Res*. 1967;2(4):282-9.
3. Costerton JW, Lewandowski Z, Caldwell DE, Korber DR, Lappin-Scott HM. Microbial biofilms. *Annu Rev Microbiol*. 1995;49:711-45.
4. Socransky SS, Haffajee AD, Cugini MA, Smith C, Kent RL, Jr. Microbial complexes in subgingival plaque. *J Clin Periodontol*. 1998;25(2):134-44.
5. Wecke J, Kersten T, Madela K, Moter A, Gobel UB, Friedmann A, et al. A novel technique for monitoring the development of bacterial biofilms in human periodontal pockets. *FEMS Microbiol Lett*. 2000;191(1):95-101.
6. Marsh PD. Dental plaque: biological significance of a biofilm and community life-style. *J Clin Periodontol*. 2005;32 Suppl 6:7-15.
7. Socransky SS, Haffajee AD. The bacterial etiology of destructive periodontal disease: current concepts. *J Periodontol*. 1992;63(4 Suppl):322-31.
8. Kornman KS, Loe H. The role of local factors in the etiology of periodontal diseases. *Periodontol 2000*. 1993;2:83-97.
9. Haffajee AD, Socransky SS. Microbial etiological agents of destructive periodontal diseases. *Periodontol 2000*. 1994;5:78-111.
10. da Costa L, Amaral C, Barbirato DDS, Leao ATT, Fogacci MF. Chlorhexidine mouthwash as an adjunct to mechanical therapy in chronic periodontitis: A meta-analysis. *J Am Dent Assoc*. 2017;148(5):308-18.
11. Hung HC, Douglass CW. Meta-analysis of the effect of scaling and root planing, surgical treatment and antibiotic therapies on periodontal probing depth and attachment loss. *J Clin Periodontol*. 2002;29(11):975-86.
12. American Academy of P. Comprehensive periodontal therapy: a statement by the American Academy of Periodontology \*. *J Periodontol*. 2011;82(7):943-9.
13. Wikesjo UM, Xiropaidis AV, Thomson RC, Cook AD, Selvig KA, Hardwick WR. Periodontal repair in dogs: rhBMP-2 significantly enhances bone formation under provisions for guided tissue regeneration. *J Clin Periodontol*. 2003;30(8):705-14.
14. Jung RE, Glauser R, Schärer P, Hämmerle CH, Sailer HF, Weber FE. Effect of rhBMP-2 on guided bone regeneration in humans. *Clin Oral Implants Res*. 2003;14(5):556-68.
15. Jung RE, Windisch SI, Eggenschwiler AM, Thoma DS, Weber FE, Hämmerle CH. A randomized-controlled clinical trial evaluating clinical and radiological outcomes after 3 and 5 years of dental implants placed in bone regenerated by means of GBR techniques with or without the addition of BMP-2. *Clin Oral Implants Res*. 2009;20(7):660-6.
16. Dohan Ehrenfest DM, Del Corso M, Diss A, Mouhyi J, Charrier JB. Three-dimensional architecture and cell composition of a Choukroun's platelet-rich fibrin clot and membrane. *J Periodontol*. 2010;81(4):546-55.
17. Schär MO, Diaz-Romero J, Kohl S, Zumstein MA, Nesic D. Platelet-rich concentrates differentially release growth factors and induce cell migration in vitro. *Clin Orthop Relat Res*. 2015;473(5):1635-43.
18. Dohan Ehrenfest DM, de Peppo GM, Doglioli P, Sammartino G. Slow release of growth factors and thrombospondin-1 in Choukroun's platelet-rich fibrin (PRF): a gold standard to achieve for all surgical platelet concentrates technologies. *Growth Factors*. 2009;27(1):63-9.

19. Castro AB, Meschi N, Temmerman A, Pinto N, Lambrechts P, Teughels W, et al. Regenerative potential of leucocyte- and platelet-rich fibrin. Part A: intra-bony defects, furcation defects and periodontal plastic surgery. A systematic review and meta-analysis. *Journal of Clinical Periodontology*. 2017;44(1):67-82.
20. Castro AB, Meschi N, Temmerman A, Pinto N, Lambrechts P, Teughels W, et al. Regenerative potential of leucocyte- and platelet-rich fibrin. Part B: sinus floor elevation, alveolar ridge preservation and implant therapy. A systematic review. *Journal of Clinical Periodontology*. 2017;44:225-34.
21. Burnouf T, Chou ML, Wu YW, Su CY, Lee LW. Antimicrobial activity of platelet (PLT)-poor plasma, PLT-rich plasma, PLT gel, and solvent/detergent-treated PLT lysate biomaterials against wound bacteria. *Transfusion*. 2013;53(1):138-46.
22. Edelblute CM, Donate AL, Hargrave BY, Heller LC. Human platelet gel supernatant inactivates opportunistic wound pathogens on skin. *Platelets*. 2015;26(1):13-6.
23. Castro AB, Cortellini S, Temmerman A, Li X, Pinto N, Teughels W, et al. Characterization of the Leukocyte- and Platelet-Rich Fibrin Block: Release of Growth Factors, Cellular Content, and Structure. *Int J Oral Maxillofac Implants*. 2019.
24. Loozen G, Boon N, Pauwels M, Quirynen M, Teughels W. Live/dead real-time polymerase chain reaction to assess new therapies against dental plaque-related pathologies. *Mol Oral Microbiol*. 2011;26(4):253-61.
25. Schindelin J, Arganda-Carreras I, Frise E, Kaynig V, Longair M, Pietzsch T, et al. Fiji: an open-source platform for biological-image analysis. *Nat Methods*. 2012;9(7):676-82.
26. Chen L, Wang C, Liu H, Liu G, Ran X. Antibacterial effect of autologous platelet-rich gel derived from subjects with diabetic dermal ulcers in vitro. *J Diabetes Res*. 2013;2013:269527.
27. Drago L, Bortolin M, Vassena C, Taschieri S, Del Fabbro M. Antimicrobial activity of pure platelet-rich plasma against microorganisms isolated from oral cavity. *BMC Microbiol*. 2013;13:47.
28. Dohan Ehrenfest DM, Andia I, Zumstein MA, Zhang CQ, Pinto NR, Bielecki T. Classification of platelet concentrates (Platelet-Rich Plasma-PRP, Platelet-Rich Fibrin-PRF) for topical and infiltrative use in orthopedic and sports medicine: current consensus, clinical implications and perspectives. *Muscles Ligaments Tendons J*. 2014;4(1):3-9.
29. Yang LC, Hu SW, Yan M, Yang JJ, Tsou SH, Lin YY. Antimicrobial activity of platelet-rich plasma and other plasma preparations against periodontal pathogens. *J Periodontol*. 2015;86(2):310-8.
30. Dohan DM, Choukroun J, Diss A, Dohan SL, Dohan AJJ, Mouhyi J, et al. Platelet-rich fibrin (PRF): A second-generation platelet concentrate. Part I: Technological concepts and evolution. *Oral Surgery, Oral Medicine, Oral Pathology, Oral Radiology, and Endodontics*. 2006;101(3):E37-E44.
31. Kour P, Pudakalkatti PS, Vas AM, Das S, Padmanabhan S. Comparative Evaluation of Antimicrobial Efficacy of Platelet-rich Plasma, Platelet-rich Fibrin, and Injectable Platelet-rich Fibrin on the Standard Strains of *Porphyromonas gingivalis* and *Aggregatibacter actinomycetemcomitans*. *Contemp Clin Dent*. 2018;9(Suppl 2):S325-S30.
32. Andrian E, Grenier D, Rouabhia M. *Porphyromonas gingivalis*-epithelial cell interactions in periodontitis. *J Dent Res*. 2006;85(5):392-403.
33. Kadowaki T, Takii R, Yamatake K, Kawakubo T, Tsukuba T, Yamamoto K. A role for gingipains in cellular responses and bacterial survival in *Porphyromonas gingivalis*-infected cells. *Front Biosci*. 2007;12:4800-9.
34. Gron H, Pike R, Potempa J, Travis J, Thogersen IB, Enghild JJ, et al. The potential role of alpha 2-macroglobulin in the control of cysteine proteinases (gingipains) from *Porphyromonas gingivalis*. *J Periodontal Res*. 1997;32(1 Pt 1):61-8.

35. Blair P, Flaumenhaft R. Platelet alpha-granules: basic biology and clinical correlates. *Blood Rev.* 2009;23(4):177-89.
36. Cieslik-Bielecka A, Dohan Ehrenfest DM, Lubkowska A, Bielecki T. Microbicidal properties of Leukocyte- and Platelet-Rich Plasma/Fibrin (L-PRP/L-PRF): new perspectives. *J Biol Regul Homeost Agents.* 2012;26(2 Suppl 1):43S-52S.
37. Tang YQ, Yeaman MR, Selsted ME. Antimicrobial peptides from human platelets. *Infect Immun.* 2002;70(12):6524-33.
38. Sreenivasan PK, Meyer DH, Fives-Taylor PM. Factors influencing the growth and viability of *Actinobacillus actinomycetemcomitans*. *Oral Microbiol Immunol.* 1993;8(6):361-9.
39. Karched M, Bhardwaj RG, Asikainen SE. Coaggregation and biofilm growth of *Granulicatella* spp. with *Fusobacterium nucleatum* and *Aggregatibacter actinomycetemcomitans*. *BMC Microbiol.* 2015;15:114.
40. Rickard AH, Gilbert P, High NJ, Kolenbrander PE, Handley PS. Bacterial coaggregation: an integral process in the development of multi-species biofilms. *Trends Microbiol.* 2003;11(2):94-100.
41. McArthur WP, Tsai CC, Baehni PC, Genco RJ, Taichman NS. Leukotoxic effects of *Actinobacillus actinomycetemcomitans*. Modulation by serum components. *J Periodontal Res.* 1981;16(2):159-70.
42. Tsai CC, Ho YP, Chou YS, Ho KY, Wu YM, Lin YC. *Aggregatibacter (Actinobacillus) actinomycetemcomitans* leukotoxin and human periodontitis - A historic review with emphasis on JP2. *Kaohsiung J Med Sci.* 2018;34(4):186-93.
43. Johansson A, Claesson R, Belibasakis G, Makoveichuk E, Hanstrom L, Olivecrona G, et al. Protease inhibitors, the responsible components for the serum-dependent enhancement of *Actinobacillus actinomycetemcomitans* leukotoxicity. *Eur J Oral Sci.* 2001;109(5):335-41.



## CHAPTER 6

### Particle release from silica-coated plastic tubes and presence in PRF matrices

Castro Ana B, Andrade Catherine, Teughels Wim & Quirynen Marc. In progress.

#### **Abstract**

**Background:** Leucocyte and platelet rich fibrin was originally developed using glass tubes, so the coagulation could start as soon as the blood contacted the inner wall of the tube. To avoid tube breaking and contamination, silica-coated plastic tubes were introduced. This coating stimulates blood clotting through the extrinsic pathway and results, as with glass tubes, in the activation of platelets and the physiological formation of a fibrin mesh. Recently, the possible contamination of the PRF matrices by silica released from the tube has been highlighted.

**Aim:** The aim of this study was to evaluate the presence of silica particles inside different PRF matrices and the influence of the centrifugation protocol on their detachment.

**Materials & Methods:** The detached particles were quantified after centrifugation with ethanol (control) and with blood (test) following three different centrifugation protocols (L-PRF, A-PRF, and A-PRF+) using silica-coated plastic tubes and glass tubes. The enzymatic degradation of all three PRF matrices were performed and the presence of silica particles was analyzed and characterized through scanning electron microscopy with energy dispersive X-Ray spectroscopy (SEM-EDX).

**Results:** The number of microparticles detached after centrifugation for the plastic tubes filled with ethanol was similar for all three protocols ( $p>0.05$ ). No particles were detected when glass tubes were used. In plastic tubes filled with blood, the amount of microparticles present at the bottom of the tube increased as the  $g$  force augmented (95% of initial particles at the bottom of the tube for the L-PRF, 60% for A-PRF, and 48% for A-PRF+). The SEM-EDX analysis confirmed that the particles detached after centrifugation were silica microparticles. Due to the contamination of the sample with other elements than Si during the enzymatic degradation of the clots, the quantification of the silica in each clot with spectrophotometer was not reliable, and thus not performed.

**Conclusions:** The centrifugation protocols influenced the amount of silica microparticles present in the PRF matrices. L-PRF presented the least amount inside the clot, and A-PRF+ the highest. The detachment rate of these particles was independent of the centrifugation protocol.

#### **Introduction**

The coagulation cascade started with an endothelial injury and involves the activation, adhesion, and aggregation of platelets as well as the deposition of a fibrin matrix to stop the bleeding. This succession of events occurs in a physiological manner with a sequence of molecules activation. When cells expressing the tissue factor (TF) protein are exposed to blood, this event immediately triggers the clotting cascade following the intrinsic pathway. When the circulating factor VII comes into contact with the TF, they form an activated complex TF-VIIa that activates factor X. From here the common pathway starts that will finalise with the transformation of fibrinogen to fibrin by thrombin. Blood clotting can be also stimulated when plasma is exposed to certain types of artificial surfaces as glass or negatively charged surfaces (i.e. silica coated). In this way, the extrinsic pathway is activated that will also result in the production of a fibrin mesh (1).



Leucocyte and platelet rich fibrin was originally developed using glass tubes to enhance the physiological coagulation cascade inside the tube. In this way, the coagulation starts as soon as the blood contacts the inner wall of the tube. Most of medical specializations are still using glass tubes to prepare L-PRF. However, in dental offices those were replaced by silica-coated plastic tubes to avoid tube breaking and contamination. Bonazza and colleagues (2016) (2) showed the influence of the material and the shape of the blood collection tube on the platelet concentrate, with differences in morphology, fibrin network architecture, and blood cell distribution.

Recently, the possible contamination of the PRF matrices by silica released from the tube has been highlighted. Tsujino and co-workers (2019) (3) found significant levels of silica microparticles incorporated into the A-PRF clot, regardless of tube brand or donor. This fact arose an important safety issue related with the use of silica-coated tubes. However, numerous silica-based materials are used in dentistry nowadays, from hydraulic calcium-silicate cements for vital pulp therapy (4) to calcium silicate-based bioceramics in bone substitutes for bone regeneration (5). The hypothetic cytotoxic effect of these particles seems to depend on their size (6, 7) and the type of exposure (inhalation, direct contact, etc.) (8).

The presence of silica particles inside different PRF matrices and the influence of the centrifugation protocol on their detachment have not been studied yet. Therefore, the primary aim of this study was to evaluate the presence of silica particles inside different PRF matrices. As a secondary aim, the impact of different centrifugation protocols (L-PRF, A-PRF, and A-PRF+) on the detachment of silica particles from the tube was considered.

## **Materials & Methods**

### **Quantification of detached particles of controls (baseline)**

Following the methodology of Tsujino et al. (2019), ethanol was added to each tube: silica-coated plastic tube (Intra-Lock, Boca Raton, Florida, USA) and glass tube (Process for PRF, Nice, France). Both ethanol-filled tubes were centrifuged at the same conditions to prepare all three protocols as described above. The suspension produced was transferred into plastic dishes. The concentration of detached particles in suspension (100µl) was quantified with a spectrophotometer set to 615 nm (Multiskan Ascent®, Rev 1.2, Thermo Electron Corporation, Vantaa, Finland). Silica-coated plastic tubes were considered as positive controls (baseline) and glass tubes as negative controls. The experiments were performed in triplicates.

### **Quantification of detached particles after blood centrifugation in each protocol**

L-PRF, A-PRF and A-PRF+ were prepared with silica-coated plastic tubes and with glass tubes following the centrifugal protocol described above. After centrifugation, the clots were removed and kept for further analysis. At the bottom of the remaining silica-coated plastic tubes, a white spot could be detected (Figure 1). The residual red thrombus was carefully removed, keeping the white particles attached at the bottom. Several centrifugation and washing steps were performed until the pellet obtained was completely clean. The concentration of detached particles in suspension (100µl) was quantified with a spectrophotometer set to 615 nm (Multiskan Ascent®, Rev 1.2, Thermo Electron Corporation, Vantaa, Finland). The experiments were performed in triplicates.

### Enzymatic degradation of PRF matrices and chemical characteristics of the particles

After centrifugation, the clots were carefully removed from the tubes, washed with Phosphate Buffered Saline (PBS) until the complete removal of red blood cells and cut into 6-8 pieces. Following the protocol described by Tsujino et al. (2019), 2 ml of trypsin 0.1% + 1mM Ethylenediaminetetraacetic acid (EDTA) were added for the degradation of the clots and incubated at 37°C overnight until almost complete fibrin degradation. Fibrin remnants and cell debris were further lysed with 2 mL of 1 M KOH until complete dissolution.

The remaining microparticles after enzymatic degradation were evaluated using a scanning electron microscope with energy dispersive X-Ray spectroscopy (SEM-EDX, Nova 600 NanoLab™ DualBeam FIB, EPFL, Switzerland). A stream of primary electrons was focused onto the sample surface resulting in a number of different waves being emitted. The secondary and backscattered electrons were used for imaging while the X-rays provided chemical characteristics of the emitted atoms. The probed depth in EDX analysis was around 1-3 µm.

The particles detached after centrifugation at the ethanol-filled tube and tube with blood were also characterized and then used as positive controls.

## **Results**

### Quantification of detached particles

The number of microparticles detached after centrifugation for the plastic tubes filled with ethanol was similar for all three protocols ( $p > 0.05$ ). No particles were detected when glass tubes were used. When evaluating the microparticles after centrifugation in plastic tubes filled with blood, the amount of microparticles present at the bottom of the tube increased as the g force augmented [L-PRF ( $0.23 \pm 0.02$ ) > A-PRF ( $0.17 \pm 0.04$ ) > A-PRF+ ( $0.11 \pm 0.02$ )]. No particles were detected when glass tubes were used.

The comparison of the results described above for each protocol showed that 95% of initial particles were sent to the bottom of the tubes for the L-PRF group. For A-PRF and A-PRF+, 60% and 48% were recovered at the bottom of the tube (Figure 2).

### SEM-EDX examination

The SEM-EDX analysis detected oxygen (O) and silica (Si) in both controls. It was confirmed that the particles detached after centrifugation were silica microparticles (Figure 3).

In all clots (L-PRF-IL, A-PRF-IL and A-PRF+-IL), not only silica was detected but also other chemical components as sulphur (S), potassium (K), and carbon (C). The presence of these other elements was due to the degradation process of the clots.

Due to the contamination of the sample with other elements than Si, the quantification of the silica in each clot with spectrophotometer was not reliable, and thus not performed.

## Discussion

This present study confirmed the influence of the centrifugation protocol on the presence of silica particles inside PRF matrices. The higher the speed and longer the centrifugation, the less particles could be found inside the clots. Moreover, it is also demonstrated that the silica particles are detached from the inner wall of a silica-coated plastic tube during centrifugation. This appeared not to be influenced by the centrifugation protocol.

Silicon, or Si, is one of the most abundant chemical components found on the Earth (9). Its oxide forms, such as silicate ( $\text{SiO}_4$ ) and silicon dioxide, also known as silica ( $-\text{SiO}_2-$ ), are the main elements of sand and quartz contributing to 90% of the Earth's crust. Due to its unique chemical and physical properties, Si based materials have been used in several industries such as construction, food industry, consumer products, electronics, and biomedical engineering/medicine (10).

The environmental and health effects of these particles seemed to be related to their size and geometry (micro-particles:  $100\mu\text{m}$  to  $100\text{ nm}$ ; nano-particles:  $100\text{ nm}$  to  $1\text{ nm}$ ) (11). For example, the aggregation behavior for amorphous SiO particles can be altered at different particle sizes ( $30$  and  $80\text{ nm}$  in diameter). Larger nanoparticles aggregate quickly, whereas smaller nanoparticles aggregate slowly (12). The geometry of the particles also influenced the clearance rates due to the alteration in the shape (13).

Due to their specific density ( $2.15\text{--}2.30\text{ g/cm}^3$ ), which is higher than the red blood cells, silica microparticles would precipitate during centrifugation. When evaluating the microparticles after blood centrifugation in silica-coated plastic tubes in this present study, the amount of microparticles at the bottom of the tube increased as the g force augmented. Thus, L-PRF presented the greatest amount at the bottom and A-PRF+ the least. So, one can hypothesize that the rest of the particles would be entrapped in the thrombus formed by the red blood cells or would remain inside the clot. The variation in the presence of silica particles in the clots obtained with different protocols has been confirmed in this present article. It is also important to notice that the composition of the particles remaining after the *in vitro* degradation of the clot was heterogeneous, so its quantification using a spectrophotometer may lead to biased results. Consequently, the results obtained by Tsujino and co-workers(3) (2019) should be considered with caution. No silica microparticles were detected when glass tubes were used.

It has been reported in literature that silica microparticles, depending on their amorphousness and size, can be harmful when inhaled (14, 15) Napierska and co-workers (16) (2012) reported a higher release of pro-inflammatory mediators by pulmonary endothelial cells not directly exposed to these particles. Most of the *in vitro* studies with epithelial human lung cells reported a time and dose-dependent decrease in proliferation induced by Si based particles, regardless of the size in the sub-micron range (17).

Several studies have evaluated the effect of Si or SiO particles when directly administered intravenously. They have shown that both particles were cleared out within a month from the body with no system toxicity (18, 19). Lu and co-workers (20), however, reported that although clearance of non-porous NPs was significantly delayed, there were no differences in cell metabolic profiles. Overall the *in vivo* studies on the cytotoxicity of Si based particles displayed no immunogenic and toxicity issues.

In the maxillofacial field, Masuki and co-workers (21) reported a significant reduction of periosteal cells proliferation and viability when in contact with silica. However, amorphous silica is actually used in a variety of products, including food and toothpaste. On the other hand, Gürbüz and co-workers (22) (2010) found also crystal-like particles on the outer surface of PRF prepared with glass tubes.

Within the limitations of this study, we can conclude that the centrifugation protocols influenced the amount of silica microparticles present in the PRF matrices. L-PRF presented the least amount inside the clot, and A-PRF+ the highest. The detachment rate of these particles was independent of the centrifugation protocol.

## Figures

Figure 1. Images of the silica-coated plastic tubes after centrifugation. The amount of particles sent to the bottom of the tubes can be clearly detected.

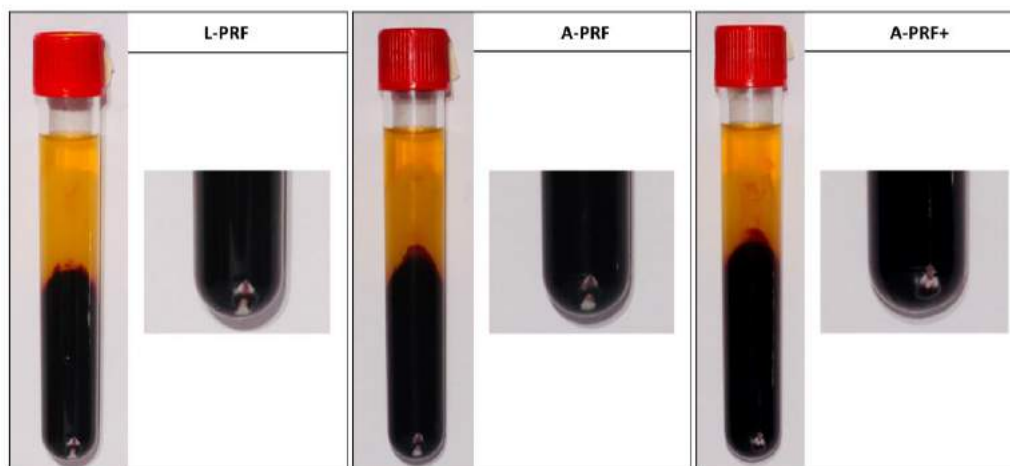


Figure 2. A. Graphical representation of the silica microparticles detached from the tube after centrifugation and the percentage of particles recovery at the bottom of the tube. B. Silica particles at the bottom of a well after drying out. Note the differences amongst the three PRF protocols when centrifuged with ethanol and the amount remaining at the bottom of the tube after blood centrifugation.

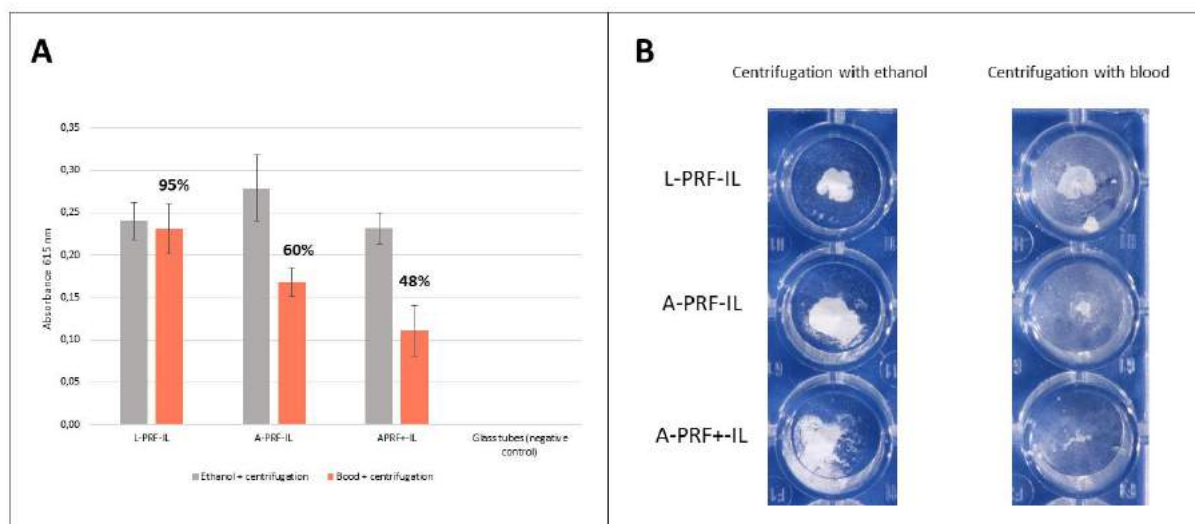
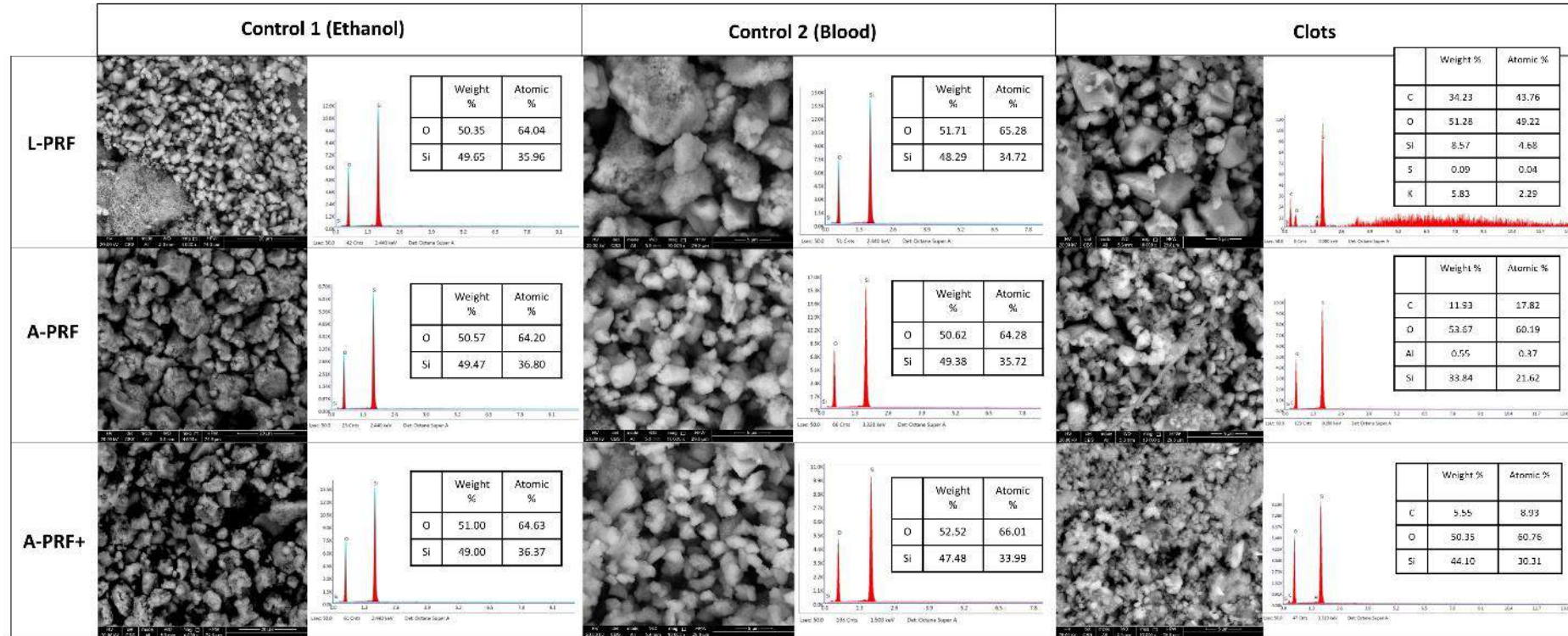


Figure 3. SEM-EDX images and percentages of each chemical element present in the PRF matrices.





## References

1. Hoffman M, Monroe DM, 3rd. A cell-based model of hemostasis. *Thromb Haemost.* 2001;85(6):958-65.
2. Bonazza V, Borsani E, Buffoli B, Castrezzati S, Rezzani R, Rodella LF. How the different material and shape of the blood collection tube influences the Concentrated Growth Factors production. *Microsc Res Tech.* 2016;79(12):1173-8.
3. Tsujino T, Takahashi A, Yamaguchi S, Watanabe T, Isobe K, Kitamura Y, et al. Evidence for Contamination of Silica Microparticles in Advanced Platelet-Rich Fibrin Matrices Prepared Using Silica-Coated Plastic Tubes. *Biomedicines.* 2019;7(2).
4. Pedano MS, Li X, Yoshihara K, Landuyt KV, Van Meerbeek B. Cytotoxicity and Bioactivity of Dental Pulp-Capping Agents towards Human Tooth-Pulp Cells: A Systematic Review of In-Vitro Studies and Meta-Analysis of Randomized and Controlled Clinical Trials. *Materials (Basel).* 2020;13(12).
5. Zhou Y, Wu C, Xiao Y. Silicate-based bioceramics for periodontal regeneration. *J Mater Chem B.* 2014;2(25):3907-10.
6. Napierska D, Thomassen LC, Rabolli V, Lison D, Gonzalez L, Kirsch-Volders M, et al. Size-dependent cytotoxicity of monodisperse silica nanoparticles in human endothelial cells. *Small.* 2009;5(7):846-53.
7. Kusaka T, Nakayama M, Nakamura K, Ishimiya M, Furusawa E, Ogasawara K. Effect of silica particle size on macrophage inflammatory responses. *PLoS One.* 2014;9(3):e92634.
8. Murugadoss S, Lison D, Godderis L, Van Den Brule S, Mast J, Brassinne F, et al. Toxicology of silica nanoparticles: an update. *Arch Toxicol.* 2017;91(9):2967-3010.
9. Ma JF. Plant Root Responses to Three Abundant Soil Minerals: Silicon, Aluminum and Iron. *Critical Reviews in Plant Sciences.* 2005;24(4):267-81.
10. Jaganathan H, Godin B. Biocompatibility assessment of Si-based nano- and micro-particles. *Adv Drug Deliv Rev.* 2012;64(15):1800-19.
11. Kreyling WG, Semmler-Behnke M, Chaudhry Q. A complementary definition of nanomaterial. *Nano Today.* 2010;5(3):165-8.
12. Li Y, Sun L, Jin M, Du Z, Liu X, Guo C, et al. Size-dependent cytotoxicity of amorphous silica nanoparticles in human hepatoma HepG2 cells. *Toxicol In Vitro.* 2011;25(7):1343-52.
13. Chung TH, Wu SH, Yao M, Lu CW, Lin YS, Hung Y, et al. The effect of surface charge on the uptake and biological function of mesoporous silica nanoparticles in 3T3-L1 cells and human mesenchymal stem cells. *Biomaterials.* 2007;28(19):2959-66.
14. Brown T. Silica exposure, smoking, silicosis and lung cancer--complex interactions. *Occup Med (Lond).* 2009;59(2):89-95.
15. Steenland K, Ward E. Silica: a lung carcinogen. *CA Cancer J Clin.* 2014;64(1):63-9.
16. Napierska D, Thomassen LC, Vanaudenaerde B, Luyts K, Lison D, Martens JA, et al. Cytokine production by co-cultures exposed to monodisperse amorphous silica nanoparticles: the role of size and surface area. *Toxicol Lett.* 2012;211(2):98-104.
17. Akhtar MJ, Ahamed M, Kumar S, Siddiqui H, Patil G, Ashquin M, et al. Nanotoxicity of pure silica mediated through oxidant generation rather than glutathione depletion in human lung epithelial cells. *Toxicology.* 2010;276(2):95-102.
18. Huang X, Li L, Liu T, Hao N, Liu H, Chen D, et al. The shape effect of mesoporous silica nanoparticles on biodistribution, clearance, and biocompatibility in vivo. *ACS Nano.* 2011;5(7):5390-9.

19. Tanaka T, Mangala LS, Vivas-Mejia PE, Nieves-Alicea R, Mann AP, Mora E, et al. Sustained small interfering RNA delivery by mesoporous silicon particles. *Cancer Res.* 2010;70(9):3687-96.
20. Lu X, Tian Y, Zhao Q, Jin T, Xiao S, Fan X. Integrated metabolomics analysis of the size-response relationship of silica nanoparticles-induced toxicity in mice. *Nanotechnology.* 2011;22(5):055101.
21. Masuki H, Isobe K, Kawabata H, Tsujino T, Yamaguchi S, Watanabe T, et al. Acute cytotoxic effects of silica microparticles used for coating of plastic blood-collection tubes on human periosteal cells. *Odontology.* 2020.
22. Gürbüz B, Pikdöken L, Tunalı M, Urhan M, Küçükodacı Z, Ercan F. Scintigraphic evaluation of osteoblastic activity in extraction sockets treated with platelet-rich fibrin. *J Oral Maxillofac Surg.* 2010;68(5):980-9.





## SECTION 3



*In vivo study*



## CHAPTER 7

### Peri-implant bone structure at early healing after implant surface functionalization with L-PRF: a micro-CT and histomorphological analysis.

Castro Ana B, Cortellini Simone, Vasconcelos Karla F, Pamuk Ferda, Duyck Joke, Jacobs Reinhilde & Quirynen Marc. In progress.

#### **Abstract**

**Aim:** To evaluate the effect of L-PRF coating on the peri-implant bone formation and angiogenesis at early healing in a pig model.

**Material & methods:** Four implants were placed in the skull of twelve domestic pigs with an oversized preparation (0.4mm): two 4.2x8mm Astra EV implants (OsseoSpeed® surface), and two 4.0x8mm Blossom implants (Osseon® surface). Implants conditions were randomised as control Astra- (Astra EV no coating), control Bloss- (Blossom no coating), test Astra+ (Astra EV coated with L-PRF), and test Bloss+ (Blossom coated with L-PRF). Two follow-up periods were settled: 7 days (6 pigs) and 28 days (6 pigs). The bone-to-implant contact (BIC) was histologically assessed for both follow-up periods. BIC was also analysed with micro-CT for the bone samples at 28-days.

**Results:** Forty-eight implants were installed following the randomisation protocol. Histological analysis at 7 days showed statistically significant higher mean BIC % values for Astra+ compared to Bloss+ ( $p=0.001$ ). Bloss+ was negatively affected by the L-PRF coating, showing the least BIC% ( $29.3\% \pm 9.2$ ). No statistically significant differences were found amongst the other groups. At 28 days, Bloss- showed significantly higher mean BIC% ( $84.4\% \pm 7.6$ ) compared to the rest of the groups. No statistically significant differences were found amongst the other groups. For the micro-CT analysis at 28 days follow-up, the mean BIC% was  $82.1\% \pm 11.0$  and  $77.7\% \pm 8.5$  for Astra+ and Astra-, respectively ( $p>0.05$ ). For Blossom implants, a mean BIC of  $89.3\% \pm 3.8$  was observed for coated implants, and  $83.9\% \pm 5.7$  for non-coated ( $p>0.05$ ). Further, none of the parameters describing the peri-implant bone microstructure as measured on micro-CT were significantly affected by L-PRF functionalization.

**Conclusion:** The effect of L-PRF coating depended on the implant surface and the healing time. The peri-implant bone formation was not improved by L-PRF implant surface functionalization.

#### **Introduction**

Osseointegration of titanium implants is a complex process involving interactions between immuno-inflammatory responses, angiogenesis, and osteogenesis, resulting in the direct contact between bone and the implant surface (1). The characteristics of the implant surface (e.g. topography and chemical modifications) were recognised as one of the key factors for its integration in bone (2).

The sequence of healing events leading to osseointegration of a titanium implant was elucidated for the first time in a dog model (3). At the first hours after implant installation, the gap between the implant surface and the implant osteotomy was occupied with a blood clot mainly composed by platelets, neutrophils, and monocytes/macrophages in a fibrin network. This coagulum was partially replaced by a primitive granulation tissue after 4 days. Already during the first week,

newly formed woven bone could be detected. In some regions, this woven bone was growing from the lateral wall of the osteotomy (distance osteogenesis). However, *de novo* formation could also be seen in direct contact with the implant surface (contact osteogenesis) especially on moderately rough surfaces. After 2 weeks of healing, bone resorption started to occur, so bone in direct contact with the implant at insertion started to disappear and was replaced by new bone. The mechanical stability of the implant at this stage was replaced by biological bonding. This bone remodelling process resulted in a fully functional bone after 6 to 8 weeks (4).

In 2011, Bosshardt and co-workers (5) studied the peri-implant bone healing and maturation in human volunteers over a period of 6 weeks. Initial bone formation was observed as early as 7 days at some distance of the implant surface. After 4 weeks, bone resorption was often found close to the implant surface. The trabecular network connecting the pristine bone with the implant surface was more mature and the new bone layer on the implant surfaces was thicker than before. At the end of the study, the overall peri-implant bone density had also increased.

The clinical success of oral implants relies on their early osseointegration. In the last decades, efforts have been made to chemically modify the implant surfaces to improve bone apposition. Several coatings have been developed including carbon, bioactive glass, fluoride or hydroxyapatite (HA) (6). Moreover, different studies demonstrated that the surface roughness of titanium implants affects the rate of osseointegration and biomechanical fixation (7-10). In the early 90's, Buser and co-workers (11) examined the influence of different surface characteristics on bone apposition. The sandblasted and acid-etched surface showed promising results, while the hydroxyapatite surface was not the first choice and is currently not recommended. At the same time, a moderately rough, microporous surface produced by anoxic oxidation was also developed (12).

The use of biological molecules on the implant surface was introduced to stimulate osteogenic cells in the early stage of osseointegration, and consequently accelerate bone formation. A range of extracellular matrix components, peptides, and growth factors have been proposed (13-15). Biomimetic dental implants may accelerate osseointegration and its application may be also useful in specific patients. For example, coating implants with factors known to induce endothelial cell differentiation and proliferation may promote greater vascularity in highly cortical bone. Coating implants with BMPs may also accelerate initial healing times during integration of the dental implant, thereby reducing overall treatment times and improving implant success rates (16, 17).

As explained above, one fundamental phase of the healing process is the formation of a stable fibrin clot in contact with the implant surface to provide a provisional scaffold for the migration of differentiating osteogenic cells towards the implant surface. Based on this, the use of platelet concentrates has also been studied for the functionalization of implant surfaces. Lollobrigida and co-workers (2018) (18) studied the behaviour *in vitro* of different implant surfaces when in contact with the L-PRF exudate and liquid fibrinogen. They concluded that both products promoted the formation of a dense fibrin clot with high cellular content on micro/nano-rough surfaces *in vitro*. Öncü and co-workers (2016) (19) reported that the application of L-PRF may increase the amount and rate of newly formed bone during early healing and provided a faster osseointegration in an animal model. However, clinical studies showed controversial results in the use of L-PRF as a coating biomaterial (20-22).

Therefore, the aim of this study was to evaluate the effect of the implant coating with L-PRF membranes on the early peri-implant bone formation and early bone-to-implant contact for two different implant surfaces. In order to observe the effect of the L-PRF on the peri-implant pristine bone and newly formed bone, implants were placed with an oversized preparation of 0.4 mm.

## **Materials and Methods**

### **Experimental animals**

Twelve female adult domestic pigs (*Sus scrofa domestica*) of 18 months old and with a weight of 200-250 kg were chosen for this study. All experimental protocols complied with the ARRIVE guidelines and were approved by the Ethical Committee for Animal Experimentation of KU Leuven (Belgium) under the file number P044/2016. The procedures were carried out in accordance with the UK Animas (Scientific Procedures) Act 1986 and EU Directive 2010/63/EU for animal experiments.

The minimum required sample size was estimated using the results of a previous animal study also comparing two different implants systems (23).

### **Dental implants**

Two types of implants were used in this study: Astra EV implants (Dentsply Sirona, Mölndal, Sweden), and Blossom implants (Intra-Lock International, Boca Raton, Florida, USA). The Astra EV™ implants with OsseoSpeed® surface are obtained after a sandblasting of the surface and a chemical modification with fluoridation. The Blossom implant (Biohorizons, Birmingham, Alabama, USA) has an Ossean® surface, a calcium phosphate low impregnated surface with a micro-nano fractal topography.

### **Blood collection and L-PRF preparation**

Eight 9-ml silica-coated plastic tubes were withdrawn from the jugular vein from each animal. The blood was immediately centrifuged with a table centrifuge (Intra-Spin, Intra-Lock, Boca Raton, Florida, USA) at 408 g for 12 min. After centrifugation, L-PRF clots were collected and transformed into membranes by gently compression using a specific box designed for this purpose (Xpression box, Intra-Lock, Biohorizons, Birmingham, Alabama, USA). The liquid released from this compression (L-PRF exudate) was also kept.

### **Surgical protocol and follow up**

Anesthesia was induced by intravenous injection of a cocktail of the following drugs: a premixed combination of tiletamine and zolazepam (Zoletil 100®, Virbac, Barneveld, the Netherlands), added at 1/6 dilution to xylazine (Vexylans, CEVA, Brussels, Belgium), and injected at 1 mL/10 kg. A concentration of 1% Propofol (Diprivan, Aspen Pharma Trading Ltd, Ireland) intravenous (10mg/kg/hour) was used to maintain anesthesia.

Implant surgery was performed in the parietal bone of the skull. Before incision, the skin of each animal was shaved and disinfected with povidone iodine and local anaesthesia was also administered. The parietal bone was exposed by a vertical incision and after releasing a full-thickness flap, four implants were inserted with an oversized preparation (0.4mm): two 4.2 x 8mm Astra EV implants (OsseoSpeed® surface), and two 4.0 x 8mm Blossom® implants (Ossean® surface). Implant conditions and positions were randomised with a computer program (Research Randomizer, version 4.0) as control Astra - (Astra EV no coating), control Bloss - (Blossom® no coating), test Astra + (Astra EV coated with L-PRF), and test Bloss + (Blossom coated with L-PRF) (Figure 1).

Each implant allocated in the test group (L-PRF coating) was firstly soaked in the L-PRF exudate. One L-PRF membrane was cut in two pieces (face: red part; body: yellow part) and the face was introduced in the osteotomy. Immediately afterwards, the coated implant was inserted (Figure 2).

The insertion torque of each implant was recorded by the Nobel Biocare iPad®-operated Osseocare Pro Drill Motor. All implants were placed following the manufacturer's surgical protocol,

except that a final extra drill (diameter 4.6 for Astra implants and 4.4 for Blossom implants) was used to obtain the oversized preparation of 0.4 mm around each implant, and were anchored apically. Full-thickness flaps were carefully repositioned and sutured in two layers (Vicryl 3/0, Ethicon Inc., New Jersey, USA; and Silk 1/0, Ethicon Inc., New Jersey, USA ).

Postoperatively, ibuprenorfine (0.005 mg/kg; im; Temgesic, Schering-Plough, Brussels, Belgium) was administered as analgesic and a single dose of amoxicillin 15mg/kg (Duphamox LA, Zoetis) as antibiotics.

#### Follow up

Two follow-up periods were settled. Half of the animals (n = 6) were euthanized 7 days after surgery and the other half after 28 days. Anesthesia was induced by intravenous injection of a cocktail of the following drugs: a premixed combination of tiletamine and zolazepam (Zoletil 100®, Virbac, Barneveld, the Netherlands), added at 1/6 dilution to xylazine (Vexylans, CEVA, Brussels, Belgium), and injected at 1 mL/10 kg, followed by overdose of barbiturate (Release, ecuphar, Belgie).

#### Specimen preparation

Implants were harvested with the surrounding bone tissue and all samples were immediately fixed in a CaCO<sub>3</sub> formalin. Those from 28-day follow-up underwent first micro-CT analysis before being processed for histology. After fixation, bone samples were dehydrated in ascending series of ethanol concentrations over a period of 15 days. Serial sections (4-µm) were made starting from the central region of the sample and perpendicular towards the long axis of the sample. Two serial sections per sample in the most central cut area were selected and stained with Masson's Trichome staining for bone-to-implant contact analysis and general morphological analysis.

#### Micro-CT scanning and analysis

Micro-CT images were taken from the bone samples at 28-days of healing. It was considered that newly formed bone would not be detected after 7 days of healing. Micro-CT scanning was performed on a SkyScan 1275 high-resolution desktop system (Bruker, Kontich, Belgium). The scan protocol was set at a source voltage of 100 kV, tube current of 100 µA, and a Cu filter of 1 mm was used to increase the transmission through the samples and consequently reduce beam hardening artefacts. The pixel resolution was established at 10 µm, a rotation step of 0.25 degrees, a frame averaging of 3, and an acquisition of 360°.

Image reconstruction was performed using the NRecon software + GPUReconServer (Bruker, Kontich, Belgium). Smoothing of the projection images prior to reconstruction was done with a value of 3. The ring artefacts were reduced with a strength of 7 and the beam hardening correction was set at 30%. Data from each animal was encoded and all measurements were performed blinded for the treatment allocation.

After reconstruction, 3D analysis of the samples was performed using CTAn software (Bruker, Kontich, Belgium). The bone-to-implant contact (BIC) was examined in a 3-D (in %) and 2-D analysis (in mm<sup>2</sup>). The BIC% in 3-D analysis was measured by the parameter percent intersection surface (S/TS%). For the 2-D analysis, the parameter intersection surface was used. Moreover, bone quality of the peri-implant area was also analysed. An axial ring was created around each implant with the same width as the oversized preparation (0.4 mm) (figure on Table 3). That ring was considered as "newly formed bone" given the oversized preparation. The bone trabecular pattern factor (Tb.Pf), percentage of bone

volume (BV/TV%), trabecular thickness (Tb.Th), trabecular number (Tb.N), and trabecular separation (Tb.Sp) were calculated.

#### Histological analysis

Digital microscopic images of histological sections from both follow-up periods (7 days and 28 days) were captured by an automated slice scanner (Axioscan, Carl Zeiss, Oberkochen, Germany). Bone-to-implant contact was calculated in percentage ( $BIC = \frac{\text{sum of the lengths of those parts of the implant surface that are in contact with bone}}{\text{total length of the implant surface}}$ ) in three different regions of each implant: coronal, middle, and apical third. Each region was determined by dividing the implant in 3 parts. Moreover, the total BIC % was calculated throughout the whole length of the implant, starting from the neck of the implant. All measurements were performed with Zeiss Zen Lite software (Carl Zeiss, Oberkochen, Germany).

#### Statistical analysis

For the histological analysis, the average of all values in duplicate were calculated and processed on the basis of a Frailty model that uses pig as a random model. Implant type, coating or not with LPRF and position were considered as fixed factors. The zero values were modelled as '<lowest quantized value>'. Comparisons were made between implant types and whether or not use of L-PRF.

For micro-CT, imaging data were analyzed using a linear mixed model with pig as random factor and implant type and L-PRF coating as fixed factors. Comparisons were made between implant types and coating L-PRF. For the analysis of the bone micro-structure around the implant a linear mixed model was also used with the pig as random factor and the ring, implant and L-PRF coating as fixed factors.

### **Results**

Forty-eight implants were installed following the randomisation protocol. One pig from the 7-day follow-up died due to complications during recovery and was considered as a control. Other animals healed uneventfully. The mean implant insertion torque recorded was  $11.8 \text{ Ncm} \pm 3.9$ , which confirmed the oversize preparation.

#### Micro-CT analysis

The oversized preparation was confirmed by the micro-CT of the control pig, with a BIC % value of 27.8%.

##### *Peri-implant ring: bone-to-implant contact*

The mean BIC% (3D analysis) after 28 days was  $89.3\% (\pm 3.8)$  and  $83.9\% (\pm 5.7)$  for Bloss+ and Bloss-, respectively ( $p > 0.05$ ). For Astra EV implants, a mean BIC of  $82.1\% (\pm 11.0)$  was observed for coated implants, and  $77.7\% (\pm 8.5)$  for non-coated ( $p > 0.05$ ).

Also the 2D analysis showed no statistically significant differences amongst groups ( $p > 0.05$ ).

##### *Peri-implant ring: bone micro-structure*

For both implant surfaces, no statistically significant differences were found for any of the variables ( $p > 0.05$ ). Data are shown in Table 3.

#### Histological analysis



*7 days follow-up*

Astra+ showed statistically significant higher mean BIC % values than Bloss+ ( $p=0.001$ ). No significant differences could be observed between Astra implants coated or not with L-PRF. Bloss- presented significant greater mean BIC % compared to Bloss+. Data are presented in Figure 3.

No statistically significant differences could be observed amongst groups at 7 days follow-up for the coronal, middle, and apical regions ( $p > 0.05$ ). Data are shown in Table 1.

The histomorphological analysis showed the presence of a thick coagulum compatible with the L-PRF membrane at the interface between the Blossom implant and the peri-implant bone. For the rest of the conditions, a thin coagulum (red interface with red blood cells) could be observed. The oversized preparation was filled with granulation tissue that was being transformed into woven bone (immature bone) (Figure 4).

*28 days follow-up*

For the total BIC %, Bloss- showed the highest mean value ( $84.4\% \pm 7.6$ ). This condition was statistically superior to the rest of the groups (Bloss+:  $73.4\% \pm 10.7$ , Astra+:  $71.2\% \pm 8.6$ , and Astra-:  $66.6\% \pm 16.9$ ). Further, no statistically significant differences could be observed between implant systems coated or not with L-PRF.

At the coronal region, Bloss- showed the highest mean BIC % ( $86.5\% \pm 4.3$ ). This condition was statistically significant higher compared to Astra- ( $66.5\% \pm 16.9$ ;  $p=0.0001$ ) and with Bloss+ ( $73.4\% \pm 10.7$ ;  $p=0.0003$ ). Data are shown in Table 2.

At the middle region, Bloss- presented also the highest mean BIC % ( $82.9\% \pm 11.1$ ). When compared to an Astra- ( $55.7\% \pm 24.9$ ), Bloss- was significantly superior ( $p=0.0001$ ). The mean BIC % for Bloss- was also statistically significant greater to Bloss+ ( $71.6\% \pm 11.9$ ;  $p=0.002$ ). For Astra implants, Astra+ showed significant higher mean BIC % values than Astra- ( $p=0.01$ ).

At the apical part, only the comparison between Bloss- vs. Astra- resulted in statistically significant differences ( $85.3\% \pm 11.7$  vs.  $69.1\% \pm 16.3$ ).

The histomorphological analysis showed the resorption or integration of the coagulum present at 7 days-follow up for the Blossom implants coated with L-PRF. The oversized preparation was filled with more matured bone in direct contact with the implant in the rest of the conditions. Bloss- presented a well-organized trabecular bone in between the implant threads (Figure 5).

## **Discussion**

This *in vivo* study investigated the effect of L-PRF implant coating on the early bone-to-implant contact (BIC) and early peri-implant bone formation around two different implant systems. Histologically at 7 days, Astra implants coated with L-PRF showed statistically significant higher mean BIC % than coated-Blossom implants. However, no significant differences could be observed between Astra implants coated or not with L-PRF. At 28 days, Bloss- showed the highest mean BIC% and this was statistically superior to the rest of the groups. No statistically significant differences could be observed between implant systems coated or not with L-PRF. Moreover, Blossom implants seemed to be negatively affected by the L-PRF coating in both follow-up periods. In the radiological analysis, the L-PRF coating provided a superior BIC %, although the differences were not statistically significant.

The domestic pig was the animal of choice in this study. Compared with small animal models, such as rodents, large animal models are superior in many aspects to study diseases and pre-clinical therapies. Because intra-oral factors such as mastication forces and disproportionate implant loading can negatively affect periimplant bone formation, an extra-oral model was used. Moreover, the maxillary bone is a very thick and massive in pigs, thus recent studies used the temporal and parietal bone given also the higher accessibility (24, 25). The skull of the domestic pig consists of a thick cortical bone with a dens trabecular bone underneath, which resembles the bone structure of the human jaws (26, 27). In literature, temporal and parietal bone segments were used to evaluate the optimal timing and long-term effects of fixation techniques (28) or for testing new biomaterials using calvarian defects (29). Furthermore, platelet rich plasma (PRP) was also tested in peri-implant bone regeneration and the pig was shown to be a suitable animal model because of the similar bone regeneration rate (1.2 – 1.5 mm/day) to the humans (1-1.5 mm/day) (30) (23) (31).

This model has certainly some limitations. Apart from a rather limited sample size, one does not have to forget that *in vivo* experiments try to resemble as much as possible the real clinical conditions. However, clinical trials remain the most accurate model. Several clinical studies evaluated the application of L-PRF on the osseointegration process, reporting statistically significant higher ISQ values when implants were coating with L-PRF (19, 20, 32, 33). Similarly, Boora et al. (2015) (34) recorded the early bone remodeling around implants coated or not with L-PRF at insertion. The L-PRF-coated implants showed 50% less initial bone loss. However, Diana and co-workers (2018) could not observed any significant effect of L-PRF coating on immediate implants with adequate primary stability.

In the present study, the face of an L-PRF membrane was placed inside the osteotomy and the implants were soaked into L-PRF exudate. Different techniques have been described in literature (e.g. wrapping the implant with an L-PRF membrane, coating only with L-PRF exudate, coating with liquid fibrinogen, etc...). The differences in the protocol may also explain the variances in the results.

While scanning samples containing metallic bodies, several methodological aspects should be take into account. The settings used for image acquisition (100 kV, 100  $\mu$ A, full 360° rotation with one frame acquired at every 0.25 rotation steps and a 1 mm copper filter) provided the best images given that a thick filter with high voltage increased the transmission through the sample and reduced beam hardening artifacts. Further artifact reduction was achieved following the protocol described by de Faria Vasconcelos et al. (2017) (35), through filtering of low-energy photons (36) and by excluding the four voxels closest to the surface of the titanium screw using an expansion tool (37, 38). Our findings showed some differences between the 2D histological and the 2D and 3D radiological analysis. The biggest difference was found for the Bloss- with the least BIC % histologically and the presence of a

thick coagulum in the gap whereas radiologically Bloss- was superior to the rest of the conditions. This might be explained by the higher density of the coagulum radiologically. Generally, micro-CT overestimates morphometric parameters when compared with histomorphometric evaluation (39). This is probably the result of an additional segmentation step used in micro-CT (40). The discrepancy between voxel size (14  $\mu\text{m}$ ) and histologic slide thickness (4  $\mu\text{m}$ ) should be addressed as this may have contributed to micro-CT overestimation, thus being a limitation of such an approach (40).

Two types of implants were used in this study. Astra EV implants (Dentsply Sirona, Molndal, Sweden) have a polished neck followed by micro-threads for ensure positive biomechanical bone stimulation and maintenance of marginal bone level (41) (42). The OsseoSpeed® surface is obtained after sandblasting and chemical modification with fluoridation. Results reported from *in vitro* experiments indicated that fluoride ions influence formation of both organic and inorganic components of bone tissue. Thus, fluoride may increase the density of trabecular bone and enhance the incorporation of collagen into bone matrix as well as alkaline phosphatase activity (43, 44). Berglundh and co-workers (2007) (45) demonstrated that the amount of new bone that formed in the chambers within the first 2 weeks of healing was larger at sites with a fluoride-modified surface (test) than with a control (TiOblast) surface. Based on these findings, it was suggested that the fluoride-modified implant surface promoted osseointegration in the early phase of healing following implant installation.

Similar to our study, Abrahamsson and co-workers (2008) (46) studied the early per-implant bone formation around fluoride-modified surfaces placed in an oversized preparation. They reported a mean BIC % of  $55.7\% \pm 9.7$  and of  $63.7\% \pm 19.3$ , after 2 weeks and 6 weeks, respectively. Those findings are in accordance to what we have observed in our study when the Astra implants were not coated with L-PRF. However, the oversized preparation in their study was of 1 mm compared to 0.4 mm from the present study. The gap size (0.4 mm) may have limited the beneficial effect of L-PRF in the distance osteogenesis. Moreover, the detection of differences in bone quality and structure with the micro-CT may have been also influenced by the gap size.

Up to now, the impact of L-PRF coating on fluoride-modified implant surfaces has not been investigated. However, Thor and co-workers (2007) (47) showed that the contact between whole blood and Ti alloy resulted in the binding of platelets to the material surface and in the generation of thrombin–antithrombin (TAT) complexes. TAT complexes are formed in response to the high thrombin level caused by coagulation. Since thrombin is rapidly bound by antithrombin, TAT is a good measure for thrombin level in the blood. With whole blood TAT levels increased 1000-fold compared with platelet rich plasma (PRP) and platelet-poor plasma (PPP), in which both almost no increase of TAT could be detected. The haemostatic plug with its fibrin network on these materials might be an optimal scaffold for regeneration of bone tissue. Augmented levels of contact activation (48) and presence of fluoride ions (49) causes generation of a less dense fibrin network and in addition enhances the fibrinolytic process as shown by Collet and co-workers, which could facilitate osteoblast migration into the area (50).

The other implant system investigated in the present study was the Blossom implant (Intra-Lock International, Boca Raton, Florida, USA). Its Ossean® surface has a calcium phosphate (Ca-P) layer that together with the fractal topography, seems to be ideal for fibrin attachment, platelet deposition and osteoblastic growth (51). The mechanical stability of the Ca-P coating requires a rough titanium surface to ensure the mechanical stability of the coating. It has been shown that such biomimetic coatings are more soluble in physiological fluids and resorbable by osteoclastic cells than high temperature coatings such as plasma-sprayed hydroxyapatite (52, 53). Pre-clinical comparative models

have demonstrated a higher BIC % for biomimetic calcium phosphate coatings than for uncoated titanium implants during the initial phase of healing and higher cell differentiation *in vitro* (51).

The interaction between L-PRF membranes and the Ossean® surface has been already investigated *in vivo*. Neiva and co-workers (2016) (54) examined the effect of L-PRF coating on bone formation after immediate implant placement in dogs with a larger gap between the implant and the surrounding bone. The Ossean® surface coated with L-PRF resulted in significantly higher bone fill of the initial gap compared to non-coated. However, in the present study the use of L-PRF on Ossean® surface seemed to negatively affect the early osseointegration. *In vitro*, titanium discs with an Ossean® surface were coated with liquid fibrinogen and with L-PRF exudate. A dense fibrin network was formed on the surface with abundant erythrocytes, platelets, and leucocytes. The authors concluded that liquid L-PRF products promoted the formation of a dense fibrin clot on micro/nano-rough implant surfaces *in vitro*. The adjunctive treatment of implant surfaces with the L-PRF exudate may provide support to the contact of the fibrin with the surface. However, it is not clear yet if this would be beneficial or detrimental for the early phases of osseointegration. The fact that a dense fibrin matrix occupies the interface between the implant and the bone might jeopardize the early steps of osseointegration on some surfaces. Plasma fibrin clots with a tight fibrin formation made of thin fibers dissolve at a slower rate than those with a loose fibrin formation made of thicker fibers (50). In the present study, traces from the L-PRF membrane could be found after 7 days in the implant-bone gap, although also remnants of a blood clot were identified. Further studies should explain how L-PRF membranes are dissolved or incorporated in the surrounding tissues and how these processes might influence osseointegration.

## **Conclusions**

The effect of the L-PRF coating seems to be dependent on the implant surface. The peri-implant bone structure seems not to be affected by L-PRF implant surface functionalization.

## **Acknowledgements**

We would like to thank both companies Dentsply Sirona and Intra-Lock International for providing the implants for this study. The company Nobel Biocare is also acknowledged for equipping us with their iPad®-operated Osseocare Pro Drill Motor.

We want to acknowledge the veterinarian Dr. Wouter Merckx, Mr. Stijn Massart and all the staff members from the Centre Zootechnique (TRANSfarm) at the KU Leven in Lovenjoel for their help during the surgeries and for taking care of the animals during the follow-up period.

Also, we would like to thank Dr. Tim Vangansewinkel and Mrs. Evelyne Van Kerckhove from Hasselt University for their help in the histological sectioning and staining of the samples.

**Figures**

Figure 1. Schematic representation of the parietal bone (skull) of the animal. The coating was randomly allocated (red cycle). Astra implants are colored in black; Blossom implants are indicated with stripes.

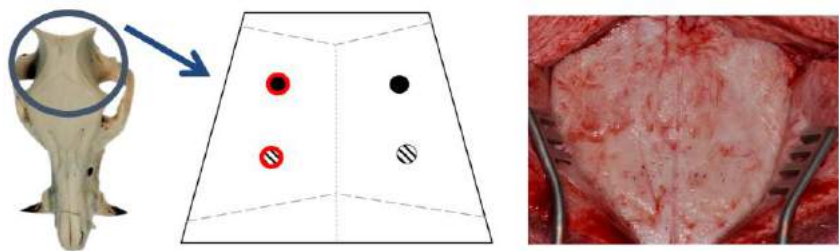


Figure 2. L-PRF coating of the tested implants. A: L-PRF clots in the Xpression box. B: ASTRA EV® implant is soaked into L-PRF exudate. C: The face of the L-PRF membrane was inserted into the osteotomy. D: implant placement with the L-PRF membrane coating the implant.

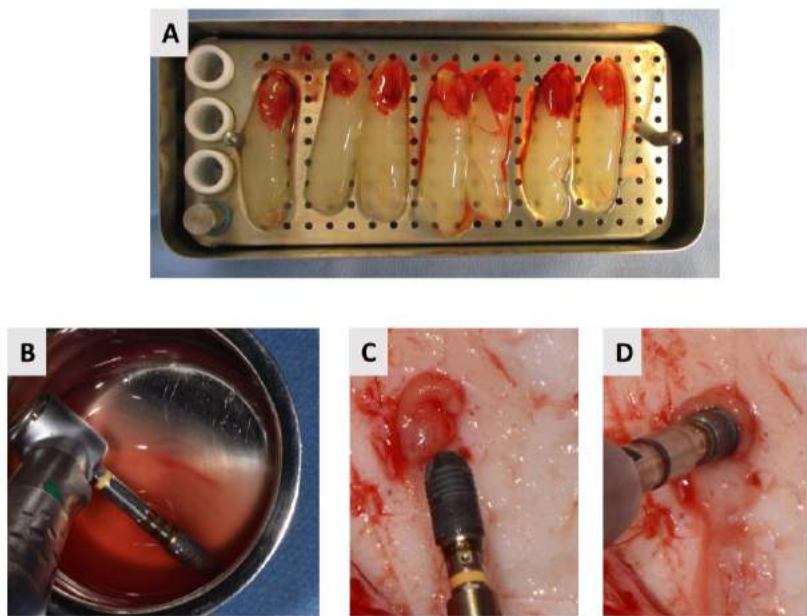


Figure 3. Total histological BIC % at 7 days and 28 days follow-up for all the conditions. St. diff.: statistical significant differences. Different letters showed statistical significant differences ( $p < 0.05$ ).

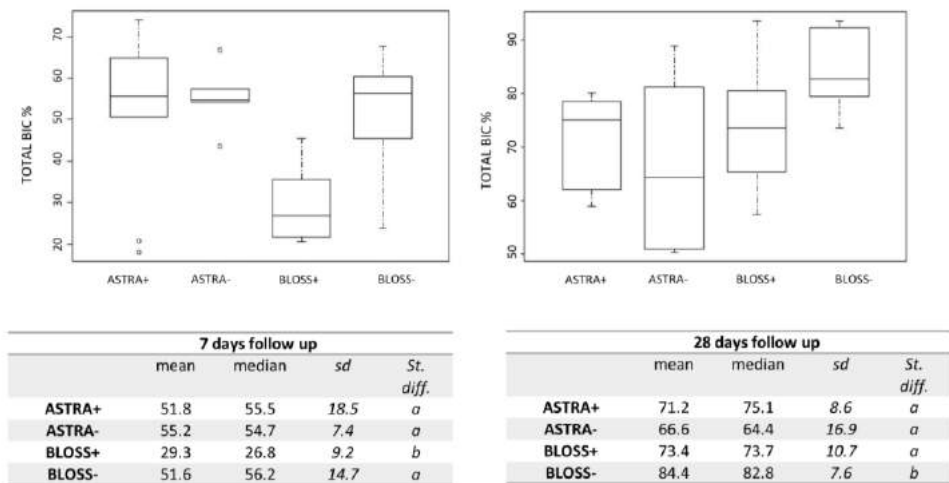




Figure 4. Histological images after 7 days follow-up. Note the oversized preparation in all images. A: Blossom implant coated with L-PRF. A thick coagulum compatible with the L-PRF membrane (in red) was present in the interface between the implant and the peri-implant bone. B: Blossom implant without coating. A thin coagulum covered the interface between the implant and the peri-implant bone. C: Astra implant coated with L-PRF. Granulation tissue and initial woven bone were present in the wound chambers. D: Astra implant without coating. Granulation tissue and initial woven bone could be observed in between the implant threads.

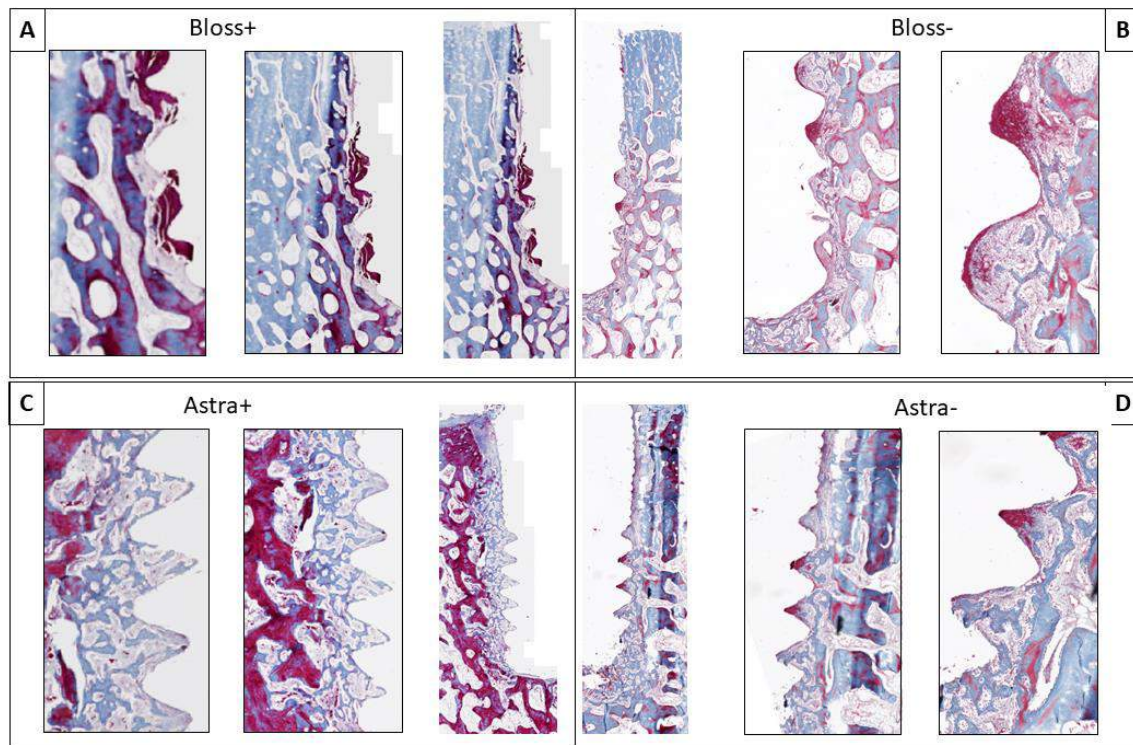
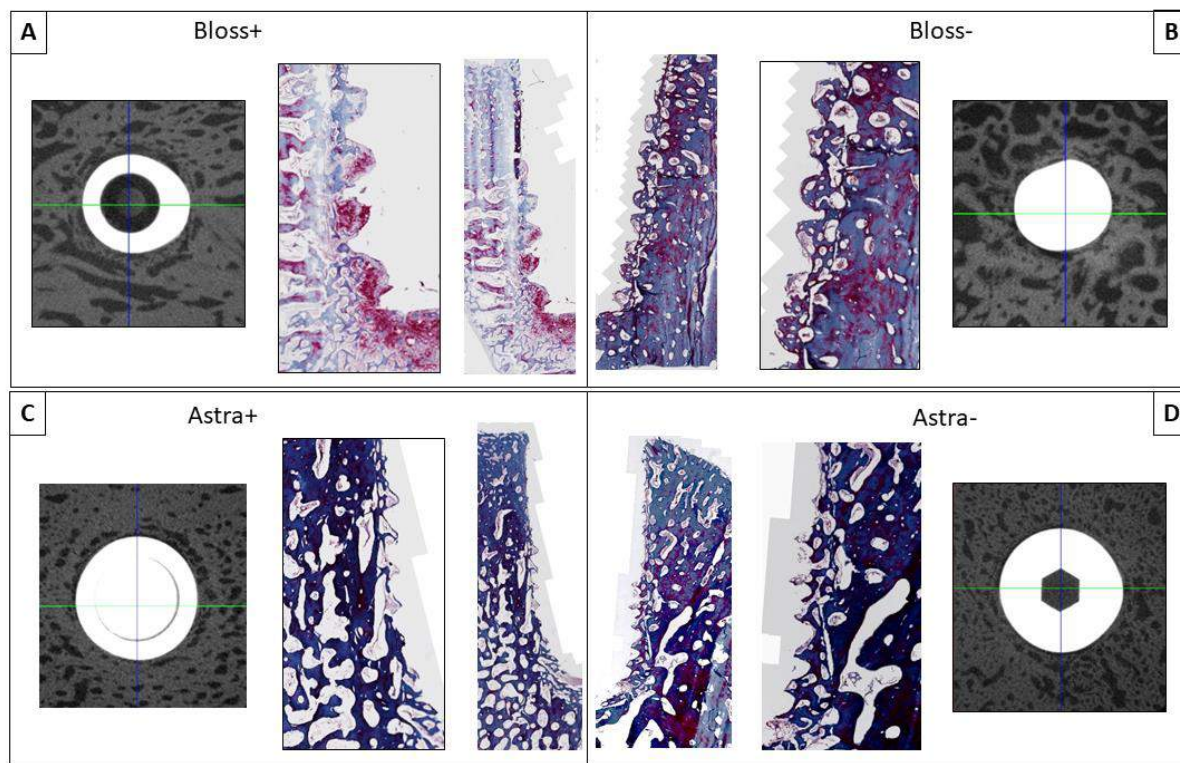


Figure 5. Histological and micro-CT images after 28 days follow-up. A: Blossom implant coated with L-PRF. Coagulum resorption was occurring while newly formed bone (woven bone) appeared in the wound chambers. B: Blossom implant without coating. More matured bone was present in between the implant threads. C: Astra implant coated with L-PRF. The oversized preparation has been filled with matured bone. D: Astra implant without coating. Woven bone is being converted into trabecular bone.



## Tables

Table 1. Percentage of bone-to-implant (BIC %) after 7 days follow-up in each implant region (coronal, middle and apical) for the histological analysis. No statistically significant differences could be found amongst groups ( $p>0.05$ ).

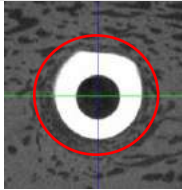
		7 days follow up		
		mean	median	<i>sd</i>
<b>CORONAL</b>	Astra+	58.4	55.8	28.4
	Astra-	54.4	58.3	14.5
	Bloss+	59.7	50.9	24.8
	Bloss-	57.1	56.3	11.0
<b>MIDDLE</b>	Astra+	51.3	50.2	27.2
	Astra-	57.2	48.3	22.7
	Bloss+	34.3	18.1	29.8
	Bloss-	52.0	53.9	21.7
<b>APICAL</b>	Astra+	48.5	51.8	13.8
	Astra-	54.6	61.6	16.5
	Bloss+	22.1	23.2	11.5
	Bloss-	48.3	53.6	15.8

Table 2. Percentage of bone-to-implant (BIC %) after 28 days follow-up in each implant region (coronal, middle and apical) for the histological analysis. Different letters showed statistical significant differences ( $p<0.05$ ).

		28 days follow up			
		mean	median	<i>sd</i>	
<b>CORONAL</b>	Astra+	73.6	73.8	11.9	<i>a,b</i>
	Astra-	72.2	74.6	12.9	<i>a</i>
	Bloss+	72.5	72.3	7.4	<i>a</i>
	Bloss-	86.5	88.2	4.3	<i>b</i>
<b>MIDDLE</b>	Astra+	71.1	74.4	10.9	<i>a</i>
	Astra-	55.7	55.3	24.9	<i>b</i>
	Bloss+	71.7	68.4	11.9	<i>a</i>
	Bloss-	82.9	86.8	11.1	<i>c</i>
<b>APICAL</b>	Astra+	71.1	68.6	11.0	<i>a,b</i>
	Astra-	69.1	65.8	16.3	<i>a</i>
	Bloss+	82.1	20.2	13.6	<i>a,b</i>
	Bloss-	85.3	86.6	11.7	<i>b</i>



Table 3. Micro-CT parameters from the ring in direct contact with the implant surface (0.4 mm wide). The bone in this region was considered newly formed bone due to the oversized preparation. No statistically significant differences could be found for any of the variables.

	Ring in contact with the implant surface							
	ASTRA +		ASTRA -		BLOSS +		BLOSS -	
	mean	<i>sd</i>	mean	<i>sd</i>	mean	<i>sd</i>	mean	<i>sd</i>
Percent intersection surface (%)	82.0	11.0	89.3	3.8	89.3	3.8	77.7	8.5
Intersection surface (mm <sup>2</sup> )	4,944.8	6,819.2	3,485.9	7,406.0	3,485.9	7,406.0	2,682.9	5,093.9
Bone micro-structure								
Trabecular thickness (mm)	0.11	0.02	0.10	0.03	0.12	0.02	0.13	0.02
Trabecular number (mm)	3.0	2.72	3.5	2.3	4.7	0.3	4.8	0.2
Trabecular separation (mm)	0.12	0.02	0.13	0.02	0.13	0.03	0.12	0.02
Trabecular pattern factor (mm)	2.0	6.9	6.6	7.1	-0.4	6.8	-3.0	4.0
Connectivity	24,810.6	9,685.5	24,435.2	11,782.6	22,878.8	11,942.6	20,934.2	11,315.1
Structure model index	0.12	0.80	0.70	0.70	0.17	0.80	-0.60	1.50
BV/TV (%)	53.8	13.2	47.7	16.7	56.0	13.2	65.4	11.4

## References

1. Feller L, Chandran R, Khammissa RA, Meyerov R, Jadwat Y, Bouckaert M, et al. Osseointegration: biological events in relation to characteristics of the implant surface. *Sadj*. 2014;69(3):112, 4-7.
2. Buser D, Broggini N, Wieland M, Schenk RK, Denzer AJ, Cochran DL, et al. Enhanced bone apposition to a chemically modified SLA titanium surface. *J Dent Res*. 2004;83(7):529-33.
3. Berglundh T, Abrahamsson I, Lang NP, Lindhe J. De novo alveolar bone formation adjacent to endosseous implants. *Clin Oral Implants Res*. 2003;14(3):251-62.
4. Salvi GE, Bosshardt DD, Lang NP, Abrahamsson I, Berglundh T, Lindhe J, et al. Temporal sequence of hard and soft tissue healing around titanium dental implants. *Periodontol*. 2000. 2015;68(1):135-52.
5. Bosshardt DD, Salvi GE, Huynh-Ba G, Ivanovski S, Donos N, Lang NP. The role of bone debris in early healing adjacent to hydrophilic and hydrophobic implant surfaces in man. *Clin Oral Implants Res*. 2011;22(4):357-64.
6. Xuereb M, Camilleri J, Attard NJ. Systematic review of current dental implant coating materials and novel coating techniques. *Int J Prosthodont*. 2015;28(1):51-9.
7. Cochran DL, Schenk RK, Lussi A, Higginbottom FL, Buser D. Bone response to unloaded and loaded titanium implants with a sandblasted and acid-etched surface: a histometric study in the canine mandible. *J Biomed Mater Res*. 1998;40(1):1-11.
8. Wennerberg A, Hallgren C, Johansson C, Danelli S. A histomorphometric evaluation of screw-shaped implants each prepared with two surface roughnesses. *Clin Oral Implants Res*. 1998;9(1):11-9.
9. Cochran DL, Buser D, ten Bruggenkate CM, Weingart D, Taylor TM, Bernard JP, et al. The use of reduced healing times on ITI implants with a sandblasted and acid-etched (SLA) surface: early results from clinical trials on ITI SLA implants. *Clin Oral Implants Res*. 2002;13(2):144-53.
10. Weber HP, Morton D, Gallucci GO, Roccuzzo M, Cordaro L, Grutter L. Consensus statements and recommended clinical procedures regarding loading protocols. *Int J Oral Maxillofac Implants*. 2009;24 Suppl:180-3.
11. Buser D, Schenk RK, Steinemann S, Fiorellini JP, Fox CH, Stich H. Influence of surface characteristics on bone integration of titanium implants. A histomorphometric study in miniature pigs. *J Biomed Mater Res*. 1991;25(7):889-902.
12. Larsson C, Thomsen P, Lausmaa J, Rodahl M, Kasemo B, Ericson LE. Bone response to surface modified titanium implants: studies on electropolished implants with different oxide thicknesses and morphology. *Biomaterials*. 1994;15(13):1062-74.
13. Kim TI, Jang JH, Kim HW, Knowles JC, Ku Y. Biomimetic approach to dental implants. *Curr Pharm Des*. 2008;14(22):2201-11.
14. Roessler S, Born R, Scharnweber D, Worch H, Sewing A, Dard M. Biomimetic coatings functionalized with adhesion peptides for dental implants. *J Mater Sci Mater Med*. 2001;12(10-12):871-7.
15. Schliephake H, Scharnweber D, Dard M, Sewing A, Aref A, Roessler S. Functionalization of dental implant surfaces using adhesion molecules. *J Biomed Mater Res B Appl Biomater*. 2005;73(1):88-96.
16. Le Guéhennec L, Soueidan A, Layrolle P, Amouriq Y. Surface treatments of titanium dental implants for rapid osseointegration. *Dent Mater*. 2007;23(7):844-54.

17. Simon Z, Watson PA. Biomimetic dental implants--new ways to enhance osseointegration. *J Can Dent Assoc.* 2002;68(5):286-8.
18. Lollobrigida M, Maritato M, Bozzuto G, Formisano G, Molinari A, De Biase A. Biomimetic Implant Surface Functionalization with Liquid L-PRF Products: In Vitro Study. *Biomed Res Int.* 2018;2018:9031435.
19. Öncü E, Bayram B, Kantarci A, Gülsever S, Alaaddinoğlu EE. Positive effect of platelet rich fibrin on osseointegration. *Med Oral Patol Oral Cir Bucal.* 2016;21(5):e601-7.
20. Öncü E, Alaaddinoğlu EE. The effect of platelet-rich fibrin on implant stability. *Int J Oral Maxillofac Implants.* 2015;30(3):578-82.
21. Diana C, Mohanty S, Chaudhary Z, Kumari S, Dabas J, Bodh R. Does platelet-rich fibrin have a role in osseointegration of immediate implants? A randomized, single-blind, controlled clinical trial. *Int J Oral Maxillofac Surg.* 2018;47(9):1178-88.
22. Alhussaini AHA. Effect of Platelet-Rich Fibrin and Bone Morphogenetic Protein on Dental Implant Stability. *J Craniofac Surg.* 2019;30(5):1492-6.
23. Vivan Cardoso M, Vandamme K, Chaudhari A, De Rycker J, Van Meerbeek B, Naert I, et al. Dental Implant Macro-Design Features Can Impact the Dynamics of Osseointegration. *Clin Implant Dent Relat Res.* 2015;17(4):639-45.
24. Lethaus B, Tudor C, Bumiller L, Birkholz T, Wiltfang J, Kessler P. Guided bone regeneration: dynamic procedures versus static shielding in an animal model. *J Biomed Mater Res B Appl Biomater.* 2010;95(1):126-30.
25. Tudor C, Bumiller L, Birkholz T, Stockmann P, Wiltfang J, Kessler P. Static and dynamic periosteal elevation: a pilot study in a pig model. *Int J Oral Maxillofac Surg.* 2010;39(9):897-903.
26. Štembírek J, Kyllar M, Putnová I, Stehlík L, Buchtová M. The pig as an experimental model for clinical craniofacial research. *Lab Anim.* 2012;46(4):269-79.
27. Kyllar M, Štembírek J, Putnová I, Stehlík L, Odehnalová S, Buchtová M. Radiography, computed tomography and magnetic resonance imaging of craniofacial structures in pig. *Anat Histol Embryol.* 2014;43(6):435-52.
28. Sims CD, Butler PE, Casanova R, Randolph MA, Ahn DK, Yaremchuk MJ. Surgical model to assess the effects and optimal timing of craniofacial fixation. *J Craniofac Surg.* 1996;7(6):412-6; discussion 7.
29. Reedy BK, Pan F, Kim WS, Gannon FH, Krasinskas A, Bartlett SP. Properties of coralline hydroxyapatite and expanded polytetrafluoroethylene membrane in the immature craniofacial skeleton. *Plast Reconstr Surg.* 1999;103(1):20-6.
30. Schlegel KA, Kloss FR, Kessler P, Schultze-Mosgau S, Nkenke E, Wiltfang J. Bone conditioning to enhance implant osseointegration: an experimental study in pigs. *Int J Oral Maxillofac Implants.* 2003;18(4):505-11.
31. Moest T, Koehler F, Prechtel C, Schmitt C, Watzek G, Schlegel KA. Bone formation in peri-implant defects grafted with microparticles: a pilot animal experimental study. *J Clin Periodontol.* 2014;41(10):990-8.
32. Hamzacebi B, Oduncuoglu B, Alaaddinoglu EE. Treatment of Peri-implant Bone Defects with Platelet-Rich Fibrin. *Int J Periodontics Restorative Dent.* 2015;35(3):415-22.
33. Öncü E, Erbeyoğlu AA. Enhancement of Immediate Implant Stability and Recovery Using Platelet-Rich Fibrin. *Int J Periodontics Restorative Dent.* 2019;39(2):e58–e63.
34. Boora P, Rathee M, Bhorla M. Effect of Platelet Rich Fibrin (PRF) on Peri-implant Soft Tissue and Crestal Bone in One-Stage Implant Placement: A Randomized Controlled Trial. *J Clin Diagn Res.* 2015;9(4):Zc18-21.

35. de Faria Vasconcelos K, Dos Santos Corpas L, da Silveira BM, Laperre K, Padovan LE, Jacobs R, et al. MicroCT assessment of bone microarchitecture in implant sites reconstructed with autogenous and xenogenous grafts: a pilot study. *Clin Oral Implants Res.* 2017;28(3):308-13.
36. Hsieh J. *Computed Tomography: Principles, Design, Artifacts, and Recent Advances* 2003.
37. Butz F, Ogawa T, Chang TL, Nishimura I. Three-dimensional bone-implant integration profiling using micro-computed tomography. *Int J Oral Maxillofac Implants.* 2006;21(5):687-95.
38. Liu S, Broucek J, Viridi AS, Sumner DR. Limitations of using micro-computed tomography to predict bone-implant contact and mechanical fixation. *J Microsc.* 2012;245(1):34-42.
39. Soares MQS, Van Dessel J, Jacobs R, da Silva Santos PS, Cestari TM, Garlet GP, et al. Zoledronic Acid Induces Site-Specific Structural Changes and Decreases Vascular Area in the Alveolar Bone. *J Oral Maxillofac Surg.* 2018;76(9):1893-901.
40. Dias DR, Leles CR, Batista AC, Lindh C, Ribeiro-Rotta RF. Agreement between Histomorphometry and Microcomputed Tomography to Assess Bone Microarchitecture of Dental Implant Sites. *Clin Implant Dent Relat Res.* 2015;17(4):732-41.
41. Rocci M, Rocci A, Martignoni M, Albrektsson T, Barlattani A, Gargari M. Comparing the TiOblast and Osseospeed surfaces. Histomorphometric and histological analysis in humans. *Oral Implantol (Rome).* 2008;1(1):34-42.
42. Dohan Ehrenfest DM, Vazquez L, Park YJ, Sammartino G, Bernard JP. Identification card and codification of the chemical and morphological characteristics of 14 dental implant surfaces. *J Oral Implantol.* 2011;37(5):525-42.
43. Shteyer A, Liberman R, Simkin A, Gedalia I. Effect of local application of fluoride on healing of experimental bone fractures in rabbits. *Calcif Tissue Res.* 1977;22(3):297-302.
44. Farley JR, Wergedal JE, Baylink DJ. Fluoride directly stimulates proliferation and alkaline phosphatase activity of bone-forming cells. *Science.* 1983;222(4621):330-2.
45. Berglundh T, Abrahamsson I, Albouy JP, Lindhe J. Bone healing at implants with a fluoride-modified surface: an experimental study in dogs. *Clin Oral Implants Res.* 2007;18(2):147-52.
46. Abrahamsson I, Albouy JP, Berglundh T. Healing at fluoride-modified implants placed in wide marginal defects: an experimental study in dogs. *Clin Oral Implants Res.* 2008;19(2):153-9.
47. Thor A, Rasmusson L, Wennerberg A, Thomsen P, Hirsch JM, Nilsson B, et al. The role of whole blood in thrombin generation in contact with various titanium surfaces. *Biomaterials.* 2007;28(6):966-74.
48. Sanchez J, Elgue G, Larsson R, Nilsson B, Olsson P. Surface-adsorbed fibrinogen and fibrin may activate the contact activation system. *Thromb Res.* 2008;122(2):257-63.
49. Di Stasio E, Nagaswami C, Weisel JW, Di Cera E. Cl- regulates the structure of the fibrin clot. *Biophys J.* 1998;75(4):1973-9.
50. Collet JP, Park D, Lesty C, Soria J, Soria C, Montalescot G, et al. Influence of fibrin network conformation and fibrin fiber diameter on fibrinolysis speed: dynamic and structural approaches by confocal microscopy. *Arterioscler Thromb Vasc Biol.* 2000;20(5):1354-61.
51. Bucci-Sabattini V, Cassinelli C, Coelho PG, Minnici A, Trani A, Dohan Ehrenfest DM. Effect of titanium implant surface nanoroughness and calcium phosphate low impregnation on bone cell activity in vitro. *Oral Surg Oral Med Oral Pathol Oral Radiol Endod.* 2010;109(2):217-24.
52. Barrère F, van der Valk CM, Dalmeijer RA, van Blitterswijk CA, de Groot K, Layrolle P. In vitro and in vivo degradation of biomimetic octacalcium phosphate and carbonate apatite coatings on titanium implants. *J Biomed Mater Res A.* 2003;64(2):378-87.

53. Habibovic P, Li J, van der Valk CM, Meijer G, Layrolle P, van Blitterswijk CA, et al. Biological performance of uncoated and octacalcium phosphate-coated Ti6Al4V. *Biomaterials*. 2005;26(1):23-36.
54. Neiva RF, Gil LF, Tovar N, Janal MN, Marao HF, Bonfante EA, et al. The Synergistic Effect of Leukocyte Platelet-Rich Fibrin and Micrometer/Nanometer Surface Texturing on Bone Healing around Immediately Placed Implants: An Experimental Study in Dogs. *Biomed Res Int*. 2016;2016:9507342.

## SECTION 4



Clinical study



## CHAPTER 8

### Effect of different platelet rich fibrin matrices for ridge preservation in multiple tooth extractions: a split-mouth randomized controlled clinical trial

Castro Ana B, Van Dessel Jeroen, Temmerman Andy, Jacobs Reinhilde & Quirynen Marc. (2021)  
*Journal of Clinical Periodontology*, 00: 1-12.

#### **Abstract**

**Aim:** To evaluate the dimensional changes in alveolar ridge and bone structure after tooth extraction when L-PRF or A-PRF+ were used in comparison to unassisted socket.

**Materials & Methods:** Twenty patients in need of at least three tooth extractions in the aesthetic zone were included. L-PRF, A-PRF+ or control were randomly assigned. CBCT scans were obtained immediately after tooth extraction and after 3 months of healing. Horizontal and vertical dimensional changes of the ridge and socket fill were calculated. Histological and micro-CT analysis of bone biopsies from the centre of the sockets were used to evaluate the bone structure after healing.

**Results:** Mean horizontal and vertical changes at 1-mm below the crest (buccal and palatal side) were similar for the 3 sites ( $p>0.05$ ). For the socket fill, L-PRF (85.2%) and A-PRF+ (83.8%) showed superior values than the control (67.9%). The histological and radiological analysis reported more newly formed bone for the PRF groups, without any differences between both.

**Conclusions:** PRF matrices failed to reduce the dimensional changes after multiple tooth extractions in the premaxilla. After 3-months healing, both PRF matrices showed radiographically a significant superiority for the socket fill. Histologically, they seemed to accelerate new bone formation.

#### **Introduction**

The alteration of the hard and soft tissue contour after tooth extraction has been extensively studied (1-3). According to a systematic review of Tan and colleagues (2012), the mean horizontal bone resorption after 6 months was  $3.8 \pm 0.2$  mm at the crest. The vertical resorption was extended to 11-22% after 6 months, whereas the horizontal resorption ranged from 29 to 63%. However, the extension of alveolar bone resorption may vary depending on tooth type as observed by Couso-Queiruga and co-workers (2021) (4) with a higher radiological horizontal bone resorption in molar sites vs non-molar sites (3.61 vs 2.54 mm). An additional bone loss of 2.4 mm in width and of 1.1 mm in height has been reported in sites with compromised buccal bone wall (5). Interestingly, these numbers only comprise single tooth extractions, making the additional ridge resorption in cases with multiple extractions less quantifiable. Consequently, bone and/or soft tissue augmentation procedures would be necessary to overcome the bone deficiency.

Different surgical techniques have been described to overcome this resorption process (6-8). Even though different treatments have been attempted to prevent this, studies failed to show a technique that totally compensates that event (9). The use of grafting biomaterials into extraction sockets has been intensively studied (10-14). In a recent systematic review with meta-analysis (15), alveolar ridge preservation (ARP) procedures were found to be effective in limiting physiologic ridge



reduction compared to natural healing. However, a certain degree of bone resorption was detected even if an ARP was used. The effect of ARP procedures is unpredictable, probably due to the influence of local and systemic factors, which are not yet fully understood.

Biological additives, for instance platelet concentrates, have also been proposed as adjunctive for bone regeneration. A second generation of platelet concentrates, leukocyte and platelet rich fibrin (L-PRF) was introduced to eliminate the drawbacks of the first generation (16). L-PRF is a 100% autologous fibrin matrix containing platelets and leucocytes obtained after blood centrifugation without anticoagulants at high spin. The three-dimensional fibrin matrix in L-PRF serves as a scaffold for the cells entrapped in it but also for the growth factors produced by these cells, resulting in a slow and gradual releasing rate (17, 18). Moreover, the absence of bone substitute remnants has been also seen as advantage for the use for this biomaterial for ARP (19, 20). It has been shown that the use of L-PRF accelerates neoangiogenesis (21), stimulates the local environment for differentiation and proliferation of surrounding cells (22), and continuously releases growth factors over a period of 7-14 days (23).

Recently, new PRF protocols [advanced platelet rich fibrin (A-PRF), and advanced platelet rich fibrin+ (A-PRF+)] have been proposed reducing the g force and duration of the centrifugation (24, 25). By reducing the relative centrifugal force, an increase in the release of growth factors and in the concentration of leucocytes and platelets was envisaged. However, the clinical relevance of these differences still needs to be demonstrated.

The aim of this study was to evaluate the dimensional changes in the alveolar ridge after tooth extraction when L-PRF or A-PRF+ were used in comparison to unassisted socket healing (control). Primary outcome variables were defined as the changes in horizontal width at crest-1 mm levels. Secondary outcome variables were established as the changes in horizontal width at crest-3 mm and -5 mm, and vertical resorption at the buccal and palatal side. The socket fill was defined as tertiary outcome variable. Finally, the % of bone volume/tissue volume (BV/TV) and bone microstructure were considered as quaternary outcome.

## **Material and Methods**

The study was approved by the Ethical Committee of the KU Leuven, UZ Leuven University Hospitals (S-57938, B322201525149) and conducted in accordance with the requirements of the Helsinki Declaration of 1975 (revised in 2008) and with the CONSORT statements (26) ([www.consort-statement.org](http://www.consort-statement.org)). The study was registered in Clinicaltrials.gov with the number NCT03268512.

### **Study population**

From August 2015 to October 2018, patients in the need of at least three tooth extractions in the aesthetic region (premaxilla, single-rooted teeth) were evaluated for initial study eligibility at the Department of Periodontology (University Hospitals Leuven, Belgium). Patients fulfilling all criteria were invited to participate in the study and provided written informed consent prior to inclusion (Table 1).

### **L-PRF and A-PRF+ preparation & surgical procedure**

Eight blood tubes per participant were collected prior to any treatment. Four sterile 9-ml silica-coated plastic tubes without anticoagulant (BVBCTP-2, Intra-Spin, Intra-Lock, Florida, USA) were used to prepare L-PRF, and another 4 sterile 10-ml glass tubes without anticoagulant (DUO, Nice, France)

for A-PRF+. These were immediately centrifuged at 2,700 rpm (RCFclot: 408 g) for 12 min to prepare L-PRF (IntraSpin, Intra-Lock, Florida, USA) (19) and at 1,300 rpm (RCFclot: 145 g) for 8 min (DUO Process, Nice, France) to prepare A-PRF+ (27). After centrifugation, each L-PRF/A-PRF+ clot was collected from the tube and carefully separated from the red blood cells with a spatula. All L-PRF/A-PRF+ clots were then transformed into 1-mm thick membranes by gentle compression using especially designed boxes for each protocol (Xpression box, Intra-Lock, Florida, USA or A-PRF+ box, DUO Process, Nice, France).

Tooth extractions were performed under local anaesthesia and sterile conditions with a flapless approach. After extraction, the sockets were carefully cleaned and randomized as control or test site by means of a computer program (Research Randomizer, version 4.0). L-PRF, A-PRF+ or control were randomly assigned, leaving one empty socket/edentulous site between conditions. The position of the extraction sites is presented in Figure 1. At the test sites (L-PRF or A-PRF+) 2-3 membranes, depending on the size of the socket, were inserted and compressed with an amalgam plunger. A 3-4 mm full-thickness envelope was created at the buccal and palatal side to create space for 1-2 folded membrane placed into this envelope to seal the socket. A crossed horizontal mattress suture (Vicryl 4.0, Ethicon™, Johnson & Johnson®, New Jersey, USA) was used to stabilize the L-PRF/A-PRF+ without any attempt for primary wound closure, followed by individual sutures for better adaptation of the material when needed. At the control site, a cross-suture was applied to stabilize the coagulum (Figure 2). Patients were unaware of the allocation of each treatment option. Immediately after tooth extractions, a first cone beam-CT (CBCT) (T0) was taken in order to record the baseline conditions.

All patients were asked to take an analgesic three times a day (Paracetamol 1 g) for 3 days, and use of an antiseptic mouth rinse (Perio-Aid™ 0.12%, Dentaïd®, Barcelona, Spain). All patients received an immediate prosthesis and were advised not to remove it the first 24 hours after surgery.

#### Follow-up

One week after tooth extraction, patients were scheduled for suture removal and the prosthesis was adapted. After three months of healing, a second CBCT (T1) was taken (Figure 3). This second CBCT was also used for the planning of the implant surgery when desired.

#### Sample size calculation

The minimum required sample size was estimated using the results of a previous study comparing L-PRF and unassisted healing for ARP (19). The power sample size was calculated to detect a difference in horizontal bone resorption of 15-20% amongst treatments and control. A power analysis in G\*Power suggested a sample size of 16 participants for a split-mouth design with three groups (L-PRF, A-PRF+, control) assuming 90% power with an  $\alpha$  of 0.05. The sample size was, however, increased to 21 patients due to a potential drop-out during follow-up.

#### CBCT acquisition and radiological analysis

To assess the alterations in the alveolar ridge, CBCT was taken immediately after tooth extraction (T0) and another after a 3 months' interval (T1) using a NewTom VGi evo CBCT (Cefla, Imola, Italy). Clinical scanning protocol was fixed to a 10x10 cm field-of-view, a voxel size of 200  $\mu$ m, 360° rotation, at 110kVp and using tube current modulation, which adapts emission according to the patient and thus eliminates any risk of exposure to an unnecessarily high dose (28) (29).

#### Radiological analysis

Both post-operative CBCT scans were spatially aligned using a rigid computer-assisted registration (MeVisLab, MeVis Medical Solutions AG, Bremen, Germany) based on selected areas of the dataset where no anatomical changes had taken place during follow-up (30) (31). Data from each patient were encoded and all measurements were performed blinded without knowing treatment allocation.

### *2D- Analysis*

The matched post-operative CBCT scans were imported into Fiji software (32) and measurements were performed using the same reference points and lines according to Temmerman and co-workers (19). The following distances were measured from the centre of the socket according to Jung and co-workers (33) and Temmerman and co-workers (19) (Figure 4):

- the thickness of the buccal bone at baseline (T0) at 1, 3, and 5 mm below the crest
- the horizontal ridge width at crest-1mm (HW-1mm), crest-3mm (HW-3mm), and crest-5mm (HW-5mm) at the buccal/palatal side, in millimeters and later transformed to percentages
- the vertical resorption on both buccal and palatal side, in millimeters
- the socket fill defined as the highest point of viewable mineralized bone at the middle of the socket; absolute values (in mm) and percentages were calculated by comparing the initial depth of the socket and the depth after three months of healing

### Biopsy collection

When patients wanted replacement of the missing teeth, implant surgery was planned. During implant surgery, the osteotomy was initially prepared with a 2.0 mm trephine bur which allowed the collection of a bone core biopsy. In the case of an edentulous ridge, a customized stent was prepared from a dental cast before extractions as reference to determine the centre of the initial socket. After collection, the biopsies were immediately frozen in liquid nitrogen and kept at -80°C.

### Micro-CT scanning

Micro-CT scanning of bone biopsies was performed on a SkyScan 1172 high-resolution desktop system (Bruker, Kontich, Belgium). The scan protocol was set at a source voltage of 100 kV, tube current of 100  $\mu$ A, and a filter of 0.5 mm to reduce beam hardening. The frozen samples were put in a vial to prevent them from drying out. This vial was then placed on the rotation stage between source and detector. The magnification was fixed with the camera in the near position with respect to the source, leading to a shorter scan time. The detector was used in the 4x4 binning mode leading to a pixel resolution of 11  $\mu$ m. With an exposure time of 158 ms, a rotation step of 0.7 degrees, a frame averaging of 6 and an acquisition over 180+ degrees, the total scan time was 9 min. The projections were reconstructed using a modified Feldkamp cone-beam algorithm (NRecon) and 2-D cross-section images of the bone samples were obtained. Smoothing of the projection images prior to reconstruction was done with a value of 3. The ring artefacts were reduced with a strength of 7 and the beam hardening correction was set at 30%. The image conversion window was [0.0 - 0.06]. Data from each patient was encoded and all measurements were performed blinded for the treatment allocation.

The 3D bone (micro)structure was evaluated in terms of ratio between bone volume (newly formed bone) and total tissue volume (%BV/TV), trabecular thickness (Tb.Th), trabecular number (Tb.N), and trabecular separation (Th.Sp).

### Histological processing and morphometric analysis

After the micro-CT scanning, bone biopsies were fixed in 4% paraformaldehyde and decalcified in 0.5M EDTA (pH 7.4)/phosphate buffered-saline at 4°C for 14 days, followed by dehydration and embedding in paraffin. Three serial sections (4-µm) were made starting from the central region of the sample and perpendicular towards the long axis, and stained with haematoxylin and eosin for general morphological analysis.

Histological sections were captured by an automated slice scanner (Axioscan, Carl Zeiss, Oberkochen, Germany), matched with the corresponding 2D micro-CT slices, and further processed in CTAn (Bruker). Newly formed bone (quantitative) was automatically determined within the same region of interest for micro-CT and histological coupes and bone volume fraction (%BV/TV) was calculated. A descriptive qualitative analysis completed the histological evaluation. Data from each patient was encoded and all measurements were performed blinded for the treatment allocation.

### Statistical analysis

Treatments were compared by creating a linear mixed model with patient as random factor and treatment as fixed factor was applied. Differences between treatments were corrected for simultaneous hypothesis testing according to Tukey. Descriptive analyses expressed data as mean values with standard deviations. All data were tested for normality using the Shapiro-Wilk test. A second mixed-model was constructed for the histology and micro-CT analysis. Non parametric comparisons between groups (Kruskal-Wallis, pairwise with automatic Bonferroni correction) were used to explore significant interaction effects. Significant differences were noted a  $p < 0.05$ .

## **Results**

### Demographic data

Twenty-one patients were included in this study (15 women, 6 men) (Table S1). Three patients were smokers of <10 cig/day. One patient did not return for the second CBCT after 3 months of healing, so he was excluded from the study (drop-out= 1). All sockets healed uneventfully. A total of 60 teeth in the premaxilla were included for analysis (central incisors: 25, lateral incisors: 16, canines: 19). The CONSORT flow chart is shown in Figure 1. Five out of the 20 included patients asked for teeth replacement with dental implants. Those patients underwent implant surgery and bone samples could be collected from the preserved sites (Table 2). The rest of the participants were provided with a definitive and well-adapted full denture.

### Radiological analysis

#### *Thickness buccal bone*

The mean thickness of the buccal plate at baseline at 1 mm below the crest was  $1.1 \pm 0.3$  mm,  $0.9 \pm 0.3$  mm, and  $1.1 \pm 0.4$  mm for L-PRF, A-PRF+, and control sites, respectively. Overall, no statistically significant differences could be found at any level below the crest amongst groups ( $p > 0.05$ ). Data is shown in Table 3.

#### *Horizontal resorption*

The mean ridge width differences between baseline (immediately after extraction) and three months of healing were measured at three levels below the crest (HW-1 mm, HW-3 mm, and HW-5 mm) on both the buccal and palatal sides (Table 4).

*Buccally:*

No statistically significant differences at any of the levels below the crest (HW-1 mm, HW-3 mm, and HW-5) were found amongst groups ( $p > 0.05$ ). For the L-PRF, A-PRF+, and unassisted sites, the values 1 mm below the crest were  $-1.6 \pm 0.8$  mm,  $-1.6 \pm 0.7$  mm,  $-1.7 \pm 1.0$ , respectively.

*Palatally:*

At the palatal side, a similar horizontal bone resorption was observed for all groups (L-PRF:  $-0.6 \pm 0.7$  mm, A-PRF+:  $-0.6 \pm 0.8$  mm, control:  $0.5 \pm 0.7$  mm). No statistically significant differences at any of the levels below the crest (HW-1 mm, HW-3 mm, and HW-5) were found amongst groups ( $p > 0.05$ ).

*Changes in the total ridge (width)*

The overall mean changes in the width at crest-1 mm were  $-28.1\% \pm 13.5$ ,  $-28.1\% \pm 11.8$ , and  $-26.4\% \pm 12.3$  for L-PRF, A-PRF+, and control, respectively. No statistical significant differences were reached amongst groups ( $p > 0.05$ ) at any level below the crest (Table 5). Bone resorption was less pronounced in all groups towards the apical part (crest-1 mm > crest-3 mm > crest-5 mm).

The fact that one socket had an unassisted socket at one or both sides or an edentulous ridge or a remnant tooth did not influence the alveolar bone resorption. No statistically significant differences could be found between positions ( $p > 0.05$ ).

*Vertical resorption*

The mean vertical height changes at the buccal side were  $0.2 \pm 1.2$  mm,  $0.2 \pm 1.1$  mm, and  $-0.2 \pm 0.8$  mm for L-PRF, A-PRF+, and control, respectively (Table 4). Differences amongst groups were however not statistically significant (L-PRF vs A-PRF+  $p = 0.9$ , tests vs control  $p = 0.3$ ). The mean vertical height changes at the palatal aspect were  $-1.1 \pm 0.9$  mm,  $-1.0 \pm 0.8$  mm, and  $-1.0 \pm 0.9$  mm, for L-PRF sites, A-PRF+ sites, and control sites, respectively. Also here, no statistical differences were reached ( $p = 0.8$ ).

*Socket Fill*

Statistically significant differences were found for the percentage of socket fill between L-PRF ( $85.2\% \pm 22.9$ ) vs. control ( $67.9\% \pm 19.2$ ) ( $p = 0.005$ ), and A-PRF+ ( $83.8\% \pm 18.4$ ) vs. control ( $67.9\% \pm 19.2$ ) ( $p = 0.01$ ) (Table 6).

Morphometrical bone analysis*Histological evaluation*

L-PRF and A-PRF+ presented a mean %BV/TV of  $47.7 \pm 7.9\%$  and  $54.5 \pm 5.6\%$ , respectively (Figure 5). No statistical significant differences could be found between test groups ( $p > 0.05$ ). Both test groups showed statistically significant more %BV/TV than the control group ( $34.7 \pm 6.9\%$ ) ( $p < 0.05$ ).

For the descriptive qualitative analysis of the samples, the main differences between test and control groups were detected at the coronal portion. In the control samples, a zone rich in connective tissue fibres (unmineralized tissue) could be found, compatible with the organic portion of bone matrix that forms prior to the maturation of bone tissue. On the contrary, a mineralized tissue with trabecular pattern was observed in both test groups.

#### *Micro-CT: 2D and 3D analysis*

For the 2D and 3D analysis of %BV/TV, no statistical significant differences could be found between test groups ( $p=0.18$  and  $p=0.71$ , respectively). When compared to the control group, A-PRF+ showed statistical significant higher newly formed bone in both 2D and 3D analysis ( $p<0.001$  and  $p=0.04$ , respectively), whereas the differences between L-PRF and control did not reach the significance ( $p=0.09$  and  $p=0.64$ ) (Figure 6).

#### **Discussion**

The present split-mouth randomized clinical trial analysed the effect of two different platelet concentrates derivatives (L-PRF and A-PRF+) on ridge preservation after tooth extraction in comparison to unassisted socket healing (blood clot). In the CBCT analysis, no statistically significant differences in the horizontal and vertical dimension could be observed amongst the 3 groups after 3 months of healing. However, both PRF matrices showed radiographically on the CBCT measurements a significant superiority for the socket fill. Histologically, PRF matrices seemed to promote higher percentage of newly formed bone in comparison to the control, after a 3-months healing period.

Over the last 20 years, the global burden of complete edentulism has diminished on average. However, in contrast to high-income countries where the prevalence of edentulism is decreasing, an opposite trend is observed in low- and middle-income countries, mainly as the result of increments in periodontal diseases and caries (34, 35). Campbell and co-workers (36) reported that edentulous patients wearing dentures had, on average, smaller residual ridges than those not wearing dentures. Increased ridge resorption was attributed to the pressure from the prostheses. Similar conclusions had been stated in the literature (37, 38).

The fact that in this study the resorption of both the buccal and palatal side barely differed amongst groups, and that the vertical bone resorption at the palatal side was more extensive than at the buccal side led us to hypothesize that the use of the full prostheses may have act as a co-founding factor, masking the effect of the platelet rich fibrin (PRF) matrices. Recently it has been hypothesized that L-PRF membranes might have the capacity to suppress the catabolic events that are caused by osteoclastic bone resorption, but that they cannot reverse the process once osteoclastogenesis has started (39, 40). After tooth extraction, osteoclasts start to resorb the bundle bone (2, 41). Osteoclastic activity can be intensified by different factors such as mechanical pressure. In the present study, all patients enrolled were provided with a full immediate removable prosthesis. Mechanical pressure transmitted continuously and/or intermittently through the prosthesis has been considered one of the causative factors for bone resorption in denture-supporting tissues (42, 43). Moreover, Alrajhi and co-workers (44) concluded that anterior maxillary areas had higher bone loss compared to posterior areas. One needs to keep in mind that this is a common protocol in daily practice after multiple tooth extractions. Consequently, ARP techniques in multiple tooth extractions when a mucosa-supported prosthesis is also used might not have the same results as in single tooth extractions. However, the evidence around the bone resorption pattern after multiple tooth extraction is scarce, what makes the comparison of our results with others, at this moment, not possible.

In single tooth extraction studies where no provisional mucosa-supported prostheses were provided, the use of PRF matrices showed promising results in the preservation of the alveolar ridge (45, 46). Temmerman and co-workers (19) reported a mean change in horizontal dimension at 1 mm below the crest of 1.4 mm (23%) and 5.0 mm (51%) for L-PRF group and control group, respectively. A recent study (47) showed a mean change in width at 1 mm below the crest of 0.9 mm and 2.2 mm for



L-PRF group and control group, respectively. Similar benefits have been reported in the literature (48-51). However, the outcome seems to be very technique-sensitive (52, 53).

Another hypothesis that might contribute to explain the findings of this article is related to the resistance of the L-PRF membranes to external forces and their stability under certain conditions. Angiogenesis is a delicate process driven by surrounding tissue's need for oxygen and nutrients, which incites production of vascular endothelial growth factor (VEGF), fibroblast growth factors (FGFs), and other pro-angiogenic stimuli (54). Recently, Ratajczak and co-workers (21) described the angiogenic potential of L-PRF in an in-vitro study by inducing key steps of the angiogenic process such as endothelial proliferation, migration, and tube formation. They also demonstrated that L-PRF was able to induce blood vessel formation in vivo with a chorioallantoic membrane assay. However, all these processes require wound stability to allow vessel sprouting to occur (55). In the present study, the use of an immediate prosthesis may have also jeopardized the angiogenic capacity of the L-PRF and A-PRF+ by decreasing their stability inside the socket.

Hard and soft tissue alterations after tooth extraction have been well documented by Cardaropoli and co-workers (1). Healing of an extraction socket was characterized by a sequence of histological events, where the buccal bone was more extensively resorbed than the palatal/lingual plate (2). This can be explained by the fact that the vestibular bone plates are generally thinner (56). In the present study, there were no differences in width of the buccal bony plates amongst test and control groups and they were in average around 1 mm thick for all groups. Given the mean values reported in literature for the aesthetic zone ( $0.8 \pm 0.4$  mm) (57), we can consider that the buccal bone plates in our study were rather thick.

Socket fill was found to statistically differ between both PRF matrices and the control group in this present study (L-PRF: 85%, A-PRF+: 83%, control: 67%). Similarly, the qualitative histological analysis also showed the lack of mineralized tissue at the coronal part of the pre-existing socket in the control group. These results are similar from those already reported in the literature for single tooth extractions (19, 50). So despite the limited effect on the horizontal dimension, the use of both L-PRF and A-PRF+ seemed to partially counteract bone resorption in the vertical dimension (mean bone gain of 0.2 mm) and showed radiographically significant greater socket fill in comparison to the control. Both parameters are crucial when considering the replacement of the missing tooth by an oral implant.

The biological characteristics of L-PRF and A-PRF+ have been extensively evaluated in vitro studies (27, 58, 59). The A-PRF+ protocol reduced the g force and the duration of the centrifugation. Some studies have reported an increase in growth factors release from A-PRF+ clots as well as a more homogenous cellular distribution throughout the membranes (El Bagdadi et al., 2017, Ghanaati et al., 2014). However, no differences could be found in the present study between L-PRF and A-PRF+ groups. It is of utmost importance to understand the properties of the biomaterials that are currently used in the clinical setting. However, it should be stressed that anatomical, functional and host factors may have a strong influence in bone resorption/regeneration patterns. Therefore, care should be taken when extrapolating in vitro results to the clinical practice.

In bone structural analysis, the present study showed more newly formed bone for both L-PRF and A-PRF+ (around 50%) compared to the control group. Nevertheless, these results need to be interpreted with caution given the limited sample size ( $n=5$ ). Even when the sample size is small, a significant difference indicates a true difference (with a minor error rate). However, the non-significant difference between the two test treatments does not assure that this difference does not exist. In order to detect a significant difference between 54.5% (A-PRF+) and 47.7% (L-PRF) with the observed variability, 22 subjects should have been included in each group for a power of 80%. However, the patients in this

study were not obliged to undergo implant surgery, otherwise it might be considered ethically questionable.

Limited evidence is reported in the literature on the qualitative/quantitative histological and radiological analysis after the use of these biomaterials in ARP techniques. For instance, Canellas and co-workers published higher values of %BV/TV for L-PRF compared to a control (L-PRF:  $55.9 \pm 11.9\%$ , control:  $36.7 \pm 11.1\%$ ) in a histomorphometrical analysis (47). They reported similar percentages in terms of newly formed bone as the ones presented in the current study. On a radiological analysis with micro-CT, Hauser and co-workers (2013) (48) also observed a tendency for higher value %BV/TV in the L-PRF group (+12.9%) compared to the control. Analysis of the trabecular morphology also revealed the superiority of L-PRF versus the control group, although in that study trabecular thickness did not reach statistical significance.

Clinicians should be aware of the limitations in the present study when using PRF matrices in multiple tooth extractions with an immediate denture. However, up to now there is no evidence about the use of PRF matrices in multiple extractions without the mechanical influence of a dental prosthesis. Moreover, one does not have to forget the trauma and post-operative pain after multiple tooth extractions. The use of L-PRF may reduce patient's discomfort and fasten soft tissue healing (20, 60). Moreover, the present study envisaged the possible acceleration of bone healing in the coronal part three months after tooth extraction by using PRF matrices. Further research is needed to confirm this hypothesis.

### **Conclusions**

Within the limitations of this study, it can be concluded that PRF matrices used for ARP failed to counteract ridge resorption that occurs after multiple extractions in the anterior maxilla after 3 months of healing. However, both PRF matrices showed radiographically a significant superiority for the socket fill compared to an unassisted socket. Histologically, they seemed to accelerate new bone formation. ARP techniques in multiple tooth extractions with the use of immediately mucosa-supported prosthesis might jeopardize the final result.

### **Acknowledgments**

We would like to acknowledge Mrs. Evelyne Van Kerckhove and Dr. Tim Vangansewinkel (Hasselt University, Belgium) for their help during the histological progressing and analysis. In addition, we would like to thank Dr. Wim Coucke for his help in the statistical analysis.



## Figures

Figure 1. CONSORT flow diagram of the progress of the study (randomized controlled clinical trial). n= number of patients.

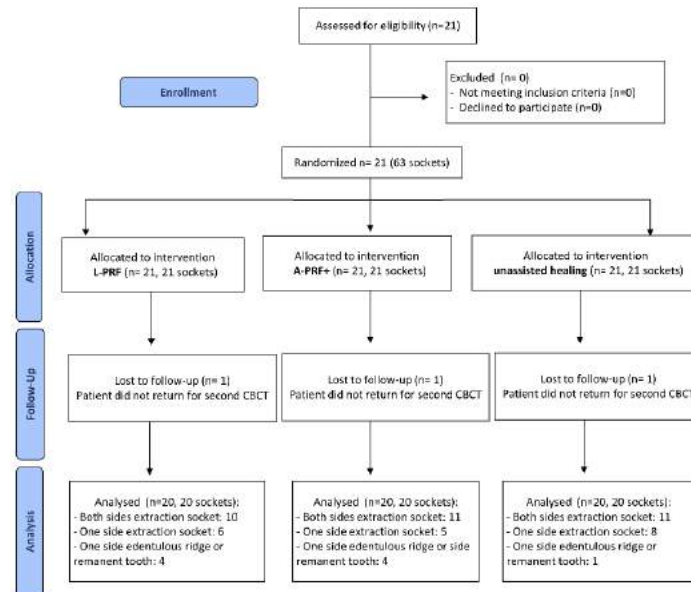


Figure 2. Surgical procedure for ridge preservation. Occlusal view of the upper jaw after tooth extraction (A) L-PRF clots (B1) and A-PRF+ clots (B2) before compression into membranes. Envelope preparation for socket sealing by insertion of the L-PRF (C1) and A-PRF+ (C2) membranes. Placement of the L-PRF membranes (D1) and A-PRF membranes (D2) into the sockets. Modified horizontal mattress suture to keep the L-PRF (E1) and A-PRF+ (E2) membranes in place without intention of primary closure.

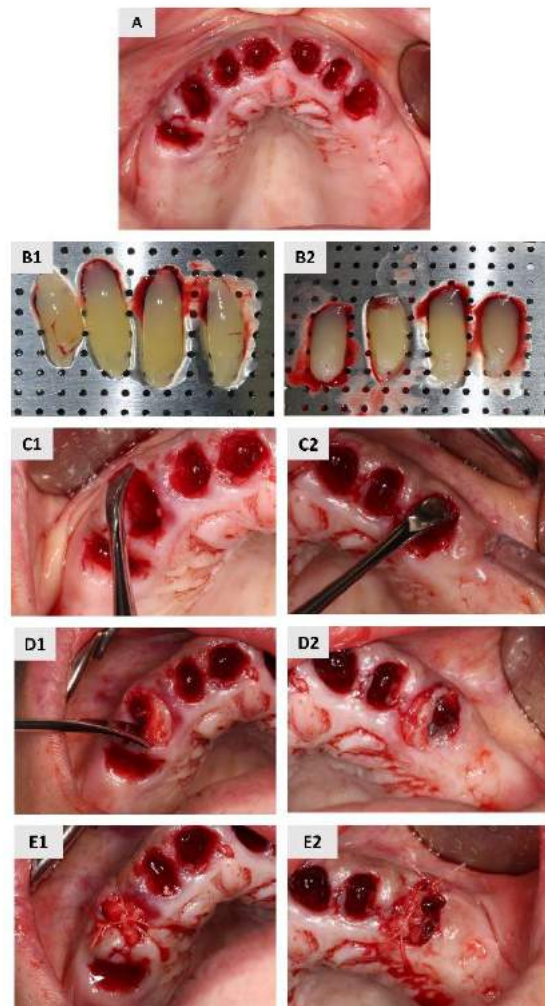


Figure 3. Representative cone-beam computed tomography of one patient at baseline (immediately after tooth extraction, T0) and after 3 months of healing (T1). (A1): CBCT T0 L-PRF group, (A2): CBCT T1 L-PRF group, (B1): CBCT T0 A-PRF+ group, (B2): CBCT T1 A-PRF+ group, (C1): CBCT T0 control group, (C2): CBCT T1 control group.

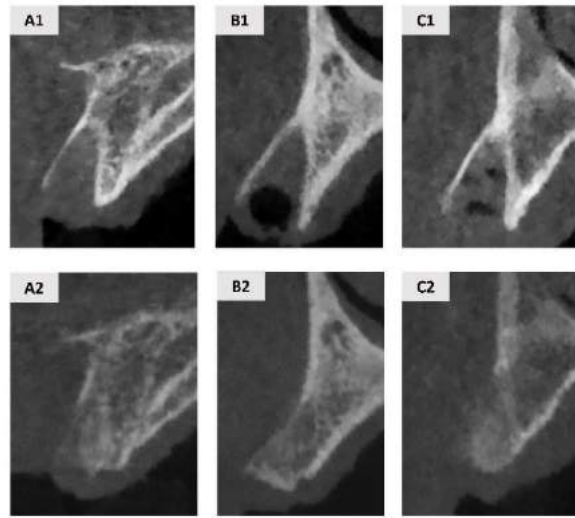


Figure 4. Linear measurements of the sockets. (A) The middle of the socket was determined at the axial view of the CBCT (T0) based on the width of each socket. A 90° line was drawn in the middle of the socket defining the cross sectional slide where the rest of the measurements were executed. (B) Cross-sectional view of a socket after tooth extraction. The apex of the extraction socket at T0 was marked, and a vertical reference line passing the apex in the centre of the socket was also drawn. Perpendicular to the vertical reference, a horizontal reference line was defined at the level of the crest, buccal HW-1 mm, HW-3 mm, HW-5 mm are representing the measurements performed at three levels below the bone crest. The depth of the socket was measured as the deepest point of the socket to the bone crest. (C1) Measurement of the initial socket depth at the middle of the socket (vertical yellow line), perpendicular to the crest. (C2) Final socket depth by measuring the distance between the bone crest and the highest bone level at the middle of the socket (blue dotted line). Socket fill is calculated by comparing the initial depth of the socket and the depth after three months of healing.

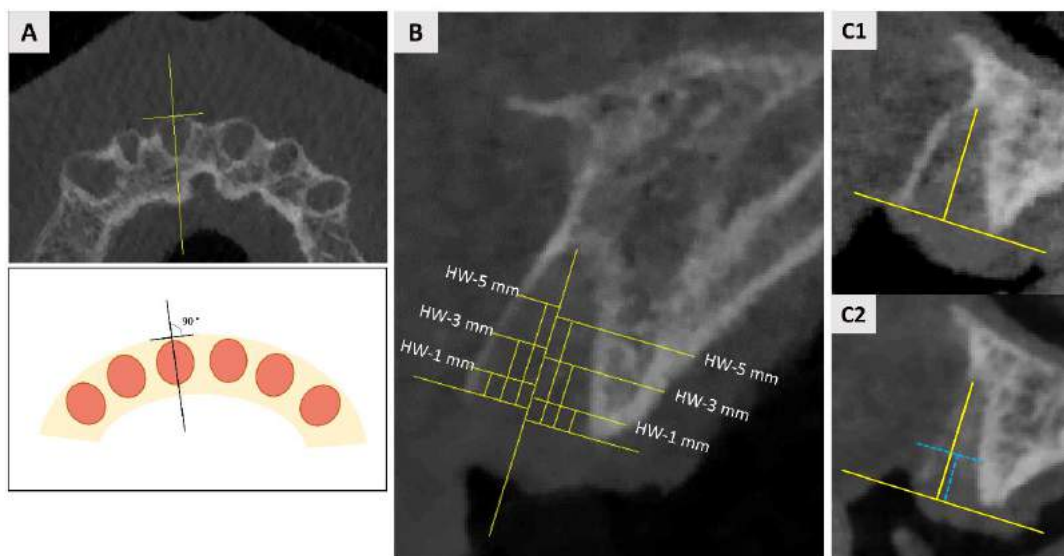


Figure 5. Histological and micro-CT 2D analysis of the bone samples. (A) L-PRF group; (B) A-PRF+ group; (C) control group, and (D) summary of results. (1) haematoxylin and eosin staining overview, (2) segmentation of bone (green) vs. soft tissue (blue), (3) micro-CT reconstruction. *sd*: standard deviation.

D	L-PRF			A-PRF+			Control		
	mean	median	<i>sd</i>	mean	median	<i>sd</i>	mean	median	<i>sd</i>
BV/TV(%)	47.7	47.0	7.9	54.5	56.7	5.6	34.7	30.0	6.9
D	L-PRF			A-PRF+			Control		
	mean	median	<i>sd</i>	mean	median	<i>sd</i>	mean	median	<i>sd</i>
BV/TV(%)	43.4	43.8	8.7	50.7	51.0	4.5	35.0	35.5	8.2

Figure 6. Micro-CT 3-D analysis of the bone samples. (A) L-PRF group; (B) A-PRF+ group; (C) control group (unassisted healing), and (D) summary of results. In the 3D reconstructions from the micro-CT, soft tissue is colored in blue, and bone in green. Tb.Th: Trabecular thickness, Tb.N: trabecular number, and Th.Sp: trabecular separation.

D	L-PRF			A-PRF+			Control		
	mean	median	<i>sd</i>	mean	median	<i>sd</i>	mean	median	<i>sd</i>
BV/TV(%)	46.6	46.9	4.6	51.8	54.4	6.9	28.3	27.2	10.2
Tb.Th (mm)	0.3	0.3	0.1	0.2	0.2	0.04	0.1	0.2	0.07
Tb.N (mm)	1.8	1.7	1.2	2.3	2.2	0.4	1.3	1.8	0.5
Tb.Sp (mm)	0.4	0.3	0.1	0.3	0.3	0.08	0.6	0.6	0.5

## Tables

Table 1. Demographic data and inclusion and exclusion criteria. ASA-score: American Society of Anesthesiologist (ASA)-score. CI: central incisor, LI: lateral incisor, C: canine. Extracted teeth in () after drop-out.

Patient demographics	
Age (years) mean $\pm$ sd	64.4 $\pm$ 12.0
Male/Female	6 / 15
Number extracted teeth	CI: 26 (25) , LI: 16, C: 21 (19)
L-PRF	CI: 8 (7), LI: 5, C: 8
A-PRF+	CI: 9, LI: 4, C: 8 (7)
Control	CI: 9, LI: 7, C: 5 (4)
Inclusion criteria	Exclusion criteria
ASA-score 1 or 2	any systemic condition that could interfere with surgical procedure
at least three teeth needed to be extracted in the anterior region (canine to canine)	any systemic condition that could interfere with surgical procedure, (2) immunosuppression, anticoagulation or platelet antiaggregation therapy
age between 18-80 years old	pregnancy or breast-feeding
	radiotherapy or chemotherapy in head and neck area
	intravenous or oral bisphosphonate therapy
	patients smoking > 10 cigarettes a day

Table 2. Distribution of implant placement and biopsy collection. The locations where an implant was placed in the same position of a preserved socket are marked in bold. Pat: patient, GBR: guided bone regeneration.

	Number of implants	Implant location	Sockets location	GBR?	Biopsy location	Type of replacement
Pat 1	4	13, 15, <b>23</b> , 25	<b>13</b> , <b>23</b> , 11	no	13, 23, 11	overdenture
Pat 2	4	<b>13</b> , 16, 21, 26	11, <b>13</b> , 22	no	11, 13, 22	overdenture
Pat 3	6	12, 14, 16, <b>22</b> , 24, 26	11, 13, <b>22</b>	no	11, 13, 22	fixed bridge
Pat 4	4	12, 14, <b>22</b> , 24	11, 13, <b>22</b>	no	11, 13, 22	overdenture
Pat 5	6	<b>11</b> , 14, 16, 21, 24, 26	<b>11</b> , 13, 22	no	11, 13, 22	fixed bridge

Table 3. Baseline radiographic measurements of the thickness of the buccal bone plate. *sd*: standard deviation. No statistically significant differences were computed amongst groups ( $p > 0.05$ ).

	L-PRF				A-PRF+				Control			
	mean	median	<i>sd</i>	range	mean	median	<i>sd</i>	range	mean	median	<i>sd</i>	range
crest-1 mm	1.1	1.0	0.3	(0.7-1.8)	1.1	0.9	0.3	(0.5-1.3)	1.1	0.9	0.4	(0.5-2.2)
crest-3 mm	1.1	1.2	0.3	(0.6-1.7)	1.0	1.0	0.2	(0.6-1.4)	1.0	1.0	0.4	(0.6-1.7)
crest-5 mm	1.1	1.2	0.4	(0.4-1.8)	1.0	0.9	0.3	(0.6-1.7)	1.0	0.9	0.6	(0.3-3.1)

Table 4. Dimensional changes at the buccal and palatal site after three months of healing for L-PRF group, A-PRF+ group, and control group. Horizontal width reduction measured at 1 mm (HW-1 mm), 3 mm (HW-3 mm), and 5 mm (HW-5 mm) below the crest. Vertical changes measured in the middle of the extraction socket both buccally and palatally. *sd*: standard deviation. Values are shown in millimeters.

	L-PRF			A-PRF+			Control		
Buccal									
	mean	median	sd	mean	median	sd	mean	median	sd
HW-1 mm	-1.6	-1.5	0.8	-1.6	-1.5	0.7	-1.7	-1.6	1.0
HW-3 mm	-1.5	-1.4	0.8	-1.2	-1.1	0.6	-1.4	-1.5	0.8
HW-5 mm	-1.0	-1.0	0.7	-0.9	-0.8	0.6	-1.0	-1.0	0.6
Vertical	0.2	0.3	1.2	0.2	0.1	1.1	-0.2	-0.2	0.8
Palatal									
	mean	median	sd	mean	median	sd	mean	median	sd
HW-1 mm	-0.6	-0.5	0.7	-0.6	-0.3	0.8	-0.5	-0.3	0.7
HW-3 mm	-0.4	-0.4	0.4	-0.4	-0.2	0.7	-0.3	-0.2	0.4
HW-5 mm	-0.2	0.0	0.4	-0.3	0.0	0.6	-0.4	-0.1	0.6
Vertical	-1.1	-0.9	0.9	-1.0	-1.0	0.8	-1.0	-0.9	0.9

Table 5. Total horizontal width (HW) reduction for L-PRF group, A-PRF+ group, and control group. Measurements performed at 1 mm, 3 mm, and 5 mm below the crest. Values are shown in millimeters (mm) and in percentages (%). HW-1mm: horizontal width reduction at 1 mm below the crest; HW-3mm: horizontal width reduction at 3 mm below the crest; HW-5mm: horizontal width reduction at 5 mm below the crest; *sd*: standard deviation.

	L-PRF		A-PRF+		CONTROL	
Millimeters (mm)						
	mean	<i>sd</i>	mean	<i>sd</i>	mean	<i>sd</i>
HW-1 mm	-2.2	1.0	-2.2	0.9	-2.2	1.1
HW-3 mm	-1.8	-1.7	-1.6	0.9	-1.7	0.8
HW-5 mm	-1.2	0.8	-1.2	0.8	-1.4	0.8
Percentage %						
	mean	<i>sd</i>	mean	<i>sd</i>	mean	<i>sd</i>
HW-1 mm	-28.1	13.5	-28.1	11.8	-26.4	12.3
HW-3 mm	-22.2	9.7	-19.4	10.1	-20.8	9.0
HW-5 mm	-14.4	10.1	-14.6	9.6	-16.3	8.1

Table 6. Socket fill measurements in L-PRF group, A-PRF+ group, and control group. Values are shown in millimeters (mm) and in percentages (%). \*: statistically significant; *sd*: standard deviation.

	L-PRF			A-PRF+			Control			<b>p-values</b>		
	mean	median	<i>sd</i>	mean	median	<i>sd</i>	mean	median	<i>sd</i>	L-PRF vs. A-PRF+	L-PRF vs. control	A-PRF+ vs. control
<b>Socket fill (%)</b>	85.2	86.5	22.9	83.8	88.9	18.4	67.9	71.8	19.2	0.9	<0.005	0.01
<b>Socket fill (mm)</b>	7.0	6.7	3.0	7.0	6.6	2.7	5.4	5.1	2.3	0.9	<0.05	<0.05

## References

1. Cardaropoli G, Araujo M, Lindhe J. Dynamics of bone tissue formation in tooth extraction sites. An experimental study in dogs. *J Clin Periodontol*. 2003;30(9):809-18.
2. Araujo MG, Lindhe J. Dimensional ridge alterations following tooth extraction. An experimental study in the dog. *J Clin Periodontol*. 2005;32(2):212-8.
3. Schropp L, Wenzel A, Kostopoulos L, Karring T. Bone healing and soft tissue contour changes following single-tooth extraction: a clinical and radiographic 12-month prospective study. *Int J Periodontics Restorative Dent*. 2003;23(4):313-23.
4. Couso-Queiruga E, Stuhr S, Tattan M, Chambrone L, Avila-Ortiz G. Post-extraction dimensional changes: A systematic review and meta-analysis. *J Clin Periodontol*. 2021;48(1):126-44.
5. García-González A, Galve-Huertas A, Aboul-Hosn Centenero S, Mareque-Bueno S, Satorres-Nieto M, Hernández-Alfaro F. Volumetric changes in alveolar ridge preservation with a compromised buccal wall: a systematic review and meta-analysis. *Med Oral Patol Oral Cir Bucal*. 2020;25(5):e565-e75.
6. Vignoletti F, Matesanz P, Rodrigo D, Figuero E, Martin C, Sanz M. Surgical protocols for ridge preservation after tooth extraction. A systematic review. *Clin Oral Implants Res*. 2012;23 Suppl 5:22-38.
7. Troiano G, Zhurakivska K, Lo Muzio L, Laino L, Cicciù M, Lo Russo L. Combination of bone graft and resorbable membrane for alveolar ridge preservation: A systematic review, meta-analysis, and trial sequential analysis. *J Periodontol*. 2018;89(1):46-57.
8. Barootchi S, Wang HL, Ravida A, Ben Amor F, Riccitiello F, Rengo C, et al. Ridge preservation techniques to avoid invasive bone reconstruction: A systematic review and meta-analysis: Naples Consensus Report Working Group C. *Int J Oral Implantol (Berl)*. 2019;12(4):399-416.
9. Chappuis V, Araujo MG, Buser D. Clinical relevance of dimensional bone and soft tissue alterations post-extraction in esthetic sites. *Periodontol 2000*. 2017;73(1):73-83.
10. Vignoletti F, Sanz M. Immediate implants at fresh extraction sockets: from myth to reality. *Periodontol 2000*. 2014;66(1):132-52.
11. Discepoli N, Vignoletti F, Laino L, de Sanctis M, Munoz F, Sanz M. Fresh extraction socket: spontaneous healing vs. immediate implant placement. *Clin Oral Implants Res*. 2015;26(11):1250-5.
12. Botticelli D, Berglundh T, Lindhe J. Hard-tissue alterations following immediate implant placement in extraction sites. *J Clin Periodontol*. 2004;31(10):820-8.
13. Barone A, Toti P, Quaranta A, Alfonsi F, Cucchi A, Negri B, et al. Clinical and Histological changes after ridge preservation with two xenografts: preliminary results from a multicentre randomized controlled clinical trial. *J Clin Periodontol*. 2017;44(2):204-14.
14. Iorio-Siciliano V, Ramaglia L, Blasi A, Bucci P, Nuzzolo P, Riccitiello F, et al. Dimensional changes following alveolar ridge preservation in the posterior area using bovine-derived xenografts and collagen membrane compared to spontaneous healing: a 6-month randomized controlled clinical trial. *Clin Oral Investig*. 2020;24(2):1013-23.
15. Avila-Ortiz G, Chambrone L, Vignoletti F. Effect of alveolar ridge preservation interventions following tooth extraction: A systematic review and meta-analysis. *J Clin Periodontol*. 2019;46 Suppl 21:195-223.
16. Dohan DM, Choukroun J, Diss A, Dohan SL, Dohan AJ, Mouhyi J, et al. Platelet-rich fibrin (PRF): a second-generation platelet concentrate. Part I: technological concepts and evolution. *Oral Surg Oral Med Oral Pathol Oral Radiol Endod*. 2006;101(3):e37-44.



17. Hachim D, Whittaker TE, Kim H, Stevens MM. Glycosaminoglycan-based biomaterials for growth factor and cytokine delivery: Making the right choices. *J Control Release*. 2019;313:131-47.
18. Castro AB, Cortellini S, Temmerman A, Li X, Pinto N, Teughels W, et al. Characterization of the Leukocyte- and Platelet-Rich Fibrin Block: Release of Growth Factors, Cellular Content, and Structure. *Int J Oral Maxillofac Implants*. 2019;34(4):855-64.
19. Temmerman A, Vandessel J, Castro A, Jacobs R, Teughels W, Pinto N, et al. The use of leucocyte and platelet-rich fibrin in socket management and ridge preservation: a split-mouth, randomized, controlled clinical trial. *J Clin Periodontol*. 2016;43(11):990-9.
20. Dragonas P, Katsaros T, Avila-Ortiz G, Chambrone L, Schiavo JH, Palaiologou A. Effects of leukocyte-platelet-rich fibrin (L-PRF) in different intraoral bone grafting procedures: a systematic review. *Int J Oral Maxillofac Surg*. 2019;48(2):250-62.
21. Ratajczak J, Vangansewinkel T, Gervois P, Merckx G, Hilken P, Quirynen M, et al. Angiogenic Properties of 'Leukocyte- and Platelet-Rich Fibrin'. *Sci Rep*. 2018;8(1):14632.
22. Dohan Ehrenfest DM, Doglioli P, de Peppo GM, Del Corso M, Charrier JB. Choukroun's platelet-rich fibrin (PRF) stimulates in vitro proliferation and differentiation of human oral bone mesenchymal stem cell in a dose-dependent way. *Arch Oral Biol*. 2010;55(3):185-94.
23. Schär MO, Diaz-Romero J, Kohl S, Zumstein MA, Nesic D. Platelet-rich concentrates differentially release growth factors and induce cell migration in vitro. *Clin Orthop Relat Res*. 2015;473(5):1635-43.
24. El Bagdadi K, Kubesch A, Yu X, Al-Maawi S, Orlowska A, Dias A, et al. Reduction of relative centrifugal forces increases growth factor release within solid platelet-rich-fibrin (PRF)-based matrices: a proof of concept of LSCC (low speed centrifugation concept). *Eur J Trauma Emerg Surg*. 2017.
25. Ghanaati S, Booms P, Orlowska A, Kubesch A, Lorenz J, Rutkowski J, et al. Advanced platelet-rich fibrin: a new concept for cell-based tissue engineering by means of inflammatory cells. *J Oral Implantol*. 2014;40(6):679-89.
26. Moher D, Hopewell S, Schulz KF, Montori V, Gotzsche PC, Devereaux PJ, et al. CONSORT 2010 explanation and elaboration: updated guidelines for reporting parallel group randomised trials. *Int J Surg*. 2012;10(1):28-55.
27. Fujioka-Kobayashi M, Miron RJ, Hernandez M, Kandam U, Zhang Y, Choukroun J. Optimized Platelet-Rich Fibrin With the Low-Speed Concept: Growth Factor Release, Biocompatibility, and Cellular Response. *J Periodontol*. 2017;88(1):112-21.
28. Stratis A, Zhang G, Lopez-Rendon X, Politis C, Hermans R, Jacobs R, et al. Two examples of indication specific radiation dose calculations in dental CBCT and Multidetector CT scanners. *Phys Med*. 2017;41:71-7.
29. Stratis A, Zhang G, Jacobs R, Bogaerts R, Bosmans H. The growing concern of radiation dose in paediatric dental and maxillofacial CBCT: an easy guide for daily practice. *Eur Radiol*. 2019;29(12):7009-18.
30. Van Dessel J, Nicolielo LF, Huang Y, Slagmolen P, Politis C, Lambrichts I, et al. Quantification of bone quality using different cone beam computed tomography devices: Accuracy assessment for edentulous human mandibles. *Eur J Oral Implantol*. 2016;9(4):411-24.
31. Van Dessel J, Nicolielo LF, Huang Y, Coudyzer W, Salmon B, Lambrichts I, et al. Accuracy and reliability of different cone beam computed tomography (CBCT) devices for structural analysis of alveolar bone in comparison with multislice CT and micro-CT. *Eur J Oral Implantol*. 2017;10(1):95-105.
32. Schindelin J, Arganda-Carreras I, Frise E, Kaynig V, Longair M, Pietzsch T, et al. Fiji: an open-source platform for biological-image analysis. *Nat Methods*. 2012;9(7):676-82.

33. Jung RE, Philipp A, Annen BM, Signorelli L, Thoma DS, Hammerle CH, et al. Radiographic evaluation of different techniques for ridge preservation after tooth extraction: a randomized controlled clinical trial. *J Clin Periodontol*. 2013;40(1):90-8.
34. Kassebaum NJ, Bernabé E, Dahiya M, Bhandari B, Murray CJ, Marcenes W. Global Burden of Severe Tooth Loss: A Systematic Review and Meta-analysis. *J Dent Res*. 2014;93(7 Suppl):20s-8s.
35. Tyrovolas S, Koyanagi A, Panagiotakos DB, Haro JM, Kassebaum NJ, Chrepa V, et al. Population prevalence of edentulism and its association with depression and self-rated health. *Sci Rep*. 2016;6:37083.
36. Campbell RL. A comparative study of the resorption of the alveolar ridges in denture-wearers and non-denture-wearers. *J Am Dent Assoc*. 1960;60:143-53.
37. Wyatt CC. The effect of prosthodontic treatment on alveolar bone loss: a review of the literature. *J Prosthet Dent*. 1998;80(3):362-6.
38. Ozan O, Orhan K, Aksoy S, Icen M, Bilecenoglu B, Sakul BU. The effect of removable partial dentures on alveolar bone resorption: a retrospective study with cone-beam computed tomography. *J Prosthodont*. 2013;22(1):42-8.
39. Kargarpour Z, Nasirzade J, Strauss FJ, Di Summa F, Hasannia S, Müller HD, et al. Platelet-rich fibrin suppresses in vitro osteoclastogenesis. *J Periodontol*. 2020;91(3):413-21.
40. Strauss FJ, Nasirzade J, Kargarpour Z, Stähli A, Gruber R. Effect of platelet-rich fibrin on cell proliferation, migration, differentiation, inflammation, and osteoclastogenesis: a systematic review of in vitro studies. *Clin Oral Investig*. 2020;24(2):569-84.
41. Trombelli L, Farina R, Marzola A, Bozzi L, Liljenberg B, Lindhe J. Modeling and remodeling of human extraction sockets. *J Clin Periodontol*. 2008;35(7):630-9.
42. Sato T, Hara T, Mori S, Shirai H, Minagi S. Threshold for bone resorption induced by continuous and intermittent pressure in the rat hard palate. *J Dent Res*. 1998;77(2):387-92.
43. Lytle RB. Complete denture construction based on a study of the deformation of the underlying soft tissues. *J Prosthet Dent*. 1959;9(4):539-51.
44. Alrajhi MS, Askar O, Habib AA, Elsyad MA. Maxillary Bone Resorption with Conventional Dentures and Four-Implant-Supported Fixed Prosthesis Opposed by Distal-Extension Partial Dentures: A Preliminary 5-year Retrospective Study. *Int J Oral Maxillofac Implants*. 2020;35(4):816-23.
45. Castro AB, Meschi N, Temmerman A, Pinto N, Lambrechts P, Teughels W, et al. Regenerative potential of leucocyte- and platelet-rich fibrin. Part B: sinus floor elevation, alveolar ridge preservation and implant therapy. A systematic review. *J Clin Periodontol*. 2017;44(2):225-34.
46. Strauss FJ, Stähli A, Gruber R. The use of platelet-rich fibrin to enhance the outcomes of implant therapy: A systematic review. *Clin Oral Implants Res*. 2018;29 Suppl 18(Suppl Suppl 18):6-19.
47. Canellas J, da Costa RC, Breves RC, de Oliveira GP, Figueredo C, Fischer RG, et al. Tomographic and histomorphometric evaluation of socket healing after tooth extraction using leukocyte- and platelet-rich fibrin: A randomized, single-blind, controlled clinical trial. *J Craniomaxillofac Surg*. 2020;48(1):24-32.
48. Hauser F, Gaydarov N, Badoud I, Vazquez L, Bernard JP, Ammann P. Clinical and histological evaluation of postextraction platelet-rich fibrin socket filling: a prospective randomized controlled study. *Implant Dent*. 2013;22(3):295-303.
49. Anwandter A, Bohmann S, Nally M, Castro AB, Quirynen M, Pinto N. Dimensional changes of the post extraction alveolar ridge, preserved with Leukocyte- and Platelet Rich Fibrin: A clinical pilot study. *J Dent*. 2016;52:23-9.



50. Alzahrani AA, Murriky A, Shafik S. Influence of platelet rich fibrin on post-extraction socket healing: A clinical and radiographic study. *Saudi Dent J.* 2017;29(4):149-55.
51. Zhang Y, Ruan Z, Shen M, Tan L, Huang W, Wang L, et al. Clinical effect of platelet-rich fibrin on the preservation of the alveolar ridge following tooth extraction. *Exp Ther Med.* 2018;15(3):2277-86.
52. Areewong K, Chantaramungkorn M, Khongkhunthian P. Platelet-rich fibrin to preserve alveolar bone sockets following tooth extraction: A randomized controlled trial. *Clin Implant Dent Relat Res.* 2019;21(6):1156-63.
53. Suttapreyasri S, Leepong N. Influence of platelet-rich fibrin on alveolar ridge preservation. *J Craniofac Surg.* 2013;24(4):1088-94.
54. Eelen G, de Zeeuw P, Treps L, Harjes U, Wong BW, Carmeliet P. Endothelial Cell Metabolism. *Physiol Rev.* 2018;98(1):3-58.
55. Ghiasi MS, Chen J, Vaziri A, Rodriguez EK, Nazarian A. Bone fracture healing in mechanobiological modeling: A review of principles and methods. *Bone Rep.* 2017;6:87-100.
56. Araújo MG, Silva CO, Misawa M, Sukekava F. Alveolar socket healing: what can we learn? *Periodontol 2000.* 2015;68(1):122-34.
57. Huynh-Ba G, Pjetursson BE, Sanz M, Cecchinato D, Ferrus J, Lindhe J, et al. Analysis of the socket bone wall dimensions in the upper maxilla in relation to immediate implant placement. *Clin Oral Implants Res.* 2010;21(1):37-42.
58. Pitzurra L, Jansen IDC, de Vries TJ, Hoogenkamp MA, Loos BG. Effects of L-PRF and A-PRF+ on periodontal fibroblasts in in vitro wound healing experiments. *J Periodontal Res.* 2020;55(2):287-95.
59. Dohan Ehrenfest DM, Pinto NR, Pereda A, Jimenez P, Corso MD, Kang BS, et al. The impact of the centrifuge characteristics and centrifugation protocols on the cells, growth factors, and fibrin architecture of a leukocyte- and platelet-rich fibrin (L-PRF) clot and membrane. *Platelets.* 2018;29(2):171-84.
60. de Almeida Barros Mourão CF, de Mello-Machado RC, Javid K, Moraschini V. The use of leukocyte- and platelet-rich fibrin in the management of soft tissue healing and pain in post-extraction sockets: A randomized clinical trial. *J Craniomaxillofac Surg.* 2020;48(4):452-7.

# GENERAL DISCUSSION AND FUTURE PERSPECTIVES





# GENERAL DISCUSSION

## 1. Benefits of L-PRF in periodontal surgery: review of the literature

The objective of this PhD thesis was to characterize different PRF matrices and to examine their regenerative potential in several oral surgical procedures. One of the objectives was achieved by systematically reviewing the literature. Section 1, with **chapters 1 and 2**, evaluated the clinical applications of L-PRF via two different systematic reviews. The first one, entitled “**Regenerative potential of leucocyte- and platelet-rich fibrin. Part A: intra-bony defects, furcation defects and periodontal plastic surgery. A systematic review and meta-analysis**” (1), thoroughly revised the evidence on the use of L-PRF in the regeneration of periodontal tissues. In this case, a meta-analysis could be performed. Superior clinical outcomes in terms of pocket depth reduction (PD), clinical attachment (CAL) gain and bone fill were observed for L-PRF when compared to open flap debridement in the treatment of infrabony defects and furcation defects. Similar conclusion have been drawn by a recent systematic review (2021) (2) where the use of PRF in conjunction with OFD statistically significantly improved PD, CAL, and bone fill, yielding to comparable outcomes to OFD + bone graft. The introduction of minimally invasive techniques for the treatment of infrabony defects led to a change in the surgical approach, giving more importance to the surgical technique than to the biomaterial used (3). At this moment, there are no clinical studies evaluating the use of L-PRF in combination with the most evidence based minimally invasive techniques (M-MIST, MIST, entire papilla preservation technique...). Further research will be of utmost importance to assess the application of L-PRF in contemporary surgical techniques.

In mucogingival surgery, the addition of L-PRF to a coronal advanced flap (CAF) did not provide better clinical results (PD reduction, CAL gain, root coverage, keratinized tissue width (KTW) gain or tissue thickness). However, when L-PRF was compared to a connective tissue graft, similar outcomes were recorded. These results are in accordance with what can be found in the most recent literature (4-6). In this line, we conducted in our department a randomized clinical trial (7) regarding the use of L-PRF to increase the keratinized tissue width (KTW) around implants compared to a free gingival graft (FGG), defined as the “gold standard” (8, 9). In literature, the use of an apical positioned flap with a FGG is considered the best combination. In our study, L-PRF was able to increase the peri-implant KTW with lower surgical time and less postoperative discomfort for the patients in comparison with a FGG. Therefore, this technique may be considered as an alternative of the FGG, although more evidence is needed with a larger sample size.

The second systematic review included in this PhD thesis (“**Regenerative potential of leucocyte- and platelet-rich fibrin. Part B: sinus floor elevation, alveolar ridge preservation and implant therapy. A systematic review**”) (10) focused on the use of L-PRF on bone augmentation procedures and osseointegration process. In this case, no meta-analysis could be conducted. The hypothesis that L-PRF would also produce bone regeneration resulted in a lot of controversy due to the lack of well-conducted randomized clinical trials (RCTs) comparing the use of L-PRF with other biomaterials. In sinus floor elevation (SFE), it has been hypothesized that bone formation might occur without using any grafting material, as a blood clot is the precursor of osteogenesis. This technique relies on the principle of space

maintenance for the blood clot allowing its differentiation. In SFE procedures, this is achieved by placing the implants simultaneously with the sinus lift where the implant serves as tent poles to keep the Schneiderian membrane lifted, avoiding its collapse (Figure 1). Golcalves Zenobio and co-workers (2019) reported a mean bone gain of  $3.2 \pm 1.5$  mm in the lateral window approach only using a blood clot after 6 months (11), whereas Molemans and co-workers (2019) observed a mean bone gain of  $5.4 \pm 1.5$  mm using L-PRF as a sole filling material (12). After 6 and 12 months, the use of L-PRF was also superior for example to the use of saline (12, 13).

In order to minimize the collapse of the membrane and provide bioactive components to the graft, the combination of L-PRF with other grafting material has also been suggested. Pichotano and co-workers (2019) reported a faster bone maturation (4 months vs. 8 months) when comparing L-PRF + DBBM or DBBM alone. A higher early graft resorption could be observed in the L-PRF + DBBM group; being however similar for the test at 4 months ( $33.1 \pm 10.7\%$ ) as for the control at 8 months ( $36.7 \pm 15.8\%$ ). In both groups, the augmented bone presented adequate volume for implant placement (14). Similarly, Nizam and co-workers (2018) performed the same comparison and they could not find any differences in newly formed bone between groups after 6 months, time of evaluation where the faster healing with L-PRF could no longer be seen (15).

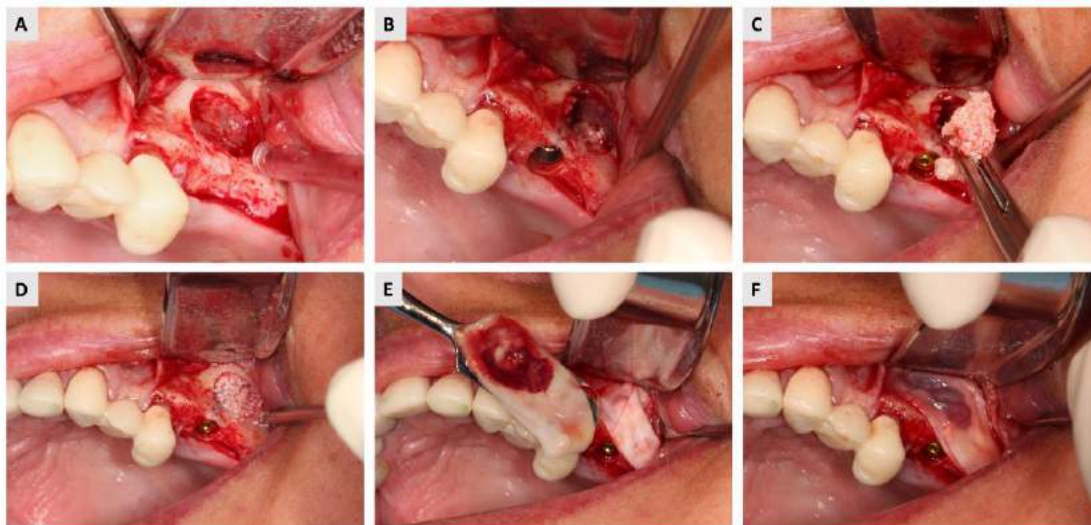


Figure 1. L-PRF block application during sinus lift with lateral window approach and immediate implant placement. A: preparation of the window at region 26. Note that the Schneiderian membrane has already been elevated. B: Implant maintaining the membrane lifted. L-PRF block was already applied at the mesial part before implant placement. C: Application of L-PRF block in the rest of the sinus cavity. D: View of the sinus cavity filled with the L-PRF block. E: Collagen membrane in place to cover the window (double layer). L-PRF membrane application as protection. F: L-PRF membranes on top of the collagen membrane before flap closure.

Another application of L-PRF during SFE procedures is when a membrane perforation occurs (16). Oncü and co-workers (2017) compared the bone formation and implant survival rate in patients with or without sinus membrane perforation. A 100% implant survival rate was observed for both groups (17). Moreover, a larger number of blood vessels and fibroblasts were observed when L-PRF was used compared to a collagen membrane to close the perforation (18).

The application of L-PRF in alveolar ridge preservation and in implant dentistry will be further discussed below.

In both systematic reviews, not only the clinical outcomes were analysed but also the surgical and centrifugation protocols. A high heterogeneity in surgical protocols was observed in terms of number of L-PRF clots/membranes used and even in the millilitres of blood withdrawn from the patient. These are important confounding variables that have to be taken into consideration. This is of outmost importance to be able to objectively compare results and standardize surgical protocols.

## 2. Characterization of PRF matrices: release of growth factors and composition

The other objective of this PhD thesis was achieved in both **chapters 3 and 4**, where the release of growth factors and cellular content of the PRF matrices (L-PRF, A-PRF, A-PRF+) were evaluated. L-PRF, A-PRF and A-PRF+ released growth factors up to 14 days (19, 20). However, no statistically significant differences amongst the 3 PRF modifications could be observed. L-PRF membrane and Liquid Fibrinogen presented high concentration of leucocytes and platelets, whereas L-PRF exudate had a low cellular content.

### ➤ Importance of growth factors released by PRF matrices

The growth factors analysed in both *in vitro* studies are crucial in wound healing. Platelets are known to be a major source of *transforming growth factor beta-1 (TGF-β1)*, which is primarily involved in inflammation, angiogenesis, epithelialization, and connective tissue regeneration. TGF-β1 facilitates the recruitment of additional inflammatory cells and augments macrophage mediated tissue debridement (21). It is also interesting to note that once the wound field is sterilized, TGF-β1 is able to deactivate superoxide production from macrophages *in vitro* which may help to protect the surrounding healthy tissue and prepare the wound for granulation tissue formation (22). Moreover, it is also involved in up regulating the main angiogenic growth factor known as *vascular endothelial growth factor (VEGF)* (23). This growth factor promotes the early events in angiogenesis, particularly endothelial cell migration and proliferation as seen in several *in vitro* studies (24, 25). Since bone is a highly vascularized organ and angiogenesis plays an important role in osteogenesis, VEGF also influences skeletal development and postnatal bone repair. VEGF is highly concentrated in the hematoma formed after bone trauma (15-fold higher than in plasma) and subsequently is involved in the initial processes of bone repair (26, 27).

Another growth factor analysed was *platelet derived growth factor (PDGF)*. PDGF is a natural protein found abundantly in bone matrix. It presents as dimers of A, B and C polypeptide chains linked by disulphide bonds. PDGF is locally released by platelets during clotting following soft or hard tissue injury. Once it is released, it binds to specific cell surface receptors promoting rapid cell migration (chemotaxis) and proliferation (mitogenesis) in the area of injury (28, 29).

But the growth factors par excellence are the group of *bone morphogenetic proteins (BMPs)*. BMPs are members of the TGF-β superfamily, originally identified as proteins that induced the formation of bone and cartilage tissues when implanted at ectopic sites in rats (30, 31). *In vitro*, BMPs have potent effects on the regulation of growth and differentiation of chondroblast and osteoblast lineage cells. Until now, at least 20 BMPs have been identified and they have been also tested in preclinical and clinical studies, showing their definite potential in osteoinduction (32). In this PhD thesis, BMP-1 was found to be released

from the L-PRF membranes. This BMP does not belong to the TGF- family but is a pro-collagen C-proteinase that cleaves procollagens and induces accumulation of extracellular matrix. Some studies suggested that BMP-1 might be also an activator of other BMPs (33, 34).

Multiple growth factors have been quantified from different platelet concentrates (35-37). Recently, the secretome of L-PRF has been deciphered and 705 proteins related to platelet and neutrophil degranulation were identified (38). After 3, 7 and 21 days of culture, more than 200 proteins were secreted, amongst them TGF- $\beta$ 1, VEGF, hepatocyte growth factor (HGF), nerve growth factor (NGF), BMP 4 and 7, matrix metalloproteinase 9 (MMP9), thrombospondin -1 (TSP1), insulin-like growth factor (IGF), and fibroblast growth factor-7 (FGF7). Proteins with antimicrobial activity such as MMP9, cationic antimicrobial protein-7 (CAP7), Myeloperoxidase (PERM), Bactericidal permeability-increasing protein (BPI), and Cathepsin G (CATG) indicate neutrophil degranulation. These proteins have not been described previously in platelet concentrates, possibly due to the fact that many of those platelet concentrates often do not contain leucocytes. Moreover, the proteomic analysis highlighted the presence of proteins derived from monocytes and CD4 lymphocytes in the secretome at day 3, confirming the presence of these cells in the L-PRF.

#### ➤ Clinical benefit and dosage

The use of biological agents in combination with grafting materials for bone regeneration has gained considerable attention in the last decades. Recently, various clinical trials have validated the safety and predictability of these approaches (39). Biologically active bone grafts could offer numerous advantages over the traditional grafts because of the presence of growth factors. The fact that the graft itself can stimulate the area to be regenerated could resemble the properties of the autogenous bone. However, the existing evidence supported by randomized controlled clinical trial is still limited. Above all, there is a lack of knowledge at a molecular and cellular level about the limit of this stimulation and about how fast the saturation would be then reached.

Several of the above-mentioned growth factors have been applied in clinical and animal studies for bone regeneration procedures (40, 41). For instance, the most commonly used and studied growth factor is the recombinant human bone morphogenetic protein-2 (rhBMP-2), which has been successfully used in bone regeneration (42, 43). On the other hand, PDGF has also been utilized for bone augmentation procedures. According to the literature, the release of this growth factor by PRP varied around 5-8 ng/ml during 7-14 days (44, 45). During the same period, the release of PDGF from L-PRF ranged between 25 to 150 ng/ml (19, 46). However, the dose used in clinical studies when the growth factor is externally applied was 300,000 ng/ml (0.3 mg/ml) (47).

Other growth factors as VEGF and TGF- $\beta$ 1 are less commonly used in the clinical setting. Schorn and co-workers (2017) (48) described the use of VEGF with a dose of 18.4  $\mu$ g/ml (184,000 ng/ml) during vertical bone augmentation in combination with rhBMP-2 in a collagenous scaffold. After 12 weeks, this combination showed significantly more bone volume density and more vertical bone gain around implants in comparison to the control group (no intervention). The use of TGF- $\beta$ 1 has also been studied in combination with  $\beta$ -tricalcium phosphate in a dose that ranges from 1 to 40 ng/ml (49). Bone height in vivo was similar with or without TGF- $\beta$ 1; however, blood vessel density was significantly higher in the



test group. The release of this factor by L-PRF varied from 40 to 120 ng/ml (19, 37), which is similar to what is given externally.

The continuous release of growth factors from the L-PRF up to 14 days may have two origins: (1) gradual fibrinolysis of the fibrin matrix and consequently the release of the growth factors attached to it; and/or (2) active production of growth factors by the living cells embedded in the fibrin mesh. One of the questions that often arises is the viability of the cells inside the PRF matrices. The **cell viability in PRF matrices** has not been specifically studied in this PhD thesis. However, the research group of Prof. Dr. Ivo Lambrechts (Hasselt University, Belgium) cultured various L-PRF clots to evaluate the viability of those cells using the outgrowth method. Outgrowth colonies appear between days 7 and 14, confirming the presence of vital cells inside the L-PRF (Figure 2).

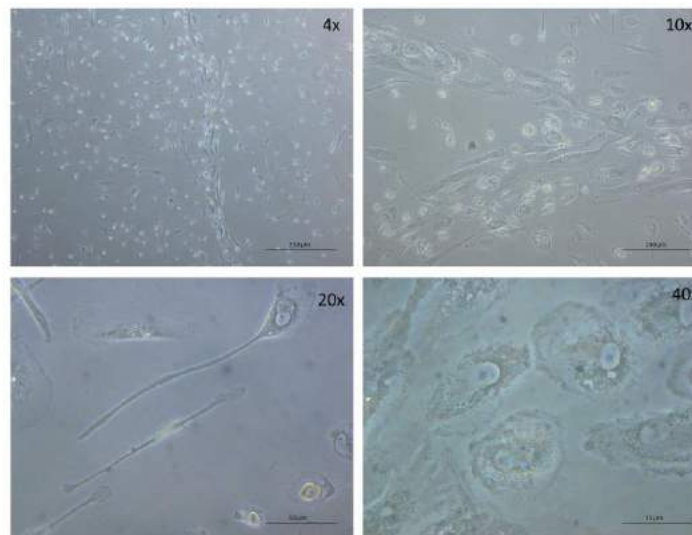


Figure 2. Outgrowth colonies after incubation of L-PRF clots. Cells compatible with early endothelial progenitor cells with a spindle-like morphology are observed. Images courtesy of Dr. J. Ratajczak and Dr. T. Vanganswinkel (Hasselt University).

#### ➤ Impact of age and gender

The macroscopic dimensions of PRF matrices (L-PRF, A-PRF, A-PRF+) have also been examined in this PhD thesis. Similarly, Miron and co-workers in 2018 (50) compared the macroscopic parameters of PRF membranes between females and males, as well as younger and older patients. They observed that the size of PRF membranes produced from females was 17% larger than those from males. This was explained by the fact that females, compared to males, generally show lower haematocrit levels in their peripheral blood. The separation between plasma layers is easier in case of lower haematocrit levels. Larger membranes were also observed in elderly patients, often showing lower concentrations of red blood cells. Yajamanya and co-workers in 2016 (51) observed that the fibrin network of L-PRF-based membranes was less dense as patient age increased. Whether these observations have a clinical impact is still unclear.



➤ Impact of g force on release of growth factors and physical characteristics

The study included in **chapter 4, “Impact of g force and timing on the characteristic of PRF matrices”**, evaluated the impact of the relative centrifugal force (RCF) on the final properties of PRF matrices. Several papers (52-54) reported contradictory data on the impact of g force on the above-mentioned release of growth factors, with some methodological shortcomings (55, 56). It has been suggested that A-PRF and A-PRF+, both with a lower RCF, presented a higher release of growth factors and a more homogenous cellular distribution inside the PRF matrices (57) (58). However, Ehrenfest and co-workers (53) (2018) compared L-PRF vs. A-PRF prepared with various centrifugation devices and concluded that the L-PRF protocol allowed producing larger clots/membranes and a more intense release of growth factors. In contrast, in a similar study El Bagdadi and co-workers (54) (2019) compared L-PRF vs. A-PRF vs. A-PRF+ and observed an increased in growth factors release when RCF was reduced. Comparing findings is complicated by the heterogeneity in methods used, such as type of tube (plastic or glass) and adaptation of RCF to the rcf-max or rcf-clot. When we adapted the settings for the different centrifuges in order to reach the same g force for each device, the previously reported differences between different protocols were no longer observed. Indeed, no statistically significant differences could be found among all membranes (L-PRF, A-PRF, A-PRF+), prepared with their specific protocols, in terms of growth factors release, cellular content, and dimensions.

Regarding the physical characteristics, the study from chapter 4 concluded that a lower g force reduced the membrane tensile strength. However, the results for the tensile testing were similar and showed no statistically significant differences for the same protocol when the g force was adapted in both centrifuges, suggesting that the adaptation of the g force may result in similar PRF matrices independently of the device used. Ockerman and co-workers (2020) (59) examined the impact of antithrombotic drugs on the structural and mechanical properties of the L-PRF. Those appeared not be affected by low doses of anticoagulant, whereas high doses impaired L-PRF generation.

➤ Impact of timing

On the other hand, we have also evaluated the importance of timing before and after centrifugation to obtain an optimal PRF construct. The results suggested that the blood should be centrifuged within the first 60 seconds after collection. Our findings are in accordance with those reported in the literature. For instance, Miron and co-workers (50) concluded that a 60- to 90-s interval between blood draw and the start of centrifugation should be respected by clinicians to avoid significant changes in the macroscopic morphology/size of fabricated PRF membranes.

The time interval between the end of centrifugation and the compression of the clot into a membrane also had an impact. The longer this time interval, the smaller the membranes. Both in length and width, statistically significant differences were found between membranes prepared immediately after centrifugation and those prepared after 2 or 3 hours ( $p < 0.05$ ).

### 3. Antimicrobial characteristics

Several studies have described the antibacterial properties of L-PRF (60, 61). The study included in this thesis **“Antimicrobial capacity of L-PRF against periodontal pathogens”** (62) assessed the antimicrobial properties of L-PRF against the main periopathogens cultured on agar plates and in planktonic solution. We could conclude that an L-PRF membrane has an antimicrobial effect, especially against *P. gingivalis*. The L-PRF exudate also showed a strong inhibition against *P. gingivalis* on agar plates and decreased the number of viable *P. gingivalis* in a dose-dependent way. Among the microorganisms isolated from patients suffering from severe periodontal pathologies, *Porphyromonas gingivalis* is the most commonly found (63, 64). This Gram-negative and obligate anaerobic bacterium produces several virulence factors that contribute to its pathogenicity by enabling the invasion of periodontal tissue and providing protection against the host defence (65). The fact that the L-PRF might inhibit or reduce the growth of this bacteria may have important clinical applications, for instance in periodontal regeneration or in the treatment of medication-related osteonecrosis of the jaws (MRONJ) or osteoradionecrosis.

However, the mechanism(s) responsible for the L-PRF antimicrobial effect against periodontal pathogens remained controversial. Existing evidence suggests that platelets may play multiple roles in the antimicrobial host defence: they generate oxygen metabolites, including superoxide, hydrogen peroxide and hydroxyl free radicals, capable of binding, aggregating, and internalizing microorganisms. In addition, platelets also release an array of potent antimicrobial peptides (66). At the Department of Periodontology at KU Leuven, we followed this research line in order to envisage the antimicrobial mechanisms of the L-PRF (67). This study confirmed that L-PRF exudate caused the growth inhibition of *P. gingivalis* on agar plates, in planktonic cultures and during the development of in vitro multispecies biofilms. This antimicrobial effect was blocked in all models by exposing the L-PRF exudate to horseradish peroxidase. Pepsin showed similar blocking effects on L-PRF exudate, with the exception of the developing multispecies biofilm model. From these results, one can conclude that L-PRF exudate may release peroxide and peptides, which may be responsible for its antimicrobial effect against *P. gingivalis*. Future research is required to evaluate the effect of L-PRF on different strains of diverse bacterial species to investigate the clinical relevance of these findings.

### 4. Characterisation of L-PRF bone block

With the project **“Characterization of the L-PRF bone block: release of growth factors, cellular content, and structure”**, a new technique was explored that combines the beneficial properties of bone blocks and particulated grafts reducing the disadvantages of both. The L-PRF block is formed by three components: (1) the L-PRF membranes, which provide a matrix rich in activated platelets secreting a wide range of bioactive molecules and growth factors, (2) the demineralized bovine bone mineral (DBBM), that offers an inorganic scaffold, and (3) the Liquid Fibrinogen, that glues the scaffold and matrix together. This last component comes also from the patient’s blood and in contact with the chopped L-PRF membranes creates a form-retaining block structure. The role of this autogenous liquid seems to be crucial and twofold: it mechanically glues all the components of the L-PRF bone block, and at the same time, it has bioactive properties (68). Because the DBBM particles are embedded in a fibrin matrix, more space is created between the graft particles, which might allow cell ingrowth from surrounding tissue, and gives

more stability to the graft. Fibrin-based matrices are well known for delivering growth factors due to the binding sites for cells, proteins and growth factors (69). Moreover, it has been suggested that DBBM might have osteoinductive properties (70). Given the active production of growth factors by the L-PRF membranes and derivatives, this might further stimulate the biological properties of DBBM particles becoming a bioactive scaffold.

#### ➤ Clinical application

Traditionally, autogenous bone blocks have been suggested for the treatment of extensive bony defects, especially in a staged approach (71). However, this technique requires a second surgical site, which increase patient morbidity and postoperative complications (72) (73). The **L-PRF bone block is a new concept in guided bone regeneration (GBR)** with a tissue engineering approach, which relies on two fundamental principles: a space-maintaining scaffold and a matrix that permits cell recruitment, neovascularization, and delivers growth factors (74). The use of surgical techniques to improve treatment outcomes and reduce patients' morbidity has to be the goal of every clinician. In this sense, bone harvesting from a secondary surgical site remains an important concern. The L-PRF bone block technique seems to be successful in the treatment of horizontal bony defects without the need of autologous bone, as reported in a proof-of-concept study performed in our department (Figure 3) (75). The combination with Liquid Fibrinogen to form the L-PRF bone block increases ease in handling and predictability of the augmentation procedure. Moreover, Mir-Mari and co-workers observed that the use of a bone substitute in a form of a block improved the horizontal volume stability and reduced displacement of the bone substitute after wound closure compared to particulate xenograft alone (76, 77). Further clinical studies with longer follow-up period and histological analysis have to confirm the use of this technique in GBR procedures.

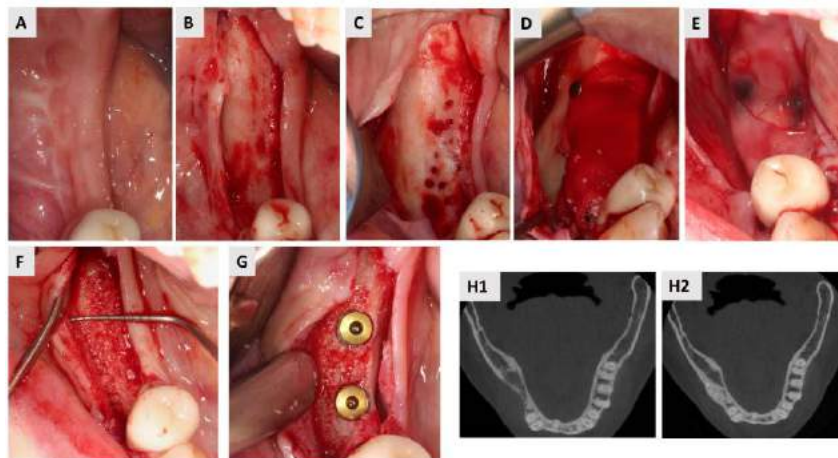


Figure 3. Guided bone regeneration (GBR) with L-PRF bone block and collagen membrane. A: pre-operative view. B: Full-thickness mucoperiosteal flap. C: Cortical perforation to stimulate vascularization to the graft. D: L-PRF bone block in situ covered with collagen membrane fixed with tacks. E: L-PRF membranes covering the collagen membrane as protection in case of a flap dehiscence. F: Bone regenerated after 9 months of healing. G: Implant placement in the regenerated bone. H1: Cone beam computed tomography (CBCT) image of the initial situation, before GBR. H2: CBCT image after GBR.

➤ Potential role of L-PRF membranes in guided bone regeneration (GBR) procedures

L-PRF has also been used as a protection of the barrier membrane (Figure 3E), in case that a flap dehiscence after bone augmentation procedures occurs. Recently it has been envisaged that L-PRF stimulates fibroblast wound closure *in vitro* (78, 79), and promotes the ability of fibroblasts to induce endothelial tube formation (79, 80). Another study (81) showed a higher cell adhesion and spreading on the expanded polytetrafluoroethylene (e-PTFE) membranes when coated with L-PRF. This is of relevant importance with this kind of membrane because of the high ratio of flap dehiscence or flap perforation (Figure 4) (82). Flap dehiscence with membrane exposure is one of the most common complication in GBR procedures with a significant detrimental influence on the outcome of bone augmentation (83). For the edentulous ridges, the sites without membrane exposure achieved 74% more horizontal bone gain than the sites with exposure. For peri-implant dehiscence defects, the sites without membrane exposure had 27% more defect reduction than the sites with exposure (84, 85).

The same principle is applied when L-PRF is used at the palatal donor site after the harvesting of a free gingiva graft or a connective tissue graft. Various studies have shown faster wound healing and less post-operative pain when using L-PRF (86, 87).

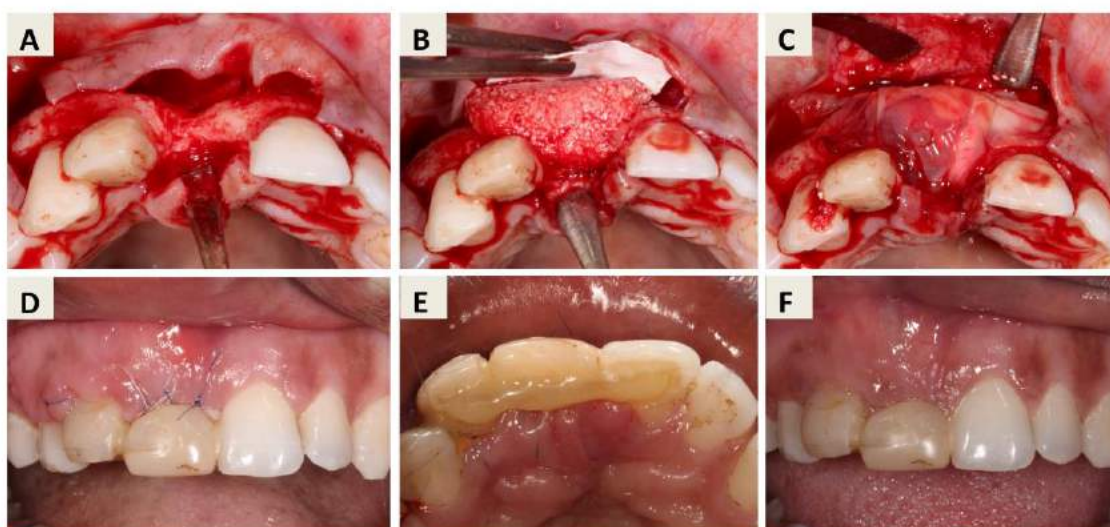


Figure 4. Guided bone regeneration (GBR) in the anterior zone (region 11). A: Visualisation of the horizontal bone defect. B: GBR at region 11 with L-PRF bone block and non-resorbable membrane (e-PTFE). C: L-PRF membranes on the e-PTFE membrane as protection D: 7 days post-op. Frontal view. E: 7days post-op occlusal view. F: 6 months post-op. No membrane exposure/perforation occurred during the healing phase.

## 5. Benefits of L-PRF in periodontal surgery: new RCT studies

➤ Alveolar ridge preservation

The application of L-PRF in alveolar ridge preservation was evaluated via a systematic review and a randomized clinical trial (**chapter 8**). The systematic review concluded that L-PRF improved the preservation of the alveolar ridge in single tooth extractions and resulted in less buccal bone resorption

compared to unassisted healing. Moreover, a better soft tissue healing and less post-operative pain was frequently reported. However, there was a high variability in the data as well as in the surgical protocols, which made the meta-analysis of the data impossible. Overall, the outcome seems to be very technique-sensitive and somehow unpredictable (88, 89). With the study of **chapter 8 (“Effect of different PRF matrices for ridge preservation in multiple tooth extractions: A split-mouth randomized controlled clinical trial”)** (90), we aimed to continue with the research line started at our department with the study of Temmerman and co-workers (91). In single tooth extraction, they reported a mean change in horizontal dimension at 1 mm below the crest of 1.4 mm (23%) and 5.0 mm (51%) for L-PRF group and control group, respectively (92). Similar benefits have been reported in the literature (93-96).

In the randomized clinical trial (RCT) included in this thesis we aimed to go further and evaluate the effect of different PRF matrices after multiple tooth extractions. The mean change in horizontal dimension at 1 mm below the crest was of 2.2 mm (26-28%) for all three groups (L-PRF, A-PRF+, and unassisted healing) three months after tooth extraction.

The main difference with our study was the use of an immediate full denture that may have jeopardized the healing of the test sites by destabilizing the L-PRF membranes inside the sockets. Mechanical pressure transmitted continuously and/or intermittently through the prosthesis has been considered one of the causative factors for bone resorption in denture-supporting tissues (97, 98). Moreover, Alrajhi and co-workers (99) concluded that anterior maxillary areas had more early bone resorption compared to posterior areas. One needs to keep in mind that the use of an immediate prosthesis is a common protocol in daily practice after multiple tooth extractions. Consequently, alveolar ridge preservation techniques in multiple tooth extractions when a mucosa-supported prosthesis is also used might not have the same results as in single tooth extractions.

Another difference with Temmerman’s study is that extraction sockets with dehiscences were included for analysis. That might explain why the control site showed more resorption than in our study with multiple tooth extractions. The evidence around the bone resorption pattern after multiple tooth extraction is limited, what makes the comparison of our results with others, at this moment, not possible.

#### ➤ Osseointegration

The use of L-PRF in Implant Dentistry was approached by a systematic review and an *in vivo* study. In the systematic review, better implant stability over time and less marginal bone loss were observed when the implants were coated with L-PRF. However, a meta-analysis could not be performed due to the heterogeneity of the data. Implant design influences primary stability and osseointegration during early healing. However, when primary stability cannot be achieved, the addition of molecules to the implant surface might improve bone to implant contact (BIC) at an early stage. L-PRF has shown to promote the formation of a dense fibrin clot on nano-rough implant surfaces, which seems to be crucial to provide a provisional scaffold for the migration of osteogenic cells (100). The section 3 (**chapter 7**) describes the project **“Peri-implant bone structure at early healing after implant surface functionalization with L-PRF: a micro-CT and histomorphological analysis. (In progress)”**, which aimed to evaluate the effect of L-PRF coating on the peri-implant bone formation at early healing in a pig model. Although beneficial results have been reported in literature, in the study included in this thesis the effect of the L-PRF coating seemed to be dependent on the implant surface. The early osteointegration of the implants with a fluoride-



modified surface (ASTRA implants, OsseoSpeed® surface) seemed to be enhanced when coated with L-PRF. However, the implants with a calcium-phosphate coating (Blossom® implants, Ossean® surface) appeared to be negatively affected by L-PRF. In vitro, the coating with L-PRF products resulted in a dense fibrin network on the Ossean® surface with abundant erythrocytes, platelets, and leucocytes. The fact that a dense fibrin matrix occupies the interface between the implant and the bone might be beneficial or detrimental for the early phases of osseointegration. In the present study, traces from the L-PRF membrane could be found after 7 days in the implant-bone gap, although also remnants of a blood clot were also identified. Further studies should explain how the L-PRF membranes are dissolved or incorporated in the surrounding tissues and how these processes influence osteointegration.

Similar to our study, Abrahamsson and co-workers (2008) (101) studied the early per-implant bone formation around fluoride-modified surfaces placed in an oversized preparation. They reported a mean bone-to-implant contact (BIC %) of  $55.7\% \pm 9.7$  and of  $63.7\% \pm 19.3$ , after 2 weeks and 6 weeks, respectively. Those findings are in accordance to what we have observed in our study when the Astra implants were not coated with L-PRF. However, the oversized preparation in their study was of 1 mm compared to 0.4 mm from the present study. The gap size (0.4 mm) may have limited the effect of L-PRF in the distance osteogenesis. Moreover, the detection of differences in bone quality and structure with the microCT may have been also influenced by the gap size.

One does not have to forget that in vivo experiments try to resemble as much as possible the real clinical conditions. However, clinical trials remain the most accurate model. Several clinical studies evaluated the benefits of the application of L-PRF on the osseointegration process (102-105). Statistically significant higher ISQ values, which increased continuously over time, have been reported in literature when implants were coating with L-PRF (104, 106). Boora et al. (2015) (107) recorded the early bone remodelling around implants coated or not with L-PRF at insertion. The L-PRF-coated implants showed 50% less initial bone loss. However, Diana and co-workers (2018) could not observed any significant effect of L-PRF coating on immediate implants with adequate primary stability. Further research is needed to envisage the effect of PRF coating on osseointegration.

## FUTURE PERSPECTIVES

---

Periodontal surgery has evolved a lot in recent years, as the demand from patients has also increased. Today we see more complex cases, in which the clinician is often limited by the extent and morphology of the bone defect, the amount of autogenous bone available, and the condition of the soft tissues. For this reason, the addition of biological agents to graft materials might help to overcome some limitations of the traditional techniques.

The use of PRF matrices started already twenty years ago, but we are still now trying to understand its healing properties. Above all, there is still a lack of knowledge at a molecular and cellular level of the extent to which we can exogenously stimulate the organism. When growth factors are added to a bone graft, the concentrations sometimes are 1,000 to 100,000 times higher than what is released by the L-PRF. Further research needs to be focused on determine the saturation point and to discard any possible negative effect of this over-stimulation.

There is quite strong evidence that PRF matrices enhance soft tissue healing. However, their application for bone regeneration somehow remains controversial. Even though it has been demonstrated that PRF matrices stimulate the migration and proliferation of osteoblasts, the clinical results seems to be very operator-sensitive. As for any other surgical technique or biomaterial, the correct handling is essential. Well-designed studies with strict and rigorous protocols are needed to envisage the real effect of PRF.

Another important perspective is to evaluate how we can further improve the characteristics of L-PRF in order to enhance its benefits. For instance, an interesting topic would be the use of L-PRF as carrier in drug delivery systems. Recently, it has been envisage the function of L-PRF as a local sustained released device for antibiotics (108). Further research will provide more details about the kinetics and the mechanisms to introduce the antibiotics in the L-PRF (109). Moreover, well-designed randomized clinical trials should assess the clinical benefit and indications of modified L-PRF membranes with antimicrobials.

Patient's characteristics need to be taken into account when using platelet concentrates. Blood composition varies amongst patients and that might affect the properties of the L-PRF too. The understanding of the ideal patient selection should be mandatory to have predictable outcomes. However, the impact of the systemic health condition as diabetes, anticoagulant medication, (auto)-immune diseases, etc. still needs to be further studied.

Nevertheless, these shortcomings might be countered by the modification of its properties during the preparation. For instance, Kawase and co-workers (110) modified the L-PRF by using heat to compress the clots. Their findings suggested that the heat-compression technique reduced the rate of biodegradation of the L-PRF membranes without sacrificing its biocompatibility. Therefore, it may be useful as a barrier membrane in guided tissue regeneration. Further improvements in the preparation of L-PRF will provide new applications of this biomaterial. The understanding of the limits of L-PRF seems of utmost importance to avoid controversial results and to provide the best treatment to our patients.

## References

1. Castro AB, Meschi N, Temmerman A, Pinto N, Lambrechts P, Teughels W, et al. Regenerative potential of leucocyte- and platelet-rich fibrin. Part A: intra-bony defects, furcation defects and periodontal plastic surgery. A systematic review and meta-analysis. *J Clin Periodontol.* 2017;44(1):67-82.
2. Miron RJ, Moraschini V, Fujioka-Kobayashi M, Zhang Y, Kawase T, Cosgarea R, et al. Use of platelet-rich fibrin for the treatment of periodontal intrabony defects: a systematic review and meta-analysis. *Clin Oral Investig.* 2021;25(5):2461-78.
3. Cortellini P, Tonetti MS. Clinical and radiographic outcomes of the modified minimally invasive surgical technique with and without regenerative materials: a randomized-controlled trial in intra-bony defects. *J Clin Periodontol.* 2011;38(4):365-73.
4. Moraschini V, Barboza Edos S. Use of Platelet-Rich Fibrin Membrane in the Treatment of Gingival Recession: A Systematic Review and Meta-Analysis. *J Periodontol.* 2016;87(3):281-90.
5. Miron RJ, Zucchelli G, Pikos MA, Salama M, Lee S, Guillemette V, et al. Use of platelet-rich fibrin in regenerative dentistry: a systematic review. *Clin Oral Investig.* 2017;21(6):1913-27.
6. Rodas MAR, Paula BL, Pazmiño VFC, Lot Vieira F, Junior JFS, Silveira EMV. Platelet-Rich Fibrin in Coverage of Gingival Recession: A Systematic Review and Meta-Analysis. *Eur J Dent.* 2020;14(2):315-26.
7. Temmerman A, Cleeren GJ, Castro AB, Teughels W, Quirynen M. L-PRF for increasing the width of keratinized mucosa around implants: A split-mouth, randomized, controlled pilot clinical trial. *J Periodontal Res.* 2018;53(5):793-800.
8. Thoma DS, Buranawat B, Hämmerle CH, Held U, Jung RE. Efficacy of soft tissue augmentation around dental implants and in partially edentulous areas: a systematic review. *J Clin Periodontol.* 2014;41 Suppl 15:S77-91.
9. Bassetti RG, Stähli A, Bassetti MA, Sculean A. Soft tissue augmentation procedures at second-stage surgery: a systematic review. *Clin Oral Investig.* 2016;20(7):1369-87.
10. Castro AB, Meschi N, Temmerman A, Pinto N, Lambrechts P, Teughels W, et al. Regenerative potential of leucocyte- and platelet-rich fibrin. Part B: sinus floor elevation, alveolar ridge preservation and implant therapy. A systematic review. *J Clin Periodontol.* 2017;44(2):225-34.
11. Zenóbio EG, Cardoso LD, Oliveira LJ, Favato MN, Manzi FR, Cosso MG. Blood clot stability and bone formation following maxillary sinus membrane elevation and space maintenance by means of immediate implant placement in humans. A computed tomography study. *J Craniomaxillofac Surg.* 2019;47(11):1803-8.
12. Molemans B, Cortellini S, Jacobs R, Pinto N, Teughels W, Quirynen M. Simultaneous sinus floor elevation and implant placement using leukocyte- and platelet-rich fibrin as a sole graft material. *Int J Oral Maxillofac Implants.* 2019;34(5):1195–201.
13. Cho YS, Hwang KG, Jun SH, Tallarico M, Kwon AM, Park CJ. Radiologic comparative analysis between saline and platelet-rich fibrin filling after hydraulic transcrestal sinus lifting without adjunctive bone graft: A randomized controlled trial. *Clin Oral Implants Res.* 2020;31(11):1087-93.
14. Pichotano EC, de Molon RS, de Souza RV, Austin RS, Marcantonio E, Zandim-Barcelos DL. Evaluation of L-PRF combined with deproteinized bovine bone mineral for early implant placement after maxillary sinus augmentation: A randomized clinical trial. *Clin Implant Dent Relat Res.* 2019;21(2):253-62.



15. Nizam N, Eren G, Akcalı A, Donos N. Maxillary sinus augmentation with leukocyte and platelet-rich fibrin and deproteinized bovine bone mineral: A split-mouth histological and histomorphometric study. *Clin Oral Implants Res.* 2018;29(1):67-75.
16. Malzoni CMA, Nicoli LG, Pinto G, Marcantonio C, Pigossi SC, Zotesso VA, et al. The effectiveness of L-PRF in the treatment of Schneiderian membrane large perforations: long-term follow-up of a case series. *J Oral Implantol.* 2020.
17. Öncü E, Kaymaz E. Assessment of the effectiveness of platelet rich fibrin in the treatment of Schneiderian membrane perforation. *Clin Implant Dent Relat Res.* 2017;19(6):1009-14.
18. Aricioglu C, Dolanmaz D, Esen A, Isik K, Avunduk MC. Histological evaluation of effectiveness of platelet-rich fibrin on healing of sinus membrane perforations: A preclinical animal study. *J Craniomaxillofac Surg.* 2017;45(8):1150-7.
19. Castro AB, Cortellini S, Temmerman A, Li X, Pinto N, Teughels W, et al. Characterization of the Leukocyte- and Platelet-Rich Fibrin Block: Release of Growth Factors, Cellular Content, and Structure. *Int J Oral Maxillofac Implants.* 2019;34(4):855-64.
20. Castro AB, Andrade C, Li X, Pinto N, Teughels W, Quirynen M. Impact of g force and timing on the characteristics of platelet-rich fibrin matrices. *Sci Rep.* 2021;11(1):6038.
21. Barrientos S, Stojadinovic O, Golinko MS, Brem H, Tomic-Canic M. Growth factors and cytokines in wound healing. *Wound Repair Regen.* 2008;16(5):585-601.
22. Tsunawaki S, Sporn M, Ding A, Nathan C. Deactivation of macrophages by transforming growth factor-beta. *Nature.* 1988;334(6179):260-2.
23. Riedel K, Riedel F, Goessler UR, Germann G, Sauerbier M. Tgf-beta antisense therapy increases angiogenic potential in human keratinocytes in vitro. *Arch Med Res.* 2007;38(1):45-51.
24. Shin Y, Jeon JS, Han S, Jung GS, Shin S, Lee SH, et al. In vitro 3D collective sprouting angiogenesis under orchestrated ANG-1 and VEGF gradients. *Lab Chip.* 2011;11(13):2175-81.
25. Adini A, Adini I, Chi ZL, Derda R, Birsner AE, Matthews BD, et al. A novel strategy to enhance angiogenesis in vivo using the small VEGF-binding peptide PR1P. *Angiogenesis.* 2017;20(3):399-408.
26. Street J, Winter D, Wang JH, Wakai A, McGuinness A, Redmond HP. Is human fracture hematoma inherently angiogenic? *Clin Orthop Relat Res.* 2000(378):224-37.
27. Hu K, Olsen BR. Osteoblast-derived VEGF regulates osteoblast differentiation and bone formation during bone repair. *J Clin Invest.* 2016;126(2):509-26.
28. Kaigler D, Avila G, Wisner-Lynch L, Nevins ML, Nevins M, Rasperini G, et al. Platelet-derived growth factor applications in periodontal and peri-implant bone regeneration. *Expert Opin Biol Ther.* 2011;11(3):375-85.
29. Javed F, Al-Askar M, Al-Rasheed A, Al-Hezaimi K. Significance of the platelet-derived growth factor in periodontal tissue regeneration. *Arch Oral Biol.* 2011;56(12):1476-84.
30. Wozney JM, Rosen V, Celeste AJ, Mitsock LM, Whitters MJ, Kriz RW, et al. Novel regulators of bone formation: molecular clones and activities. *Science.* 1988;242(4885):1528-34.
31. Reddi AH. Role of morphogenetic proteins in skeletal tissue engineering and regeneration. *Nat Biotechnol.* 1998;16(3):247-52.
32. De Biase P, Capanna R. Clinical applications of BMPs. *Injury.* 2005;36 Suppl 3:S43-6.

33. Anastasi C, Rousselle P, Talantikite M, Tessier A, Cluzel C, Bachmann A, et al. BMP-1 disrupts cell adhesion and enhances TGF- $\beta$  activation through cleavage of the matricellular protein thrombospondin-1. *Sci Signal*. 2020;13(639).
34. Bilezikian J.P. RLG, Martin J. *Principles of Bone Biology*. 3rd ed 2008.
35. Qiao J, An N, Ouyang X. Quantification of growth factors in different platelet concentrates. *Platelets*. 2017;28(8):774-8.
36. Lei L, Yu Y, Han J, Shi D, Sun W, Zhang D, et al. Quantification of growth factors in advanced platelet-rich fibrin and concentrated growth factors and their clinical efficacy as adjunctive to the GTR procedure in periodontal intrabony defects. *J Periodontol*. 2020;91(4):462-72.
37. Schär MO, Diaz-Romero J, Kohl S, Zumstein MA, Nesic D. Platelet-rich concentrates differentially release growth factors and induce cell migration in vitro. *Clin Orthop Relat Res*. 2015;473(5):1635-43.
38. Hermida-Nogueira L, Barrachina MN, Morán LA, Bravo S, Diz P, García Á, et al. Deciphering the secretome of leukocyte-platelet rich fibrin: towards a better understanding of its wound healing properties. *Sci Rep*. 2020;10(1):14571.
39. Avila-Ortiz G, Bartold PM, Giannobile W, Katagiri W, Nares S, Rios H, et al. Biologics and Cell Therapy Tissue Engineering Approaches for the Management of the Edentulous Maxilla: A Systematic Review. *Int J Oral Maxillofac Implants*. 2016;31 Suppl:s121-64.
40. Susin C, Fiorini T, Lee J, De Stefano JA, Dickinson DP, Wikesjö UM. Wound healing following surgical and regenerative periodontal therapy. *Periodontol 2000*. 2015;68(1):83-98.
41. Donos N, Dereka X, Calciolari E. The use of bioactive factors to enhance bone regeneration: A narrative review. *J Clin Periodontol*. 2019;46 Suppl 21:124-61.
42. Boyne PJ, Marx RE, Nevins M, Triplett G, Lazaro E, Lilly LC, et al. A feasibility study evaluating rhBMP-2/absorbable collagen sponge for maxillary sinus floor augmentation. *Int J Periodontics Restorative Dent*. 1997;17(1):11-25.
43. Jung RE, Glauser R, Schärer P, Hämmerle CH, Sailer HF, Weber FE. Effect of rhBMP-2 on guided bone regeneration in humans. *Clin Oral Implants Res*. 2003;14(5):556-68.
44. Kobayashi E, Flückiger L, Fujioka-Kobayashi M, Sawada K, Sculean A, Schaller B, et al. Comparative release of growth factors from PRP, PRF, and advanced-PRF. *Clin Oral Investig*. 2016;20(9):2353-60.
45. Masuki H, Okudera T, Watanebe T, Suzuki M, Nishiyama K, Okudera H, et al. Growth factor and pro-inflammatory cytokine contents in platelet-rich plasma (PRP), plasma rich in growth factors (PRGF), advanced platelet-rich fibrin (A-PRF), and concentrated growth factors (CGF). *Int J Implant Dent*. 2016;2(1):19.
46. He L, Lin Y, Hu X, Zhang Y, Wu H. A comparative study of platelet-rich fibrin (PRF) and platelet-rich plasma (PRP) on the effect of proliferation and differentiation of rat osteoblasts in vitro. *Oral Surg Oral Med Oral Pathol Oral Radiol Endod*. 2009;108(5):707-13.
47. Thoma DS, Cha JK, Sapata VM, Jung RE, Hüsler J, Jung UW. Localized bone regeneration around dental implants using recombinant bone morphogenetic protein-2 and platelet-derived growth factor-BB in the canine. *Clin Oral Implants Res*. 2017;28(11):1334-41.
48. Schorn L, Sproll C, Ommerborn M, Naujoks C, Kübler NR, Depprich R. Vertical bone regeneration using rhBMP-2 and VEGF. *Head Face Med*. 2017;13(1):11.

49. Elimelech R, Khoury N, Tamari T, Blumenfeld I, Gutmacher Z, Zigdon-Giladi H. Use of transforming growth factor- $\beta$  loaded onto  $\beta$ -tricalcium phosphate scaffold in a bone regeneration rat calvaria model. *Clin Implant Dent Relat Res*. 2019;21(4):593-601.
50. Miron RJ, Dham A, Dham U, Zhang Y, Pikos MA, Sculean A. The effect of age, gender, and time between blood draw and start of centrifugation on the size outcomes of platelet-rich fibrin (PRF) membranes. *Clin Oral Investig*. 2019;23(5):2179-85.
51. Yajamanya SR, Chatterjee A, Babu CN, Karunanithi D. Fibrin network pattern changes of platelet-rich fibrin in young versus old age group of individuals: A cell block cytology study. *J Indian Soc Periodontol*. 2016;20(2):151-6.
52. Fujioka-Kobayashi M, Miron RJ, Hernandez M, Kandalam U, Zhang Y, Choukroun J. Optimized Platelet-Rich Fibrin With the Low-Speed Concept: Growth Factor Release, Biocompatibility, and Cellular Response. *J Periodontol*. 2017;88(1):112-21.
53. Dohan Ehrenfest DM, Pinto NR, Pereda A, Jimenez P, Corso MD, Kang BS, et al. The impact of the centrifuge characteristics and centrifugation protocols on the cells, growth factors, and fibrin architecture of a leukocyte- and platelet-rich fibrin (L-PRF) clot and membrane. *Platelets*. 2018;29(2):171-84.
54. El Bagdadi K, Kubesch A, Yu X, Al-Maawi S, Orlowska A, Dias A, et al. Reduction of relative centrifugal forces increases growth factor release within solid platelet-rich-fibrin (PRF)-based matrices: a proof of concept of LSCC (low speed centrifugation concept). *Eur J Trauma Emerg Surg*. 2017.
55. Miron RJ, Pinto NR, Quirynen M, Ghanaati S. Standardization of relative centrifugal forces in studies related to platelet-rich fibrin. *J Periodontol*. 2019;90(8):817-20.
56. Pinto N, Quirynen M. Letter to the editor: RE: Optimized platelet-rich fibrin with the low-speed concept: Growth factor release, biocompatibility, and cellular response. *J Periodontol*. 2019;90(2):119-21.
57. Ghanaati S, Booms P, Orlowska A, Kubesch A, Lorenz J, Rutkowski J, et al. Advanced platelet-rich fibrin: a new concept for cell-based tissue engineering by means of inflammatory cells. *J Oral Implantol*. 2014;40(6):679-89.
58. Choukroun J, Ghanaati S. Reduction of relative centrifugation force within injectable platelet-rich-fibrin (PRF) concentrates advances patients' own inflammatory cells, platelets and growth factors: the first introduction to the low speed centrifugation concept. *Eur J Trauma Emerg Surg*. 2018;44(1):87-95.
59. Ockerman A, Braem A, EzEldeen M, Castro A, Coucke B, Politis C, et al. Mechanical and structural properties of leukocyte- and platelet-rich fibrin membranes: An in vitro study on the impact of anticoagulant therapy. *J Periodontal Res*. 2020;55(5):686-93.
60. Burnouf T, Chou ML, Wu YW, Su CY, Lee LW. Antimicrobial activity of platelet (PLT)-poor plasma, PLT-rich plasma, PLT gel, and solvent/detergent-treated PLT lysate biomaterials against wound bacteria. *Transfusion*. 2013;53(1):138-46.
61. Edelblute CM, Donate AL, Hargrave BY, Heller LC. Human platelet gel supernatant inactivates opportunistic wound pathogens on skin. *Platelets*. 2015;26(1):13-6.
62. Castro AB, Herrero ER, Slomka V, Pinto N, Teughels W, Quirynen M. Antimicrobial capacity of Leucocyte-and Platelet Rich Fibrin against periodontal pathogens. *Sci Rep*. 2019;9(1):8188.
63. Davey ME. Techniques for the growth of *Porphyromonas gingivalis* biofilms. *Periodontol* 2000. 2006;42:27-35.

64. Brunner J, Scheres N, El Idrissi NB, Deng DM, Laine ML, van Winkelhoff AJ, et al. The capsule of *Porphyromonas gingivalis* reduces the immune response of human gingival fibroblasts. *BMC Microbiol.* 2010;10:5.
65. Xu W, Zhou W, Wang H, Liang S. Roles of *Porphyromonas gingivalis* and its virulence factors in periodontitis. *Adv Protein Chem Struct Biol.* 2020;120:45-84.
66. Tang YQ, Yeaman MR, Selsted ME. Antimicrobial peptides from human platelets. *Infect Immun.* 2002;70(12):6524-33.
67. Rodríguez Sánchez F, Verspecht, T., Castro, A.B., Pauwels, M., Rodríguez Andrés, C., Quirynen, M., Teughels, W. Antimicrobial mechanisms of leucocyte- and platelet rich fibrin exudate against *Porphyromonas gingivalis* and multi-species biofilm: a pilot study. Submitted.
68. Serafini G, Lopreiato M, Lollobrigida M, Lamazza L, Mazzucchi G, Fortunato L, et al. Platelet Rich Fibrin (PRF) and Its Related Products: Biomolecular Characterization of the Liquid Fibrinogen. *J Clin Med.* 2020;9(4).
69. Brown AC, Barker TH. Fibrin-based biomaterials: modulation of macroscopic properties through rational design at the molecular level. *Acta Biomater.* 2014;10(4):1502-14.
70. Schwartz Z, Weesner T, van Dijk S, Cochran DL, Mellonig JT, Lohmann CH, et al. Ability of deproteinized cancellous bovine bone to induce new bone formation. *J Periodontol.* 2000;71(8):1258-69.
71. Sanz-Sánchez I, Ortiz-Vigón A, Sanz-Martín I, Figuero E, Sanz M. Effectiveness of Lateral Bone Augmentation on the Alveolar Crest Dimension: A Systematic Review and Meta-analysis. *J Dent Res.* 2015;94(9 Suppl):128s-42s.
72. Nkenke E, Neukam FW. Autogenous bone harvesting and grafting in advanced jaw resorption: morbidity, resorption and implant survival. *Eur J Oral Implantol.* 2014;7 Suppl 2:S203-17.
73. Khoury F, Hanser T. Mandibular bone block harvesting from the retromolar region: a 10-year prospective clinical study. *Int J Oral Maxillofac Implants.* 2015;30(3):688-97.
74. De Witte TM, Fratila-Apachitei LE, Zadpoor AA, Peppas NA. Bone tissue engineering via growth factor delivery: from scaffolds to complex matrices. *Regen Biomater.* 2018;5(4):197-211.
75. Cortellini S, Castro AB, Temmerman A, Van Dessel J, Pinto N, Jacobs R, et al. Leucocyte- and platelet-rich fibrin block for bone augmentation procedure: A proof-of-concept study. *J Clin Periodontol.* 2018;45(5):624-34.
76. Mir-Mari J, Benic GI, Valmaseda-Castellón E, Hämmerle CHF, Jung RE. Influence of wound closure on the volume stability of particulate and non-particulate GBR materials: an in vitro cone-beam computed tomographic examination. Part II. *Clin Oral Implants Res.* 2017;28(6):631-9.
77. Mir-Mari J, Wui H, Jung RE, Hämmerle CH, Benic GI. Influence of blinded wound closure on the volume stability of different GBR materials: an in vitro cone-beam computed tomographic examination. *Clin Oral Implants Res.* 2016;27(2):258-65.
78. Pitzurra L, Jansen IDC, de Vries TJ, Hoogenkamp MA, Loos BG. Effects of L-PRF and A-PRF+ on periodontal fibroblasts in in vitro wound healing experiments. *J Periodontol Res.* 2020;55(2):287-95.
79. Bi J, Intriago MFB, Koivisto L, Jiang G, Häkkinen L, Larjava H. Leucocyte- and platelet-rich fibrin regulates expression of genes related to early wound healing in human gingival fibroblasts. *J Clin Periodontol.* 2020;47(7):851-62.
80. Ratajczak J, Vanganswinkel T, Gervois P, Merckx G, Hilkens P, Quirynen M, et al. Angiogenic Properties of 'Leucocyte- and Platelet-Rich Fibrin'. *Sci Rep.* 2018;8(1):14632.

81. Talon I, Schneider A, Ball V, Hemmerlé J. Functionalization of PTFE Materials Using a Combination of Polydopamine and Platelet-Rich Fibrin. *J Surg Res.* 2020;251:254-61.
82. Soldatos NK, Stylianou P, Koidou VP, Angelov N, Yukna R, Romanos GE. Limitations and options using resorbable versus nonresorbable membranes for successful guided bone regeneration. *Quintessence Int.* 2017;48(2):131-47.
83. Lim G, Lin GH, Monje A, Chan HL, Wang HL. Wound Healing Complications Following Guided Bone Regeneration for Ridge Augmentation: A Systematic Review and Meta-Analysis. *Int J Oral Maxillofac Implants.* 2018;33(1):41–50.
84. Machtei EE. The effect of membrane exposure on the outcome of regenerative procedures in humans: a meta-analysis. *J Periodontol.* 2001;72(4):512-6.
85. Garcia J, Dodge A, Luepke P, Wang HL, Kapila Y, Lin GH. Effect of membrane exposure on guided bone regeneration: A systematic review and meta-analysis. *Clin Oral Implants Res.* 2018;29(3):328-38.
86. Femminella B, Iaconi MC, Di Tullio M, Romano L, Sinjari B, D'Arcangelo C, et al. Clinical Comparison of Platelet-Rich Fibrin and a Gelatin Sponge in the Management of Palatal Wounds After Epithelialized Free Gingival Graft Harvest: A Randomized Clinical Trial. *J Periodontol.* 2016;87(2):103-13.
87. Lektemur Alpan A, Torumtay Cin G. PRF improves wound healing and postoperative discomfort after harvesting subepithelial connective tissue graft from palate: a randomized controlled trial. *Clin Oral Investig.* 2020;24(1):425-36.
88. Areewong K, Chantaramungkorn M, Khongkhunthian P. Platelet-rich fibrin to preserve alveolar bone sockets following tooth extraction: A randomized controlled trial. *Clin Implant Dent Relat Res.* 2019;21(6):1156-63.
89. Suttapreyasri S, Leepong N. Influence of platelet-rich fibrin on alveolar ridge preservation. *J Craniofac Surg.* 2013;24(4):1088-94.
90. Castro AB, Van Dessel J, Temmerman A, Jacobs R, Quirynen M. Effect of different platelet-rich fibrin matrices for ridge preservation in multiple tooth extractions: A split-mouth randomized controlled clinical trial. *J Clin Periodontol.* 2021.
91. Temmerman A, Vandessel J, Castro A, Jacobs R, Teughels W, Pinto N, et al. The use of leucocyte and platelet-rich fibrin in socket management and ridge preservation: a split-mouth, randomized, controlled clinical trial. *J Clin Periodontol.* 2016;43(11):990-9.
92. Canellas J, da Costa RC, Breves RC, de Oliveira GP, Figueredo C, Fischer RG, et al. Tomographic and histomorphometric evaluation of socket healing after tooth extraction using leukocyte- and platelet-rich fibrin: A randomized, single-blind, controlled clinical trial. *J Craniomaxillofac Surg.* 2020;48(1):24-32.
93. Hauser F, Gaydarov N, Badoud I, Vazquez L, Bernard JP, Ammann P. Clinical and histological evaluation of postextraction platelet-rich fibrin socket filling: a prospective randomized controlled study. *Implant Dent.* 2013;22(3):295-303.
94. Anwandter A, Bohmann S, Nally M, Castro AB, Quirynen M, Pinto N. Dimensional changes of the post extraction alveolar ridge, preserved with Leukocyte- and Platelet Rich Fibrin: A clinical pilot study. *J Dent.* 2016;52:23-9.
95. Alzahrani AA, Murriky A, Shafik S. Influence of platelet rich fibrin on post-extraction socket healing: A clinical and radiographic study. *Saudi Dent J.* 2017;29(4):149-55.
96. Zhang Y, Ruan Z, Shen M, Tan L, Huang W, Wang L, et al. Clinical effect of platelet-rich fibrin on the preservation of the alveolar ridge following tooth extraction. *Exp Ther Med.* 2018;15(3):2277-86.

97. Sato T, Hara T, Mori S, Shirai H, Minagi S. Threshold for bone resorption induced by continuous and intermittent pressure in the rat hard palate. *J Dent Res*. 1998;77(2):387-92.
98. Lytle RB. Complete denture construction based on a study of the deformation of the underlying soft tissues. *J Prosthet Dent*. 1959;9(4):539-51.
99. Alrajhi MS, Askar O, Habib AA, Elsyad MA. Maxillary Bone Resorption with Conventional Dentures and Four-Implant-Supported Fixed Prosthesis Opposed by Distal-Extension Partial Dentures: A Preliminary 5-year Retrospective Study. *Int J Oral Maxillofac Implants*. 2020;35(4):816-23.
100. Lollobrigida M, Maritato M, Bozzuto G, Formisano G, Molinari A, De Biase A. Biomimetic Implant Surface Functionalization with Liquid L-PRF Products: In Vitro Study. *Biomed Res Int*. 2018;2018:9031435.
101. Abrahamsson I, Albouy JP, Berglundh T. Healing at fluoride-modified implants placed in wide marginal defects: an experimental study in dogs. *Clin Oral Implants Res*. 2008;19(2):153-9.
102. Hamzacebi B, Oduncuoglu B, Alaaddinoglu EE. Treatment of Peri-implant Bone Defects with Platelet-Rich Fibrin. *Int J Periodontics Restorative Dent*. 2015;35(3):415-22.
103. Öncü E, Alaaddinoğlu EE. The effect of platelet-rich fibrin on implant stability. *Int J Oral Maxillofac Implants*. 2015;30(3):578-82.
104. Öncü E, Bayram B, Kantarci A, Gülsever S, Alaaddinoğlu EE. Positive effect of platelet rich fibrin on osseointegration. *Med Oral Patol Oral Cir Bucal*. 2016;21(5):e601-7.
105. Öncü E, Erbeyoğlu AA. Enhancement of Immediate Implant Stability and Recovery Using Platelet-Rich Fibrin. *Int J Periodontics Restorative Dent*. 2019;39(2):e58–e63.
106. Torkzaban P, Khoshhal M, Ghamari A, Tapak L, Houshyar E. Efficacy of Application of Platelet-Rich Fibrin for Improvement of Implant Stability: A Clinical Trial. *J Long Term Eff Med Implants*. 2018;28(4):259-66.
107. Boora P, Rathee M, Bhorla M. Effect of Platelet Rich Fibrin (PRF) on Peri-implant Soft Tissue and Crestal Bone in One-Stage Implant Placement: A Randomized Controlled Trial. *J Clin Diagn Res*. 2015;9(4):Zc18-21.
108. Polak D, Clemer-Shamai N, Shapira L. Incorporating antibiotics into platelet-rich fibrin: A novel antibiotics slow-release biological device. *J Clin Periodontol*. 2019;46(2):241-7.
109. Rafiee A, Memarpour M, Taghvamanesh S, Karami F, Karami S, Morowvat MH. Drug Delivery Assessment of a Novel Triple Antibiotic-Eluting Injectable Platelet-Rich Fibrin Scaffold: An In Vitro Study. *Curr Pharm Biotechnol*. 2021;22(3):380-8.
110. Kawase T, Kamiya M, Kobayashi M, Tanaka T, Okuda K, Wolff LF, et al. The heat-compression technique for the conversion of platelet-rich fibrin preparation to a barrier membrane with a reduced rate of biodegradation. *J Biomed Mater Res B Appl Biomater*. 2015;103(4):825-31.



SUMMARY







# SUMMARY

---

The **overall objective** of this PhD thesis was to characterize different PRF matrices and to examine their regenerative potential in several oral surgical procedures. The **general hypothesis** was that PRF products have a positive effect when used alone or as adjuvant in bone grafting. This hypothesis was divided in four subcategories: systematic reviews, *in vitro*, *in vivo*, and clinical studies. Each subcategory presented some specific sub-hypotheses.

The first subcategory comprises **two systematic reviews** of the literature and a **meta-analysis** of randomised controlled clinical trials regarding the application of L-PRF in oral surgery. In the both systematic reviews, an electronic and hand search were conducted in three databases (*Medline*, *Embase* and *Cochrane*). Only randomized clinical trials were selected and no follow-up limitation was applied. In the first systematic review (**chapter 1**), three subgroups were created: intra-bony defects (IBDs), furcation defects, and periodontal plastic surgery. Meta-analysis was performed in all the subgroups. Pocket depth (PD), clinical attachment level (CAL), bone fill, keratinized tissue width (KTW), recession reduction and root coverage (%) were considered as outcome. The main results of the quantitative analysis were that the use of L-PRF resulted in a reduction of the pocket depth and a higher bone fill in intrabony defects and furcation defects compared to open flap debridement. When L-PRF was compared to a connective tissue graft in mucogingival surgery around teeth, similar outcomes were obtained. In the second systematic review (**chapter 2**), the use of L-PRF in bone regeneration and implant procedures was studied. Fourteen studies were included and three subcategories were created depending on the application: sinus floor elevation (SFE), alveolar ridge preservation, and implant therapy. In SFE, for a lateral window as well as for the trans-alveolar technique, histologically faster bone healing was reported when L-PRF was added to most common xenografts. L-PRF alone improved the preservation of the alveolar width after single tooth extraction, resulting in less buccal bone resorption compared to natural healing. In implant therapy, better implant stability over time and less marginal bone loss were observed when L-PRF was applied. Meta-analyses could not be performed due to the heterogeneity of the data.

The subcategory of ***in vitro* studies** involves 4 studies where the PRF matrices were characterized. In **chapter 3**, the biological characteristics of the L-PRF membranes, L-PRF exudate, Liquid Fibrinogen as well as of the L-PRF block were extensively studied. L-PRF membranes and the L-PRF block released growth factors up to 14 days. L-PRF exudate and the Liquid Fibrinogen could also release growth factors at the moment of collection. The L-PRF exudate presented a low cellular content in comparison with the L-PRF membranes with more than 80% of platelets and more than 70% of leucocytes in the initial blood sample. The microCT and SEM images revealed the bone substitute particles surrounded by platelets and leucocytes, embedded in a dens fibrin network. In **chapter 4**, the biological and physical characteristics of 3 types of PRF membranes (L-PRF, A-PRF and A-PRF+) using two different centrifuges (Intra-Spin and Duo) with adapted relative centrifugal forces (RCF) were compared. Moreover, the impact of timing (blood draw - centrifugation and centrifugation - membrane preparation) was assessed morphologically including scanning electron microscopy. We concluded that the adaptation of the RCF for each centrifuge did not

result in differences in terms of release of growth factors, cellular content, dimensions, and mechanical properties. However, the time between blood collection and centrifugation strongly influenced the dimension and structure of the L-PRF membranes obtained. The antimicrobial capacity of the L-PRF membranes and exudate against periodontal pathogens was evaluated in **chapter 5**. L-PRF membrane showed antimicrobial effect against the main periopathogens, especially against *Porphyromonas gingivalis*. The L-PRF exudate showed a strong inhibition against *P. gingivalis* on agar plates but no inhibition could be observed for the rest of the bacterial strains. *Aggregatibacter actinomycetemcomitans* showed increased growth in contact with L-PRF. However, the L-PRF exudate has an antimicrobial effect against *P. gingivalis* in a dose-dependent way. The last *in vitro* study described in **chapter 6** evaluated the detachment of particles from the silica-coated tubes and its presence in different PRF matrices compared to glass tubes. It was concluded that the centrifugation protocols influenced the amount of microparticles present in the PRF matrices. L-PRF presented the least amount inside the clot, and A-PRF+ the highest. The detachment rate of these particles was independent of the centrifugation protocol. Due to the contamination of the sample with other elements than Si during the enzymatic degradation of the clots, the quantification of the silica in each clot with spectrophotometer was not reliable, and thus not performed.

The third subcategory was an ***in vivo* study** where the effect of L-PRF coating on the early peri-implant bone formation and angiogenesis was evaluated in a pig model (**chapter 7**). Four implants were placed in the skull of twelve domestic pigs with an oversized preparation (0.4mm). Implants conditions with or without L-PRF were randomised and two follow-up periods were settled: 7 days and 28 days. To assess the bone-to-implant contact, histological and micro-CT images were taken from the bone samples. The early osteointegration of the implants with a fluoride-modified surface (ASTRA implants) seemed to be enhanced when coated with L-PRF. However, the implants with a calcium-phosphate coating appeared to be negatively affected by L-PRF. Thus, the effect of the L-PRF coating seemed to be dependent on the implant surface. For both implant surfaces, the bone microarchitecture were not significantly affected by the L-PRF functionalization.

In **chapter 8**, a **randomised controlled clinical study** evaluated the alveolar ridge changes and bone structure after multiple tooth extraction when L-PRF or A-PRF+ were used for ridge preservation in comparison to unassisted socket. Twenty patients in need of at least three tooth extractions in the aesthetic zone were included. L-PRF, A-PRF+ or control were randomly assigned. CBCT scans were obtained immediately after tooth extraction and after 3 months of healing. Horizontal and vertical dimensional changes of the ridge and socket fill were calculated. Histological and micro-CT analysis of bone biopsies from the centre of the sockets were used to evaluate the bone structure after healing. It was concluded that PRF matrices failed to reduce the dimensional changes after multiple tooth extractions in the premaxilla. After 3-months healing, both PRF matrices showed radiographically a significant superiority for the socket fill. Histologically, they seemed to accelerate new bone formation.

SAMENVATTING





# SAMENVATTING

Het doel van dit proefschrift was om verschillende PRF-matrices te karakteriseren en hun regeneratief potentieel te onderzoeken in verschillende orale chirurgische applicaties. De hypothese was dat PRF-producten een positief effect hebben wanneer ze alleen of als adjuvans bij bottransplantaties worden gebruikt. Deze hypothese werd onderzocht in niveaus: systematische reviews, *in vitro*, *in vivo* en klinische studies. Elke niveau onderzocht specifieke aspecten van de hypothese.

Het eerste deel omvat **twee systematische reviews** en een **meta-analyse** van gerandomiseerde gecontroleerde klinische studies met betrekking tot de toepassing van L-PRF bij orale chirurgie. In beide systematische reviews werd elektronisch en handmatig gezocht in drie databases. Er werden alleen gerandomiseerde klinische studies geselecteerd en er werd geen follow-up beperking toegepast. In de eerste systematische review (**hoofdstuk 1**) werden drie subgroepen onderscheiden: intra-bony defecten (IBD's), furcatie defecten en parodontale plastische chirurgie. Meta-analyse werd uitgevoerd op alle subgroepen. Pocketdiepte (PD), klinisch aanhechtingsniveau (CAL), bone fill, gekeratiniseerde gingiva breedte (KTW), recessievermindering en wortelbedekking (%) werden als uitkomst beschouwd. De belangrijkste resultaten van de kwantitatieve analyse waren de volgende: het gebruik van L-PRF resulteerde in een vermindering van de pocketdiepte en een hogere botvulling in intra-bony en furcatie defecten in vergelijking met open flap debridement. Wanneer L-PRF werd vergeleken met een bindweefselgreffe bij mucogingivale chirurgie rond tanden werden vergelijkbare resultaten verkregen. In de tweede systematische review (**hoofdstuk 2**) werd het gebruik van L-PRF bij botregeneratie en implantaattherapie bestudeerd. Veertien studies werden geïnccludeerd en er werden drie subcategorieën onderscheiden, afhankelijk van de toepassing: sinus lift (SFE), behoud van alveolaire kam en implantaattherapie. In SFE, zowel voor een lateraal venster als voor de trans-alveolaire techniek, werd histologisch snellere botgenezing gerapporteerd wanneer L-PRF werd toegevoegd aan de meest voorkomende xenografts. L-PRF alleen verbeterde het behoud van de alveolaire breedte na de verwijdering van een tand. Dit resulteerde in minder buccale botresorptie in vergelijking met natuurlijke heling. Bij implantaattherapie werd een betere implantaatstabiliteit in de loop van de tijd en minder marginaal botverlies waargenomen wanneer L-PRF werd aangebracht. Meta-analyses konden niet worden uitgevoerd vanwege de heterogeniteit van de gegevens.

Het deel van de **in vitro-studies** omvat 4 studies waarin de PRF-matrices werden gekarakteriseerd. In **hoofdstuk 3** werden de biologische eigenschappen van de L-PRF membranen, het L-PRF exsudaat, het vloeibaar fibrinogeen en van het L-PRF blok uitgebreid bestudeerd. L-PRF-membranen en het L-PRF-blok geven groeifactoren vrij tot 14 dagen na bereiding. L-PRF exsudaat en het vloeibare fibrinogeen geven ook groeifactoren af op het moment van verzamelen. Het L-PRF-exsudaat vertoonde een lage cellulaire inhoud in vergelijking met de L-PRF-membranen, met meer dan 80% bloedplaatjes en meer dan 70% leukocyten in het aanvankelijke bloedstaal. De microCT- en SEM-beelden onthulden dat de xenograft partikels omgeven door bloedplaatjes en leukocyten, ingebed in een dicht fibrinenetwerk. In **hoofdstuk 4** werden de biologische en fysische eigenschappen van 3 typen PRF-membranen (L-PRF, A-PRF en A-PRF +) in functie van de relatieve centrifugaal krachten (RCF) vergeleken. Bovendien werd de impact van timing (bloedafname - centrifugeren en centrifugeren - membraanpreparatie) morfologisch beoordeeld met

inbegrip van scanning elektronenmicroscopie. We concludeerden dat een aanpassing van de RCF voor elke centrifuge niet resulteerde in verschillen in termen van afgifte van groeifactoren, cellulaire inhoud, dimensies en mechanische eigenschappen. De tijd tussen bloedafname en centrifugatie had echter een sterke invloed op de opmeting en structuur van de L-PRF-membranen. In **hoofdstuk 5** werd de antimicrobiële capaciteit van de L-PRF membranen en exsudaat tegen parodontale pathogenen geëvalueerd. Het L-PRF membraan vertoonde een antimicrobieel effect tegen de belangrijkste periopathogenen, vooral tegen *Porphyromonas gingivalis*. Het L-PRF-exsudaat vertoonde een sterke groei remming van *P. gingivalis* op agarplaten, maar er kon geen inhibitie worden waargenomen voor de rest van de bacteriestammen. *Aggregatibacter actinomycetemcomitans* vertoonde een sterkere groei in contact met L-PRF. Het L-PRF-exsudaat heeft echter een antimicrobiële werking tegen *P. gingivalis* op een dosisafhankelijke manier. In **hoofdstuk 6** evalueerde de laatste in vitro studie het loslaten van partikels uit de silica-gecoate buisjes en de aanwezigheid ervan in verschillende PRF-matrices in vergelijking met glazen buisjes. De conclusie was dat de centrifugatieprotocollen de hoeveelheid microdeeltjes in de PRF-matrices beïnvloedden. L-PRF bevat de kleinste hoeveelheid van alles in het stolsel en A-PRF + de grootste. De mate van loslaten van deze partikels was onafhankelijk van het centrifugatieprotocol.

Het derde deel was een **in vivo studie** waarin het effect van L-PRF coating op de vroege peri-implantaire botvorming werd geëvalueerd in een varkensmodel (**hoofdstuk 7**). Vier implantaten werden in de schedel van twaalf huis varkens geplaatst met een over-preparatie van 0.4 mm. Implantaatcondities met of zonder L-PRF werden gerandomiseerd en er werden twee follow-up tijden bepaald: 7 dagen en 28 dagen. Om het contact tussen bot en implantaat te beoordelen, werden histologische en micro-CT-beelden van de botmonsters genomen. L-PRF coating van implantaten met een fluoride gemodificeerde oppervlak (ASTRA®-implantaten) lijkt de vroege osteointegratie van de implantaten te verbeteren. De implantaten met een calciumfosfaatcoating (Blossom®-implantaten) bleken echter negatief te worden beïnvloed door L-PRF. Het effect van L-PRF-coating leek dus afhankelijk te zijn van het implantaatoppervlak. Voor beide implantaatoppervlakken werd de botmicroarchitectuur niet significant beïnvloed door L-PRF-coating.

**Hoofdstuk 8** bespreekt een **gerandomiseerde gecontroleerde klinische studie** die de alveolaire kamveranderingen en botstructuur na extractie van meerdere tanden evalueerde wanneer L-PRF of A-PRF + werden gebruikt voor het behoud van de kam in vergelijking met natuurlijke heling. Twintig patiënten die minstens drie tandextracties in de esthetische zone nodig hadden, werden geïnccludeerd. L-PRF, A-PRF + of controle werden willekeurig toegewezen. CBCT-scans werden onmiddellijk na het verwijderen van tanden en na 3 maanden genezing genomen. Horizontale en verticale veranderingen van de alveolaire kam werden berekend. Histologische en micro-CT-analyse van botbiopsies vanuit het midden van de sockets werden gebruikt om de botstructuur na heling te evalueren. Er werd geconcludeerd dat PRF-matrices de dimensionale veranderingen na meerdere tandextracties in de premaxilla niet konden verminderen. Na 3 maanden genezing vertoonden beide PRF-matrices radiografisch een significante superioriteit voor de socketvulling. Histologisch leken ze de vorming van nieuw bot te versnellen.

CURRICULUM VITAE







# CURRICULUM VITAE

---

## PERSONAL

Name: Ana Belén Castro Sardá

Place of birth: Albelda (Huesca), Spain

Date of birth: 26 August 1986

Contact address: Kapucijnenvoer 7, blok a – box 7001  
3000 Leuven, Belgium

Phone: +32 484 71 94 73

E-mail: [anabelen.castrosarda@kuleuven.be](mailto:anabelen.castrosarda@kuleuven.be); [anabelencastro@hotmail.com](mailto:anabelencastro@hotmail.com)

---

## EDUCATION

2021 PhD in Biomedical Sciences  
*Periodontology & Oral Microbiology (KU Leuven), Leuven, Belgium*

2020 Master in Science of Specialised Oral Health Care,  
specialisation in Periodontology (summa cum laude)  
*EFP accredited program (KU Leuven), Leuven, Belgium*

2020 Postgraduate Studies in Periodontology (magna cum laude)  
*Periodontology & Oral Microbiology (KU Leuven), Leuven, Belgium*

2012 Master of Science (MSc) in Biomedical Engineering  
*University of the Basque Country, Bilbao, Spain*

2010 Master of Science (MSc) in Dentistry  
*University of Barcelona, Barcelona, Spain*

2007 Bachelor of Dental Science (BDS)  
*University of Barcelona, Barcelona, Spain*

2004 Secondary school option Biological Sciences (cum laude)  
*La Llitera college, Tamarite, Spain*

---

## RELEVANT CERTIFICATES

2021 EF Good Clinical Practice (GCP) Certificate on Clinical Studies

2019 Certificate for the use of CBCT in dentomaxillofacial diagnostics

2018 FELASA B Certificate – Laboratory Animal Science, Belgium

---

## PROFESSIONAL CAREER

2020 - present	Periodontist-Implantologist in private practice in Belgium
2020 - present	Clinical instructor at the Department of Periodontology <i>KU Leuven, Belgium</i>
2015-2020	Clinical assistant at the Department of Periodontology <i>KU Leuven, Belgium</i>
2014-2021	PhD part-time Researcher, Department of Periodontology <i>KU Leuven, Belgium</i>
2012-2014	General dentist in private practice in The Netherlands
2010-2012	General dentist in private practice in Spain

---

## PUBLICATIONS

Temmerman A, Vandessel J, **Castro AB**, Jacobs R, Teughels W, Pinto N, Quirynen M. The use of leucocyte and platelet-rich fibrin in socket management and ridge preservation: a split-mouth, randomized, controlled clinical trial. *J Clin Periodontol*. 2016 Nov;43(11):990-999. doi: 10.1111/jcpe.12612. Epub 2016 Sep 21.

Anwandter A, Bohmann S, Nally M, **Castro AB**, Quirynen M, Pinto N. Dimensional changes of the post extraction alveolar ridge, preserved with Leukocyte- and Platelet Rich Fibrin: A clinical pilot study. *J Dent*. 2016 Sep;52:23-9. doi: 10.1016/j.jdent.2016.06.005. Epub 2016 Jun 20.

Meschi N, **Castro AB**, Vandamme K, Quirynen M, Lambrechts P. The impact of autologous platelet concentrates on endodontic healing: a systematic review. *Platelets*. 2016 Nov;27(7):613-633. Epub 2016 Sep 22.

**Castro AB**, Meschi N, Temmerman A, Pinto N, Lambrechts P, Teughels W, Quirynen M. Regenerative potential of leucocyte- and platelet-rich fibrin. Part B: sinus floor elevation, alveolar ridge preservation and implant therapy. A systematic review. *J Clin Periodontol*. 2017 Feb;44(2):225-234. doi: 10.1111/jcpe.12658. Epub 2017 Jan 10.

**Castro AB**, Meschi N, Temmerman A, Pinto N, Lambrechts P, Teughels W, Quirynen M. Regenerative potential of leucocyte- and platelet-rich fibrin. Part A: intra-bony defects, furcation defects and periodontal plastic surgery. A systematic review and meta-analysis. *J Clin Periodontol*. 2017 Jan;44(1):67-82. doi: 10.1111/jcpe.12643. Epub 2016 Nov 24.

**Castro AB**, Politis C, De Hous C, Teughels W, Quirynen M. The role of vascularization in the development of peri-implantitis. *J Parodontologie et d'implantologie Orale* 2018;136 (37): 145-152.

Cortellini S, **Castro AB**, Temmerman A, Van Dessel J, Pinto N, Jacobs R, Quirynen M. Leucocyte-and platelet -rich fibrin block for bone augmentation procedure: A proof-of-concept study. *J Clin Periodontol* 2018 May;45(5):624-634. doi: 10.1111/jcpe.12877. Epub 2018 Apr 10.

Temmerman A, Cleeren GJ, **Castro AB**, Teughels W, Quirynen M. L-PRF for increasing the width of keratinized mucosa around implants: A split-mouth, randomized, controlled pilot clinical study. *J Periodontal Res* 2018 J Oct;53(5):793-800. doi: 10.1111/jre.12568. Epub 2018 Jun 2.

**Castro AB**, Cortellini S, Oud V, Sanaan B, Vanderstuyft T, Wylleman A, Temmerman A, Teughels W, Quirynen M. Review of article: Restoration contour is a risk indicator for peri-implantitis: a cross sectional radiographic analysis . *JCP digest* 2018-2.

De Winter S, Hoflack M, **Castro AB**, Quirynen M, Teughels W. Impact of history of periodontitis on incidence of peri-implantitis. *J Parodontologie et d'Implantologie Orale* 2018; 136(37):133-143.

**Castro AB**, Cortellini S, Temmerman A, Li X, Pinto N, Teughels W, Quirynen M. Characterization of the Leucocyte- and Platelet Rich Fibrin Block: release of growth factors, cellular content, and structure. *Int J Oral Maxillofac Impl* 2019, Feb 11. doi: 10.11607/jomi.7275. [Epub ahead of print].

**Castro AB**, Rodriguez ER, Slomka V, Pinto N, Teughels W, Quirynen M. Antimicrobial capacity of Leucocyte-and Platelet Rich Fibrin against periodontal pathogens. *Sci Rep* 2019, 9(3): 8188.

Vanderstuyft T, Tarce M, Sanaan B, Oud V, De Greef A, Temmerman A, Quirynen M, Teughels W, **Castro AB**. Review of article: Evaluation of peri-implant marginal tissues around tissue-level and bone-level implants in patients with a history of chronic periodontitis. *JCP digest* 2019.

Ockerman A, Braem A, EzEldeen M, **Castro AB**, Coucke B, Politis C, Verhamme P, Jacobs R, Quirynen M. Mechanical and structural properties of Leukocyte- and Platelet Rich Fibrin membranes: an in vitro study on the impact of anticoagulant therapy. *J Periodontal Res* 2020, 55; 686-693.

**Castro AB**, Andrade C, Li X, Pinto N, Teughels W, Quirynen M. Impact of g force and timing on the characteristics of platelet-rich fibrin matrices. *Scie Rep* 2021, 11; 6038.

**Castro AB**, Van Dessel J, Temmerman A, Jacobs R, Quirynen M. Effect of different platelet rich fibrin matrices for ridge preservation in multiple tooth extractions: a split-mouth randomized controlled clinical trial. *J Clin Periodontol* 2021, 48: 984-995.

Alami M, Germonpré PJ, Ntovas N, Robben J, Rodríguez Sánchez F, Siawasch SAM, Sidiropoulou N, Teughels W, **Castro AB**. Correlation between dental-plaque accumulation and gingival health in periodontal-maintenance patients. *JCP digest* 2021.

Rodríguez Sánchez F, Verspecht T, **Castro AB**, Pauwels M, Rodríguez Andrés C, Quirynen M, Teughels W. Antimicrobial mechanisms of leucocyte-and platelet rich fibrin exudate against planktonic *Porphyromonas gingivalis* and within multi-species biofilm: a pilot study. *Front Cell Infect Microbiol*. 2021. Accepted.

---

## CHAPTER IN BOOKS

### Het tandheelkundig jaar 2017

Temmerman A, De Coster I, **Castro AB**, Pinto N, Teughels W, Quirynen M. Weefselregeneratie door middel van L-PRF: 'van mythe tot realiteit'. Bohn Stafleu van Loghum, ISBN 978-90-368-1029-6.

### Newman and Carranza's Clinical Periodontology (Chapter 66)

Pinto N, Temmerman A, **Castro AB**, Cortellini S, Teughels W, Quirynen M. Leucocyte- and Platelet Rich Fibrin: biological properties and applications. 13th Edition. Elsevier. 2019. Pages: 664-675.

---

## PARTICIPATION AT NATIONAL AND INTERNATIONAL MEETINGS

**Castro AB**, Rodriguez ER, Slomka V, Pinto N, Teughels W, Quirynen M. L-PRF: cellular content and antibacterial capacity (**Oral presentation**). Congress Enhanced Natural Healing in Dentistry L-PRF (Belgium, 2016).

**Castro AB**, Rodriguez ER, Slomka V, Pinto N, Teughels W, Quirynen M. Leucocyte- and Platelet Rich Fibrin has antibacterial effect against the main periodontal pathogens (**Oral presentation**). International Association for Dental Research (IADR) General Session (San Francisco, USA, 2017).

**Castro AB**, Cortellini S, Temmerman A, Li X, Pinto N, Teughels W, Quirynen M. Biological properties of the L-PRF block: release of growth factors and cellular content (**Poster presentation**). Congress of the European Association for Osseointegration (EAO) (Madrid, 2017).

**Castro AB**, Cortellini S, Temmerman A, Li X, Pinto N, Teughels W, Quirynen M. L-PRF block as a living tissue: analysis of its bioactive nature and structure (**Poster presentation**). Congress of the European Federation of Periodontology (EFP) Europerio9 (The Netherlands, 2018).

**Castro AB**, Andrade C, Li X, Pinto N, Teughels W, Quirynen M. Are the centrifuge and timing a key factor for the preparation of platelet concentrates? (**Oral presentation**). Congress Enhanced Natural Healing in Dentistry L-PRF (Belgium, 2018)

**Castro AB**, Cortellini S, Vasconcelos KF, Duyck J, Jacobs R, Quirynen M. Peri-implant bone and microvessel density after implant functionalization with L-PRF (**Poster presentation**). Congress of the European Association for Osseointegration (EAO) (Lisbon, 2019)

**Castro AB**, Cortellini S, Temmerman A, Teughels W, Quirynen M. Application of cellular therapy on the current surgical techniques in Implantology (**Oral presentation**). Belgian Symposium for Tissue Engineering (Belgium, 2019).

# ACKNOWLEDGEMENTS AND CONFLICT OF INTEREST





# ACKNOWLEDGEMENTS AND CONFLICT OF INTEREST

---

## Scientific acknowledgement

First, I would like to acknowledge the scientific and personal support of my promoter, **Prof. Marc Quirynen**, and both my co-promoters, **Prof. Reinhilde Jacobs** and **Prof. Joke Duyck**. Moreover, I would like to thank all the co-authors of the articles included in this PhD thesis for their scientific contribution and input to enhance the quality of this thesis.

Many thanks to **Dr. Martine Pauwels**, **Dr. Esteban Rodriguez Herrero**, **Dr. Vera Slomka** and all members from the **laboratory of Oral Microbiology** (KU Leuven) for their help and patience teaching me how to work in a lab. It was a very enriching experience and I hope to continue working together in the future. Moreover, I would like to thank **Dr. Tim Vangansewinkel** and **Mrs. Evelyne Van Kerckhove** from Hasselt University for their unconditional help in the histological processing and **Dr. Ferda Pamuk** for her support in the histological analysis of the *in vivo* study.

Thanks to **Dr. Xin Li**, **Dr. Jeroen Van Dessel** and **Dr. Karla de Faria Vasconcelos** for their help in the acquisition and analysis of scanning electron microscopy images and micro-CT images, respectively. These data enriched enormously the scientific evidence of the studies.

I would like to show my gratitude to **Dr. Wim Coucke** for his availability and nice discussions about the statistical analysis of the data from the studies of this PhD thesis.

Also thanks to **Dr. Nastaran Meschi** and **Prof. Emer. Paul Lambrechts** for their help and teamwork on both systematic reviews. I cannot forget **Drs. Catherine Andrade** and **Prof. Nelson Pinto** from the University of Los Andes (Chile) for their pleasant collaboration.

Finally yet importantly, I would like to thank **Prof. Wim Teughels**, **Prof. Andy Temmerman**, **Drs. Simone Cortellini** and all members of the **Department of Periodontology** for their support and help throughout this PhD thesis.

## Personal contribution

This PhD thesis was written by Ana B. Castro Sardá and reviewed by the promotor Prof. Marc Quirynen. All manuscripts included in this thesis were written by the PhD candidate and revised by all co-authors.

## Conflict of interest

### ***Systematic reviews***

#### **Regenerative potential of leucocyte- and platelet-rich fibrin. Part A and Part B**

No conflict of interest

### ***In vitro studies***

#### **Characterization of Leucocyte- and Platelet Rich Fibrin Block (L-PRF block): release of growth factors, cellular content, and structure**

No conflict of interest



The department of Periodontology and the department of Prosthetic Dentistry at KU Leuven are holders of a research chair from Intra-Lock International; devoted to optimizing osseointegration. The consumables of this project were paid by this chair.

#### **Impact of g force and timing on the characteristics of platelet-rich fibrin matrices**

No conflict of interest

The department of Periodontology and the department of Prosthetic Dentistry at KU Leuven are holders of a research chair from Intra-Lock International; devoted to optimizing osseointegration. The consumables of this project were paid by this chair.

#### **Antimicrobial capacity of Leucocyte- and Platelet Rich Fibrin against periodontal pathogens**

No conflict of interest

The department of Periodontology and the department of Prosthetic Dentistry at KU Leuven are holders of a research chair from Intra-Lock International; devoted to optimizing osseointegration. The consumables of this project were paid by this chair.

#### **Particle release from silica-coated plastic tubes and presence in PRF-matrices**

No conflict of interest

The department of Periodontology and the department of Prosthetic Dentistry at KU Leuven are holders of a research chair from Intra-Lock International; devoted to optimizing osseointegration. The consumables of this project were paid by this chair.

#### ***In vivo study***

##### **Peri-implant bone structure after implant surface functionalization with L-PRF at early healing: a micro-CT and histomorphological analysis**

No conflict of interest

The department of Periodontology and the department of Prosthetic Dentistry at KU Leuven are holders of a research chair from Intra-Lock International; devoted to optimizing osseointegration. The consumables of this project were paid by this chair.

#### ***Clinical study***

##### **Effect of different platelet rich fibrin matrices for ridge preservation in multiple tooth extractions: a split-mouth randomized controlled clinical trial**

No conflict of interest

Part of this project was partially financed by the Research Foundation – Flanders (FWO) appointed to Prof. Andy Temmerman within the frame of a TBM project for applied biomedical research with a primary social finality (grant number: T003018N – L-PRF in cranial and oral surgery).

The department of Periodontology and the department of Prosthetic Dentistry at KU Leuven are holders of a research chair from Intra-Lock International; devoted to optimizing osseointegration. The consumables of this project were paid by this chair.